Investigating the effect of altered nutrition on signalling via *Drosophila* class 1A phosphatidylinositol-3 kinase (PI3K), and functional analysis of PI3K mutated within its Ras-binding domain.

Gemma Louise Bradley

Thesis submitted to the University of London
for the degree of Master of Philosophy
July 2003

Growth Regulation Laboratory
Cancer Research UK
44 Lincoln's Inn Fields
London WC2A 3PX

Department of Biochemistry
University College London
Gower Street
London WC1 6BT

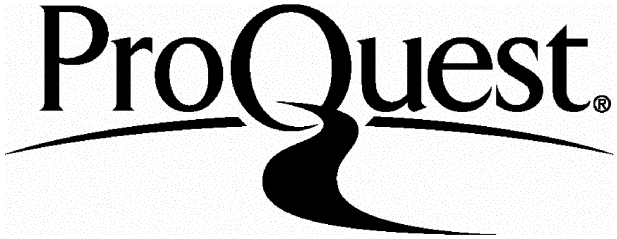

Abstract

Adult *Drosophila* size is determined during larval life, by the growth of internal epithelial structures known as imaginal discs. These discs metamorphose during pupal development to form the adult epidermal structures. The insulin/PI3K signalling pathway in *Drosophila* has been shown to regulate disc, final organ and organism size. Disruption of this signalling pathway inhibits *Drosophila* growth and generates smaller than wild-type flies whereas increasing PI3K signalling increases growth, generating larger flies.

As the nutritional state of larvae also has a bearing on final organism size, with malnourished larvae generating small adults, my initial aim was to evaluate whether nutrition acts through the PI3K signalling pathway to affect growth. Levels of PI3K signalling were monitored in whole-larval lysates via the phosphorylation and activation of the PI3K target dAkt. Preliminary experiments showed that dAkt phosphorylation decreased with reduced nutritional input. Kinase assays confirmed that dAkt activity was reduced co-ordinately. However, despite extensive optimisation, the reproducibility of these results was poor. I concluded that whole larval extracts were not a suitable system for monitoring physiological changes in dAkt activity.

Drosophila embryos lacking the class IA PI3K catalytic sub-unit, Dp110, arrest development late in larval life and contain no visible imaginal discs. A similar phenotype is observed in Ras/MAPK pathway loss of function mutants. Further to this, many biochemical data from mammalian cell systems suggest that Ras-family GTPases interact with and activate PI3K catalytic sub-units via a Ras binding domain (RBD). However, the biological importance of this interaction is unclear. My second aim was to establish the functional significance of the RBD in Dp110. Larvae with only one copy of the Dp110 gene containing a non-conservative mutation within the RBD (6N3) remain small and fail to pupate, raising the possibility that RBD integrity is essential for Dp110 function. However, the mutation may equally reduce protein stability, binding to the adapter, p60, or catalytic activity. These possibilities were tested in turn, using a cell culture system. Other RBD mutants of Dp110 were tested in parallel. Results suggest that the 6N3 mutation partially disrupts Dp110 catalytic activity. However, this and other properties of Dp110 remain unimpaired in other RBD mutants, indicating that these proteins could be used in further studies to establish the significance of this domain *in vivo*.

Table of Contents

Table of Figures

Table of Tables

List of Abbreviations

4E-BP	eIF4E-binding protein
α–	Anti- (precedes protein name for antibodies)
aa	Amino acid
AED	After egg deposition
ATP	Adenosine triphosphate
BCR	Breakpoint cluster homology
C-terminal	Carboxy-terminal
CHO	Chinese hamster ovary
$CuSO_4$	Copper sulphate
d4E-BP	*Drosophila* eIF4E binding protein
dAkt	*Drosophila* Akt
deIF4E	*Drosophila* eukaryotic initiation factor 4E
DILP	*Drosophila* insulin like peptide
dINR	*Drosophila* insulin receptor
DNA	Deoxyribonucleic acid
Dp110	*Drosophila* p110 (catalytic subunit of *Drosophila* PI3K)
dPDK	*Drosophila* phosphoinositide dependent kinase
Dpp	Decapentaplegic
DPTEN	*Drosophila* phosphatase and tensin homolog deleted from chromosome ten
Dras	*Drosophila* Ras
dS6K	*Drosophila* S6 kinase
dTOR	*Drosophila* target of rapamycin
dTSC	*Drosophila* tuberous sclerosis
eIF4E	Eukaryotic initiation factor 4E
ERT	Endoreplicating tissue
FBP	FKBP12-rapamycin binding domain
GAP	GTPase activating domain
GDP	Guanine diphosphate
GEF	Guanine nucleotide exchange factor
GFP	Green fluorescent protein
GFP-PH	PIP_3 binding PH domain fused to GFP
GSK-3β	Glycogen synthase kinase-3β
GTP	Guanine triphosphate
HA	Haemagglutinin
HEK293	Human embryonic kidney 293
HRP	Horse radish peroxidase
IDGF	Imaginal disc growth factor
IGF	Insulin like growth factor
ILK	Integrin linked kinase
IP	Immunoprecipitation
IRS	Insulin receptor substrate
KA	Kinase assay
KLH	Keyhole limpet hemacyanin
m-NSC	Median neurosecretory cell
MAPK	Mitogen activated protein kinase
Mt	Metallothionein
MT	Mitotic tissue
N-terminal	Amino terminal

NF	Normal food
PBS	Phosphate buffered saline
PDGF	Platelet derived growth factor
PDK	Phosphoinositide dependent kinase
p-dAkt	Phosphorylated *Drosophila* Akt
PI	Phosphatidylinositol
PI3K	Phosphoinositide 3-kinase
PI(4)P	Phosphatidylinositol 4-phospate
PIF	PDK1 interacting fragment
PIP_2	Phosphatidylinositol 4,5-bisphosphate
PIP_3	Phosphatidylinositol 3,4,5-trisphosphate
PH	Pleckstrin homology
PKB	Protein kinase B
PP2A	Protein phosphatase 2A
PRK2	Protein kinase C related kinase 2
PTB	Phosphotyrosine binding
PTEN	Phosphatase and tensin homolog deleted from chromosome ten
RBD	Ras binding domain
RNA	Ribonucleic acid
RTK	Receptor tyrosine kinase
S2	Schneider 2
S6K	S6 kinase
SDS-PAGE	SDS-polyacrylamide gel electrophoresis
SF	Standardised food
SH2	Src homology 2
SH3	Src homology 3
SK50	Anti-Dp110 antibody
TOR	Target of rapamycin
TSC	Tuberous sclerosis
WT	Wild type

Chapter 1: Introduction

1.1 Overview

The growth of single celled organisms is tightly regulated by the availability of nutrients. For example, yeast monitor amino acids levels and respond accordingly, in part by altering their ability to grow and divide. In multicellular organisms cells have retained this ability to be directly influenced by amino acids and they too modulate their growth or division accordingly (see section 1.3.5). However, as the growth of multiple cells needs to be tightly coordinated in order to produce organs and organisms of the correct dimensions, these nutritional signals must integrate with intrinsic growth control mechanisms such as patterning cues (see section 1.3.2). Moreover, the availability of nutrients is not simply monitored on a cellular basis. In addition, organismal nutrient levels are assessed by specialised organs, which secrete humoral growth factors in a nutrient-dependent fashion (see section 1.3.4).

One such humoral signal is the hormone insulin. In mammals, insulin is produced in the β-cells of the pancreas and secreted in response to high blood glucose levels (for more details see section 3.1). Insulin acts at a distance to induce liver cells, muscle cells and adipose tissue to take up glucose and can regulate cell growth, in part, via the promotion of protein synthesis (see section 1.3.6). The molecules involved in transducing the insulin signal are discussed in section 1.2. These include the heterodimeric lipid kinase, phosphoinositide (3) kinase (PI3K), and the serine/threonine kinase, Akt.

The work in this thesis investigates the regulation of the insulin/PI3K signalling pathway in the fruit fly *Drosophila melanogaster* by nutrition, and its potential regulation by Ras-family small GTPases. Hence this introduction will firstly give an overview of the mammalian and *Drosophila* insulin/PI3K signalling pathways. This will be followed by general introduction to the regulation of growth in *Drosophila*, and the role that PI3K signalling and nutrition play in this process.

1.2 Insulin/PI3K signalling pathway

1.2.1 Phosphoinositide 3-kinases.

Phosphatidylinositol (PI) is the basic building block for all the phosphoinositide lipids found in eukaryotic cell membranes. It consists of D-*myo*-inositol-phosphate linked via its phosphate group to diacylglycerol. Although there are five free hydroxyl groups on the inositol ring that could be linked to phosphate groups, no reports of the 2

and 6 positions becoming esterified with phosphate *in vivo* have been documented. However the 3, 4 and 5 positions can be phosphorylated *in vivo* (Vanhaesebroeck et al., 2001). Phosphoinositide 3-kinases (PI3Ks) are an evolutionary conserved family of lipid kinases that catalyse the phosphorylation of the 3´ hydroxyl position of the inositol ring (Stephens et al., 1993). This family is divided into three groups, I, II and III, according to structure and substrate specificity (Vanhaesebroeck et al., 1997a). Class I PI3K have been best characterised, and will be the focus of the discussion below.

Class I PI3Ks are heterodimers made up of a 110kDa catalytic subunit, and an adaptor/regulatory subunit. Although *in vitro* these kinases can utilise PI, phosphatidylinositol 4-phosphate (PI(4)P) and phosphatidylinositol 4,5-bisphosphate (PIP_2), as substrates, their preferred substrate *in vivo* appears to be PIP_2. The class I enzymes are subdivided into two groups, class IA and class IB, which are activated by tyrosine kinases and the β/γ subunit of heterotrimeric G-proteins, respectively (see section 1.2.2). Mammals have three class IA catalytic subunits: p110α, p110β and p110δ, and at least seven class IA adaptor subunits that are generated through the alternative splicing of three different genes. Each of the catalytic subunits can bind to any of the adaptor subunits (Vanhaesebroeck et al., 1997a). The only known class IB PI3K, which exists exclusively in mammals, consists of the p110γ catalytic subunit and the p101 regulatory subunit (Stephens et al., 1997). The fruit fly *Drosophila melanogaster* contains only one class I PI3K. This is a class IA enzyme made up from the catalytic subunit Dp110 and the adaptor subunit p60 (Leevers et al., 1996; Weinkove et al., 1997).

1.2.1.1 Structure of Class I PI3Ks

All PI3K catalytic subunits share a homologous region that consists of a catalytic core domain, a helical domain and a membrane-binding C2 domain. In addition, the class I catalytic subunits contain N-terminal adaptor binding and Ras-binding domains (see figure 1.1A). The crystal structure of p110γ minus its N-terminal adaptor-binding region has been solved (Walker et al., 1999). As this section of the molecule is highly conserved between this and other catalytic subunits, the structure has given researchers further insight into how the PI3K molecules function, are regulated and are inhibited (for a review see (Djordjevic and Driscoll, 2002).

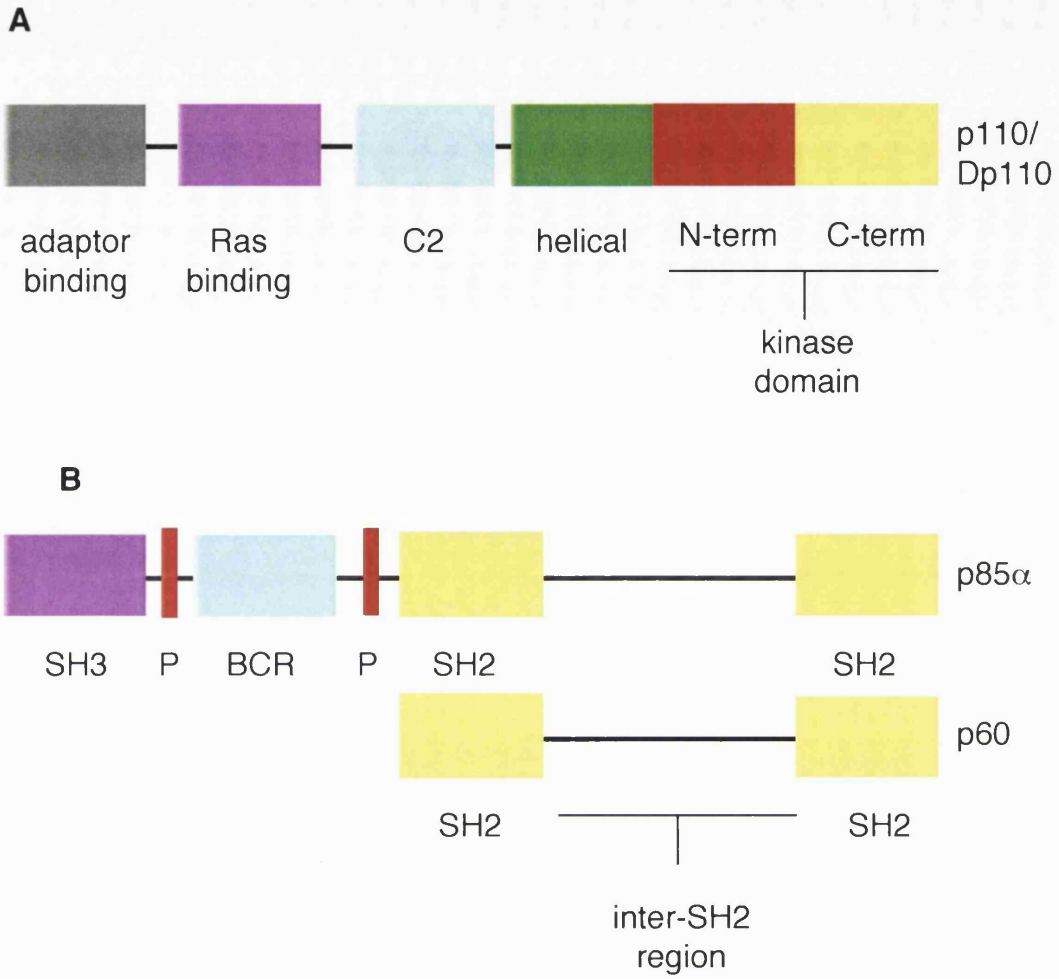

Figure 1.1 Mammalian and *Drosophila* class IA PI3K

A shows a schematic of the domain structure of the class I PI3K catalytic subunits, p110 and Dp110. The structures of the *Drosophila* and mammalian p110 molecules are highly homologous. **B** shows a schematic of the mammalian class IA adaptor subunit, p85α and the *Drosophila* homolog, p60. Note that P marks the proline rich motifs.

The structural data revealed that the catalytic subunits have a modular structure. The helical domain acts like a scaffold, from which the catalytic, C2 and Ras-binding domains hang. The catalytic domain has the typical double-lobed structure that is seen in other ATP-dependent kinases, with a small N-terminal lobe and a large C-terminal lobe. The Ras-binding domain (RBD) contacts the N-terminal lobe and to a lesser extent the C-terminal lobe of this kinase domain (Walker et al., 1999). This proximity means that Ras-p110γ binding can cause a conformational change in the catalytic domain (Pacold et al., 2000). This may well alter the activity of the molecule (for further details see section 4.1).

The adaptor subunits of class IA PI3K contain two Src homology 2 (SH2) domains that can bind phosphorylated tyrosine residues (see figure 1.1B). The region between the two SH2 domains is predicted to adopt a helical conformation. The p110 binding site falls within this inter-SH2 region (Holt et al., 1994). More recent experiments have shown that an isoleucine, lysine and arginine rich domain in this region seems to act in synergy with Ras to promote downstream signalling, and a leucine, glutamate and aspartate rich domain seems to negatively regulate PI3K catalytic activity (Chan et al., 2002). In addition a sub-class of mammalian adaptors, the p85 molecules, contain an N-terminal SH3 domain, which can bind proline rich motifs *in vitro,* and a breakpoint cluster region (BCR) homology domain. BCR homology domains have structural homology with GTPase activating domains (GAPs) but are not thought to possess any GAP activity, thus their function is unclear. The adaptors also contain varying numbers of proline rich sequences, and it is possible that these are bound by the SH3 domains of other p85 adaptor subunits, leading to the dimerisation of PI3K molecules (Layton et al., 1998). p101, the class IB PI3K adaptor, is unrelated to any known sequence and its only domain of note is a proline-rich domain, in the centre of the molecule (Stephens et al., 1997).

1.2.1.2 Activation of Class I PI3Ks

When cells are treated with ligands that stimulate receptor tyrosine kinases (RTKs), or that signal via intracellular tyrosine kinases or G-proteins, the intracellular levels of PIP_3 increase rapidly (for review see (Stephens et al., 1993). This implies that PI3K molecules become activated upon trans-membrane receptor activation (see figure 1.2 for details).

After binding extracellular ligands, such as insulin or platelet derived growth factor (PDGF), the cognate RTK, which could be either a constitutive dimer (e.g.

insulin receptor) or a monomer that dimerises upon stimulation (e.g. PDGF receptor), transphosphorylates on key exposed tyrosine residues, leading to its activation (Feige and Chambaz, 1987; Hunter et al., 1992). Once activated, the insulin receptor binds and tyrosine phosphorylates an insulin receptor substrate (IRS) protein that acts as a membrane-targeted adaptor (Myers et al., 1994). The amino acid sequence that surrounds the phosphotyrosines specify which proteins can bind to these residues. For example phosphotyrosine in the context of a pYXXM consensus motif, where X can be any amino acid, is specifically recognised and bound by the two SH2 domains in PI3K adaptor molecules (Songyang et al., 1993). The IRS protein contains such a motif and is therefore bound by PI3K adaptors, which brings the catalytic subunit to the membrane where it can contact its substrates (Kotani et al., 1994). The need for the adaptor subunit to target p110 to the membrane can be bypassed experimentally by the addition of peptides that become post-translationally farnesylated or myristylated to one of the termini of p110. Such tagged proteins when over expressed have been shown to be constitutively active (Klippel et al., 1996; Leevers et al., 1996). These data suggest that controlling the localisation of p110 proteins regulates their *in vivo* activity. This hypothesis is supported by the result that purified Class IA PI3K in complex with their adaptors are constitutively active *in vitro* (See section 4.6 and (Hiles et al., 1992).

However, other studies have suggested that translocation to the membrane is not sufficient for full activation of the Class IA PI3Ks (e.g. (Backer et al., 1992; Klippel et al., 1996). These experiments suggest that when the PI3K complex is in the cytosol the adaptor subunit acts to inhibit the catalytic activity of p110. This repression is relieved when the adaptor subunit binds to phosphotyrosine containing peptides (for further discussion see section 4.16.1). Furthermore, when the adaptor subunit binds to phosphotyrosines the activity of the associated catalytic subunit is enhanced. The resulting activity is higher than can be achieved by monomeric p110. The part of the adaptor subunit that plays this activating role has been mapped to the inter-SH2 region of p85 (Chan et al., 2002).

The regulation of class IB PI3Ks is less well characterised, though they are known to be activated through association with the β/γ subunits of heterotrimeric G-proteins (Stephens et al., 1997). As both the class IA and class IB PI3K catalytic subunits contain Ras-binding domains, the binding of Ras in its active GTP-bound form has been postulated to be a further mechanism by which both classes of catalytic subunit could be activated. In the case of the class IA molecules, the activation by

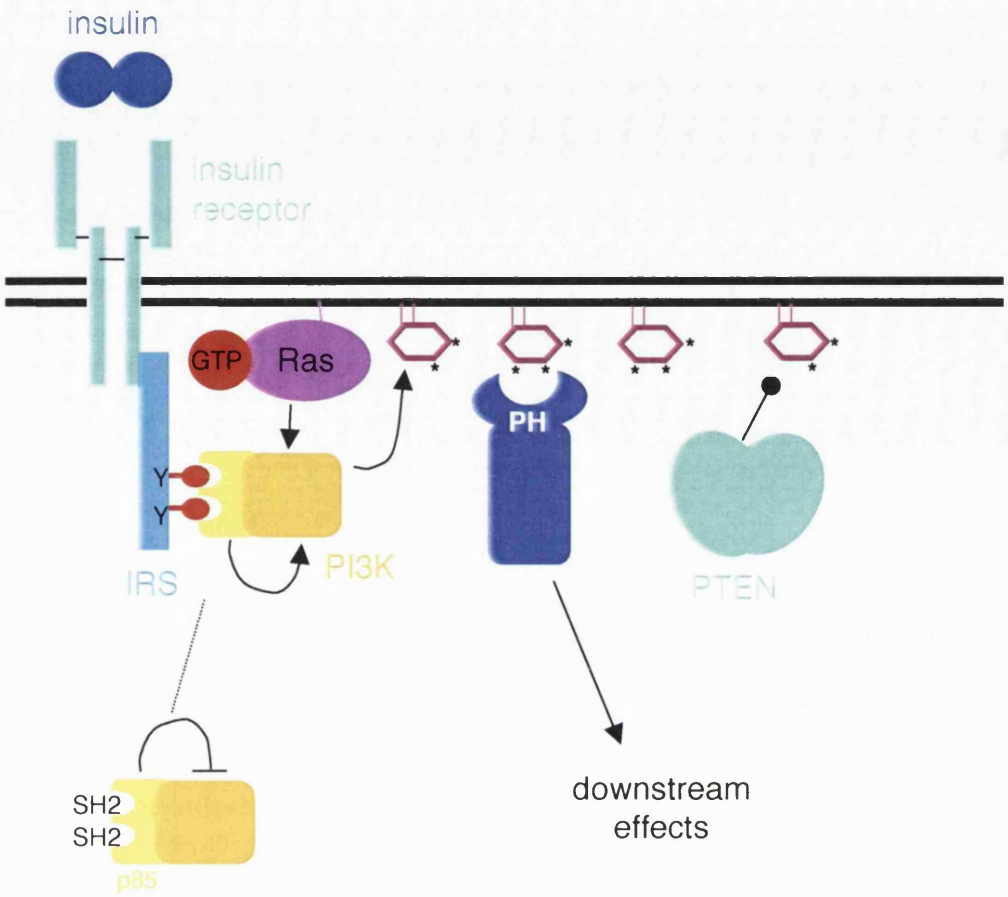

Figure 1.2 Production of phosphatidyl inositol (3.4.5) trisphosphate

The details of this signalling pathway are described in the text. Briefly, upon ligand binding, the insulin receptor, which exists as a constitutive dimer, autophosphorylates on intracellular tyrosine residues. Insulin receptor substrate proteins (IRS) bind to these motifs, and are tyrosine phosphorylated by the receptor. PI3K is brought to the membrane by the adaptor subunit binding via its SH2 domains to IRS phosphotyrosines. This binding also relieves the repression exerted by the adaptor on the catalytic subunit. PI3K then phosphorylates PIP_2 at the 3´ position to produce PIP_3. PIP_3 is bound by PH domain containing molecules that consequently generate downstream signals. The production of PIP_3 is antagonised by the lipid phosphatase, PTEN.

constitutively active Ras has been shown to act in synergy with the activation via adaptor-phosphotyrosine binding (Rodriguez-Viciana et al., 1996a). The binding of GTP-bound Ras to p110 is thought to cause an allosteric change in the catalytic domain of p110, thereby leading to its activation (Pacold et al., 2000). A possible explanation of how this works is that the new conformation increases the affinity of the catalytic subunit for its substrates (Suire et al., 2002). Although many experiments have been carried out to investigate whether this mode of regulation is important under physiological conditions, the answer remains elusive (see section 4.1 for further details).

1.2.3 Down regulation of Class I PI3K activity

The down regulation of PI3K pathway activity is discussed at length in section 4.16.2. Briefly, although binding to the adaptor subunit stabilises the p110 protein it also inhibits its basal catalytic activity (Kodaki *et al.*, 1995). As discussed, the binding of phosphorylated tyrosine residues to the class IA adaptor subunit SH2 domains relieves this inhibition. There is also evidence that p110δ autophosphorylates on serine 1039 after activation by CD28 in Jurkat cells, leading to a reduction in its catalytic activity (Vanhaesebroeck et al., 1999). The phosphorylation of the adaptor subunit on serine 608 by p110α and p110β has also been postulated to be a mechanism for down regulation of PI3K activity, but the relevance of this event *in vivo* is not clear (Dhand et al., 1994).

Class I PI3K signalling is antagonised by the lipid phosphatase and tumour suppressor, PTEN (phosphatase and tensin homolog deleted from chromosome ten). Despite showing homology with protein tyrosine phosphatases, recombinant PTEN is a lipid phosphatase that can dephosphorylate $PI(3,4)P_2$ and $PI(3,4,5)P_3$ specifically at the 3′ hydroxyl position of the inositol ring *in vitro* (Maehama and Dixon, 1998). Consistent with this observation, cells isolated from *pten* null mouse embryos contain elevated levels of PIP_3 (Stambolic et al., 1998). The structure of PTEN has been solved and shows that PTEN contains a C2 domain. This domain enables PTEN to associate with phospholipid membranes, and positions the catalytic domain so that it can act on the membrane localised phosphoinositides (Lee et al., 1999). Mutation of the *pten* gene in the germ line can lead to various autosomal cancer-predisposing syndromes including Cowden disease and Bannayan-Zonna syndrome. In addition, the gene is mutated or deleted in a large proportion of sporadic cancers (Li et al., 1997). These observations suggest that increasing PI3K signalling plays a role in inducing the overgrowth phenotypes that are associated with such diseases (see section 1.3.4).

Class IA PI3K activity can also be antagonised by the cell-permeable, low molecular weight compounds, wortmannin (Wymann et al., 1996) and LY294002 (Vlahos et al., 1994). The specificity of these compounds is only ensured when they are used at between 20 and 50nM and between 1 and 2 μM respectively, and even then LY294002 can inhibit the phosphoinositide kinase (PIK) related kinases, including mammalian Target of rapamycin (mTOR) and DNA protein kinase (Vanhaesebroeck et al., 2001; Wymann et al., 1996). However, together they can be and have been used effectively to investigate the functions of PI3K signalling.

1.2.2 Downstream of PI3K signalling

Once generated $PI(3,4)P_2$ and PIP_3 function as signal transduction intermediates, influencing the activity of a number of downstream signalling molecules. These in turn activate or inhibit a wide range of cellular processes such as cell survival, cell and tissue growth, DNA synthesis, and cytoskeletal reorganisation (for a review see (Vanhaesebroeck et al., 2001). These signalling molecules are able to act downstream of PI3K by binding to 3-phosphoinositides via integral pleckstrin homology (PH) lipid-binding domains.

PH domains are globular protein motifs of around 100 amino acids, originally identified in pleckstrin, the major phosphorylation target of protein kinase C in platelets (Mayer et al., 1993). Although the level of primary sequence identity between PH domains is low, crystal structure data has shown that their tertiary structure is highly conserved (Lemmon et al., 1996). Upon binding to phosphoinositides, the PH domain-containing molecule localises to the cell membrane (Maffucci and Falasca, 2001). The activation of such molecules may simply be a function of this relocation if, for example, it brings the protein into contact with its substrate. Alternatively, the relocation could bring together the PH domain-containing protein and a membrane-bound activator. A further possibility is that binding the lipid itself induces a conformational change in the effector that leads to its activation. It is clear that these mechanisms can also work in parallel (see section 1.3.2).

PH domains have been found in well over 100 different eukaryotic proteins, yet only a subset of these domains specifically binds to PIP_3. The diversity of proteins containing such domains explains how PI3K signalling can influence so many different processes. These PI3K target proteins include tyrosine kinases of the Tec family, adaptor molecules such as Gab1, phospholipase Cγ, and guanine nucleotide exchange

factors and GTPase-activating proteins for Arf (centaurin α) or Ras (e.g. GAP) (Vanhaesebroeck et al., 2001). I will focus, in particular, on the activation of one PI3K effector, protein kinase B/Akt. A large number of studies have indicated that this molecule mediates many of the events downstream of the PI3K lipid products (Alessi and Downes, 1998).

1.2.2.1 The function of protein kinase B/Akt.

Protein kinase B (PKB)/Akt is a serine/threonine protein kinase that belongs to the AGC family of kinases. It is also the cellular homolog of the oncogenic viral protein v-Akt. Mammals have three closely related *pkb/ akt* genes encoding the isoforms PKBα/Akt1, PKBβ/Akt2 and PKBγ/Akt3. Each of the proteins is around 57kDa in size and contains an N-terminal PIP_3-binding PH domain (see figure 1.3).

The consensus site for Akt phosphorylation is RXRXXS/T, where X represents any amino acid (Obata et al., 2000). This sequence is contained in many proteins and Akt is able to phosphorylate a large proportion of these *in vitro* (Lawlor and Alessi, 2001). To identify the *in vivo* targets of Akt is difficult and some molecules may have been falsely credited as being biologically relevant Akt targets. This is because many studies have used the ectopic over-expression of constitutively active or dominant negative Akt as a means by which to investigate this issue, and these experiments are prone to artefact (Lawlor and Alessi, 2001). For instance, other AGC kinases share similar substrate specificity to Akt, so ectopic expression of Akt may result in its non-physiological phosphorylation of or interaction with substrates that are normally regulated by other kinases. For example, high levels of dominant negative Akt in the cell may sequester a substrate away from another kinase and prevent it from being phosphorylated by this kinase. This observation could lead to the false hypothesis that Akt is the substrate's physiological kinase.

However, despite these problems, some proteins have been shown to be targeted by Akt in multiple ways, and are therefore highly likely to be biologically relevant Akt targets. These include the pro-apoptotic Bcl-2 family member, Bad, which is inhibited by phosphorylation, thereby promoting cell survival (Blume-Jensen et al., 1998; Datta et al., 1997). The Forkhead family of transcription factors, which control of cell cycle progression, are also phosphorylated and inhibited by Akt (Burgering and Medema, 2003). Furthermore, Akt promotes the increase of glycogen synthesis, via the phosphorylation and inhibition of Glycogen synthase kinase 3β (Cross et al., 1995).

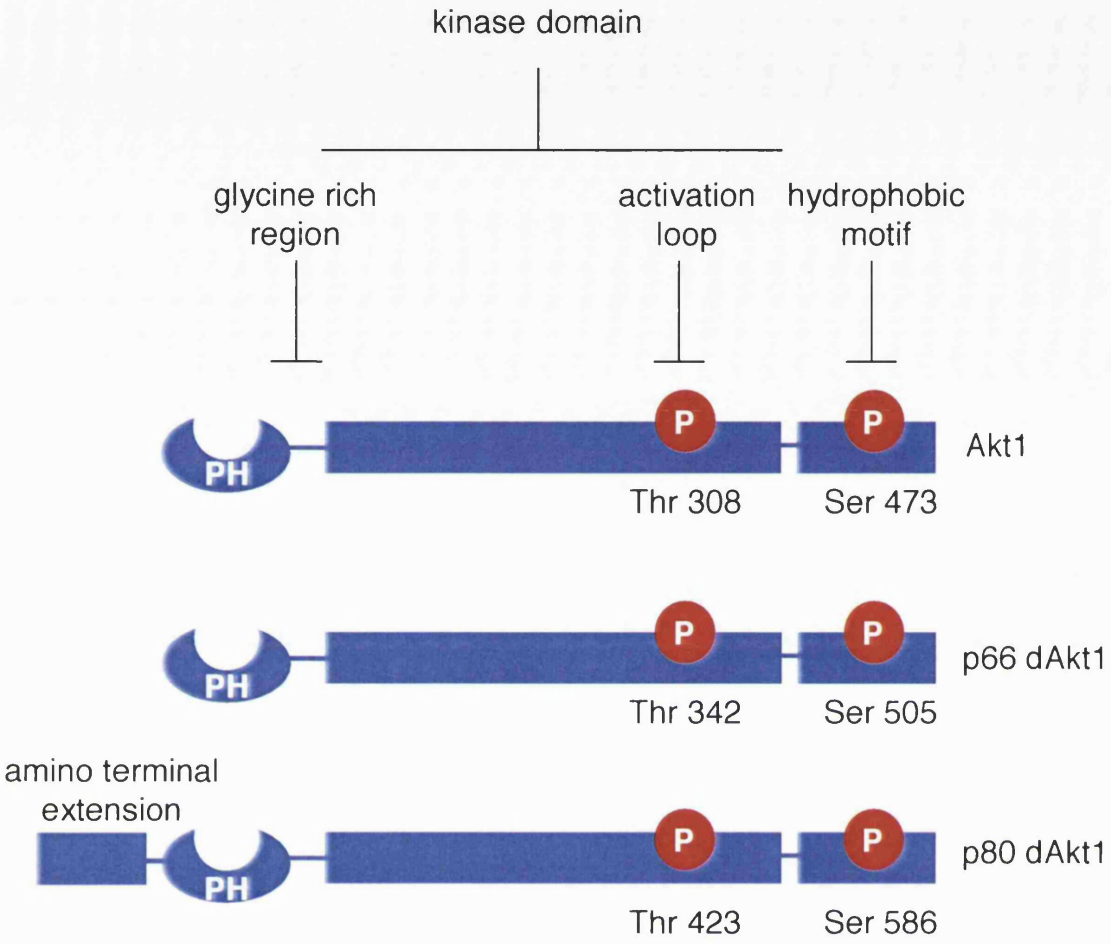

Figure 1.3 Mammalian and *Drosophila* Akt

A schematic comparison of the major domains and phosphorylation sites in mammalian Akt1 and *Drosophila* Akt. Note that *Drosophila* cells express two Akt isoforms generated through the use of alternative translation initiator codons. This results in the expression of a 66kDa isoform and a longer 80kDa variant. The latter possesses an additional amino-terminal extension that is rich in serine, threonine and proline residues.

1.2.2.2 Activation of Akt

Experiments showing that ligand stimulated Akt activation is inhibited if cells are pre-treated with wortmannin or other PI3K inhibitors indicate that Akt is activated downstream of PI3K activation (Alessi et al., 1996). The overall activation mechanism of Akt is complex and not completely understood. However, it is known to involve a combination of allosteric regulation by PIP_3 binding and regulation via phosphorylation by one or more activating kinase (Vanhaesebroeck and Alessi, 2000). The activation of Akt1 by insulin and growth factors is accompanied by its phosphorylation on threonine 308 in the activation loop of the kinase domain and on serine 473 in the so-called C-terminal hydrophobic motif of the kinase (see figure 1.4). For maximal activation of Akt1, both these residues must be phosphorylated (Alessi et al., 1996).

A common characteristic of AGC kinases is that under basal conditions the activation loop acts to inhibit kinase function, yet upon phosphorylation the structure of the loop is modified to allow ATP and the kinase substrate to access the catalytic site. The kinase that phosphorylates Akt1 on threonine 308 and Akt2 and Akt3 on the equivalent residues is phosphoinositide-dependent kinase 1 (PDK1). This kinase is so named as the ability of the kinase to phosphorylate Akt at this residue *in vitro* is absolutely dependent on the inclusion of $PI(3,4)P_2$ or PIP_3 in the reaction mixture (Alessi et al., 1997b). Further experiments have shown that in fact PDK1 does have kinase activity in the absence of phosphoinositides but its ability to phosphorylate Akt is enhanced by the presence of these lipids.

PDK1 is a ubiquitously expressed 63kDa protein containing a PH domain and a consensus kinase domain (Alessi et al., 1997a). Unlike Akt, PDK1 appears to be constitutively active (Alessi et al., 1997b). The PH domain of PDK1 binds to 3-phosphoinositides with a higher affinity than Akt (Dowler et al., 1999; Stephens et al., 1998) and some studies have shown that it can also bind to $PI(4,5)P_2$ (Currie et al., 1999). This binding-affinity allows PDK1 to be membrane localised by the low levels of PIP_3 that are present in resting cells. PDK1 is also present in the cytoplasm, and excluded from the nucleus of resting cells (Anderson et al., 1998; Currie et al., 1999). The localisation of PDK1 has been observed in resting and growth factor stimulated cells. Although some experiments showed that the membrane concentration of PDK1 did increase after treatment with IGF1 (Anderson et al., 1998) , another group used the more sensitive method of immunoelectron microscopy and found that insulin stimulation did not alter PDK1 localisation in HEK293 cells (Currie et al., 1999). If this

latter experiment can be believed, additional factors must be involved in regulating PDK1 membrane localisation. If the PDK1-PH domain were the only factor, the increase in PIP_3 concentration downstream of insulin-stimulated PI3K activity would increase the PDK1 concentration at the membrane (Currie et al., 1999).

If the localisation or activity of its activating kinase does not alter, how does growth factor stimulation lead to the observed increase in Akt activity? The answer could well be that PI3K activation modifies the proximity and responsiveness of Akt to PDK1. Upon PI3K activation Akt translocates to the plasma membrane by binding the generated PIP_3. (Andjelkovic et al., 1997). This translocation increases the local concentration of PDK1 near Akt, thereby increasing the likelihood of threonine 308 phosphorylation. This theory is supported by experiments which show that mutations in the PH domain that abrogate phosphoinositide binding, inhibit the phosphorylation of Akt by PDK1 (Franke et al., 1995; Stokoe et al., 1997). However, two experiments suggest that the PH domain of Akt has a further function. If the PH domain of Akt is removed completely, the resulting deletion mutant can be phosphorylated by PDK1 in the absence of PIP_3 (Stokoe et al., 1997). Furthermore, PIP_3 is still needed to activate Akt if a truncated PDK1 that lacks a PH domain is used in the *in vitro* kinase assay (Stephens et al., 1998). These two experiments suggest that the PH domain acts to mask the threonine 308 site from cytosolic PDK1, thereby inhibiting the phosphorylation event. Phosphoinositide binding removes this inhibition, perhaps by inducing a conformational change in dAkt that reveals this site.

Together then, the mechanism proposed for activation of Akt is as follows (see figure 1.4): PDK1 resides in a constitutively active form both in the cytosol and at the plasma membrane, and its activity is enhanced when it is bound to phosphoinositide lipids. Akt resides in an inactive state in the cytosol, allosterically inhibited by the conformation of its own PH domain. When activated, PI3K generates increased levels of membrane PIP_3 and $PI(3,4)P_2$, which induce the membrane localisation of Akt via 3-phosphoinositide-PH-domain interactions. These interactions unmask the threonine 308 site in the Akt activation loop, which can then be phosphorylated by membrane-bound PDK1. As mentioned before, for its full activation Akt also needs to be phosphorylated on a serine residue in its hydrophobic tail by a kinase referred to as PDK2. After these two phosphorylation events, Akt is thought to detach itself from the membrane and either remain in the cytosol or translocate to the nucleus, via an

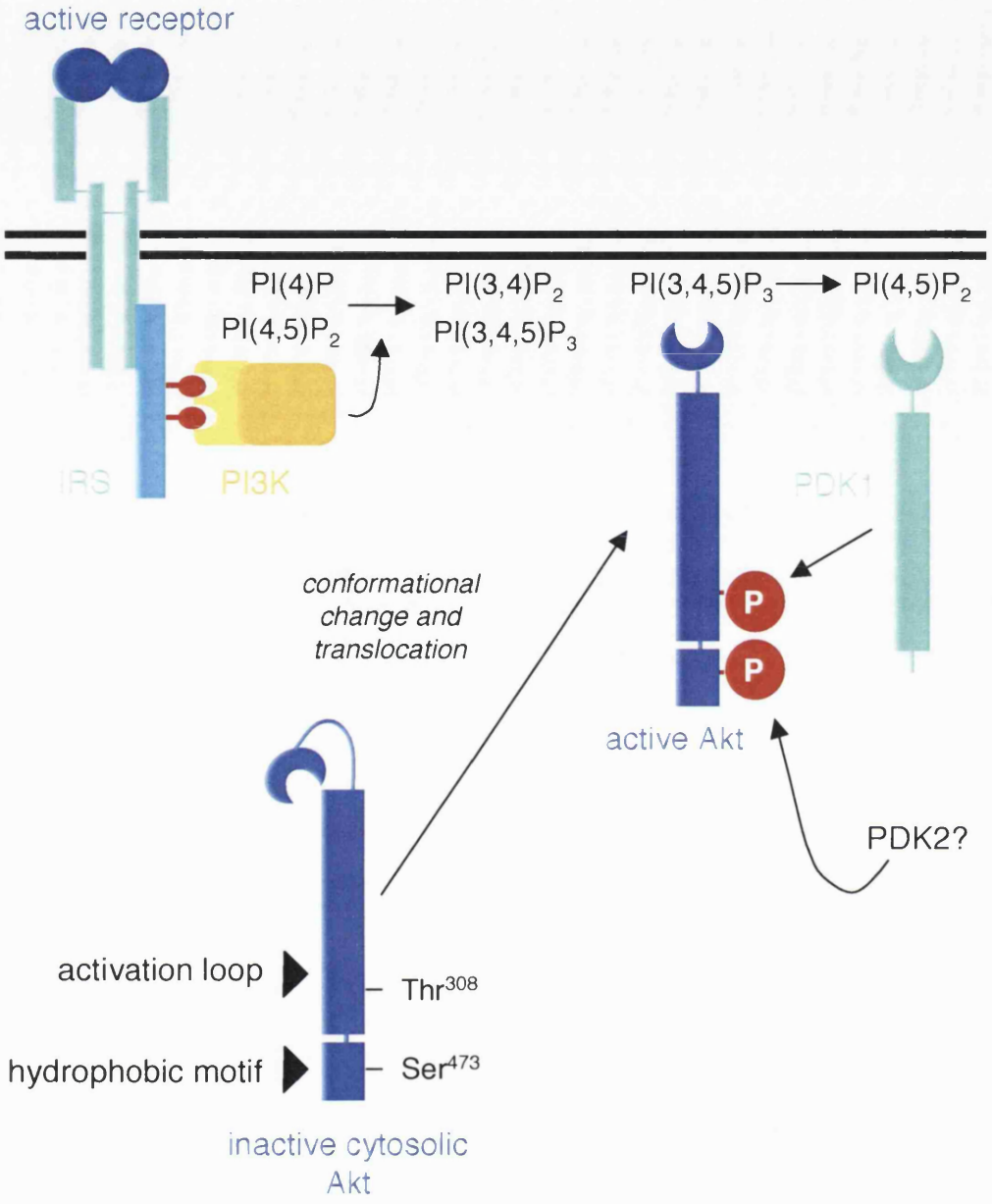

Figure 1.4 The activation of Akt

A diagram showing how Akt becomes activated downstream of active PI3K. Briefly, the activation of dAkt requires both allosteric activation by PIP_3 binding, and dual phosphorylation by one or more serine/threonine kinase. For further details, see the main text.

unknown mechanism, where it activates its downstream effectors (Andjelkovic et al., 1997).

There has been much debate about the identity of PDK2, and although several candidates have been proposed, the identity of PDK2 has not been definitively established. Immunoprecipitates of Integrin-linked kinase (ILK) have been shown to phosphorylate Akt on serine 473 *in vitro* (Delcommenne et al., 1998). However, ILK lacks some of the key amino acids that are conserved across protein kinases making its ability to phosphorylate Akt somewhat controversial. More recently, other experiments showed that ILK immunoprecipitates do not possess significant protein kinase activity towards multiple substrates including Akt itself (Lynch et al., 1999). Instead ILK seems to act indirectly to promote Akt phosphorylation.

An alternative hypothesis is that PDK1 itself possesses PDK2 activity when it is associated with a C-terminal fragment of another kinase, protein kinase C-related kinase 2 (PRK2) (Balendran et al., 1999). This peptide fragment is known as the PDK1 interacting fragment or PIF-tide. However, the PIF binding pocket on PDK1 has been identified and it has been shown that disrupting this pocket does not abrogate the phosphorylation of the Akt hydrophobic tail (Biondi et al., 2001).

Yet another theory is that Akt autophosphorylates on serine 473 (Toker and Newton, 2000). These researchers suggest that Akt kinase activity and phosphorylation of the activation loop site are necessary for serine 473 phosphorylation. Importantly, phosphorylation of Akt at serine 473 still occurs in cells that lack the *pdk1* gene (Williams et al., 2000). This strongly suggests that neither Akt activation nor PIF-bound PDK1 is required for phosphorylation of Akt on the PDK2 site.

1.2.2.3 Down regulation of Akt

Akt is dephosphorylated by protein phosphatase 2A (PP2A) *in vitro*. That this kinase plays the same role *in vivo* is supported by evidence that Akt activity is stimulated in cells treated with okadaic acid, a toxin that originates from marine sponges and inhibits PP2A (Andjelkovic et al., 1996).

1.2.2.4 p70 S6 kinase

Akt is not the only substrate of PDK1. This kinase phosphorylates a number of other AGC kinase family members on homologous activation loop residues. These include p70 S6 kinase (S6K), which is phosphorylated by PDK1 on threonine 229 (Pullen et al., 1998; Toker and Newton, 2000). This phosphorylation event requires the

priming phosphorylation of several S6K residues including threonine 389 (Dennis et al., 1996; Park et al., 2002). Threonine 389 phosphorylation is sensitive to both the PI3K inhibitor, wortmannin, and rapamycin, a specific inhibitor of the TOR protein kinase (Dennis et al., 1996). Indeed, TOR is thought to play a central role in mediating S6K activity in the presence of amino acids (Dufner and Thomas, 1999). Once activated, S6K phosphorylates the 40S ribosomal S6 protein, thereby promoting the translation of a subset of mRNAs that have oligopyrimidine tracts at their 5′ transcriptional start site (Jefferies et al., 1997; Jefferies et al., 1994). This subset includes many transcripts that encode ribosomal proteins and other components of the translational machinery. S6K activation thus leads to an increase in the translational activity of the cell (Dufner and Thomas, 1999).

1.2.3 The Drosophila *insulin/PI3K pathway*

Various genetic and biochemical studies in *Drosophila melanogaster* have established the existence of an insulin/PI3K signalling pathway that plays an essential role in the control of cell, organ and organismal growth (see section 1.3.4; (Garofalo, 2002). Both the structure of the molecules on the pathway and their relationships to one another are similar in fruit flies and mammals (see figure 1.5).

A bioinformatic-based approach was taken to search the *Drosophila* genome for insulin or insulin-like growth factor (IGF) homologs and seven such genes were identified (Brogiolo et al., 2001). These ligands, named DILP1-7 (for *Drosophila* insulin-like peptide), are most homologous to mammalian insulin in structure. Like insulin, the DILPs are predicted to be translated as pro-hormones, which need to be cleaved in two places to remove an internal peptide fragment known as the C-peptide. The two remaining fragments, the A and B chains, dimerise via disulphide bonds, to generate the active hormone. *In situ* experiments have shown that the different DILPs have distinct expression patterns. For example, DILPs 2, 3 and 5 are all expressed in a set of seven median neurosecretory cells (m-NSCs) in the fly brain (Brogiolo et al., 2001; Ikeya et al., 2002; Rulifson et al., 2002). Visualisation of the projections from the m-NSCs by expressing GFP downstream of the *dilp2* promoter showed that they terminate on the surface of the heart and the corpora cardiaca compartment of the ring gland (Ikeya et al., 2002; Rulifson et al., 2002). It is thought that these sites are the ligands' main entry points into the freely circulating larval hemolymph, the insect equivalent of blood.

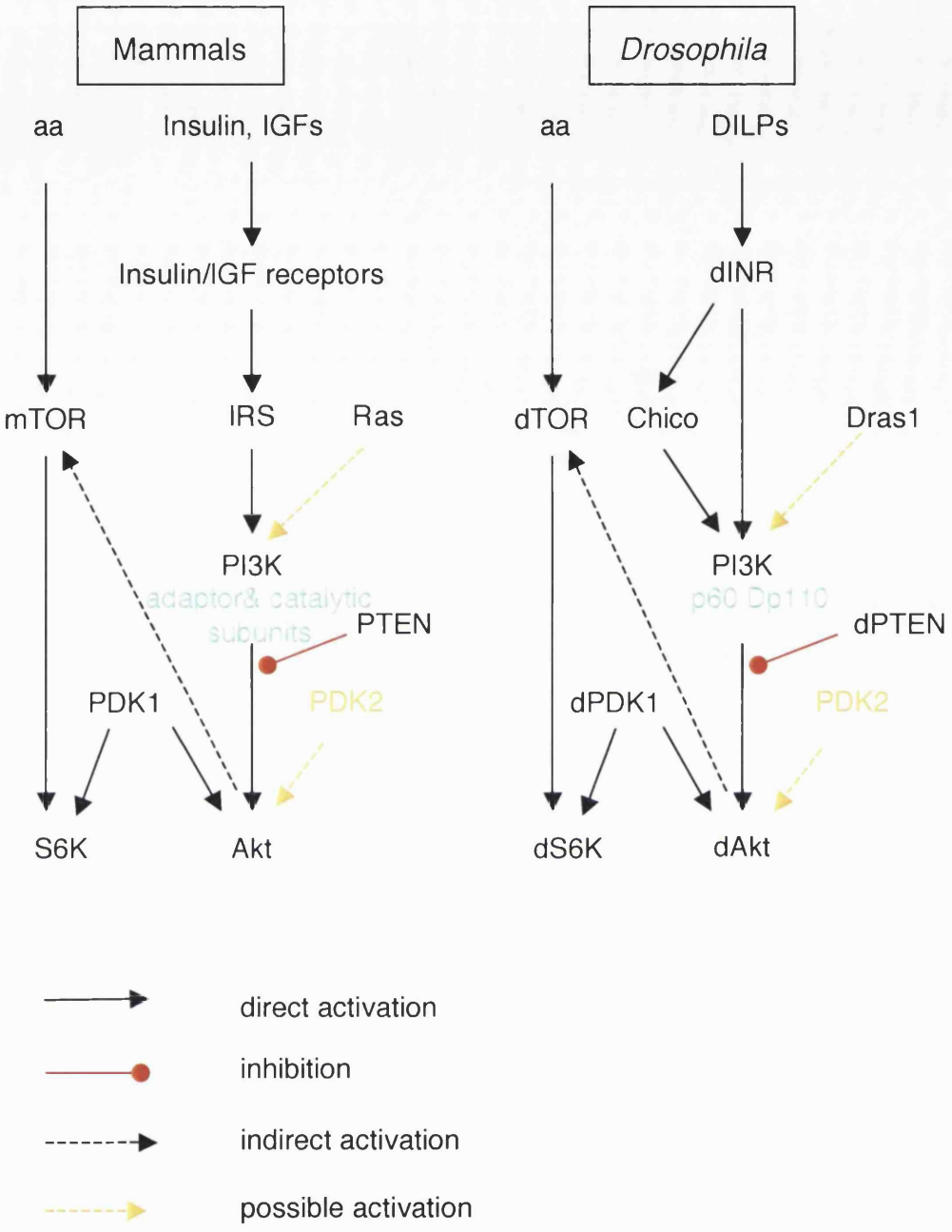

Figure 1.5 Mammalian and *Drosophila* insulin/PI3K signalling pathways

Diagrams showing the intermolecular links of the mammalian and *Drosophila* insulin/PI3K pathways. These pathways are described in detail in the text.

The DILPs signal via tetrameric transmembrane receptors that consist of two extracellular α chains and two transmembrane β-chains, connected to one another via disulphide bonds (Brogiolo et al., 2001; Fernandez et al., 1995; Yenush et al., 1996). The β-chains of the *Drosophila* insulin receptor (dINR), like their mammalian counterparts, contain intracellular tyrosine kinase domains, and undergo activating autophosphorylation on tyrosine residues within their activation loop upon ligand stimulation (Brogiolo et al., 2001; Fernandez et al., 1995; Yenush et al., 1996). However, they also have an additional C-terminal extension that is not present in the mammalian homologs, and that is sometimes cleaved in *Drosophila* cells (Fernandez et al., 1995; Yenush et al., 1996). This extension contains three tyrosine residues in YXXM motifs, which when phosphorylated fit the consensus binding sites for the adaptor subunit of *Drosophila* PI3K (p60), and an additional putative binding site for the Ras/MAPK pathway adaptor protein, Drk. These observations suggest that unlike the mammalian receptors, dINR can signal independently of an IRS protein.

Despite this, *Drosophila* possess an insulin receptor subunit homolog known as Chico. Chico is an adaptor protein containing multiple tyrosine phosphorylation sites, which become docking sites both for p60 and other downstream effectors of insulin signalling, when phosphorylated. In addition it contains a PH domain and a phosphotyrosine-binding (PTB) domain (Bohni et al., 1999). The latter is used to bind to the activated receptor, after which Chico is phosphorylated by the RTK. The phenotypes of flies that are null for *chico* are weaker than those that result from the mutation of other pathway members, suggesting that only a fraction of insulin signalling is mediated via this subunit (Bohni et al., 1999), see section 1.3.4).

As was discussed in section 1.2.1, *Drosophila* have one Class IA PI3K, which consists of the adaptor, p60 and the catalytic subunit, Dp110. The *Drosophila* PI3K is thought to be regulated in an analogous way to its mammalian homolog. Thus, the binding of p60 to the phosphorylated dINR or Chico brings the constitutively bound p110 to the membrane, where it can phosphorylate membrane localised phosphoinositides (Oldham et al., 2002). The resulting increase in membrane PIP_3 concentration is antagonised by the fly homolog of the lipid phosphatase PTEN, termed DPTEN (Gao et al., 2000; Goberdhan et al., 1999; Oldham et al., 2002; Smith et al., 1999).

As in mammalian systems, PIP_3 acts as a signal transduction intermediate, and increased PIP_3 levels lead to the activation of the *Drosophila* Akt homolog, dAkt

(Scanga et al., 2000; Verdu et al., 1999). This activation is dependent on phosphorylation of dAkt by dPDK1 (Cho et al., 2001), and by an unidentified serine/threonine kinase, dPDK2. It is of interest to note that two isoforms of dAkt are produced from the same transcript, owing to the presence of a weak alternative transcriptional start site, upstream of the major initiator sequence. The larger p80 isoform, which contains an N-terminal extension that bears no homology to any known sequence, is present at approximately one sixth of the concentration of the shorter p66 isoform (Andjelkovic et al., 1995).

The *Drosophila* homolog of S6K, dS6K, is activated by platelet derived growth factor (PDGF) in a wortmannin and rapamycin sensitive manner when transfected into mammalian COS or NIH3T3 cells (Watson et al., 1996). Furthermore the insulin stimulation of fly cells also leads to increased S6K activity (Radimerski et al., 2002a). Together these data suggest that, like its mammalian counterpart, the activation of dS6K is dependent both on PI3K and *Drosophila* TOR (dTOR) activity. However, more recent data has controversially indicated that although dS6K activity in flies is dependent on dPDK1 function, it does not require PI3K activation (Radimerski et al., 2002b). As these observations are in direct contrast to previous observations made in mammalian cells, it is hard to know how to interpret them. The control of dTOR activity and the downstream targets of dAkt and dS6K will be discussed later, in sections 1.3.5, 1.3.6 and 1.3.8.

1.3 The regulation of growth during development

The final size of an animal is determined by many factors. Most obviously, final size is a product of an organism's rate of growth, where growth is synonymous with mass increase, and the duration of its growth period (Stern and Emlen, 1999). Observations of animal sizes reveal that animals of the same species grow to very similar though not identical sizes, containing organs whose relative size is tightly regulated. This observation suggests that genetic factors play a major role in determining size. Environmental factors, such as nutritional levels, can also affect growth and final size, and these must be carefully integrated with the genetic growth control mechanisms.

Other observations of growth in different experimental situations have led to the idea that the growth of a specific tissue is subject to intrinsic and extrinsic controls. The intrinsic control mechanisms somehow allow developing organs to "know" what size

they are supposed to be and to stop growing accordingly. The mammalian liver provides a good example of this process. Liver cells are able to grow and divide throughout life, unlike many mammalian somatic cells. If two thirds of a rat liver is surgically removed, the remaining cells will activate the cell cycle and begin to grow and divide to regenerate the lost liver cells. This will only continue until the liver has reached its original size (Michalopoulos and DeFrances, 1997). The mechanisms through which growth could be intrinsically controlled will be discussed in more detail in sections 1.3.2 and 1.3.3.

Extrinsic signals include hormones that are secreted by specific organs in response to a variety of signals, such as total developmental time or nutritional levels, which act at a distance to modulate organ growth. These hormones could inhibit or promote tissue growth or control the development of the whole organism, for example by instructing the organism that it is time to move on to the next stage of its life cycle (Stern and Emlen, 1999). In *Drosophila* the insulin/PI3K signalling pathway and the pathway downstream of dTOR have been identified as playing a major role in responding to extrinsic growth promoting signals, thereby autonomously controlling the growth of individual organs (see section 1.3.4 and 1.3.5).

In this section, the imaginal discs of *Drosophila* will be used as a model system through which these issues will be examined more thoroughly.

1.3.1 Imaginal disc development

Drosophila larvae hatch from eggs about 24 hours after the eggs are laid. During larval life the animals' main functions are to eat and grow. As they do this they moult, shedding their cuticle. This occurs twice during larval life. Each stage is called an instar. The *Drosophila* larva has no wings or legs. These, and other organs emerge when the larva undergoes metamorphosis after the third larval instar. Metamorphosis takes place within a pupa, from which the adult fly emerges, between nine and ten days after the original egg was fertilised (for further details see (Lawrence, 1992; Wolpert et al., 1998)

The epithelial structures of an adult fly, such as their wings, eyes, or legs, originate from epithelial cells that are specified during embryonic life. The patterning of the embryo means that even at this early stage when the cells are first specified, they contain information regarding their positional identity. For example cells that express the homeotic gene *engrailed* are destined to generate the posterior compartments of

* The abdominal segments of the adult fly originate from the larval histoblasts. These sets of epidermal cells do not dissociate from the larval epidermis, and contribute to its patterning. They can be distinguished from the larval epidermal cells as they remain diploid throughout their existence.

future organs (Morata and Lawrence, 1975). These specified cells invaginate into the body cavity to form sacs known as imaginal discs. The discs that will go on to make up the wing contain around 40 cells when the first instar larvae hatch. Growth and cell division then occur throughout larval life such that at the end of the third larval instar the number of cells has increased to about 50,000 (Madhavan and Scheiderman, 1977). During this larval growth period (four days at 25°C), the disc is patterned by regulated cell-cell signalling events that are initiated downstream of the patterning information that was established in the embryo (Whittle, 1990). During metamorphosis the discs undergo a dramatic reorganisation to generate the final organs.

The development of the *Drosophila* imaginal discs thus resembles the development of many mammalian or vertebrate organs, in that it involves coordinated growth, cell division, and pattern formation. Scientists have used imaginal disc development in conjunction with the powerful tool of *Drosophila* genetics as a model system in which to study the regulation of tissue and organ growth *in vivo*.

1.3.2 Patterning and the intrinsic control of imaginal disc growth

Numerous observations support the idea that imaginal disc growth is controlled by mechanisms intrinsic to the disc. Firstly, if growing discs are excised from the developing larvae and transferred to a permissive environment, such as the abdomen of an adult female fly, the discs continue to grow. Remarkably, even under these circumstances, growth stops once the disc reaches the size at which it would have stopped growing had it remained inside the larva (Bryant and Simpson, 1984). Secondly, if a developing disc is damaged, metamorphosis is delayed until that disc is repaired. However, in this event the remaining, undamaged discs do not overgrow. Instead, they will stop growing as soon as they have reached an organ-appropriate size (Bryant and Simpson, 1984). Furthermore, the regenerating damaged disc will also stop growing when it reaches the appropriate size (Milan et al., 1997). Thirdly, if one body part is homeotically transformed into another from the beginning of development, for example if a haltere is turned into a wing, the newly specified wing will grow to the same size as a normal wing (Lewis, 1978)

All the above observations imply that individual organs somehow know how big they should be. There are several mechanisms by which this could occur. If we assume that the disc is bathed in growth factors, one possibility is that the growing disc cells produce a secreted factor that acts in a paracrine fashion to inhibit cell growth or cell

division, or to induce cell death. Disc growth would lead to increases in the concentration of this factor and some point in time an equilibrium will be reached when no further growth is possible. This situation would arise either because the local concentrations of the growth inhibitory factor are greater than those of the growth promoting factor, so all cells are inhibited from growing or dividing, or because any further increase in cell number results in an increase in levels of the inducer of cell death, which thus causes an equivalent number of cells to die (Conlon and Raff, 1999).

A second possible mechanism for intrinsic growth control is linked with the patterning of discs, and involves the spatially restricted production of limiting amounts of growth factors or mitogens (Conlon and Raff, 1999; Day and Lawrence, 2000). This can be explained more clearly by using the wing disc as an example. The secreted signalling molecule Dpp is produced in a thin stripe at the anterior-posterior boundary in the centre of the developing wing disc. Dpp protein then spreads from here in a graded fashion towards the edges of the disc. Differential gene transcription is achieved in different parts of the disc, as different genes are have different sensitivities to Dpp. Genes that are more sensitive to Dpp will be transcribed a greater distance from the signalling source than those that are less sensitive (Day and Lawrence, 2000). To determine disc dimensions, such a signal would have to exert a growth promoting effect or act as a cell survival factor. Cells that are further away from the signal source would receive less signal and either growth of these distant cells would arrest or, if growth did take place, the resulting cells will not survive in the absence of the growth factor, thus limiting the size of the organ (Day and Lawrence, 2000). From this model then we would predict that cell proliferation occurs at a higher rate in the centre of the disc. This is not observed. Rather, cell proliferation occurs uniformly across the disc (Gonzalez-Gaitan et al., 1994).

A third model to explain why growth ceases when tissues reach an appropriate size has been proposed based on the evidence from regeneration experiments in the cockroach. These experiments showed that if a cockroach leg was amputated at a proximal position and a distal leg fragment was then reattached to the proximal fragment, the leg would re-grow to its original length (French et al., 1976). The model presupposes that cells have a positional identity, and that this identity can be recognised by its neighbours. If the cells identify that they are not supposed to be next to one another, they initiate growth and cell division to regenerate, or intercalate, the tissue that should be between them (for a review see (Wolpert et al., 1998). One possible

mechanism by which this is achieved requires that the cells can monitor the slope of a morphogen gradient and that there is a target value for this slope at which growth ceases. Although this is an attractive model, its relevance to disc growth is unclear. Furthermore, if Dpp were the growth promoting morphogen, the ectopic expression of Dpp throughout the disc would be predicted to prevent disc growth, as the morphogen gradient would effectively be zero. This is not the observed outcome. Rather growth under these conditions is greatly enhanced along the anterior-posterior axis (Nellen et al., 1996).

1.3.3 Monitoring final organ size – cell size or cell number?

The models proposed above are thought to monitor organ size primarily by measuring the distance between two points. I have not however considered the alternative possibility that the number of cell divisions is the monitored parameter. Tissue growth is a product of cell size and cell number (this itself being a function of cell division and cell death). As such, by counting the number of cell divisions the resulting organ size would be fixed, as long as cell size and the rate of cell death were known constants. In reality, a number of experiments have excluded such a mechanism from consideration.

Increasing the chromosomal content of cells increases the size of those cells in a proportional manner. For example, tetraploid cells, which contain four sets of each chromosome, are twice as big as diploid cells, which contain only two sets. If the size of salamanders, composed of these tetraploid cells or the normal diploid cells are compared, both salamanders are approximately the same size. Thus the organs of the tetraploid salamander must contain around half the number of the larger cells (Fankhauser, 1952). Similarly, in natural *Drosophila* populations, cell size and cell number tend to show negative covariance. That is, wings made from larger cells contain fewer cells, and wings made from smaller cells contain a greater number of cells. Through this relationship wing size remains constant (McCabe et al., 1997).

Negative covariance was also observed in wing discs when cell cycle regulators were expressed in clones of cells. In this situation, compensatory mechanisms should be pushed to the limits. The *Drosophila* E2F transcription factor increases the rate of cell division by stimulating the production of the G1 cyclin, Cyclin E, and increasing the production of the *Drosophila* cdc25 homolog, String, thereby promoting G2 to M progression (Neufeld et al., 1998). Over-expression of dE2F in clones thus leads to the

increased proliferation of cells in those clones. However, this increase in cell number is not accompanied by an increase in clone size. Rather, the size of the constituent cells is reduced so that the resulting clone is equivalent in size to neutral clones induced at the same time point (Neufeld et al., 1998). These are known as sister clones.

Katrin Weigmann and colleagues made similar observations when they increased the levels of the mitotic cyclin dependent kinase, Cdc2, in wing-disc clones (Weigmann et al., 1997). If the cell cycle is blocked, by over-expression of the dE2F inhibitor, dRBF (the *Drosophila* homolog of the tumour suppressor, retinoblastoma), the resulting reduction in cell division rate reduces the final number of cells in the wing disc clone. However those cells are still able to grow, and as division is blocked the cells reach a larger size than cells outside the clone. As before, mutant and sister clone reach equivalent sizes. It is important to note that if dRBF expressing clones are made very early on in disc development a small difference in size between mutant clone and sister clone can be seen. This could well be because, although cell growth can continue in the absence of division, at some point the amount of DNA in the clone cells becomes growth limiting (Neufeld et al., 1998).

These observations therefore support the models of intrinsic growth regulation that have already been presented in section 1.3.2, where growth is determined by the dimensions of an organ rather than by the number of its constituent cells. In addition, they show that in order to increase tissue growth the size and number of the constituent cells must be increased co-ordinately.

1.3.4 Insulin signalling and the control of growth by hormones

Although, as discussed, the size of imaginal discs is remarkably resistant to perturbation, there are situations in which disc size can alter. For example, if developing larvae are malnourished, the resulting flies will be smaller than those raised with plentiful food (see section 3.6). This is caused by a reduction in the size of the imaginal discs from which the adult is generated. Another experiment has shown that by removing the hind wing imaginal discs from a caterpillar larva, the resulting butterfly develops abnormally large forewings and forelegs (Nijhout and Emlen, 1998). This result too is likely to be caused through altering the size of the relevant precursor imaginal discs.

Both these observations are consistent with the existence of regulators of disc growth extrinsic to the disc itself. The first example could be interpreted in two ways.

Firstly, imaginal disc cells could respond directly to nutrients (for further details see section 1.3.5). Secondly, nutrition could regulate the production of a growth factor that acts at a distance (for further details see sections 3.1 and 3.12). The second example indicates that imaginal discs compete for limiting amounts of an extrinsic signal. Removing one competing disc allows the remaining discs to grow more, presumably because they receive increased levels of this signal. An alternative explanation of this second result is that discs produce a growth inhibitory signal that acts on neighbouring disc structures, and this growth repression is removed alongside the disc. As the structures that are most influenced by the removal of one disc are those that were closest to that disc before it was removed, it is likely that such a signal would act in a local rather than a humoral manner.

Extrinsic regulators of disc growth are likely to function by modulating the activity of signalling pathways within the disc leading to alterations in disc growth. The extrinsic and intrinsic controls on disc growth must be carefully co-ordinated. Although the extrinsic regulators can modify growth, the disc-intrinsic controls, which provide the disc with the "knowledge" of how big it should be and determine the organ's shape, cannot be completely overridden. The components of the mechanisms that extrinsic growth signals modulate should be identifiable by the following properties: increasing the concentration of positive signalling components throughout the disc would be expected to increase the size of the disc; whereas reducing the levels of such components would reduce disc size. In neither case would pattern be affected. The intracellular components of the *Drosophila* insulin signalling pathway all display these hallmarks.

The first indication that the *Drosophila* insulin signalling pathway could play a role in growth regulation came from experiments where Dp110 was over expressed in the developing wing disc. The resulting wings were larger than wild type wings, primarily as a result of increased cell size, although in addition cell number was slightly but significantly increased. Inhibiting signalling through the pathway by over expressing a catalytically inactive and therefore dominant negative version of Dp110 reduced final wing size through reducing both cell size and cell number (Leevers et al., 1996). Multiple publications have now established the *Drosophila* insulin signalling pathway as a mechanism through which final organ size can be altered (reviewed in (Garofalo, 2002; Kozma and Thomas, 2002).

Flies that contain null mutations in *chico* or a combination of hypomorphic *dinr, dpdk1 or dAkt* mutant alleles are viable, but small (Bohni et al., 1999; Brogiolo et al., 2001; Rintelen et al., 2001). Ablation of the m-NSCs that produce some of the DILPs can also reduce final fly size (Ikeya et al., 2002; Rulifson et al., 2002). This clearly demonstrates that DILPs can act as humoral signals to influence growth of tissues at a distance. In all cases the size reduction is caused by reductions in cell size and number.

Null mutations in most pathway components lead to embryonic or larval lethality. For example, *Drosophila* lacking *p60* or *dp110* arrest growth as small larvae whose imaginal disc structures are small or missing, respectively (Weinkove et al., 1999). To study the cellular effects of such lethal mutations, clones of mutant cells were made in developing discs and examined either at the end of larval development or in the adult fly. Results of such experiments using various pathway components have confirmed that reducing signalling through the *Drosophila* insulin/PI3K pathway reduces cell size and number in a cell autonomous manner (Brogiolo et al., 2001; Goberdhan et al., 1999; Huang et al., 1999; Weinkove et al., 1999). Increasing signalling through the pathway invariably increases clone size, which is consistently accompanied by cell autonomous increases in cell size (Goberdhan et al., 1999; Verdu et al., 1999; Weinkove, 1999). Reports on whether increasing insulin/PI3K signalling is sufficient to increase cell number vary. An interesting observation is that activation of components further up the pathway such as the receptor can increase cell number (Brogiolo et al., 2001), whereas activation of components further downstream in the pathway cannot (Verdu et al., 1999). This difference could explain the variability of the phenotypes seen, as the upstream pathway components may be additionally activating parallel pathways that stimulate cell division. Alternatively, it may simply reflect the fact that these upstream molecules are more effective as growth drivers.

A further interesting observation is that the growth response to *Drosophila* insulin/PI3K signalling is graded. By generating flies with heads that had different capacities for PIP_3 generation, Sean Oldham and colleagues showed that the size of the fly head correlated with the ability of the constituent cells to produce PIP_3 (Oldham et al., 2002). These data are consistent with cells reading the level of insulin/PI3K signalling and responding appropriately by enhancing or restricting their growth and division rates.

The *Drosophila* insulin/PI3K signalling pathway has thus been identified as a pathway intrinsic to the disc, that is capable of responding to externally produced

signals and modulating the growth of the disc in a cell- and disc-autonomous manner. However, as yet the regulators of DILP production have not been discussed, and these are clearly of great importance, being the ultimate controllers of growth via this signalling pathway. In mammals the production and secretion of insulin is activated primarily in response to high blood glucose concentrations. It is therefore tempting to hypothesise that the carbohydrate levels in the *Drosophila* larval hemolymph are able to influence DILP release from the m-NSCs. The nutritional regulation of signalling downstream of PI3K in *Drosophila* will be discussed at greater length in chapter 3.

One last issue to consider is that *dilp2* RNA is expressed in imaginal discs (Brogiolo et al., 2001). From this, it could be inferred that although the insulin/PI3K signalling pathway can modulate disc growth downstream of externally produced DILPs, which may be regulated by environmental factors such as nutritional levels, it could also be activated by ligands acting in a paracrine fashion. As such, the insulin/PI3K signalling pathway could be controlled via the intrinsic growth regulatory mechanisms, for example patterning cues could influence the production of DILP2 in order to influence growth. Although this hypothesis is attractive, *dilp2* RNA appears to be produced uniformly across the disc (Brogiolo et al., 2001).

1.3.5 TOR and the regulation of growth by amino acids

So far, the discussion of the nutritional control of growth has been limited to the predicted regulation of DILP production by circulating carbohydrate levels. If this were the only regulatory mechanism in operation, the following observation would be difficult to explain. *Drosophila* larvae raised on diets of 20% sucrose do not grow past the first instar stage (Britton and Edgar, 1998). Under these conditions we would expect that *Drosophila* larvae would have high levels of DILP production, resulting in activation of signalling via dINR and hence growth. The observed result therefore suggests that other nutritional factors, such as amino acids play a role in controlling growth. These could function directly on tissues, they could regulate the release of DILPs, they could alter the responsiveness of cells to DILPs or indeed they could regulate the secretion of another independent, but essential growth factor. At least one of the ways in which amino acids act is directly on tissues to regulate dTOR activity (for a further discussion of the nutritional control of insulin release and growth see section 3.12).

TOR is a member of the subset of phosphoinositide kinases that lack lipid kinase activity but do exhibit serine/threonine protein kinase activity. This family is known as the phosphoinositide kinase-related kinase (PIKK) family. Other members of this group include the DNA dependent protein kinases DNA-PK, ATM and ATR that are involved in DNA repair processes (for a review see (Schmelzle and Hall, 2000). Mammalian TOR is a 250kDa large protein containing N-terminal α-helical HEAT repeats that are involved in protein-protein interactions. It also contains a FAT domain, whose function is unknown, an "FBP domain", which binds to the inhibitory FKBP12-rapamycin complex and, near to the C-terminus, a kinase domain (see figure 1.6, (Schmelzle and Hall, 2000). *Drosophila* TOR (dTOR) has a similar domain structure to mammalian TOR, with the highest level of identity in the kinase and FBP domains (Zhang et al., 2000).

The fungal macrolide, rapamycin, specifically inhibits TOR and has been used extensively by researchers to identify targets of TOR. Importantly two key TOR targets, S6K and 4E-BP1, are also modulated by insulin/PI3K signalling. Hypophosphorylated 4E-BP1 binds and inhibits the translation initiation factor eIF4E. This inhibition is relieved when 4E-BP1 is phosphorylated downstream of growth factor stimulation as hyperphosphorylated 4E-BP1 cannot bind the initiation factor (Lin et al., 1994). Free eIF4E then acts as part of a complex to bring mRNA molecules together with 40S ribosomal subunits, thereby leading to translation initiation (for review see (Gingras et al., 1999). As discussed in section 1.2.2.4, phosphorylation of S6K downstream of TOR activity is necessary for its activation (Dennis et al., 1996). dTOR targets dS6K and d4E-BP in a similar manner to its mammalian homolog. Rapamycin treatment of *Drosophila* S2 cells results in the inhibition of serum-dependent dS6K phosphorylation and insulin-dependent phosphorylation of 4E-BP, yet has no effect on dS6K phosphorylation if cells are additionally transfected with a rapamycin-resistant form of dTOR (Jaeschke et al., 2002; Zhang et al., 2000). It is important to note that these two targets may not be directly downstream of dTOR. A TOR interacting kinase that binds TOR tightly and is therefore present in TOR immunoprecipitates may be responsible. Equally, TOR could also act to down regulate the activity of a bound phosphatase (Barbet et al., 1996; Di Como and Arndt, 1996).

Experiments in yeast indicate that TOR plays a role in mediating responses to changes in amino acid concentrations. If yeast cells are treated with rapamycin the resulting phenotype resembles that of amino acid starvation. Cells arrest growth in

Figure 1.6 Mammalian TOR

A diagram showing the domain structure of mammalian TOR (after Schmelzle and Hall, 2000). The HEAT repeats are involved in protein-protein interactions. Each HEAT motif comprises approximately 40 amino acids that form a pair of anti-parallel helices. The function of the FAT domain is unknown. The FRB domain is a FKBP12-Rapamycin binding domain through which Rapamycin exerts its inhibitory effect on TOR. The extreme C-terminal sequence of TOR has been termed a FATC domain. FATC domains only occur in combination with FAT domains and may be important for the catalytic activity of PIKKs.

early G1, accumulate glycogen, reduce protein synthesis and up regulate the transcription of genes that aid survival on poor nitrogen sources (Cardenas et al., 1999; Schmidt et al., 1998). Results in higher eukaryotic cells demonstrate that this role of TOR is conserved through evolution. For example, transferring Chinese hamster ovary (CHO) cells to amino acid free culture medium leads to the dephosphorylation of 4E-BP1. This dephosphorylation can be reversed by reintroducing amino acids to the medium, but the reversal is blocked if rapamycin is added at the same time (Hara et al., 1998). The way in which amino acid concentrations influence TOR activity is still unknown. One proposed mechanism has uncharged transfer RNAs inhibiting TOR, possibly directly (Iiboshi et al., 1999). This hypothesis is interesting, considering that other members of the PIKK family are already known vary their activity in a nucleic acid dependent manner.

As in yeast, reducing TOR signalling in *Drosophila* generates a phenotype similar to that induced by amino acid starvation. *Drosophila* larvae contain not only the imaginal discs, but also larval tissues such as the fat body or salivary glands that grow via endoreplication, through increases in cell size. When larvae are starved of amino acids these two tissue types respond in different ways. The cells of the endoreplicating tissues stop DNA synthesis, while the imaginal disc cells continue to grow and divide, albeit at a slower rate than in fully fed larvae (Britton and Edgar, 1998). Furthermore, under amino acid starvation conditions, the morphology of the larval fat body alters, with lipid vesicles increasing in size (Britton and Edgar, 1998). Larvae with weak loss of function mutations in *dTOR* grow more slowly than normal. In these mutants, larval imaginal disc tissue still grow but this is at the expense of the endoreplicating tissues, which stop synthesising DNA once the maternal TOR protein has been degraded. Nucleolar size is also reduced, concomitant with a reduction in protein synthesis. In addition, fat body morphology alters in a similar manner is seen to after amino acid starvation (Oldham et al., 2000; Zhang et al., 2000).

In contrast, strong *dTOR* mutants closely resemble insulin/PI3K signalling pathway mutants. This is not particularly surprising as the effectors of dTOR, dS6K and d4E-BP, are also targeted by *Drosophila* Insulin/PI3K signalling. Strong *dTOR* mutant animals arrest growth during larval development, and can survive for up to thirty days without pupating. Clones of $dTOR^{-/-}$ imaginal disc tissue are reduced in size compared with their wild-type twin spot and this is caused by a decrease in cell size and cell number, reminiscent of clones containing mutations in the *Drosophila* insulin/PI3K

pathway. Furthermore, strong *dTOR* mutant clones contain an increased number of cells in G1, and a co-ordinately reduced number of cells in S-phase and G2. If *dTOR*$^{-/-}$ clones are made in the endoreplicating tissue of the salivary gland, the cells within the clone stop synthesising DNA. All these phenotypes are cell autonomous (Oldham et al., 2000; Zhang et al., 2000).

Together these data indicate that dTOR activity can influence growth downstream of dietary amino acid levels in a cell autonomous manner. These effects on growth are at least in part mediated through dS6K and d4E-BP, indicating that there is considerable cross talk between the dTOR and PI3K signalling pathways in *Drosophila*, and hence between the control of growth by carbohydrates and by amino acids. However, the starvation phenotype associated with weak *dTOR* mutations suggests that dTOR has targets independent of the insulin signalling pathway.

1.3.6 Protein synthesis as a mechanism of growth regulation

It seems straightforward to assign much of the ability of the *Drosophila* insulin and TOR signalling pathways to stimulate growth to their ability to promote protein synthesis via activation of dS6K and inactivation of d4E-BP. However, there is a significant problem with this explanation: other mutations that affect translation do not have the same mutant phenotypes as dTOR and *Drosophila* insulin/PI3K pathway mutants.

A class of dominant mutations exist in *Drosophila* that are collectively known as the *Minutes*. Many of these mutations are within ribosomal genes, so would be expected to impair the rate of translation when present (Lambertsson, 1998). *Drosophila* that are homozygous for *Minute* mutations die early in development. Heterozygous animals have a characteristic dominant phenotype, which includes developmental delay during the larval period, and long slender bristles in the adult fly. In contrast to the loss of function mutation of *Drosophila* insulin/PI3K pathway components, the vast majority of *Minute* mutations do not have any effects on final body size. This is probably because the extended developmental time compensates for any reductions in growth rate in *Minute* heterozygotes. Although weak mutations in the *Drosophila* insulin/PI3K signalling pathway do cause some developmental delay, it appears that this delay is not sufficient to compensate for the reduced growth rates induced, and the resulting adult flies are therefore reduced in size.

Likewise the clonal phenotype of *Minute* mutations is not comparable to that of *Drosophila* insulin/PI3K pathway mutations. Although if the whole animal is made up of *Minute* heterozygous cells these cells can survive, slow-growing *Minute* heterozygous cells present in clones that are surrounded by wild type tissue are rapidly eliminated. This effect has been ascribed to a process known as cell competition, where healthy cells can proliferate at the expense of genetically weaker cells (Morata and Ripoll, 1975). This observation can be contrasted with the clonal phenotypes of loss of function mutations in the *Drosophila* insulin/PI3K pathway, in which slow growing mutant clones are able to survive, even if mutations are strong. However the clones are smaller than any wild-type twin spot clones, and consist of small cells (Neufeld et al., 1998).

How can we reconcile the observations that reducing rates of translation doesn't seem to lead to overall changes in disc size but reducing insulin/PI3K signalling does? Also, why do *Minute* heterozygous cells that survive in an entirely mutant animal disappear when they are in competition with wild type cells, whereas heterozygous *Drosophila* insulin/PI3K mutant clones do not disappear in this way? One possibility is that while mutations in the *Minute* genes lead to a reduced rate of global protein synthesis, Dp110-mediated post-translational modifications of dS6K or d4E-BP affect the translation rate of only a subset of RNAs. As I have discussed earlier (in section 1.2.2.4) the phosphorylation of the ribosomal protein S6 by S6K enhances the translation of mRNAs that contain a 5′ terminal oligopyrimidine tract, many of which encode ribosomal proteins or translation elongation factors (Dufner and Thomas, 1999). In addition, different mRNAs display different abilities to compete for binding of the initiation complex that contains eIF4E. So modulating the availability of eIF4E by controlling 4E-BP phosphorylation could also alter the pattern of mRNA translation as opposed to simply altering its rate.

Although this may not be a complete explanation, it is clear that dS6K and eIF4E are able to alter growth of the fruit fly in a manner that is not achieved by mutations in the *Minute* genes. The phenotype of *ds6k* mutant flies has already been described in section 1.3.4. Studies in *Drosophila* examining the effects of d4E-BP1 over-expression, and deIF4E phosphorylation on growth have also recently been carried out, and will be described below.

The *Drosophila* 4E-BP, also known as Thor, was originally characterised as playing a role in the immune response (Bernal and Kimbrell, 2000). Furthermore,

although interactions of d4E-BP with *Drosophila* eIF4E (deIF4E) have been seen in S2 cells, the consensus eIF4E-binding site in d4E-BP is not completely conserved. This raises the question of whether d4E-BP is as important as its mammalian counterpart in translational regulation. The strength of d4E-BP-deIF4E binding could be enhanced by reverting the binding site sequence to the consensus, in a mutant protein known as $4E\text{-}BP^{LL}$ (Miron et al., 2001). Over-expression of this mutant protein led to cell autonomous reductions in cell size. Moreover, over-expression of $4E\text{-}BP^{LL}$ in the eye disc was able to reduce the overgrowth phenotype associated with over-expression of dAkt, and its over-expression in the wing could enhance the size reductions associated with expression of dominant negative Dp110 (Miron et al., 2001).

As expression of wild-type d4E-BP had none of the above effects, these results alone do not demonstrate that d4E-BP normally plays a role in *Drosophila* growth regulation. However, the data does clearly point to such a role for the initiation factor, deIF4E in imaginal disc growth regulation, and this is corroborated by the observation that homozygous *deIF4E* mutants arrest growth during larval development. Mammalian eIF4E is phosphorylated in response to growth factors, on serine 209. The homologous residue in deIF4E is serine 251. Flies whose *deIF4E* gene is mutated so that it encodes a non-phosphorylatable protein, in which serine 251 is mutated to alanine, have a reduced viability. Any escapers are small, but remain appropriately proportioned. It is interesting to note that, in contrast to *ds6K* mutants, where only cell size is affected, both the size and the number of cells in $deIF4E^{S251A}$ flies are affected.

Although the differences in patterns of translation caused by *Minute* mutations, and mutations in the *Drosophila* insulin/PI3K pathway may cause the differences in observed phenotype, an alternative explanation is possible: Insulin/PI3K signalling may affect more than just translation rates. For example, other biosynthetic pathways may be modulated by the levels of insulin/PI3K signalling present in a cell.

1.3.7 Cyclin E and the translational control of the cell cycle

As was discussed in section 1.3.5, disc cells that are homozygous for strong *dTOR* mutations have an altered cell cycle profile, with a larger G1 population than heterozygous cells from the same imaginal discs (Zhang et al., 2000). A similar observation has been made in cells that over express a truncated from of p60, Δp60, which cannot bind to Dp110 (Weinkove et al., 1999). Δp60 is thought to act as a dominant negative protein, by competing with Dp110-bound p60 and hence reducing

insulin/PI3K signalling in cells where it is expressed (Weinkove et al., 1999). Conversely, cells from clones that are null for *dpten* or that that over express Dp110 have an increased G2 population and a reduced G1 population (Weinkove et al., 1999; Zhang et al., 2000). In contrast, the cell cycle distribution of *ds6k* and *chico* null cells is no different from wild type, though this phenotype may reflect the fact that neither dS6K nor Chico is an essential component of *Drosophila* insulin/PI3K signalling. Together these observations suggest that *Drosophila* insulin/PI3K and TOR signalling can promote the G1 to S transition.

These data raise the question of how growth promoters such as Dp110 or dTOR can regulate the cell cycle. In yeast, the G1 cyclin Cln3p is regulated at the translational level. This is achieved as the *cln3* transcript has a long 5´ untranslated region that contains many short open reading frames (ORFs), which reduce access to the start codon on the *cln3* message (Polymenis and Schmidt, 1997). Increasing translational rates are thus hypothesised to increase 'leaky' scanning of these ORFs, thereby allowing more translation from the *cln3* start codon to occur (Coelho and Leevers, 2000). In flies, the homologous G1 cyclin, Cyclin E, is the prime candidate for a translation-dependent cell cycle regulator. Cyclin E associates with and activates the cyclin-dependent kinase cdk2, leading to entry into S phase. As with *cln3,* the mRNA of *Drosophila cyclin E* contains untranslated ORFs at its 5´ terminus (Richardson et al., 1993), suggesting that a similar mechanism could be at work in *Drosophila* cells and yeast. Further to this, although there is no direct evidence that insulin/PI3K signalling increases Cyclin E levels in *Drosophila*, over-expression of other growth regulators including Dras1 and dMyc (see section 1.3.9) does increase the amount of Cyclin E protein in imaginal disc clones (Prober and Edgar, 2000). Moreover, the levels of *Drosophila* Cyclin E expression were reduced by about 30% on immunoblots of *dTOR* null larvae compared with wild type larvae of the same size, and ectopically expressing Cyclin E can bypass the cell cycle arrest seen in these mutants (Zhang et al., 2000).

1.3.8 TOR and insulin signalling: two halves of the same pathway?

As the TOR and insulin/PI3K signalling pathways converge on the two effectors S6K and 4E-BP1, it makes sense to question at which point this convergence occurs. Is it only at the level of these effectors, or does insulin/PI3K signalling feed in higher up the pathways, at the level of TOR for example? Early work showed that mammalian TOR was phosphorylated on serine 2448 in an Akt dependent manner *in vitro* (Nave et

al., 1999). However mutation of this site to a non-phosphorylatable alanine does not inhibit TOR activity, calling into question the relevance of these phosphorylation events *in vivo* (Sekulic et al., 2000). Regardless of this, the activity of TOR in immunoprecipitates from cells that over express Akt is increased compared to those from untransfected cells (Scott et al., 1998). Recent work in *Drosophila* has confirmed that dTOR is activated in a dAkt dependent manner, and has clarified the mechanism of this activation. It seems that, unlike the previous biochemical work suggested, dAkt does not act directly on dTOR but indirectly through the inhibition of a dTOR inhibitory complex (see figure 1.7 and (Marygold and Leevers, 2002).

This inhibitory complex is made up of two proteins known as dTSC1 and dTSC2. The mammalian homologs of these proteins, known additionally as hamartin and tuberin respectively, act as tumour suppressors. Loss of heterozygosity of either mammalian gene results in a relatively common disease known as tuberous sclerosis. This disease manifests itself as a widespread development of benign growths called hamartomas, some of which contain big cells. It is still unclear exactly how dTSC1 and dTSC2 act to inhibit dTOR function, although dTOR phosphorylation is sensitive to dTSC1/2 levels (Inoki et al., 2002). Unfortunately, the structures of the two proteins do not give us many clues: dTSC1 has a coiled-coiled region that may be used in protein-protein interactions, and a predicted single trans-membrane domain; dTSC2 contains a putative GTPase activating (GAP) domain and a leucine zipper like sequence.

What is clear is that dTSC1 and dTSC2 function in a complex. Firstly, they are able to bind one another *in vitro* (Gao et al., 2002; Potter et al., 2001). Secondly, over-expression of one component on its own has no effect, whereas over-expression of both components together leads to the restriction of tissue growth via reductions in cell growth and cell proliferation (Potter et al., 2001; Tapon et al., 2001). This over-expression phenotype resembles that caused by loss of function mutations in the *Drosophila* insulin/PI3K signalling pathway. Furthermore, loss of dTSC1 or dTSC2 in clones promotes G1 to S transition in clone cells, and increases clone cell size, a phenotype that is reminiscent of *pten* null clonal phenotypes (Ito and Rubin, 1999). Interestingly in these clones, the expression of cyclin E is increased (Tapon et al., 2001).

By performing genetic epistasis experiments where the phenotypes of mutations in individual insulin/PI3K pathway components or the dTSC1/2 complex were

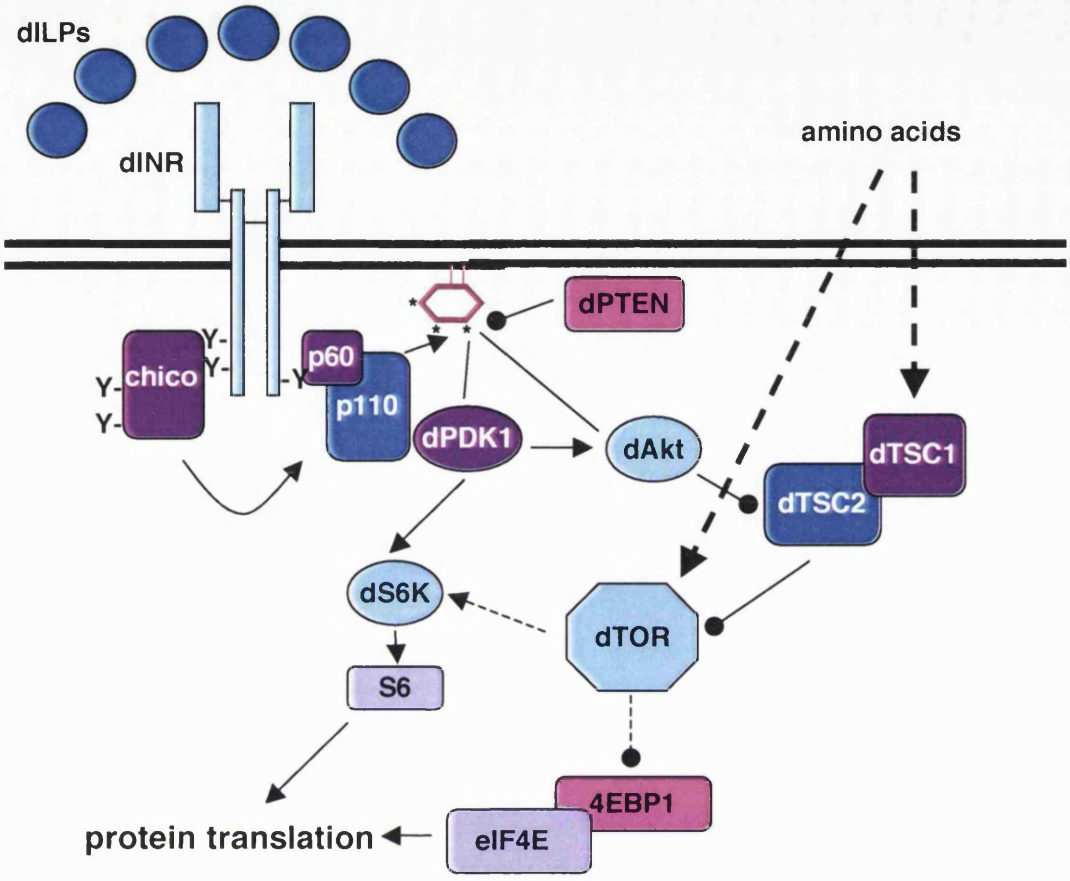

Figure 1.7 The *Drosophila* insulin like peptide/ PI3K signalling pathway

One of the major downstream effects of *Drosophila* insulin/PI3K signalling is the increased translation of a subset of proteins, which leads to cell and organismal growth. This effect is mediated through the dTOR dependent activation of dS6K and deIF4E. dTOR activity is inhibited by the binary complex of dTSC1 and dTSC2. Insulin/PI3K signalling pathway activity, which leads to the activation of dAkt, removes this inhibition. Specifically, the phosphorylation of dTSC2 by dAkt inhibits the activity of the dTSC1/dTSC2 complex. dTOR is also responsive to amino acid levels, although it is unclear whether it monitors these levels itself or whether this is the role of other proteins, for example the dTSC1/dTSC2 complex.

compared with those induced by mutations in both, dTSC1 and dTSC2 were placed upstream of dS6K and downstream of dAkt (Gao and Pan, 2001; Potter et al., 2001; Tapon et al., 2001). Thomas Radimerski and colleagues confirmed this positioning using biochemical tests and additionally showed that the activation of dS6K that resulted from the removal of dTSC1 by double stranded RNA interference was blocked by the presence of a dTOR inhibitor (Radimerski et al., 2002a). Similarly, removal of dTSC2 increases the phosphorylation of dS6K at the rapamycin sensitive site, threonine 389 (Inoki et al., 2002).

The inhibition of the dTSC1/2 complex by dAkt is mediated directly by phosphorylation of dTSC2. dTSC2 contains four putative Akt phosphorylation sites, two of which are important for its *in vivo* function. If either of these sites is mutated to a non-phosphorylatable alanine, the inhibitory effects of dTSC1/2 on dS6K activity are enhanced (Potter et al., 2002). Conversely, if they are mutated to phosphomimetic residues, then the ability of dTSC2 to inhibit TOR is reduced (Inoki et al., 2002). Together with the earlier results, these data suggest that at least some of the growth effects of insulin/PI3K signalling are mediated via dTOR. However, this may not be the only route through which increases in PIP_3 can increase growth. The increase in clone size caused by loss of *dTSC1* can be further enhanced by loss of *pten*, suggesting that independent pathways are also utilised (Gao and Pan, 2001).

One further issue that remains to be resolved is how the dTOR signalling pathway senses amino acids. We already know that dTOR function is dependent on the presence of amino acids and on the absence of functional dTSC1/2, yet how these two inputs coordinated has not been discussed. Two sets of experiments have been carried out to investigate this issue. These experiments found firstly that the ability of nutrient stimulation to increase phosphorylation of dS6K is inhibited by the over expression of dTSC1/2 (Inoki et al., 2002). Secondly, the rapid decrease in dS6K phosphorylation upon shifting S2 cells to medium lacking amino acids does not occur if dTSC2 is depleted in these cells (Gao et al., 2002). These results suggest that the dTSC1/2 complex, rather than dTOR, is the primary nutrient sensor in the cell, and that the presence of amino acids acts to neutralise the dTSC1/2 inhibitory function. An alternative hypothesis is that dTSC1/2 acts on dTOR and enhances its responsiveness to amino acids. Thus the more dTSC1/2 present, the more nutrient sensitive dTOR is (Marygold and Leevers, 2002; McManus and Alessi, 2002).

1.3.9 Other growth regulators: CyclinD/Cdk4, Ras and Myc

Although the *Drosophila* insulin/PI3K signalling pathway and the associated pathway downstream of dTOR are major growth regulatory pathways, other molecules have been associated with growth control. These molecules are capable of stimulating growth, and in some cases cell division, to lead to an increase in overall tissue growth.

The *Drosophila* G1 cyclin, Cyclin D, and its associated kinase, dCdk4, are able to promote the growth of targeted tissues, when over-expressed (Datar et al., 2000; Meyer et al., 2000). The over-expression of the *Drosophila* cyclin D/dCdk4 complex does not alter cell size or the cell cycle profile, but does reduce cell-doubling time. This situation therefore leads to an increase in tissue mass by virtue of an increase in growth and cell number (Datar et al., 2000). dCdk4 might accelerate cell cycle progression via the phosphorylation of dRBF, leading to a derepression of dE2F mediated transcription and progression through both the G1 to S phase and G2 to M phase transitions. However, although the over-expression of dE2F results in a decreased doubling time, it also reduces cell size and does not promote growth. The fact that dCdk4 promotes both growth and cell cycle progression argues for the existence of additional *Drosophila* Cyclin D/dCdk4 targets that regulate cell size to ensure that cell size remains constant as proliferation rates increase.

Other regulators of *Drosophila* growth include the small GTPase, Ras and the basic-helix-loop-helix-zipper transcription factor, Myc. *Myc* family genes are frequently rearranged and deregulated in a wide range of tumours in many animal species (Pelengaris et al., 2002). Although Myc has been proposed to function mainly in cell cycle regulation how this is achieved is not well established despite the identification of multiple Myc targets. *Drosophila* that carry mutations in *dmyc* exhibit decreased body size, decreased cell size and decreased viability (Johnston et al., 1999). Furthermore, over-expression of dMyc, like Dp110, accelerates progression through G1 (Johnston et al., 1999) and also leads to an increase in Cyclin E levels (Prober and Edgar, 2002). Perhaps of greatest interest is that the levels of dMyc expression appear to be regulated by the patterning molecule, Wingless. This interaction suggests a putative mechanism through which patterning cues influence the growth of imaginal discs (Johnston et al., 1999).

Ras, like other small GTPases adopts a different conformation when it is bound to GDP or GTP. Thus Ras is able to act as a molecular switch that is 'on' when it is bound to GTP and 'off' when it is GDP-bound. The nucleotide binding state of Ras is

influenced by exchange factors that promote GTP binding, and GTPase activating proteins (GAPs) that promote the GTPase activity of Ras itself, thus increasing the proportion of Ras that is GDP-bound (Downward, 1992). Ras GEFs, and hence Ras activity, are frequently activated by extracellular growth factors. The most well known effector of Ras is the serine/threonine kinase Raf, which in turn activates the MAPK pathway.

Dras1, the most closely related homolog of Ras in *Drosophila*, has been shown to play a role in many processes in the developing fly, perhaps most notably the differentiation of the photoreceptors of the compound eye (Diaz-Benjumea and Hafen, 1994; Dickson et al., 1992; Halfar et al., 2001). However, it has also been implicated in cell proliferation and apoptosis (Karim and Rubin, 1998; Prober and Edgar, 2000). More recently, David Prober and Bruce Edgar have shown that Dras1, like Myc and Dp110, promotes cell and tissue growth and S-phase entry (see section 4.1, (Prober and Edgar, 2000). Notably, activation of Dras1 in clones results in the stabilisation of dMyc, and Dras1 null clones express reduced levels of dMyc, suggesting that Dras1 promotes growth at least in part through Myc (Prober and Edgar, 2002). The possibility that Dras1 also acts through Dp110 to promote growth will be discussed in greater detail in chapter 4.

1.3.10 Regulation of mammalian growth by the insulin/IGF/PI3K pathway

The role of the insulin/IGF/PI3K pathway in tissue growth appears to be conserved throughout evolution, as demonstrated by a number of transgenic/'knock-out' studies. For example, mice that lack functional IGF-1 receptor are severely growth retarded during embryonic development, and are only 45% of the size of wild type mice at birth (Efstratiadis, 1998). Consistent with these observations, mice that are null for *irs1* or *irs2* also show growth defects (Araki et al., 1994; Tamemoto et al., 1994; Withers et al., 1999). Furthermore, S6K1-deficient mice are proportionally smaller than wild type mice (Shima et al., 1998).

More recent experiments have shown that increasing or decreasing the ability of individual cells to produce PIP_3, by targeted over-expression or inhibition of PI3K or PTEN can result in cell and organ growth phenotypes. Tetsuo Shioi and colleagues generated transgenic mice that expressed constitutively active or kinase dead forms of the PI3K catalytic subunit, p110α, specifically in the heart. These mice had larger or smaller hearts respectively and this size alteration was accompanied by a comparable

change in cardiac myocyte size (Shioi et al., 2000). Later experiments confirmed that this growth effect was mediated through Akt1 (Shioi et al., 2002). Furthermore, the proportions of each heart chamber, the myocardial architecture and the cardiac function were not significantly perturbed by the modulation of p110α or Akt1 activity. Other groups have shown that inactivation of PTEN in differentiated mouse neurons increases the size of the neuronal cell bodies by up to two times (Backman et al., 2001; Kwon et al., 2001). No proliferative defects were seen in these cells. In contrast, both cell growth and cell proliferation were increased if *pten* was deleted in neuronal stem cells (Groszer et al., 2001). This difference has been attributed to the difference in mitotic capability of the stem cells and differentiated cells (Backman et al., 2001).

In summary, observations from experiments in mammals and flies show that the insulin/PI3K pathway is an evolutionarily conserved critical regulator of growth.

1.4 Overview of the thesis

The nutritional regulation of growth by amino acids via dTOR has been extensively studied (see section 1.3.5). However, it is likely that levels of circulating nutrients also activate upstream components of the *Drosophila* insulin/PI3K signalling pathway. This possibility is further examined in chapter 3, through experiments in which variations in the level of dAkt phosphorylation and activation in larvae raised on different diets were examined. Furthermore, models to explain how nutrient sensing leads to the generation of humoral growth promoting signals, and how these interact with the cell autonomous monitoring of nutrient availability are presented.

The mechanisms of Dp110 activation are still not fully characterised. In chapter 4 the role of the evolutionarily conserved Dp110 Ras-binding domain (RBD) in the function of the catalytic subunit is evaluated. This chapter will show how generating inducible cell lines, which express wild type Dp110 or Dp110 containing mutations within its RBD, allowed the biochemical properties of the different Dp110 proteins to be tested. Furthermore, the phenotype of larvae carrying null mutations in *dp110* is compared to that of larvae carrying $dp110^{6N3}$, a mutant *dp110* gene that contains a non-conservative mutation in its RBD. Although these experiments do not conclusively prove that the RBD of Dp110 is important for its catalytic activity, ways that this preliminary data could be used to further examine this question are discussed.

Chapter 2: Materials and Methods

2.1 Cell culture

Drosophila Schneider S2 cells were grown at 22-25°C in Schneider's *Drosophila* medium (Invitrogen) supplemented with 10% (v/v) heat-inactivated foetal bovine serum and penicillin-streptomycin (Life Technologies) at a final concentration of 50 units penicillin G and 50μg streptomycin sulphate per millilitre of medium. Selective culture medium for control transfected or pMT-HA-p60/pMT-myc-Dp110* cell lines was also supplemented with 300μg/ml of Hygromycin B (Invitrogen) to maintain selection (see sections 2.6.2 and 4.5). For general maintenance the cells were grown in 75 cm^2 or 175cm^2 tissue culture flasks. Cells were split to a density of 2×10^6 cells/ml when the cell density had reached between 8 and 20×10^6 cells/ml. Cells that were to be harvested for Western blot analysis were usually plated into 90mm dishes or six-well plates at a density of 5×10^6 cells/ml and cultured for between one and two days.

2.1.1 Insulin and $CuSO_4$ treatment

All reagents were from Sigma. Cells were treated with porcine insulin at a concentration of 1μM for 30 min. For induction of the metallothionein responsive promoter in the pMT-HA-p60/pMT-myc-Dp110* cell lines, cells were exposed to 700mM $CuSO_4$ for the lengths of time indicated in the figure legends. When no time is specified, the treatment lasted for 16 hours.

2.2 Fly culture

For general maintenance, flies were raised in tubes and bottles containing fly food (1× Normal food) at 18°C or 25°C depending on the experimental requirements. The composition of this food is: 0.8% (w/v) agar, 8.8% (w/v) yeast, 5.5% (w/v) cornmeal, 1% (w/v) flour, 7.5% (w/v) sucrose, 4% (v/v) Nipagin and 0.8% (v/v) proprionic acid.

2.2.1 Composition of fly foods used in nutrition experiments

60mm dishes containing 'highly defined diets' were used to raise larvae from hatching (see section 3.2). 'Starved' larvae were raised on 1% (w/v) agar in phosphate buffered saline (PBS). This was supplemented with 0.75% (w/v) sucrose, or 20% (w/v) sucrose, on which 'amino acid starved' larvae, or 'amino acid starved (2)' larvae were raised respectively. 'Sugar starved' larvae were raised on 1% (w/v) agar in PBS, supplemented with 5.5% (w/v) casein (BDH). 'Fed' larvae were raised on 1% (w/v) agar in PBS, supplemented with 5.5% (w/v) casein and 0.75% (w/v) sucrose.

The nutritional components of Normal food (NF) were diluted down, in order to calorically restrict larvae (see section 3.4). All dilutions of NF contained 1% (w/v) agar, 4%

(v/v) Nipagin and 0.8% (v/v) proprionic acid. The percentage amounts of nutrients added to each dilution are shown in the table below:

	NF concentration (w/v)			
	0.5×	0.25×	0.1×	0.05×
Yeast extract	4.4%	2.2%	0.88%	0.44%
Cornmeal	2.75%	1.375%	0.55%	0.275%
Flour	0.5%	0.25%	0.1%	0.05%
Sucrose	3.75%	1.875%	0.75%	0.375%

'Standardised food' (SF, see section 3.6) contained the same concentrations of agar, Nipagin and proprionic acid as NF. However, yeast extract and sucrose were the only nutrient sources added. The percentage amounts of these added to SF dilutions are shown below:

	SF concentration (w/v)				
	1×	0.5×	0.25×	0.1×	0.05×
Yeast extract	8.8%	4.4%	2.2%	0.88%	0.44%
Sucrose	7.5%	3.75%	1.875%	0.75%	0.375%

The food used to re-feed larvae that had been raised for 16 hours from 80 hours development on 0.05× SF (see section 3.9) contained 0.44% yeast extract, 0.375% (w/v) sucrose, 1% (w/v) agar, 4% (v/v) Nipagin and 0.8% (v/v) proprionic acid, as 0.05× SF. In addition, it was supplemented with 5.24% casein hydrolysate (BDH) and sucrose to a final concentration of 0.75% (w/v).

2.2.2 Harvesting embryos and larvae

Flies were allowed to lay eggs on apple juice/agar plates that had been supplemented with yeast paste for the lengths of time specified in the text. Embryos were washed in distilled water, and counted manually on apple juice/agar plates.

First instar larvae were harvested from plates using a paintbrush. They were then washed in PBS. Third instar larvae were harvested by adding 30% (v/v) glycerol to the food vials and using a paintbrush to break up the food. The larvae then floated to the surface and were collected using a paintbrush or a spatula. Larvae were counted manually on cooled apple juice/agar plates and weighed using a microbalance. If larvae were to be lysed they were placed in Eppendorf tubes and lysed immediately or snap frozen by immersing the tubes in liquid nitrogen (for details see text).

2.3 Production of Rabbit antisera against Dp110 peptides

Peptides Dp110-1, Dp110-2 and Dp110-3 (section 4.3) were synthesised in the Peptide Synthesis Laboratory at Cancer Research UK London Research Institute. A cysteine residue and an aminohexanoic acid linker were added to the N-termini of peptides Dp110-2 and Dp110-3. This allowed the lyophilised Dp110-2 and Dp110-3 peptides to be coupled via the N-terminal thiol group to Imject maleimide-activated keyhole limpet hemacyanin (KLH) as directed by Pierce, at a weight to weight ratio of 1:1, and then purified by gel filtration.

Dp110-1 was coupled to KLH using glutaraldehyde, via the exposed amino groups on the N-terminal lysine residues. KLH and lyophilised Dp110-1 were dissolved in 0.1M $NaHCO_3$, to a final concentration of 2mg/ml of each. An excess of glutaraldehyde was added, to a final concentration of 0.05%, and the solution was stirred overnight. Glycine ethyl ester (pH8) was then added to a final concentration of 0.1M and the solution was incubated at room temperature for 30 min to quench the excess glutaraldehyde. Four volumes of acetone (at –20°C) were added and the coupled peptide was precipitated at –70°C for 30 min. The protein was pelleted by centrifugation at 10,000×*g* for 5 min in a Beckmann centrifuge. The pellet was air dried then resuspended to 1mg/ml in 0.9% NaCl solution.

Two rabbits (A and B) were immunised with each coupled peptide by Harlan-Sera Lab. For each initial immunisation 200μg of immunogen was injected into each rabbit and 100μg immunogen was used for each additional boost. The immunisation and bleeding schedule are shown in the table below:

Day	**Procedure**
0	Prebleed (10ml) and immunisation
14	Boost 1
28	Boost2
35	Test bleed 1 (10ml)
42	Boost 3
49	Test bleed 2 (10ml)
56	Boost 4
63	Test bleed 3 (10ml)
70	Boost 5
77	Terminal bleed

The crude sera were stored at –20°C, or at 4°C with 0.03% NaN_3.

2.4 Biochemical Techniques

2.4.1 Preparation of lysates

To prepare cell lysates, the cells were loosened with a sharp tap on the culture dish and mixed gently to ensure even distribution. An aliquot of 50µl was removed to assess the cell density of the culture. The remaining cell suspension was transferred to an Eppendorf (1.5ml) or a Falcon (15ml or 50ml) tube, depending on the volume of cells to be lysed. The cells were then pelleted by centrifugation at 1,200×*g* for 3 min. The supernatant was aspirated and the pellet washed in a minimum of five volumes of PBS. The centrifugation was repeated and the supernatant was aspirated again. All subsequent steps were performed at 4°C or on ice. 1ml lysis buffer (50mM HEPES pH7.5, 1% (v/v) Triton X-100, 150mM NaCl, 2mM EDTA, 2mM EGTA, 50mM NaF, 1mM $NaVO_4$, 10µg/ml pepstatin A, 10µg/ml aprotinin, 15µM N-α-p-tosyl-L-lysine chloromethyl ketone (TLCK), 0.9µg/ml leupeptin and 1mM phenylmethysulphonyl fluoride (PMSF)) was added per 10^8 cells. The lysis reaction was allowed to proceed for 30 min. Nuclei and membranes were pelleted at 14,000×*g* for 10 min, then the supernatant was removed and used for further studies.

Larval lysates for Western blot analysis were prepared using the lysis buffer described above. Initially 5µl lysis buffer was added per 1mg larvae. Larvae were homogenised using a small pestle in an Eppendorf tube, then the homogenate was incubated for 10 min on ice. Later (see section 3.8), 15µl lysis buffer was added per 1mg larvae and 30 min were allowed for lysis, as this gave higher protein concentrations. Again, lysates were clarified by centrifugation at 14,000×*g* for 10 min and the supernatant was used for further studies.

Larval lysates for dAkt kinase assays were prepared initially by adding 5µl kinase assay (KA) lysis buffer per 1mg larvae. Larvae were lysed by homogenisation, as described, followed by incubation on ice for 30 min. Later, when Tricine gels were used in the analysis of dAkt activity, 15µl KA lysis buffer was added to each mg larvae. The reaction was allowed to proceed for 30 min on ice as before. KA lysis buffer contains 50mM Tris pH 7.5, 120mM NaCl, 1% (v/v) NP40, 1mM EDTA pH 8.0, 1mM EGTA, 20mM β-glycerophosphate, 15mM NaPPi, 1mM DTT, 25mM NaF, 100µM $NaVO_4$, 10µg/ml pepstatin A, 1µg/ml aprotinin, 0.9µg/ml leupeptin, 1mM PMSF. These lysates were clarified by centrifugation at 14,000×*g* for 10 min and the supernatant was used for further studies.

2.4.2 Protein assays

The approximate protein concentration yielded by lysis of resuspended cells and larvae was determined by a detergent-compatible assay (Bio-Rad DC protein assay). This procedure was based on a modified Lowry protein assay (Lowry *et al.*, 1951). Using known concentrations of protein standards a standard curve was constructed and the protein concentration of each sample was determined. The protein standards that were used were

made from known concentrations of bovine serum albumin reconstituted in the same buffer as the samples.

2.4.3 Affinity purification

Affinity purification was performed using Actigel beads (Sterogene) that had been coupled to the phosphopeptide (GGpYMDMSKDESVDpYVPML) as described (Fry et al., 1992). This phosphorylated YXXM motif is taken from the human PDGFβ receptor and binds selectively to the *Drosophila* Class IA PI3K adaptor, p60 (Weinkove et al., 1997). For each purification 30μl of a 1:1 slurry of beads and lysis buffer was added to S2 cell lysate (18mg protein) and incubated at 4 C with constant tumbling for 90 to 120 min. The beads were washed three times in lysis buffer and twice in 2× lipid kinase assay buffer (40mM Tris-HCl pH 7.4, 200mM NaCl, 1mM EGTA).

2.4.4 Immunoprecipitation from cell lysates

All incubations were performed at 4°C in lysis buffer or KA lysis buffer containing protease inhibitors, with constant tumbling on a rotating wheel. For immunoprecipitations (IPs) that were analysed by Western blot, α-myc (9E10, (Evan et al., 1985) or α-HA (12CA5, (Niman et al., 1983) were incubated with constant tumbling for 1 hour with cell lysate (1μl antibody/1.25-1.5mg protein). 30μl of a 1:1 slurry of lysis buffer and protein A sepharose beads (Pharmacia, pre-washed three times in PBS and twice in lysis buffer) was then added, and the mixture incubated for a further 45 min. Alternatively, 8μl α-p60 (Weinkove et al., 1997) was incubated with each ml cell lysate for 45 min. 40μl of a 1:1 slurry of lysis buffer and pre-washed protein A sepharose beads was then added to each ml of lysate, and the mixture incubated for a further 45 min. After washing four times in lysis buffer, the beads were resuspended in an appropriate amount of 1× SDS gel sample buffer (62.5mM Tris pH 6.8, 2% (w/v) SDS, 10% (w/v) glycerol, 0.2% (w/v) bromophenol blue, 100mM dithiothreitol (DTT)) and heated to 98°C for 3-5 min.

For IPs that were analysed by lipid kinase assay, 3μl α-myc was incubated with constant tumbling for 1 hour with cell lysate (18mg protein). 50μl of a 1:1 slurry of lysis buffer and pre-washed protein G sepharose beads (Pharmacia) was then added, and the mixture was incubated for a further 45 min. Beads were then washed three times in lysis buffer and twice in 2× lipid kinase assay buffer.

After optimisation (see section 4.11) the IP method was altered: 3μl α-myc antibody was added per ml lysate, and 6μl 1:1 slurry of pre-washed protein G sepharose beads and lysis buffer was added per mg protein. All other elements of the method remained the same.

2.4.5 Immunoprecipitation from larval lysates

All incubations were performed at 4°C in lysis buffer or KA lysis buffer containing protease inhibitors, with constant tumbling on a rotating wheel. In α-dAkt immunoprecipitations (IPs) from larval lysates that were used for kinase assays using the scintillation counting method, 3μl crude polyclonal α-dAkt antisera was incubated for one hour with between 85μl and 100μl larval lysate. In α-dAkt IPs that were used for kinase assays utilising the Tricine gel method, 3μl crude polyclonal α-dAkt antisera was incubated for one hour with between 300μl and 500μl lysate. 25μl of a 1:1 slurry of KA lysis buffer and protein A sepharose beads, which had been pre-washed three times in PBS and twice in KA lysis buffer, was added and the mixture incubated for a further 45 min. The beads were then washed three times in KA lysis buffer, once in salt wash (100mM Tris pH7.5, 0.5M NaCl) and once in kinase assay wash (50mM Tris pH7.5, 10mM $MgCl_2$, 1mM DTT).

2.4.6 Protein kinase assays

dAkt kinase activity was measured by assessing the capacity of α-dAkt immunoprecipitates to phosphorylate a peptide substrate (Crosstide) corresponding to the sequence in mammalian glycogen synthase kinase 3β surrounding serine 9 that is phosphorylated by Akt (GRPRTSSFAEG; (Cross et al., 1994)). This peptide was manufactured in the Peptide Synthesis Laboratory, Cancer Research UK London Research Institute. Beads from α-dAkt IPs were washed at 4°C as described above. Kinase assays were performed in 50μl of 50mM Tris-HCl pH7.5, 10mM $MgCl_2$, 1mM DTT, 50μM ATP containing 2μCi [γ-^{32}P]-ATP (6Ci/μmol) and 30μM Crosstide for 30 min at 30°C. Following incubation, the reaction was briefly centrifuged at 14,000×*g* for 10 seconds and transferred to ice. 40μl of the supernatant was spotted onto p81 phosphocellulose paper (Whatman), which was then washed extensively in 75mM phosphoric acid. Following this, the P81 paper was rinsed once in acetone and allowed to dry completely. The amount of [γ-^{32}P] incorporation was quantified by Cerenkov counting, using a liquid scintillation counter (Beckmann).

Alternatively, after centrifugation, 40μl of the reaction supernatant was added to 40μl 2× Tricine gel sample buffer (8% (w/v) SDS, 24% (v/v) glycerol, 100mM Tris pH6.8, 2% (v/v) β-mercaptoethanol, 0.01% (w/v) Coomassie brilliant blue G-250 (BDH)) and incubated at 40°C for 30 min. The reaction mix was then resolved by SDS-polyacrylamide gel electrophoresis (PAGE) in the Tris-tricine buffer system (see section 2.4.8 for method). Gels were dried (see section 2.4.9), exposed to a phosphoimager screen for 16 hours and the phosphoimage was visualised using a phosphoimager (Storm).

25μl 1× sample buffer was added to the beads and these were separated by electrophoresis on polyacrylamide gels.

2.4.7 Lipid kinase assays

Dp110 lipid kinase activity was measured by assessing the capacity of α-myc immunoprecipitates or affinity purified Dp110 to phosphorylate phosphatidylinositol vesicles. Control or Dp110-bound beads were washed at 4°C as described above. Kinase assays were performed in 60μl of 20mM Tris-HCl pH 7.4, 100mM NaCl, 500μM EGTA, 2.5mM $MgCl_2$, 100μM ATP containing 5mCi [γ-^{32}P]-ATP (6Ci/μmol) and 200μM sonicated phosphatidylinositol (Sigma). The reaction was incubated for 30 min at 30°C with constant agitation and terminated by the addition of 100μl 1M HCl. 200μl of chloroform: methanol (1:1) was added, and the mixture was vortexed at maximum speed and then separated via centrifugation at 14,000×*g* for 2 min to extract the lipids. 80μl of the non-aqueous phase was spotted onto TLC plates (Whatman) that had been pre-soaked in 1% oxalic acid, 1mM EDTA, 40% (v/v) methanol, and preheated to 110°C. The lipids were resolved overnight with 65% propan-1-ol, 0.7M acetic acid, 50mM H_3PO_4. After drying, the TLC plate was wrapped in Saran wrap and exposed to a phosphoimager screen for 3 hours and the phosphoimage was visualised using a phosphoimager (Storm).

2.4.8 SDS polyacrylamide gel electrophoresis

SDS-PAGE was performed using a procedure modified from that of Laemmli, 1970. 0.75mm, 1mm or 1.5mm thick mini gels (6cm × 9cm) or large gels (16cm × 20cm) were run using Bio-Rad apparatus. Resolving gels contained 8.0% (w/v) acrylamide: bisacrylamide in a ratio of 37.5:1 (Amresco), 375mM Tris-HCl pH8.8 and 0.1% (w/v) SDS. Stacking gels consisted of 125mM Tris-HCl pH6.8, 4% (w/v) acrylamide: bisacrylamide and 0.1% (w/v) SDS. Both resolving and stacking gels were polymerised by the addition of ammonium persulphate and TEMED (NNN'N'-Tetramethylethylenediamine). Samples were electrophoresed at 150V (mini-gels) or 60V (large gels) in running buffer (25mM Tris-base pH8.3, 192mM glycine and 0.1% SDS). Sample buffer was added to all samples that were loaded onto gels. The following list gives the final concentrations of the sample buffer constituents in the protein samples: 62.5mM Tris pH6.8, 2% (w/v) SDS, 10% (w/v) glycerol, 0.2% (w/v) bromophenol blue, 100mM DTT.

Discontinuous SDS-PAGE in the Tris-Tricine buffer system was performed using a procedure modified from that of Schägger and von Jagow, 1987. 1mm thick large gels (16cm × 20cm) were run using Bio-Rad apparatus. Resolving gels contained 16% (w/v) acrylamide: bisacrylamide (32:1), 1M Tris pH8.45, 0.1% (w/v) SDS, 0.1% (v/v) glycerol. Stacking gels contained 4% acrylamide: bisacrylamide (32:1), 0.75M Tris pH8.45, 0.075% (w/v) SDS. Both resolving and stacking gels were polymerised by the addition of ammonium persulphate and TEMED. Samples were electrophoresed at 100V using a discontinuous buffer system. The

anode buffer was 200mM Tris-base, pH8.9. The cathode buffer contained 100mM Tris-base, 100mM Tricine, 0.1% (w/v) SDS.

2.4.9 Drying SDS-PAGE gels under vacuum

Gels were placed on two sheets of damp 3MM paper (Whatman) and the paper was cut so that it remained slightly larger than the gels. The gel was covered with Saran wrap and dried under vacuum for 90 min at 80°C on a gel drier (Hoefer).

2.4.10 Electroblotting PAGE-resolved proteins

Resolved proteins were transferred onto a polvinylidene difluoride (PVDF) membrane (Immobilon-P, Millipore) by the Trans-Blot system (Bio-Rad) for 90-120 min at 200mA. The Immobilon membranes were pre-wet in methanol prior to use. Electroblotting was performed in transfer buffer (38mM glycine, 50mM Tris-base, 0.0375% (w/v) SDS and 20% (v/v) methanol).

2.4.11 Immunoprobing of Western blots

Membranes were blocked for 45-60 min at room temperature with agitation on a rotary shaker either in Tris-buffered saline (20mM Tris pH7.4, 150mM NaCl) containing 0.1% (v/v) Tween-20 (TBS-T) and 5% (w/v) powdered milk (Marvel) or in Odyssey blocking buffer (LI-COR). Primary antisera were diluted in the same blocking solution at the appropriate dilution, and agitated overnight with the blot at 4°C. Standard dilutions used are shown in the table below:

Antibody	**Reference**	**Dilution**
α-p-Ser586	(Alrubaie, 2002)	1:1000
a-dAkt	(Alrubaie, 2002)	1:1000
α-β-tubulin (E7, Developmental Studies Hybridoma Bank)	(Chu and Klymkowsky, 1989)	1:200
α-Dp110 (SK50)	(Leevers et al., 1996)	1:1000
α-p60	(Weinkove et al., 1997)	1:1000
α-myc	(Evan et al., 1985)	1:1000
α-HA	(Niman et al., 1983)	1:5000

The crude antisera raised against peptides Dp110-1, Dp110-2 and Dp110-3 were all used at a dilution of 1:1000.

After overnight incubation in primary antibody, the membranes were rinsed three times and washed four times for 5 min each in TBS-T at room temperature. The immunoblots were then incubated for 60 min with an appropriate secondary antibody. Secondary antibodies

conjugated to horseradish peroxidase (DAKO) were diluted 1:10,000 in TBS-T containing 5% (w/v) milk powder. Secondary antibodies conjugated to either IRDye 800 (Rockland) or Alexa Fluor 680 were diluted in Odyssey blocking buffer containing 0.1% Tween-20. α-rabbit-680 was used at 1:8000, α-mouse-800 and α-rabbit-800 were used at 1:2500.

Following secondary antibody incubation, the blots were rinsed and washed as above. Horseradish peroxidase conjugated antibodies were visualised using a chemiluminescence kit. The standard chemiluminescence reagent used was Supersignal West Pico (Pierce). However, Supersignal West Dura (Pierce) was used on the immunoblots of larval lysates. Excess moisture was removed from the immunoblots, by touching a paper towel to their edge. The immunoblots were then incubated for 5 min with the chemiluminescence reagents. Excess moisture was then removed as above and the blots were covered in Saran wrap and exposed to X-ray film (Fuji). For those blots where fluorophore conjugated secondary antibodies were used, the washed blots were rinsed once in PBS and scanned using the Odyssey infrared imaging system (LI-COR).

The Odyssey IR imaging system uses two solid-state diode lasers to simultaneously provide light excitation at 680 and 780nm. These lasers excite the IR dyes that are coupled to the secondary antibodies, which then emit light with non-overlapping spectra. A scanner collects this light and a mirror is used to sort the fluorescent signals, by transmitting the light above 810nm (from IR-800), and reflecting light below 750nm (from Alexa Fluor 680). This light is then converted to an electrical signal and, after multiple amplification and filtration steps, is co-ordinated with the positional data to create an image file. In this file, the light above 810nm is represented in green and the light below 750nm is represented in red. (For further details see the operator's manual).

2.4.12 Quantification of Western blots

The blots that were visualised using the Odyssey IR imaging system were quantified using the associated software package. A rectangle was drawn around the bands and the 'integrated intensity' of the pixels inside the rectangle was calculated. This is the sum of the intensity values for all the pixels enclosed by the rectangle, multiplied by the area of the shape. The background signal was calculated as the mean intensity of the pixels that fall within three pixels above, or below the defined shape.

The blots that were visualised using chemiluminescent reagents were quantified on the FLUOR-S Max MultiImager (Bio-Rad). Images of the blots were quantified in much the same way, using the associated software package, Quantity One. In this case the 'pixel volume' was calculated, which is equivalent to 'integrated intensity'. The background signal was calculated by taking an average of the 'pixel volume' of two control rectangles drawn on the image within the lanes of the gel, but where no bands were seen.

2.4.13 Quantification of phosphoimages

After scanning the exposed screen on the phosphoimager, the bands on the resulting image were quantified using the ImageQuant software. Again, rectangles were drawn around the bands and the 'volume' of the shape was calculated. This 'volume' is calculated in the same way as 'integrated intensity' or 'pixel volume'.

2.5 Molecular biological techniques

Basic molecular biology techniques were performed essentially as described in (Sambrook et al., 2001). All restriction enzymes, other modifying enzymes and kits were used according to the manufacturer's instructions. Only significant differences from standard techniques will be described in this section.

2.5.1 Transforming E. coli with plasmid DNA

Ligated DNA was transformed into either SoloPack Gold Supercompetent cells (Stratagene) or XL10-Gold Ultracompetent cells (Stratagene), as directed, unless otherwise stated.

2.5.2 DNA purification

Plasmid DNA was purified from bacterial cultures using QIAprep Spin Miniprep Kits (QIAGEN), or QIAGEN Plasmid Midi Kits (QIAGEN), as directed. Alternatively, the QIAprep 96 Turbo BioRobot Kit was used in conjunction with the BioRobot 8000 (QIAGEN) by Graham Clark, Equipment Park, Cancer Research UK London Research Institute.

2.5.3 Design, synthesis and purification of oligonucleotides

In order to increase the number of useful restriction enzyme sites 5′ of the myc-Dp110 sequence in pBluescript(SKII)-myc-Dp110 (pSL56, Sally Leevers), a linker was designed that could be inserted into the *KpnI* site immediately 5′ of the Dp110 coding sequence in this vector. This linker contained the sequences that are recognised by *KpnI*, *XhoI* and *EcoRV*. Further details of this procedure can be found in section 2.5.4.2. The oligonucleotides designed were: *KpnI* linker forward: CCTCGAGGATATCGTAC; and *KpnI* linker reverse: CATGGGAGCTCCTATAG.

Oligonucleotides were used as primers to add the Ras-binding domain mutations into pBluescript(SKII)-myc-Dp110 using the QuikChange Site Directed Mutagenesis Kit (Stratagene). For further details see section 2.5.4.2. The following criteria were taken into consideration when designing primers:

1) Both the mutagenic primers must contain the desired mutation(s) and anneal to the same sequence on opposite strands of the plasmid

2) Primers should be between 25 and 45 bases in length and the melting temperature of the primers should be greater or equal to 78°C.
3) The desired mutation(s) should be in the middle of the primer, with c.10-15 bases of correct sequence on both sides
4) The primers optimally should have a minimum GC content of 40% and should terminate in one or more C or G bases.

The sequence of the primers used is shown below:

Name	**Sequence (5′ to 3′)**
D260N (6N3) forward	CGGTCGCAGATGAAAATGAACAACCGGACCTCCG
D260N (6N3) reverse	CGGAGGTCCGGTTGTTCATTTTCATCTGCGACCG
T231D forward	CGAGAACGACCAGAGCACGTTTGACTTGTCGGTGAACGAGCAGG
T231D reverse	CCTGCTCGTTCACCGACAAGTCAAACGTGCTCTGGTCGTTCTCG
K250A, R253A forward	GCACGCTGCAGGCGATGAATGCGTCGCAGATGAAAATGAACG
K250A, R253A reverse	CGTTCATTTTCATCTGCGACGCATTCATCGCCTGCAGCGTGC
K250A, R253A, K257A forward	GCACGCTGCAGGCGATGAATGCGTCGCAGATGGCAATGAACGACC
K250A, R253A, K257A reverse	GGTCGTTCATTGCCATCTGCGACGCATTCATCGCCTGCAGCGTGC

Oligonucleotides were synthesised, purified and quantified using an Applied Biosystems 3948 DNA synthesiser and dried down by the Oligonucleotide Synthesis Service, Cancer Research UK.

2.5.4 Subcloning and plasmid construction

2.5.4.1 pMTIZ-HA-p60

See figure 2.1 for a schematic of the following cloning strategy. pBluescript(SKII)-HA-p60 (Weinkove, 1999) was digested overnight with *XbaI* and *NotI* and the resulting fragments were resolved on TAE-agarose gels (1% (w/v) agarose, 40mM Tris-acetate, 1mM EDTA, 0.5mg/ml ethidium bromide) using TAE buffer (40mM Tris-acetate, 1mM EDTA). The 1.6kB fragment was excised from the gel and purified using a QIAquick gel extraction kit (QIAGEN), as directed, and subcloned into *XbaI/ NotI* digested pMTIZ (from Pascal Meier).

*2.5.4.2 pMK33-myc-Dp110**

The *KpnI* linker oligonucleotides were phosphorylated, using T4 polynuclotide kinase (New England Biolabs), as directed, and then mixed at a 1:1 ratio. They were annealed by heating to 80°C for 10 min followed by slow cooling. The linker sequence was then ligated into *KpnI* digested pSL56 that had been treated with Calf Intestinal Alkaline Phosphatase (CIP, New England Biolabs). The vector produced was named pGB01.

See figure 2.2 for a schematic of the following cloning strategy. The QuickChange Site-Directed Mutagenesis Kit (Stratagene) was used, as directed, to introduce the Ras-binding

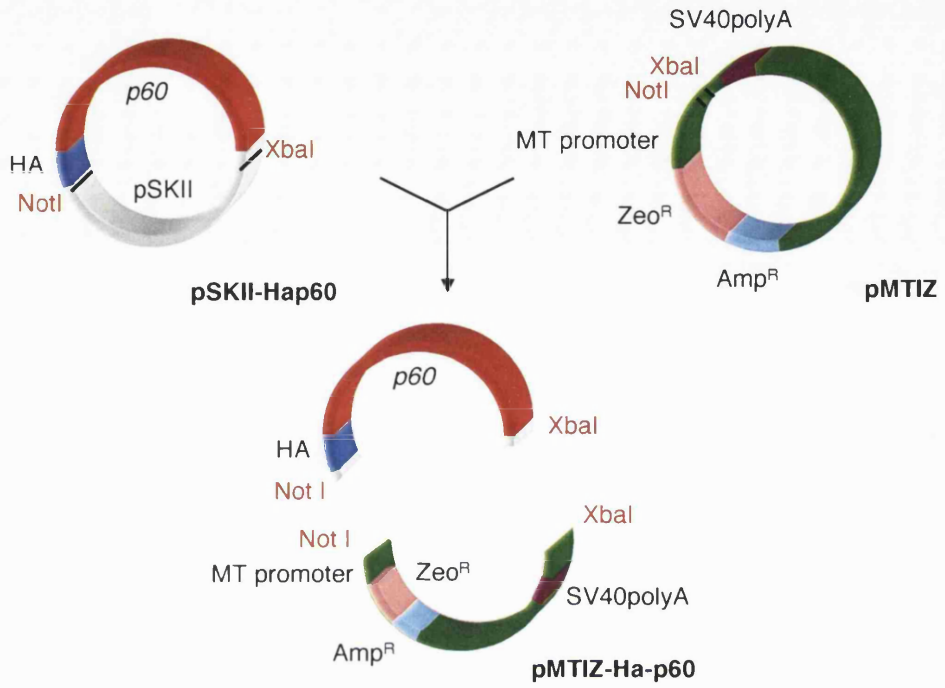

Figure 2.1 Generating pMTIZ-HA-p60

For details of cloning strategy see the text. Briefly, pBluescript (SKII)-HA-p60 was digested with *NotI* and *XbaI*. The HA-p60 containing fragment was then subcloned into *NotI/XbaI* digested pMTIZ.

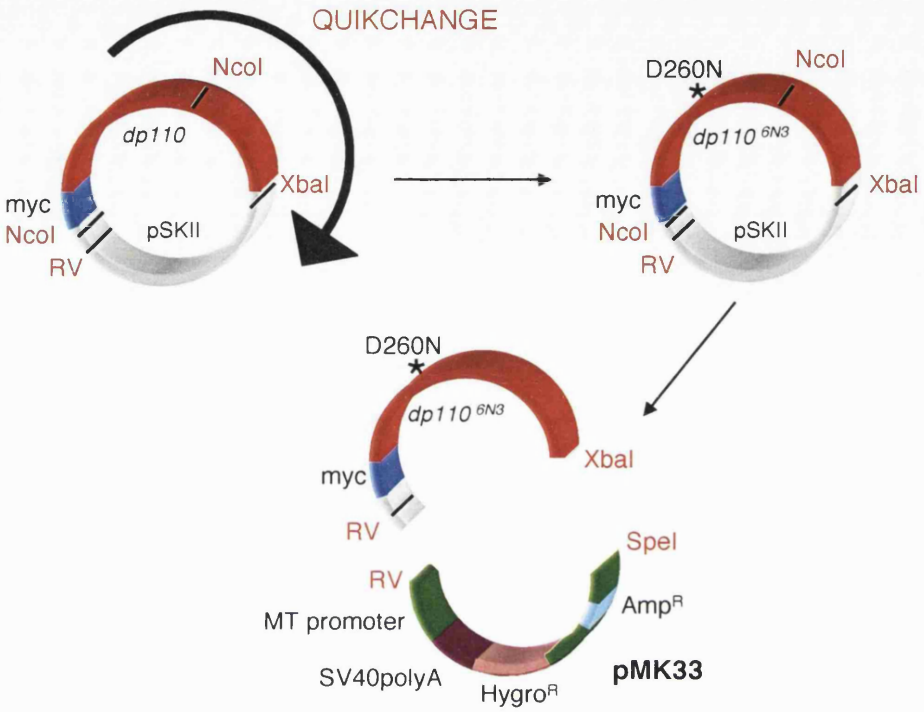

Figure 2.2 Generating pMK33-myc-Dp110* vectors

For details of cloning strategy see the text. Briefly, the QuikChange Site Directed Mutagenesis kit (Stratagene) was used to introduce Ras-binding domain mutations into the *myc-dp110* DNA sequence that was resident in the pBluescript SKII backbone. The resulting vector was digested with *EcoRV* and *XbaI* and the myc-Dp110* containing fragment was subcloned into *EcoRV/SpeI* digested pMK33.

domain mutations into pGB01. The kit uses a polymerase chain reaction (PCR) based method to introduce mutations. Two oligonucleotide primers containing the mutations of choice (see section 2.5.3), were annealed to opposite sides of the vector, and extended during temperature cycling by the Pfu Turbo DNA polymerase (Stratagene). Incorporation of the oligonucleotide primers generated a mutated plasmid containing staggered nicks. Following temperature cycling, the product was treated with the *DpnI* endonuclease, which specifically targets methylated DNA and therefore only digests the parental DNA that was methylated during bacterial culture. The nicked vector is transformed into XL1-Blue supercompetent cells. Several sets of mutagenesis reactions were carried out to create vectors containing the desired mutations.

1) D260N forward and reverse → $Dp110^{6N3}$
2) T231D forward and reverse, followed by K250A, R253A forward and reverse → $Dp110^{TKR}$
3) T231D forward and reverse, followed by K250A, R253A, K257A forward and reverse → $Dp110^{TKRK}$

The pBluescript(SKII)-myc-Dp110* vectors were then digested overnight with *XbaI*, *EcoRV* and *PvuI*. The resulting fragments were resolved on TAE agarose gels, as above, and the 3.3kB fragment was excised and purified, and subcloned into *EcoRV/ SpeI* digested PMK33.

2.5.5 DNA sequencing

Sequencing reactions were carried out in 20µl reaction volumes, using the cycle sequencing method as directed by Applied Biosystems. Reactions were cleaned using the DyeEx 2.0 Spin Kit (QIAGEN) and resolved on an ABI Prism 377 DNA Sequencer (Applied Biosystems). The sequence immediately 5′ to the coding sequence of the *dp110* gene, and the first 2000 bases of the dp110* coding sequence in pBluescript(SKII)-myc-$Dp110^{6N3}$, pBluescript(SKII)-myc-$Dp110^{TKR}$ and pBluescript(SKII)-myc-$Dp110^{TKRK}$ was sequenced to confirm the presence of the introduced mutations. The entire dp110* coding sequence in PMK33-myc-$Dp110^{WT}$, PMK33-myc-$Dp110^{6N3}$, PMK33-myc-$Dp110^{TKR}$ and PMK33-myc-$Dp110^{TKRK}$ was sequenced to confirm the presence of the myc-tag and the Ras-binding domain mutations and the absence of any other mutations introduced during the mutagenesis or cloning procedures. M13 forward primers and internal Dp110 primers were used in each case.

2.6 Generation of polyclonal stable inducible cell lines.

2.6.1 Transfection of S2 cells

For each transfection reaction, six 3.5cm wells of Schneider S2 cells were used. 2ml S2 cells (5×10^6 cells/ml) were added to each well of a six-well plate (Falcon), and left for one

hour to adhere to the bottom of the well. The excess media was then aspirated, and replaced with 2ml fresh media. The cells were transfected using the Calcium Phosphate Transfection Kit (Invitrogen) as directed. Each well was transfected with 5μg DNA that was made up of the appropriate PMK33 and pMTIZ vectors at a 1:1 mass ratio. After incubation for 16 hours, the media was aspirated and 2ml fresh media was added to each well. Selection began 56 hours later.

2.6.2 Selection of transfected cells

The media in each well was gently but repeatedly pipetted up and down using a P1000 pipette (Gilson), to loosen cells. The cell suspension from five wells of each plate was pooled in a 15ml tube (Falcon) and then pelleted by centrifugation at 1,200×*g* for 3 min. The media was aspirated and cells were resuspended in 5ml selective culture media that contained 300μg/ml Hygromycin (Invitrogen). Cells were carefully observed and repeatedly passaged. After three weeks, the surviving cells looked healthy and were used for further experiments.

2.7 Phenotypic analysis

2.7.1 Drosophila lines used in experiments

Oregon R was used as a wild type control line where indicated.

Genotype	Source	References
yw; *dp110*^{A}, p[gH, ry^{+}] / TM3, Sb, Kr-Gal4 UAS-GFP	-	(Leevers et al., 1996), (Casso et al., 2000)
y^{+} w; *dp110*^{6N3}/ TM3, Sb, Kr-Gal4 UAS-GFP	Ernst Hafen	(Casso et al., 2000)
y^{+} w; *dp110*^{1C1}/ TM3, Sb, Kr-Gal4 UAS-GFP	Ernst Hafen	(Casso et al., 2000)

2.7.2 Light microscopy and digital photography

All light microscopy was carried out using a dissecting microscope (Leica - MZFL111), including the assessment of GFP presence in larvae. Images were captured with a digital camera (Nikon - DXM1200), using Act-1 software

2.7.3 Larval length measurement

The recorded digital images were imported into Adobe Photoshop 6.1 and the lengths of larvae were measured using the measuring tool. By referring to measurements from an image of a scale that had been photographed and manipulated in parallel, larval lengths on the images could be converted into actual larval lengths.

2.8 Immunostaining of cells

All incubations and washes were performed at room temperature. Coverslips that were fixed to the bottom of uncoated microwell dishes (MatTek) were covered with 200µl 0.01% poly-L-lysine solution for 1 hour. Excess solution was then aspirated and the dishes left uncovered for 10-20 min, in a sterile environment to dry. 100µl cell suspension was added to the surface of the coverslip and left for 1 hour for the cells to adhere. Excess culture was aspirated and cells were fixed in 3.7% formaldehyde in PBS for 20 min, and then permeablilised in 0.1% Triton X-100 for 3 min. Cells were then washed three times in excess PBS. Cells were incubated on a rotary shaker for 1 hour with α-myc-FITC (Zymed Laboratories Inc.) diluted 1:500 in PSN buffer (PBS with 0.1% saponin and 1% normal goat serum). After rinsing five times and then washing three times for 10 min in PBS, excess moisture was aspirated from the coverslips and coverslips were removed from the dishes and mounted on glass slides in 30µl DAPI containing mountant (Vectashield). Immunofluorescent cells were analysed using a Zeiss Axioplan 2 imaging microscope and Zeiss AxioVision 3.0 software. Images were processed and assembled in Adobe Photoshop 6.1.

2.9 Statistical analysis

All statistical analysis described in this thesis was performed using the two-tailed T-test method for samples with unequal variance. On graphs presented in the thesis, * indicates the p-values obtained for all comparisons were less than 0.1; ** indicates the p-values of all the comparison were less than 0.05. These p-values equate to confidence limits of 99% and 99.5%, respectively.

Chapter 3: The effect of altered nutrition on the phosphorylation state and activity of larval dAkt

3.1 Introduction

As discussed in chapter one, the growth of *Drosophila*, as with all unicellular and multicellular organisms, is regulated by the integration of multiple signalling pathways that are activated downstream of genetic or environmental cues. For example, early experiments showed that reducing the temperature at which *Drosophila* larvae were grown increased the size of the flies generated, primarily through increasing cell number (Robertson, 1959). More recent experiments have demonstrated clearly that the over-expression of patterning genes in clones in developing wing imaginal discs can lead to overgrowth phenotypes (for a review see (Day and Lawrence, 2000).

Knowledge of the availability of nutrition is of vital importance to any developing organism. Without nutritional input the organism will not have the building blocks for growth and so if nutritional levels begin to dwindle the organism must respond appropriately. Potential responses to this situation are numerous. Some organisms modulate their behaviour, perhaps by searching for food or by entering hibernation. Some organisms, such as *C. elegans,* enter an alternative developmental pathway (Riddle, 1997), others arrest or delay their development.

The way in which *Drosophila* responds to the reduction or removal of nutrition is determined by the timing and the severity of the caloric restriction. Early in the third (and final) larval instar, hormonal events are initiated that determine when pupariation will take place. These events are associated with larvae reaching a 'critical weight'. If larvae are starved before this point is reached, they fail to pupariate despite, under certain conditions, being able to survive past the time at which this normally occurs (Britton and Edgar, 1998). In contrast, larvae starved after this time successfully pupariate but generate small adult flies (Bakker, 1959; Robertson, 1963). If larvae are fed a restricted diet rather than starved, for example if they are raised under crowded conditions or on defined diets with specific nutritional deficiencies, they may experience developmental delay and generate small flies (Atkinson, 1979; Robertson, 1959). In both these cases the size reduction is mediated through a reduction in both cell size and cell number (Robertson, 1959).

The survival of any species depends on the production of fertile adults. In *Drosophila* the adult epidermal structures and brain are made from mitotic tissues that grow and are patterned during larval development. The survival of these tissues, which include the imaginal discs and the neuroblasts, is therefore vital if viable adults

are to be formed. However, the majority of the larva is made up of endoreplicating tissues (ERTs). These tissues, as their name suggests, grow via their constituent cells undergoing multiple rounds of DNA replication without intervening mitoses (Smith and Orr-Weaver, 1991). These ERTs, which include the larval epidermis, the fat body and the salivary glands, have various functions during larval life but during metamorphosis the majority of their biomass is used to provide nutrients to the developing imaginal tissues. Unsurprisingly, these differences in function are taken into account in the larval response to nutritional deprivation, resulting in a differential response of the two tissue types to starvation. The ERTs are highly sensitive to nutritional levels, with component cells exiting the cell cycle soon after larvae are starved of amino acids. In contrast, the cells in the smaller number of mitotic tissues are still able to replicate their DNA, and possibly complete the cell cycle, if nutrition is removed, so long as dietary amino acids have initiated cell cycling (Britton and Edgar, 1998): Thus it seems that under starvation conditions imaginal discs are spared at the expense of ERTs.

The level of nutrients to which the larva is exposed could be monitored in a number of ways. One or more larval organ could be nutrient sensitive and release a nutrition dependent signal that can bind and stimulate other tissues. This is reminiscent of the mammalian pancreas, which secretes insulin in response to high blood glucose levels. Alternatively, individual cells could assess the level of nutrients in the surrounding medium. In doing so the cells would be able to gauge the appropriateness of intercellular growth signals (for a review of nutritional sensing by higher eukaryotic cells see (Kimball and Jefferson, 2000). The observation that loss of dTOR function in clones in the developing *Drosophila* imaginal discs, or in larval ERTs, induce an autonomous reduction in cell size and cell number suggests that individual cells do normally monitor amino acid levels directly via dTOR, and respond by modulating their growth accordingly (Oldham et al., 2000; Zhang et al., 2000). However, the replication block experienced by ERTs cultured *in vivo* in the absence of amino acids can be overcome by the over-expression of G1/S regulators (Britton and Edgar, 1998), indicating that amino acids are not necessary for endoreplication to take place. Furthermore, amino acids alone are not sufficient to initiate cell cycling in quiescent mitotic tissues or to promote the replication of ERTs grown in culture (Britton and Edgar, 1998). These latter observations are consistent with the production of

nutrition-dependent humoral signals being necessary to regulate growth of larval tissues in a non-autonomous manner.

During larval stages the fat body accumulates large stores of proteins, lipids and carbohydrates, which are normally degraded by autophagy during metamorphosis to provide nutrients to the developing imaginal tissues. Upon starvation fat body morphology alters rapidly and dramatically. Lipid vesicles remobilise to support proliferating mitotic tissues causing the organ to change both its texture and its opacity (Britton and Edgar, 1998) and to reduce in size. These observations lend support to the hypothesis that the fat body is able to sense the level of nutrients in the larval hemolymph. Furthermore, early experiments showed that in order to achieve maximal imaginal disc growth in culture the culture medium should be pre-conditioned with larval fat body as well as being supplemented with insulin and juvenile hormone (Davis and Shearn, 1977). Further to this, co-culturing quiescent neuroblasts with fat bodies from fed larvae is sufficient to initiate cell cycling (Britton and Edgar, 1998). This observation suggests that the fat body is able to produce a growth-promoting signal. The identity of this signal is unknown, but one group of candidates are the imaginal disc growth factors (IDGFs). These proteins were isolated from media conditioned by growing clonal imaginal disc cells, and the proliferation of these cells can be stimulated by the addition of recombinant IDGFs alone to supplement free culture media. Furthermore, the endogenous proteins are expressed in the larval fat body (Kawamura et al., 1999).

As discussed in chapter one, the level of amino acids in the larval diet alters the growth of the larvae and the size of the resulting fly at least in part by altering the activity of dTOR. The dTOR signalling pathway affects growth by altering the phosphorylation of dS6K and d4E-BP, which in turn alters patterns of protein translation. *Drosophila* PI3K signalling co-operates with dTOR signalling to regulate these proteins, and so larvae that contain weak loss of function mutations in the *Drosophila* insulin / PI3K pathway unsurprisingly resemble starved larvae, generating small flies via reductions in cell size and cell number. However, the *Drosophila* insulin/PI3K pathway could also be regulated by nutrition further upstream, at the level of the ligand of the receptor (for a schematic, see figure 3.1).

The nutritional regulation of mammalian insulin and IGF occurs at numerous levels in the ligand production process. To produce functional insulin or IGF the ligands must first be transcribed and translated. Following this, the translation product

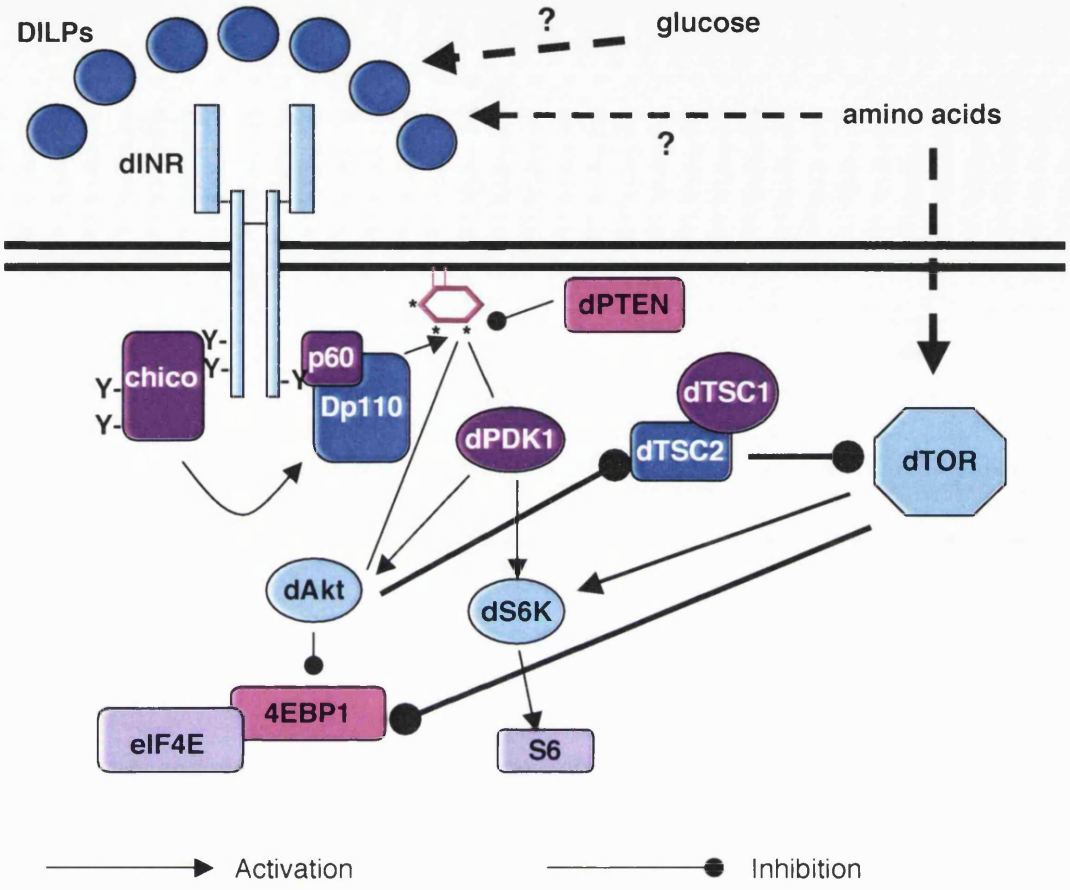

Figure 3.1 Nutritional regulation of the *Drosophila* PI3K signalling pathway

The activation of dTOR by high concentrations of amino acids has been well documented, although it the exact mechanism behind this activation remains unclear. Activation of dTOR leads to the activation of dS6K, a downstream member of PI3K signalling. Studies in mammalian cell culture suggest that nutrients may play an additional role in regulating the PI3K signalling pathway further upstream. Glucose and amino acids have been shown to regulate the transcription of mammalian insulin and insulin like growth factor respectively. In addition, to produce functional insulin, insulin mRNA must be translated, the translation product must be cleaved by endo- and ecto-peptidases and the cleaved protein must be secreted. Each of these steps has been shown to be nutritionally regulated. It is an intriguing possibility that the *Drosophila* insulin like peptides (DILPs), are regulated in the same way.

must be cleaved by endo- and ecto-peptidases in order to create a functional protein. The ligand is then stored in vesicles until finally it is secreted into the blood stream to act on responsive tissues. Each of these stages is subject to nutritional regulation. Transcription of insulin is glucose dependent (Ohneda et al., 2000), and transcription of IGF-1 in cultured ovine hepatocytes is modulated by the concentration of amino acids in the surrounding medium (Wheelhouse et al., 1999). Translation of insulin mRNA can be stimulated fifty-fold by an increase in glucose levels and although the exact mechanism is unclear, structural regulatory sequences that are involved in the glucose dependent translational up regulation have been mapped to the 5′ and 3′ untranslated regions of the preproinsulin mRNA (Goodge and Hutton, 2000). Glucose also regulates the conversion of proinsulin to functional insulin by regulating the biosynthesis of the endoproteases that are required for the cleavage reaction (Goodge and Hutton, 2000). Furthermore, glucose plays a major role in the induction of insulin release (Deeney et al., 2000). Even after release, nutritional regulation of the ligands continues through the regulated production of binding proteins that modulate the ligands' behaviour.

The molecules in *Drosophila* that are analogous to mammalian insulin and IGFs are the *Drosophila* Insulin like peptides (DILPs). It remains an intriguing possibility that the production and release of these ligands are similarly regulated by nutrition. If this is the case, there are two ways in which nutritional regulation of these upstream *Drosophila* insulin/PI3K signalling pathway components in larvae could translate into nutritional regulation of PI3K signalling in the larva as a whole, and hence larval growth. The first possibility is that all larval tissues could respond directly to the levels of circulating DILPs. A second possibility is that signalling downstream of the DILPs is required in the fat body, or other larval organ, for the production of the nutrition dependent humoral signal(s). These two possibilities are of course not mutually exclusive.

By inhibiting Inr/PI3K signalling specifically in the larval fat body, growth is arrested and larvae are indistinguishable from those that have been starved of amino acids (Britton et al., 2002). In contrast, if PI3K signalling is enhanced in the fat body by the over-expression of Dp110, the fat-body cells become opaque as they take up more nutrients, and the larvae are less able to survive when deprived of amino acids than wild-type larvae, surviving two or three days as opposed to eight or more days (Britton et al., 2002). There could be several explanations for the latter observation.

One thought is that over-expression of Dp110 in the fat body inhibits the remobilisation of stored nutrients that would normally occur upon amino acid starvation, leading to a faster than normal rate of nutrient depletion of the larval hemolymph. Alternatively, when Dp110 is over expressed the putative nutrient dependent fat body signal may be produced inappropriately causing the larval tissues to behave as if nutrients were plentiful, using up their own small supplies of nutrients more rapidly than is advisable, thereby reducing the animal's viability. If either hypothesis were true, we would deduce that PI3K activity, at least in the fat body, is normally high in fed larvae and low in starved larvae.

3.1.1 Background to the project

The initial aim of the work presented in this chapter was to discover, using biochemical techniques, whether nutrition is able to modulate PI3K signalling upstream of dTOR in *Drosophila* larvae. If this was the case, we hoped to move on to investigate which component of the diet, carbohydrates or amino acids, is more critical in promoting Dp110 activity.

The phosphorylation state and activity of dAkt in whole larval lysates were used to assess signalling flux through the pathway. This method was chosen as we had available an anti-phosphoSer586 antibody that recognises dAkt only when it is phosphorylated at Serine-586 in the hydrophobic loop of the protein (α–p-Ser586) (Alrubaie, 2002). As discussed in chapter one, phosphorylation of this site occurs only when PI3K is active, and is necessary for the full activation of dAkt (Alessi et al., 1996). An anti-dAkt antibody that recognises the C-terminal of dAkt was also available (α-dAkt). Not only would this second antibody enable me to assess the total amount of dAkt present in larval lysates but it is also capable of immunoprecipitating dAkt from these lysates, therefore allowing me to carry out in-vitro dAkt kinase assays.

Although this approach does not measure PI3K activity directly, PI3K is required for dAkt activation. Direct assessment of Dp110 activity could have been achieved by studying the *in vitro* phospho-inositide kinase activity of α-dINR or α-phospho-tyrosine immunoprecipitates. However, as well as being more technically demanding, this method could be open to the criticism that association of Dp110 with phosphorylated tyrosine motifs is not synonymous with its *in vivo* activation.

Restraints on Dp110 kinase activity are removed in the *in vitro* system and elevated activity levels may thus be recorded.

An alternative method of assessing Dp110 activity would have been to visualise the change in localisation of a PH domain that is able to bind specifically to phosphatidylinositol 3,4,5-trisphosphate (PIP_3) and has been fused to the green fluorescent protein (GFP-PH). When Dp110 is active, levels of PIP_3 within the cell membrane increase. This increase would be seen as an increase in membrane localisation of GFP as the fusion protein binds to the PIP_3 via its PH domain. This method was not used, as we believed that quantification of GFP-PH protein levels would be prone to difficulties, especially in imaginal disc cells owing to their small, compact nature.

After extensive investigation of the phosphorylation state and activity of dAkt in lysates of larvae that had been subjected to altered diets of various sorts, I concluded that this system was not well-suited to monitoring physiological changes in endogenous dAkt. Although the activity of dAkt could be monitored, the signals obtained were often less than twice as large as the background signal, and this led to many experiments failing to produce conclusive results. In addition to this, the reproducibility of results was poor. In this chapter I have presented a selection of the experiments performed, in order that the reader can assess the data for themselves, and appreciate why I felt unable to take this project further.

3.2 Development of larvae hatched on highly defined diets

As discussed, the *Drosophila* larva is made predominantly of endoreplicating tissues that are highly sensitive to levels of nutrition. In contrast, the cells in the smaller number of mitotic tissues, such as the neuroblasts of the larval brain and the imaginal discs, are still able to replicate their DNA, and possibly complete the cell cycle, if nutrition is removed, so long as dietary amino acids have initiated cell cycling (Britton and Edgar, 1998). The dependence of adult fly size on imaginal disc size, and my desire to investigate the role of PI3K in the nutritional control of growth, made me decide to assess the level of signalling downstream of Dp110 in larvae that hatched and were raised on food containing varying levels of nutrients. Using this routine the mitotic tissues would also be highly regulated by larval nutritional input, and it was hoped that extreme variations in larval growth ability and PI3K signalling would result, facilitating the investigations.

Figure 3.2A shows the composition of the defined diets. The nutritional components of 'Normal' food are yeast extract, cornmeal, flour and sugar (see figure 3.3A and section 2.2.1 for further details). The concentrations of 0.75% sucrose and 5.5% casein used in the other diets are based on those recommended by Sang in his defined medium for *Drosophila* culture (Sang, 1978). The 20% sucrose regime was also used to starve larvae of amino acids, to allow comparison with previously published literature (Britton and Edgar, 1998; Oldham et al., 2000; Zhang et al., 2000).

Embryos from an overnight egg-lay of wild type flies (Oregon R strain) were seeded on to plates of food at a density of 100 embryos per plate. Development of larvae on the different regimes was assessed over a period of 12 days (see figure 3.2B). Those on normal fly food (fed) began to pupate after five days, and flies began to emerge after nine days. The larvae that lacked amino acids in their diet were unable to grow past the early first-instar stage. The majority of fully starved larvae and larvae raised on agar with 0.75% sucrose (amino acid (aa) starved) perished within two or three days. In contrast, those raised on 20% sucrose (aa starved (2)) were able to survive for up to eight days.

Growth was seen in *Drosophila* larvae raised on casein (sugar starved) and casein with sucrose ('fed'), but development was delayed compared with the larvae grown on complete fly food and the larval viability was also reduced. On both regimens containing casein the first pupae were seen after seven days. Flies from 'fed' larvae were first seen at day 12, and flies from sugar-starved larvae were first observed on day 13. Although the 'fed' regimen was supposed to mimic Normal food this was not the case, as 'fed' flies began to emerge three days after those on Normal food. A likely explanation for this difference was that the casein and sucrose food was not supplemented with the vitamins and minerals thought to be provided by the yeast extract in Normal food. Furthermore, full dissolution of the casein was hard to achieve.

3.3 Phosphorylation of dAkt in first-instar larvae raised on defined diets

To investigate the effect of these defined diets on the phosphorylation of larval dAkt, embryos were seeded onto plates of defined food as before. After growing for 24 hours at 25 C, larvae were harvested using a paintbrush. This time point was chosen as it was the latest time at which larvae from all regimens remained alive. Larvae were rinsed in PBS, weighed and then lysed in 5µl lysis buffer per mg larvae. Lysates were assayed for the amount of protein they contained and equivalent amounts

A

	1% agar in PBS	5.5% casein	0.75% sucrose	20% sucrose	Normal fly food
Fed					✓
'fed'	✓	✓	✓		
Starved	✓				
Sugar starved	✓	✓			
aa starved	✓		✓		
aa starved (2)	✓			✓	

B

DAY	1	2	3	4	5	6	7	8	9	10	11	12	13
Fed	≈	≈	≈	≈	P	P	P	P	✈	✈	✈	✈	✈
'fed'	≈	≈	≈	≈	≈	≈	P	P	P	P	P	✈	✈
Starved	≈	☨	☨										
Sugar starved	≈	≈	≈	≈	≈	≈	P	P	P	P	P	P	✈
aa starved	≈	☨	☨										
aa starved (2)	≈	≈	≈	≈	≈	≈	≈	☨	☨				

≈ - larvae P - pupae ✈ - flies ☨ - dead

Figure 3.2 Development of and dAkt phosphorylation in first-instar larvae raised on a defined diet.

Sets of 100 wild-type (OregonR) embryos from an overnight egg-lay were transferred to plates of defined food. See **A** for recipes. The developmental ability of *Drosophila* raised from hatching on these diets is shown in **B**. See text for further details. After growing at 25 C for 24 hours, larvae were harvested, rinsed in PBS and lysed. **C** Lysates were separated on two 8% SDS-PAGE gels and Western blots were probed with either α-Akt, or α-pSer586, which recognises phosphorylated dAkt (p-dAkt), and α-β-tubulin. Bands were quantified using the BioRad FLUOR-S multi-imaging system. Relative levels of p-dAkt and total dAkt were assessed by dividing the appropriate signal by the amount of β–tubulin in the respective lane. These values are shown in **D**. Note that the values for –sucrose are not shown, as the low levels of β-tubulin (marked by †) artificially increased the values for phosphorylated and total dAkt. Only the p66 isoform of p-dAkt was considered in the analysis, as a cross-reacting band specific to apoptosing cells could be masking the p80 isoform of dAkt (see asterisk).

n = 1

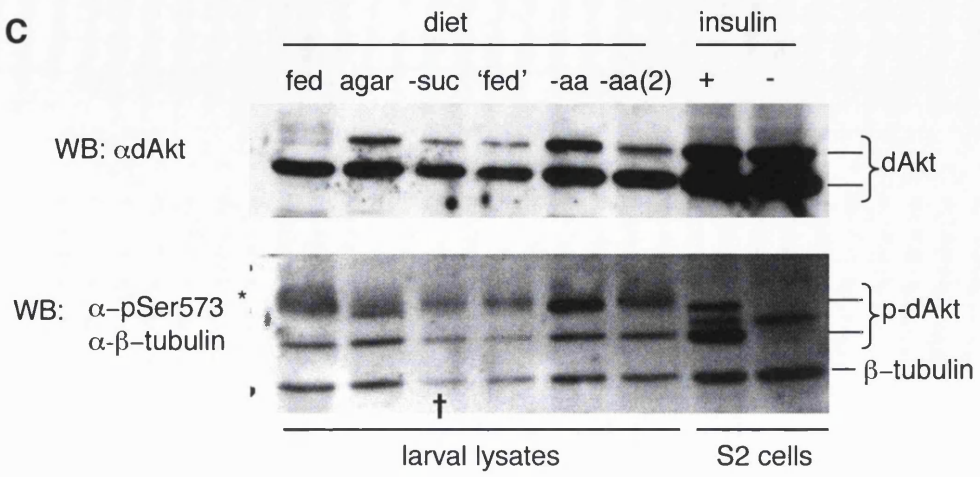

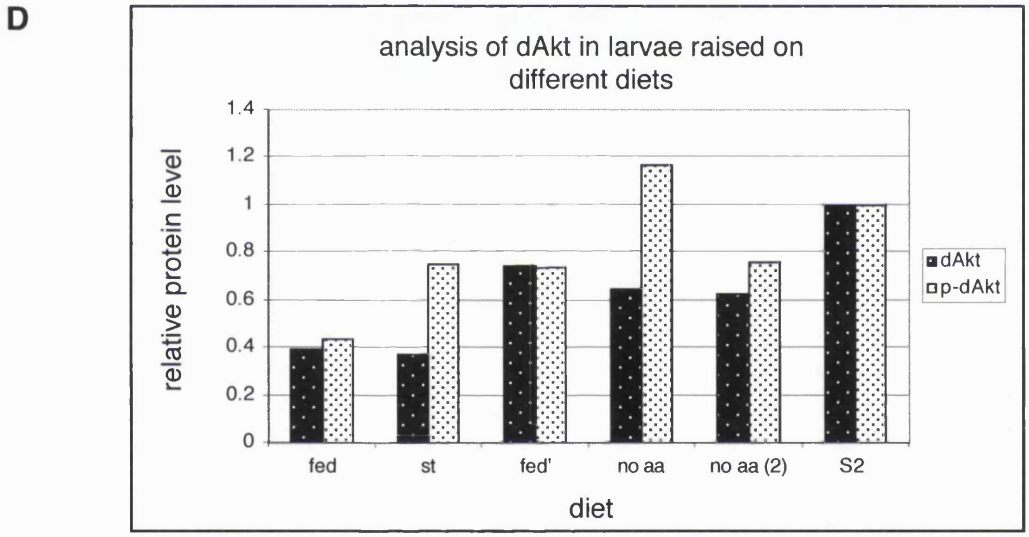

Figure 3.2 cont. Development of and dAkt phosphorylation in first-instar larvae raised on a defined diet.

of each larval lysate (c. 30μg), and lysates of serum starved (-) and insulin stimulated (+) Schneider S2 cells (c. 60μg) were loaded onto two SDS-PAGE gels (8%) and separated. Western blots of the separated proteins were probed first with α-dAkt or with α-p-Ser586 and α-β-tubulin primary antibodies together. The amount of β-tubulin in the lanes was to be used as a loading control. The blots were then probed with Horseradish Peroxidase (HRP)-conjugated α-mouse and α-rabbit secondary antibodies. Signals were visualised using a chemiluminescent HRP substrate (Pierce) see figure 3.2C for an example. The stimulated or unstimulated S2 cell lysates acted as reference points, showing the position on the immunoblot of the two dAkt isoforms, p66 and p80. In addition, they confirmed that the Western blots had been probed with the correct antibodies, as dAkt remains unphosphorylated under serum-starved conditions yet is recognised by the phospho-specific antibody in lysates of Schneider S2 cells treated for 30 minutes with 1μM porcine insulin.

Although equal loading was attempted it was often very hard to achieve. This was due to the fact that protein assays quantified the level of all protein present in the lysates, regardless of whether that protein originated from the larval tissues or was present in the gut, prior to lysis. I frequently found in these experiments that very little larval protein was seen in the lysates of fed, 'fed' or sugar-starved larvae.

I decided that it was necessary to quantify the Western blots so that meaningful results could be obtained even when equal amounts of cellular protein were not present in every lane. The BioRad FLUOR-S Max Multi-imager is able to quantify chemiluminescence directly from Western blots. Using this machine, I assessed the amount of total dAkt and phosphorylated dAkt (p-dAkt) present in each lane, relative to the total amounts of protein present (represented by the β-tubulin signal). The values obtained for total and p-dAkt levels are presented in figure 3.2D. It is important to point out that only the p66 isoform was considered when quantifying the levels of phosphorylated dAkt. This is because at the time that I was performing these experiments Saif Alrubaie discovered the presence of an apoptosing-cell specific protein which cross reacted with the α-p-Ser586 antibody, and ran on SDS-PAGE gels at the same level as the p80 isoform (Alrubaie, 2002).

The data are hard to interpret. If absolute levels of p-dAkt are used as an indicator of PI3K pathway activity, then no differences would be ascribed to the dAkt in larvae raised on agar, 20% sucrose or 0.75% sucrose and 5.5% casein, and the larvae raised on 0.75% sucrose alone would have relatively high levels of pathway activity. Alternatively if the

fraction of total dAkt that is phosphorylated were considered to be the appropriate measure of signalling flux through PI3K, then fully- or amino acid-starved larvae would have much higher levels of signalling assigned to them than the larvae raised on the other diets.

Unfortunately the levels of protein that could be extracted from these first instar larvae were so low that the experimental system was pushed to its limits, frequently leading to a low signal to background ratio. The simple measure of increasing the amount of starting material in order to overcome this problem was impractical, owing to the time taken to harvest larvae. In addition to this, the miscalculation of amounts of larval protein in the samples was sometimes so severe that no fed, 'fed', or sugar-starved larval protein could be visualised on the immunoblots. These factors reduced the reproducibility of results.

In addition, upon closer examination of larval development on the different defined diets, I noticed that a small number of fully- or amino acid-starved larvae were able to grow, although they never pupated. These larvae must have found an alternative source of nutrients, perhaps by feeding off dead larvae present on the plates. This observation reduced the reliability of data further.

Another difficulty with interpretation of data may have arisen as we were examining larval growth under discreet and extreme conditions. As discussed, we were trying to assess what happens to larval dAkt when amino acids, sucrose, or both are not present, compared to dAkt in fully fed larvae.

These four problems – low protein levels, miscalculation of cellular protein concentrations, larval cannibalism and the discreet nature of starvation regimens – led me to propose a new experimental approach. In order to increase the amount of starting material without substantially increasing the amount of time taken to harvest larvae, more developed and therefore larger larvae were transferred to test foods. Although mitotic tissues would no longer be under such strict nutritional control if larvae were transferred at a later time point, reduction in larval growth and adult fly size have been recorded if amino acid starvation takes place at 80 hours after egg deposition (AED, (Partridge et al., 1999). To remove the problems associated with the protein concentration calculations, in the new method, the amount of lysis buffer added to the larvae was to be proportional to the mass of those larvae, and equal volumes of lysate were to be used in experiments. Furthermore, I hypothesised that reducing down dietary components in a graded manner and looking at trends would

improve our ability to draw firm conclusions. This final alteration would have the added benefit that fewer variables would be introduced to the system, as the different diets would contain the same components with only the concentration of those components varying. It was also hoped that reducing the severity of the treatment from starvation to caloric restriction would decrease the likelihood of larvae being forced to turn to cannibalism.

3.4 Assessing the phosphorylation of dAkt in third-instar larvae raised on different dilutions of normal food.

The level of dAkt protein phosphorylation in larvae subjected to these new treatments was assessed. Wild-type embryos from a three-hour egg lay were raised in vials on Normal food (NF) at 25 C (100 embryos/vial). After 72 hours, developing third-instar larvae were harvested and transferred at a density of 50 larvae per vial to varying dilutions of Normal food (see figure 3.3A for details). The recipes for diluted foods, ranging from 1× NF to 0.05× NF, were created by diluting down the nutritional components of Normal food while leaving the concentrations of agar and fungicides, namely Nipagin and proprionic acid, constant. After a further 24 hours, larvae were harvested, weighed and lysed (5 µl lysis buffer/mg larvae). Equivalent volumes of lysate were separated on two SDS-PAGE gels (8%). Western blots were probed with either α-p-Ser586 or α-dAkt and α–β-tubulin, as before (figure 3.3B), and quantified on the BioRad FLUOR-S Max multi-imager (see figure 3.3C). Further information on the method can be found in chapter 2.

The larval transfer time point of 72 hours was chosen as by this time *Drosophila* larvae should have reached their critical weight. As discussed in section 3.1, once critical weight has been reached the time to pupariation is defined, regardless of further nutritional input. Lack of food after the critical weight has been reached does not induce a delay in development, unlike the situation if food removal occurs before this time point. In the latter case, the size of the resulting flies is altered; flies become smaller as nutritional input is reduced. It would have been wise to test directly whether the critical weight had been reached at 72 hours, as environmental conditions can vary developmental timing. This could have been achieved by comparing developmental timing in larvae that were starved and fed after 72 hours development (see section 3.6)

A

'Normal' food recipes

Food Concentration	1x	0.5x	0.25x
Yeast Extract	8.8%	4.4%	2.2%
Cornmeal	5.5%	2.75%	1.375%
Flour	1.0%	0.5%	0.25%
Sucrose	7.5%	3.75%	1.875%
Agar	0.8%	0.8%	0.8%
Nipagin	4.0%	4.0%	4.0%
Proprionic Acid	0.8%	0.8%	0.8%

B

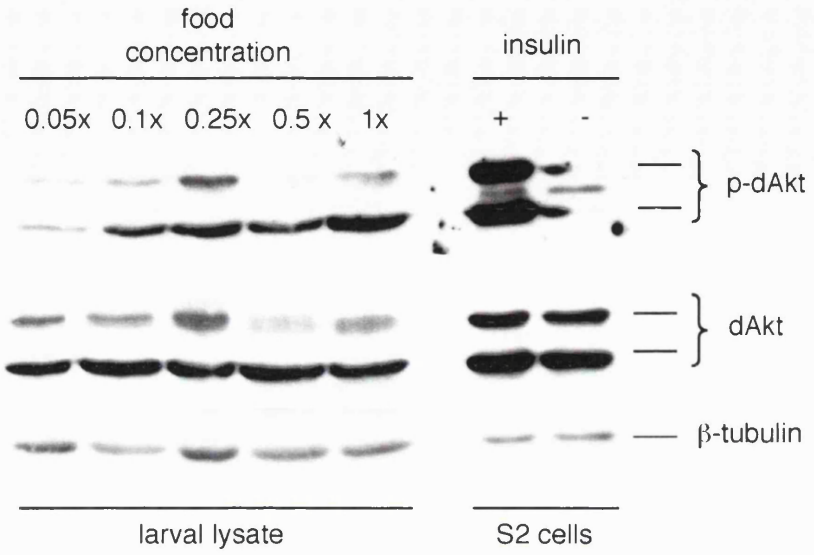

C

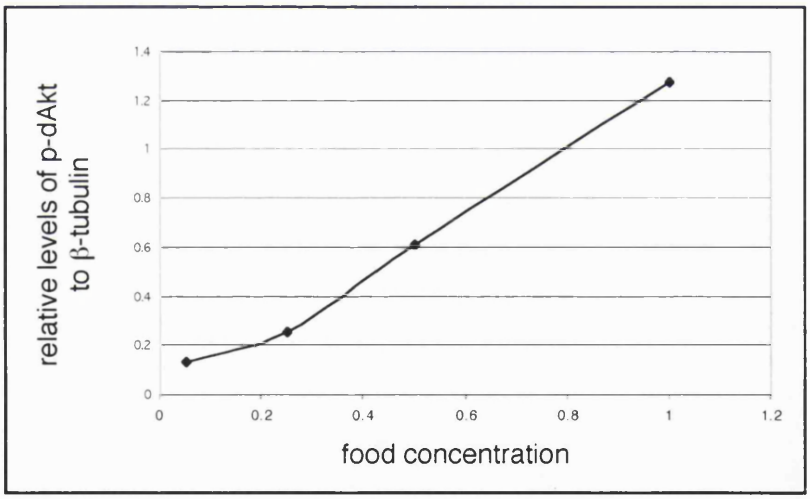

Figure 3.3 Phosphorylation of dAkt in calorically restricted third-instar larvae.

Sets of 100 wild-type embryos were grown at 25 C on 1x Normal food for 72 hours and then transferred to food with the same concentration of agar and fungicides, but with varying nutritional content. (See **A** for recipes of diluted 'Normal' food). After a further 24 hours, larvae were harvested and lysed (5μl lysis buffer/mg larvae), and lysates were run on two 8% SDS-PAGE gels. **B** Western blots were probed with α-pSer586 or α-dAkt and α-β-tubulin. **C** The Bio-Rad FLUOR-S was used to quantify the immunoblot. Relative p-dAkt levels were calculated by dividing the amount of p-dAkt in each lane, by the respective amount of β-tubulin. dAkt appears to become more phosphorylated as food concentration increases.

n = 2

The larvae were harvested between 24 and 40 hours post-transfer, as after that point, larvae began to wander away from the food to start the pupariation process. This behaviour could add a further variable to the experiment and confuse the results obtained, as even the larvae defined as fully fed may have stopped eating prior to pupariation, thereby potentially altering the level of signalling through PI3K.

Normalising the amount of protein loaded onto the SDS-PAGE gels by lysate volume rather than apparent protein concentration reproducibly led to more equal loading of lanes, assessed by comparing the amounts of β-tubulin in each lane.

The results from the experiment shown indicate that phosphorylation of dAkt reduces as the 72 hour-old larvae are provided with less nutrition. This trend is also seen if the fraction of dAkt that is phosphorylated is assessed. These results indicate that larval nutritional levels do feed into PI3K signalling upstream of Dp110.

3.5 Assessing the activity of dAkt in third-instar larvae raised on different dilutions of normal food.

In order to confirm that the dAkt in calorically restricted larvae was less active than that in fully fed larvae, *in vitro* kinase assays of α-dAkt immunoprecipitates from the larval lysates were performed. Larvae were reared and lysates prepared in a similar manner to before but using a different lysis buffer (see section 3.4 and section 2.4.1). 3μl of α-dAkt antibody was added to 85μl of lysate and rotated at 4 C for one hour. Washed protein-A sepharose beads (25μl/point) were used to capture antibody-antigen complexes. "Beads alone" controls were prepared by adding the same amount of protein-A sepharose beads to 85μl of pure lysate. The dAkt kinase activity of the immunoprecipitates was assayed *in vitro* as described in materials and methods section 2.4.6. Briefly, after repeated washing, each of the dAkt immunoprecipitates were incubated with 50μM ATP containing 2μCi [γ-^{32}P]-ATP, and a dAkt peptide substrate called Crosstide (30μM), created from a sequence in mammalian GSK-3β (Cross et al., 1994). Following incubation at 30 C for 30 min, the protein-A sepharose beads were pelleted by centrifugation. 80% of the reaction mix was spotted onto squares of P81 phosphocellulose paper (Whatman), which were then rinsed extensively in 75mM orthophosphoric acid. The amount of γ-^{32}P incorporated into the Crosstide was quantified using a liquid scintillation counter (Beckmann). Background signals, obtained from the "beads alone" controls, were subtracted from the signals gained from the immunoprecipitates, and the results

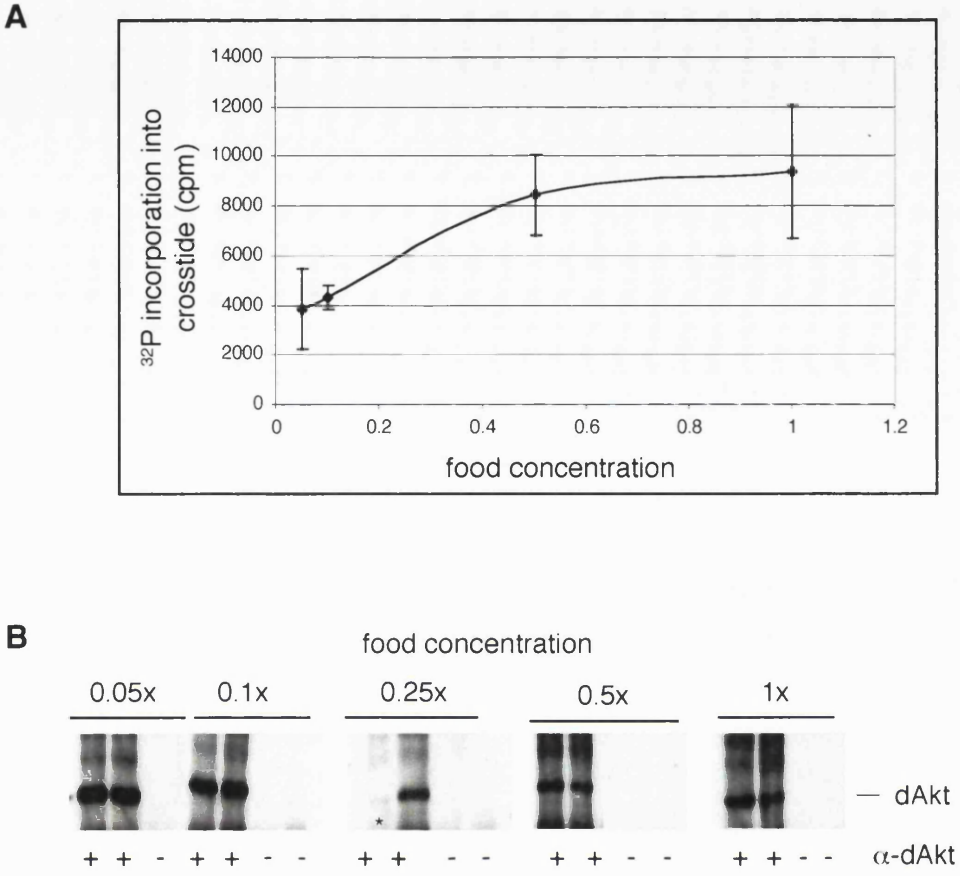

Figure 3.4 dAkt kinase activity in larvae that were calorically restricted 72 hours after egg deposition

α-dAkt was used to immunoprecipitate dAkt from lysates of larvae fed for 72 hours and then calorically restricted on dilutions of 'Normal' food for 24h. **A** Duplicate immunoprecipitates were tested for dAkt kinase activity by assessing their ability to phosphorylate the dAkt peptide substrate, Crosstide in the presence of γ-^{32}P-ATP (Cross et al., 1994). The incorporation of γ -^{32}P was quantified by adhering the phosphorylated Crosstide to P81 phospho-cellulose paper and measuring counts per minute in a liquid scintillation counter. A background signal, obtained from the beads alone controls, has been subtracted from all the values. Immunoprecipitates were then separated using SDS-PAGE (8% gels). **B** shows the Western blots, probed with α-dAkt to visualise the amount of dAkt loaded into each assay. Despite the initial observation that larval dAkt activity reduced as the concentration of food fed to the larvae decreased (see **A**), the differences in activity were not significant (see text). The lane marked with an asterisk on the gel was poorly loaded and as such shows a reduced amount of protein. This point was ignored during analysis.

n = 2

Error bars show standard deviation

displayed on a graph (see figure 3.4A). The immunoprecipitates were resolved on SDS-PAGE gels (8%) and Western blots were probed with α-dAkt in order to visualise the amount of dAkt present in each assay (see figure 3.4B).

Initially, when the absolute amount of ^{32}P incorporation was considered, I believed that the activity of dAkt was reduced as the caloric intake of the larvae decreased. However, on recent re-examination of the raw data, student t-tests indicate that the apparent differences seen are not significant ($p>0.1$). From the Western blots of the immunoprecipitates it is clear that more dAkt was present in the assays of lysates of larvae fed on 0.05× food and 0.1× food than in those from fully fed larvae. Perhaps if dAkt activity levels had been normalised to the amount of protein present in the individual assays, the significance of the differences seen may have been increased. Alternatively, incorporation of this factor may have added a further level of error to the experiment, so differences would have remained statistically insignificant.

The high degree of error associated with these experiments meant that the nutritional control of dAkt activity, and by implication the nutritional regulation of PI3K signalling upstream of Dp110, was neither confirmed nor disproved.

3.6 Comparing *Drosophila* development when third-instar larvae are transferred at different times to diluted normal or standardised food.

As discussed in the introduction (section 3.1) my ultimate aim was to identify which of the dietary components, amino acids or carbohydrates, were more important in PI3K activation. The diet that I had been using up until this point was too complex to allow for dilution of only one component, as both cornmeal and flour contained a degree of both types of nutrient. A new set of diets that contained no cornmeal or flour was trialled (for recipes see figure 3.5A and section 2.2.1). In these diets only yeast extract and sucrose were used to provide nutrients to the developing larvae. Although yeast extract itself contains more than just amino acids, when a further standardised diet (Sang, 1978) was tested, the larvae appeared not to like the food, did not eat, and hence did not develop. The 'standardised' foods (SF) were a compromise solution.

It was important to compare the development of larvae transferred to dilutions of this standardised diet to that of larvae raised on the diluted Normal food (see 3.2A for composition), to see whether experiments carried out on the new food could be compared to those already performed. Several parameters were tested: larval mass 24

hours after transfer, fly size three days after emergence and developmental timing. Two different times of larval transfer were examined: 72 hours and 80 hours.

Figure 3.5B shows the larval masses 24 hours after transfer to dilutions of either NF or SF. The larvae that were given a further eight hours to develop on 1× NF prior to transfer were larger than the larvae transferred 72 hours AED. In addition, if the masses of those larvae on dilutions of NF are compared to the masses of the larvae on the same concentrations of SF, fewer differences are seen when the larvae were transferred at 80 hours as opposed to 72 hours AED.

After transfer, two vials of larvae for each point were left at 25 C until flies emerged. Pictures of the flies formed from larvae transferred after 80 hours development on 1× NF to 0.1×, 0.5×, or 1× SF are shown in figure 3.5C. Note the reduced size of both male and female flies from larvae that were raised from 80 hours on food containing one tenth of the nutritional content of 1× food.

The developmental timing of the larvae on the different regimens was also monitored. The data collected were used to assess whether the larvae had reached their critical mass by the time of transfer. This was important as if critical mass had not been reached, the experiments would contain a further uncontrolled variable of developmental stage that could be responsible for changes in dAkt phosphorylation or activity levels.

A delay in development is seen if larvae are transferred to 0.25× Normal food after 72 hours of development (data not shown). This delay becomes more severe as larvae are further calorically restricted, or if cornmeal and flour are removed from the diet. Very few of the larvae raised from 72 hours on 0.05× NF or SF ever form pupae, and although 70% of larvae on 0.1× NF pupariate this number fell to less than 50% if larvae were transferred to 0.1×SF. Less developmental delay under all conditions was seen if larvae were transferred at 80 hours AED. A delay of around one day is seen in larvae raised on 0.1×SF, and a greater delay is seen in further calorically restricted larvae. However, larvae do pupate, and viable flies are produced on all regimens. In contrast to the increase in developmental time seen between larvae raised from 72 hours AED on dilutions of SF in comparison to those raised on the same dilutions of NF, few timing differences between larvae that were given and denied cornmeal and flour were seen if larvae were transferred from 1× NF after 80 hours.

Figure 3.5 Size of calorically restricted third instar larvae and flies.

A new, more standardised, food was tested which contained only yeast extract as a source of protein and pure sucrose as a carbohydrate source. See **A** for details. Larvae were raised at 25°C for 72 or 80 hours on normal fly food (100 larvae/vial), and then transferred at a density of 50 larvae per vial to dilutions of either the Normal food (+), or the standardised food (-) at the dilutions shown for a further 24 hours. **B** The mean mass the larvae raised on the different regimes (n=20) were calculated after this time. There is less difference in mass between larvae raised on Normal (+) and standardised (-) food if transfer takes place after 80 hours of development. Note the reduction in larval mass as the food is diluted more than twice. **C** If the larvae, transferred to dilutions of the standardised food after 80 hours are left to develop further they will form viable adult flies. The flies generated from highly calorically restricted larvae (0.1x) are smaller than those from well-fed larvae (1x).

A

'Standardised' Food recipes

Food Concentration	1x	0.5x	0.25x
Yeast Extract	8.8%	4.4%	2.2%
Sucrose	7.5%	3.75%	1.875%
Agar	0.8%	0.8%	0.8%
Nipagin	4.0%	4.0%	4.0%
Proprionic Acid	0.8%	0.8%	0.8%

B

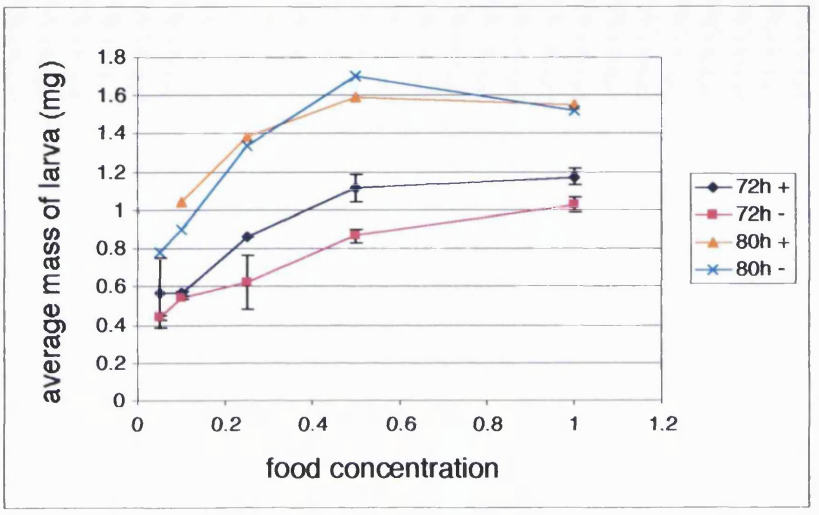

Error bars show standard error of the mean

C

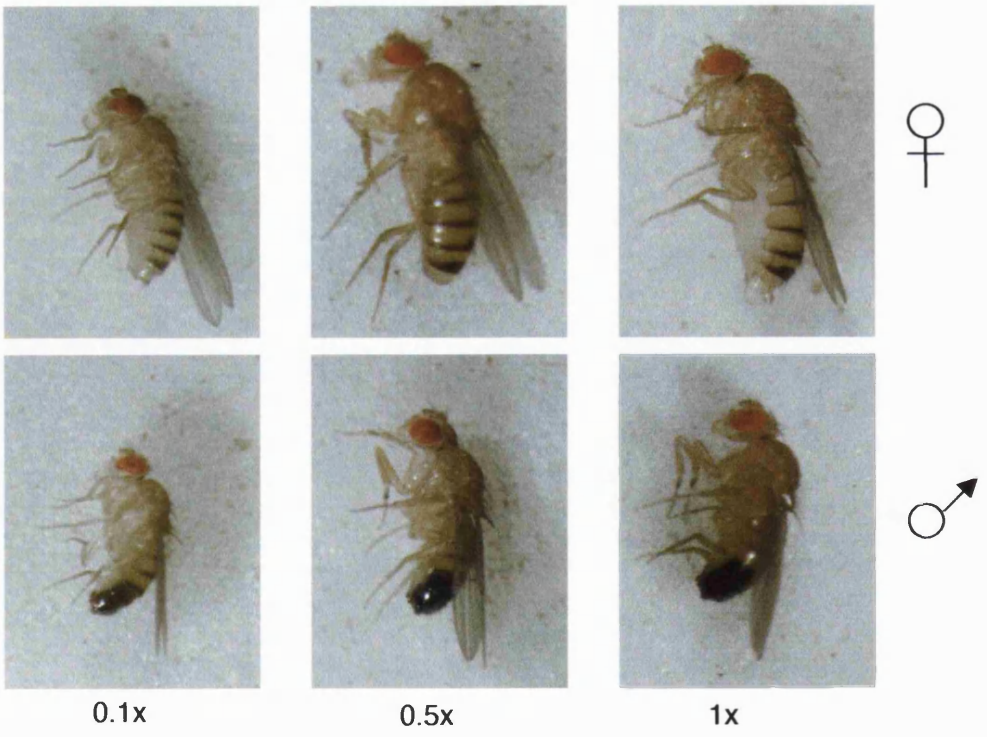

From these results I can conclude that critical mass was not reached even by 80 hours after egg deposition, as developmental delay was seen when larvae were transferred to highly diluted foods. However, less developmental delay and fewer differences in the ability to develop and developmental timing were observed between larvae raised on the diluted Normal or standardised food regimens when larvae were transferred after 80 hours of development. Therefore, this time point was used in further experiments.

3.7 Assaying dAkt activity in third-instar larvae raised on varying dilutions of standardised food.

Larvae were transferred to dilutions of standardised food after 80 hours on 1× Normal food, at a density of 50 larvae per vial. After a further 24 hours, larvae were harvested and lysed, and dAkt activity of the lysates was assayed as described in sections 3.5 and 2.4.6. The dAkt activity in the different lysates is presented in figure 3.6A and Western blots of the α–dAkt immunoprecipitates are shown in figure 3.6B.

Statistical analysis of the data confirmed that the dAkt activity in lysates of larvae fed 0.05× SF for 24 hours was significantly lower than that in lysates of larvae fed 0.1× or 0.5× SF ($p<0.1$). However, it was not significantly lower than the activity in lysates of larvae fed 1x SF. This may be explained by the variable amounts of dAkt seen in the immunoprecipitates from lysates of the "1× larvae".

This result suggests that there is a decrease in dAkt activity as larvae are fed less concentrated food and that therefore larval nutritional levels do feed in to PI3K signalling. However, it also highlights how the variable nature of individual results can reduce the significance of these apparent differences. The technique being used for assessing γ–^{32}P incorporation into the peptide substrate, Crosstide led to low signal to background ratios. Often the activities of immunoprecipitates were less than three times the activities of the beads alone controls. If this low differential between signal and background increased further in individual experiments, owing to lower-than-normal [γ^{32}P]-ATP activity or dAkt concentrations, it became impossible to interpret the resulting data. In an attempt to avoid these difficulties, a new method for assaying Crosstide phosphorylation was adopted.

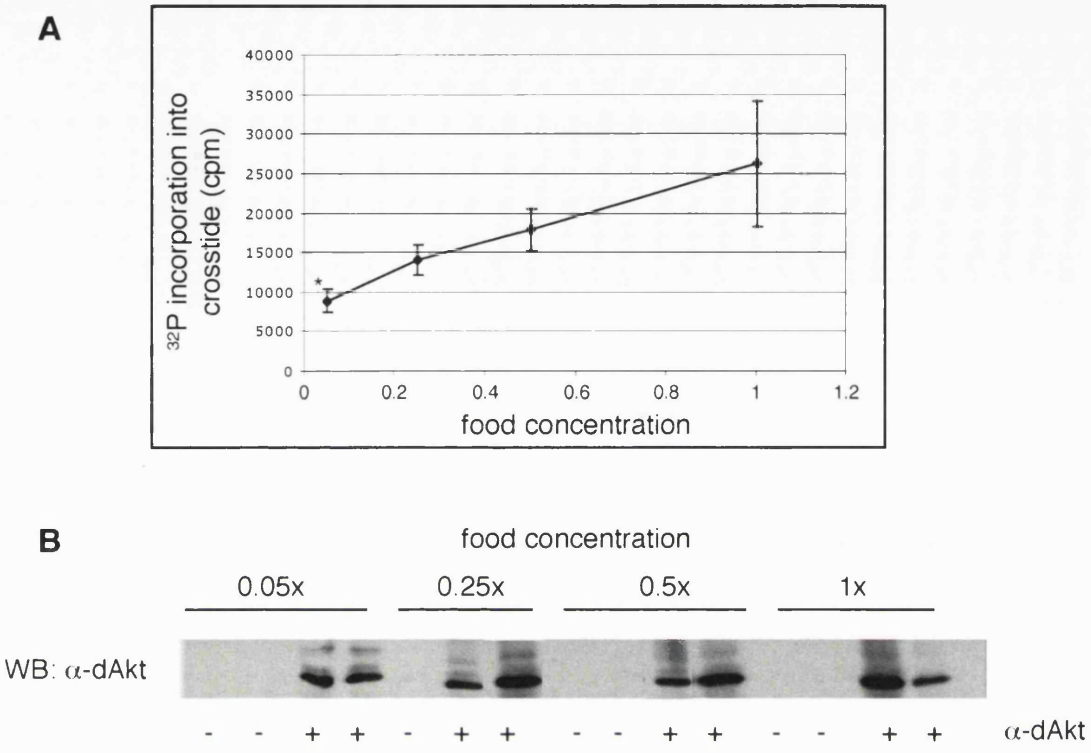

Figure 3.6 dAkt activity in larvae that were calorically restricted 80 hours after egg deposition.

α-dAkt was used to immunoprecipitate dAkt from lysates of larvae fed for 80 hours and then calorically restricted on varying concentrations of the standardised diet for 24h. **A** Immunoprecipitates were tested for dAkt kinase activity as before. An average background activity level calculated from the beads alone controls was subtracted from all values and the data are presented graphically. Immunoprecipitates were then separated using SDS-PAGE (8% gels). **B** Western blots were probed with α-dAkt to visualise the amount of dAkt loaded into each kinase assay. The activity of dAkt in the larvae reduces as the concentration of food fed to the larvae is lowered. The large error seen in the activity of dAkt from larvae raised on 1x food can be explained by the variable amounts of dAkt protein present in the immunoprecipitates.

n = 1

Error bars show standard deviation

3.8 Using Tricine gels to assay larval dAkt kinase activity.

SDS-Polyacrylamide gel electrophoresis in a discontinuous Tris-Tricine buffer system can be used to resolve small peptides and proteins that are between 5–20kDa in weight. The modifications to the buffer system used in traditional Laemmli SDS-PAGE remove the problems associated with non-separation of these small peptides from SDS (Schagger and von Jagow, 1987). By separating the components of 80% of the kinase assay mix on a Tricine gel, then drying the gel and exposing it to a phosphoimager screen I was able to directly visualise the phosphorylated Crosstide using a Storm phosphoimager (see section 2.4.6 for details). The Tricine gel method allowed full separation of the peptide from any unincorporated radioactive ATP. In this way I hoped to reduce the kinase assay background relative to the assay signal.

As the kinase assay method had altered, I optimised both the lysis and immunoprecipitation procedures for the new method. Lysis time was increased from 10 to 30 min and a larger amount of lysis buffer was used (15µl buffer/mg larvae). Lysates made in this way also gave good signals on immunoblots. The larger amount of lysis buffer used was likely to lead to more complete lysis of the larvae and ensure less degradation of constituent proteins, as the ratios of proteinase and phosphatase inhibitors to larval material were increased. In addition, I tested whether "snap-freezing" larvae or lysate in liquid nitrogen affected the final dAkt activity level. It appeared that snap-freezing larvae prior to lysis increased the recorded dAkt activity, presumably by increasing the lysis efficiency. Thus the method was further amended to include a snap-freezing step. The method for immunoprecipitation was slightly altered by reducing the antibody: lysate ratio (see section 2.4.5 for details).

Results from one such experiment, in which the ability of dAkt to phosphorylate Crosstide was monitored on Tricine gels, is shown in figure 3.7. Larvae were transferred to 1×-, 0.1×-, or 0.05×-standardised food at 80 hours AED. After a further 24 hours, larvae were harvested, snap-frozen and lysed. dAkt activity of the lysates was then assessed. Figure 3.7A shows the image of the gel recorded by the Storm phosphoimager. Phosphorylated Crosstide is marked. Figure 3.7B shows the quantification of the phosphoimage. Statistical analysis of the data by student's t-test confirmed that the α-dAkt immunoprecipitates from the lysates of larvae grown for 24 hours on 0.05× standardised food, contained a lower dAkt kinase activity than those from larvae fed 1× standardised food ($p<0.05$). This reduction in activity was not caused by a reduced amount of dAkt protein, as can be seen from the Western blots of

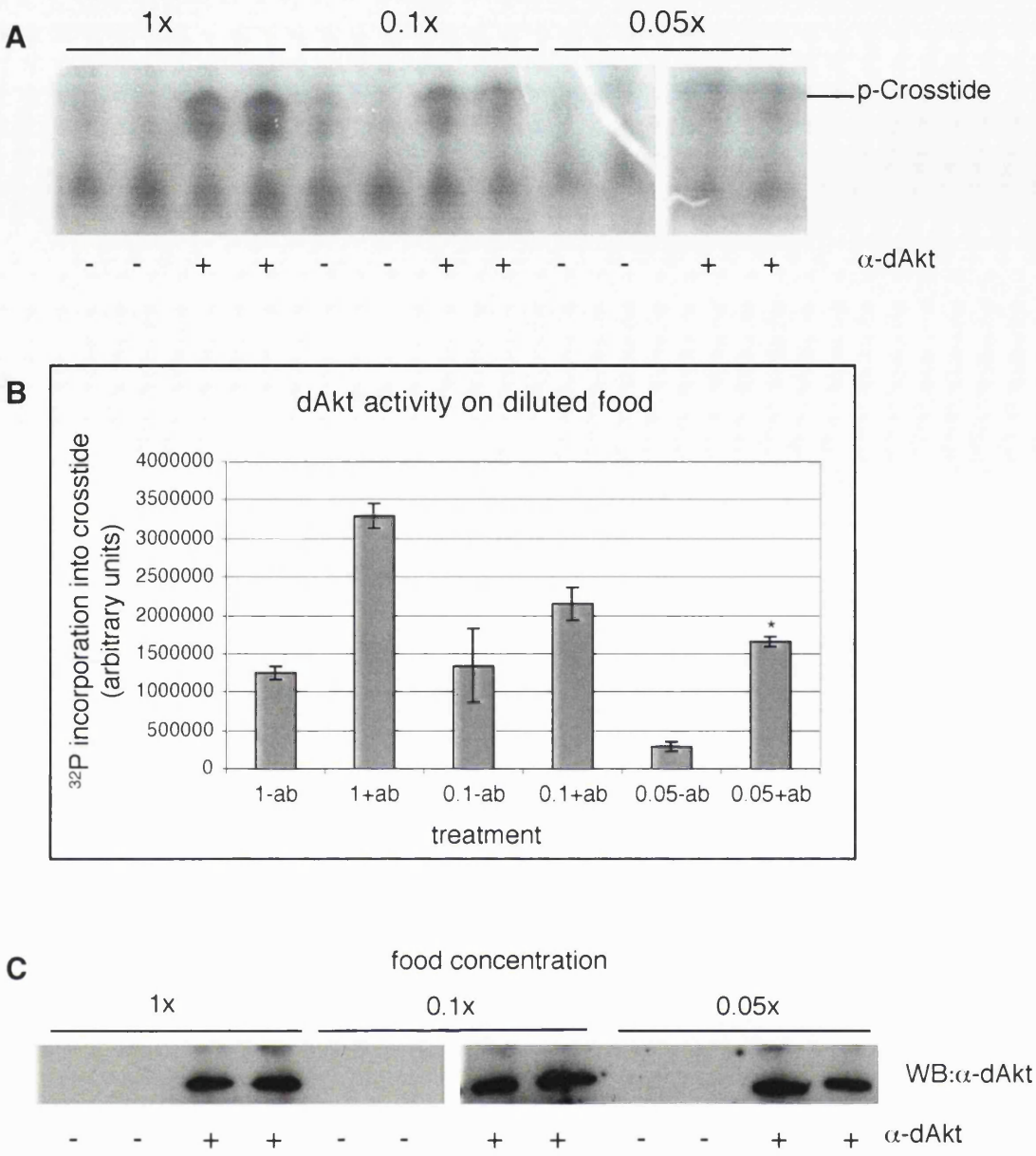

Figure 3.7 Measuring dAkt activity in calorically restricted third instar larvae using Tricine gels

Sets of 100 embryos were grown up on 1x Normal food at 25 C for 80 hours. Larvae were then harvested and transferred to diluted standardised food (50 larvae/vial) for a further 24 hours, and then snap frozen in liquid nitrogen and lysed (15μl lysis buffer/mg larvae). 3μl α-dAkt was used to immunoprecipitate dAkt from the lysates (600μl) and the immunoprecipitates were assayed for dAkt kinase activity. **A** The kinase reaction was separated by SDS-PAGE using the Tris-Tricine discontinuous buffer system. **B** ^{32}P incorporation into the substrate, Crosstide, was quantified from the gel using a phosphoimager. A reduction in dAkt kinase activity was seen in those larvae fed 0.05x food for 24 hours compared to the fully fed larvae. **C** shown western blots of the immunoprecipitates probed with α-dAkt. These show that the reduction in dAkt activity seen was not caused by a reduced dAkt protein level in the assays.

n = 1

Error bars show standard deviation

the immunoprecipitates, probed with α–dAkt (see figure 3.7C). These results indicate that dAkt activity can be regulated by nutrition, and hence Dp110 activity too is likely to be influenced by the levels of larval nutrition. However, the use of Tricine gels failed to increase the signal to background ratio. In fact dAkt kinase activities recorded from immunoprecipitates were less than twice as large as those from beads alone controls.

3.9 dAkt activity in fed, starved and re-fed third-instar larvae

My concern that the diverse composition of yeast extract would not allow the individual effects of sucrose and amino acids on dAkt phosphorylation and activity to be tested, and the reluctance of larvae to develop on more defined food have already been discussed (see section 3.6). In order to overcome these difficulties, I decided to try a different experimental approach involving re-feeding. This approach is analogous to methods used in tissue culture systems, where cells are serum-starved prior to stimulation with a specific reagent, allowing the basal and stimulated states to be compared.

For a schematic of the method used, see figure 3.8A. Briefly, larvae were fed on 1× Normal food until 80 hours AED, at a density of 100 larvae per vial. They were then transferred to either 1×- or 0.05×-Standardised food at a density of 50 larvae per vial for a further 16 hours. Some larvae were then harvested and snap-frozen (to later generate 'fed 16h' or 'starved 16 h' larval lysate), some were left where they were and some of the starved larvae were re-fed by transferring them at the same density to 0.05× food supplemented with sucrose and amino acids to the concentrations recommended by Sang. This re-feeding food contained 0.44% yeast extract (as found in 0.05× standardised food), 5.24% casein hydrolysate (to make up the amino acid concentration to that recommended by (Sang, 1978), 7.5% sucrose, 0.8% agar, 0.8% proprionic acid and 4% Nipagin. After a further four hours, all remaining larvae were harvested and snap frozen.

Lysates of the frozen larvae were made the following day, and dAkt kinase activity was assessed, as before, using the 'Tricine-gel method'. The resulting phosphoimage was quantified (see figures 3.8B and C). Analysis showed that there was no difference in dAkt activity in larvae that were fed for 20 hours and larvae that were starved for 16 hours, which seemed surprising. Furthermore, although a lower dAkt activity was recorded in lysates of larvae that were starved for 20 hours, this

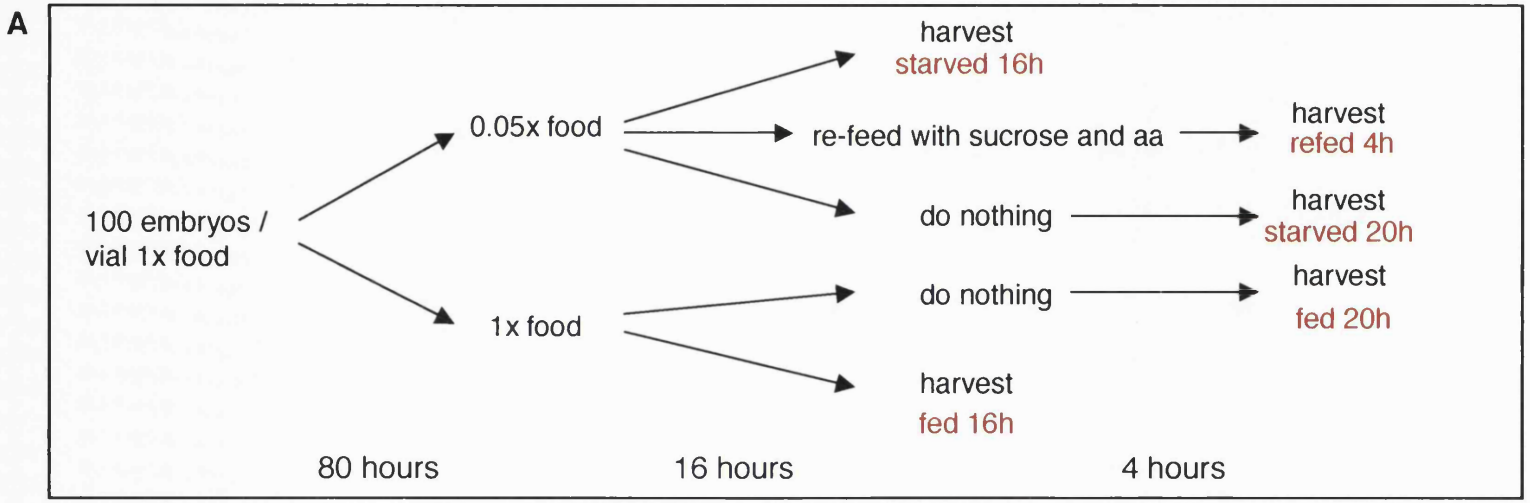

Figure 3.8 dAkt activity in fed, starved and re-fed larvae.

A An outline of the method followed during the re-feeding experiment. Wild-type embryos were allowed to develop on Normal food for 80 hours at 25 C. The larvae (50 larvae/vial) were then transferred to either 1x standardised food (fed) or 0.05x standardised food (starved). After a further 16 hours larvae were either left where they were, or harvested. Half of the harvested starved larvae were re-fed on food containing the concentration of amino acids and sucrose recommended by Sang, 1978. All other harvested larvae were snap-frozen and lysed. After four hours all remaining larvae were harvested, frozen and lysed. α-dAkt was used to immunoprecipitate dAkt from the lysates (400ml). Kinase assays were carried out on the immunoprecipitates and 80% of the resulting assay mix was separated on a tricine gel (**B**). The dAkt kinase activity in each of the lysates was assessed, by quantifying the intensity of the phosphorylated Crosstide band using a phosphoimager (**C**). It is clear from the graph that background levels were high. The dAkt activity in larvae that have been starved for 16 hours, and those that were fed for 20 hours is very similar. The lower level of activity seen in larvae starved for 20 hours may have been because these kinase assays contained less dAkt.

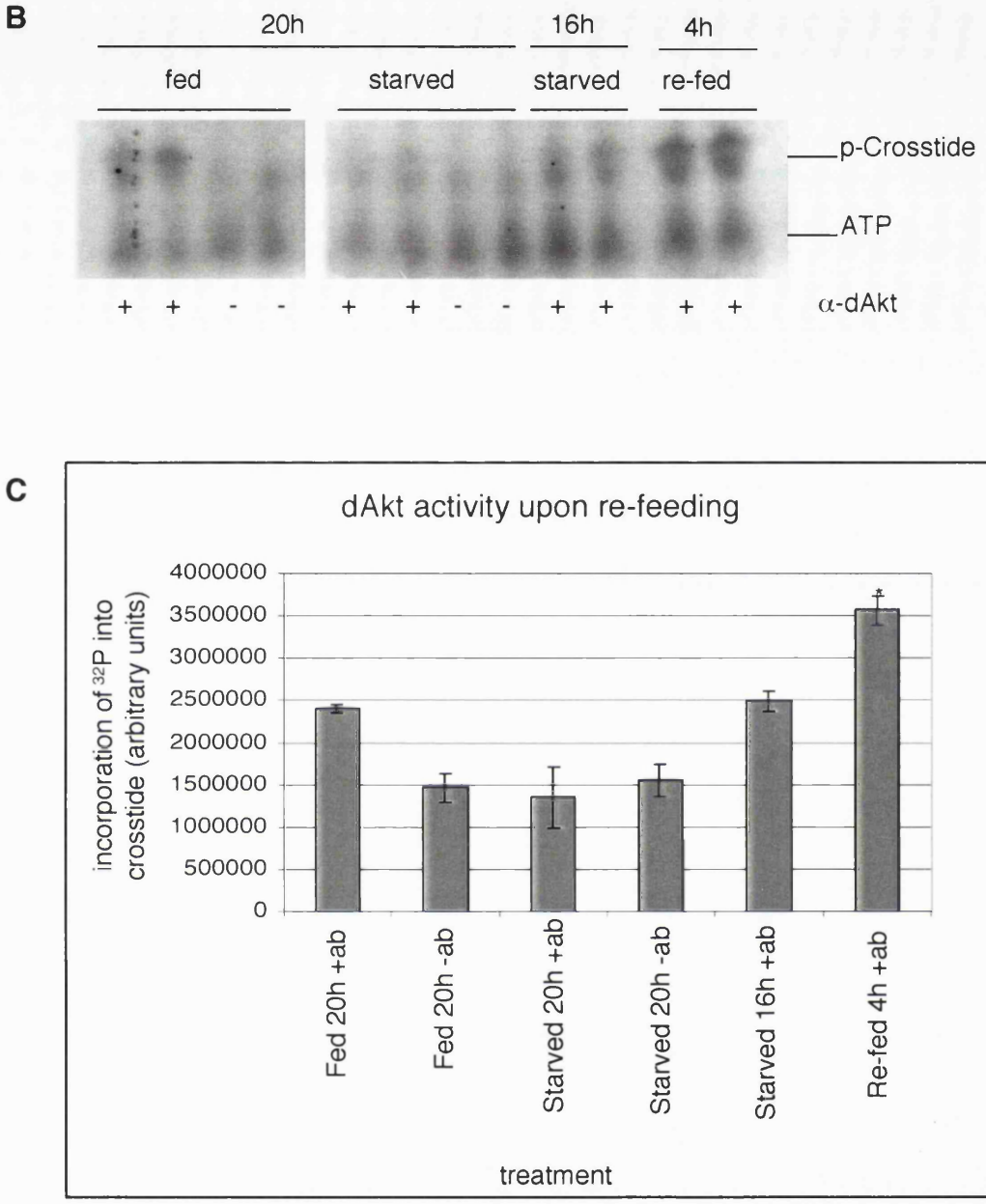

Figure 3.8 cont. Measuring dAkt activity in calorically restricted third instar larvae using Tricine gels

reduction was not statistically significant. However, the larval dAkt activity after re-feeding was significantly increased compared to the activity in 'starved 20h' or 'starved 16h' larvae. The increase in 're-fed' larval dAkt activity compared to 'fed 20h' activity was also significant.

Although these results imply that re-feeding does increase larval dAkt activity compared to that seen in starved larvae, the low signal to background ratio hindered data analysis. Further to this, the increase in dAkt activity upon re-feeding was not seen upon repetition of the same experiment, suggesting that the Tricine-gel method was still subject to poor reproducibility.

3.10 Phosphorylation of dAkt in calorically restricted third-instar larvae, revisited

So far, a number of different experimental approaches have been described that were used to analyse changes in larval dAkt phosphorylation or activation upon modulation of larval nutritional input. The failure of all these methods to provide reproducible results suggests that the overall approach of trying to assess dAkt activity in whole larval extracts may be flawed or over-ambitions. Furthermore, several of the recent experiments failed to detect statistically significant differences between the dAkt activities in lysates of starved or fed larvae.

One final experiment was performed to investigate whether differences in dAkt activity could still be observed in lysates of larvae that were raised from 80 hours of development on varying dilutions of standardised food for 24 hours. Kinase assays were carried out using the Tricine-gel method, but no differences in dAkt activity were seen (data not shown).

I then re-assessed the phosphorylation of dAkt in lysates of calorically restricted larvae, using Western blot analysis. Owing to the recent acquisition of a LI-COR Odyssey infrared scanner I was able once again to quantify Western blots. This had not been possible for several months, as the laboratory had moved location. The LI-COR Odyssey system relies on the use of secondary antibodies that are directly coupled to infrared dyes. Two different dyes are available that allow simultaneous two-colour detection. This is made possible by the lack of overlap in the emittance spectra of the two dyes. The immunoblots are scanned directly and the captured image data can be quantified. As the system does not rely on a chemical reaction for visualisation, the relationship between the quantified data and the amount

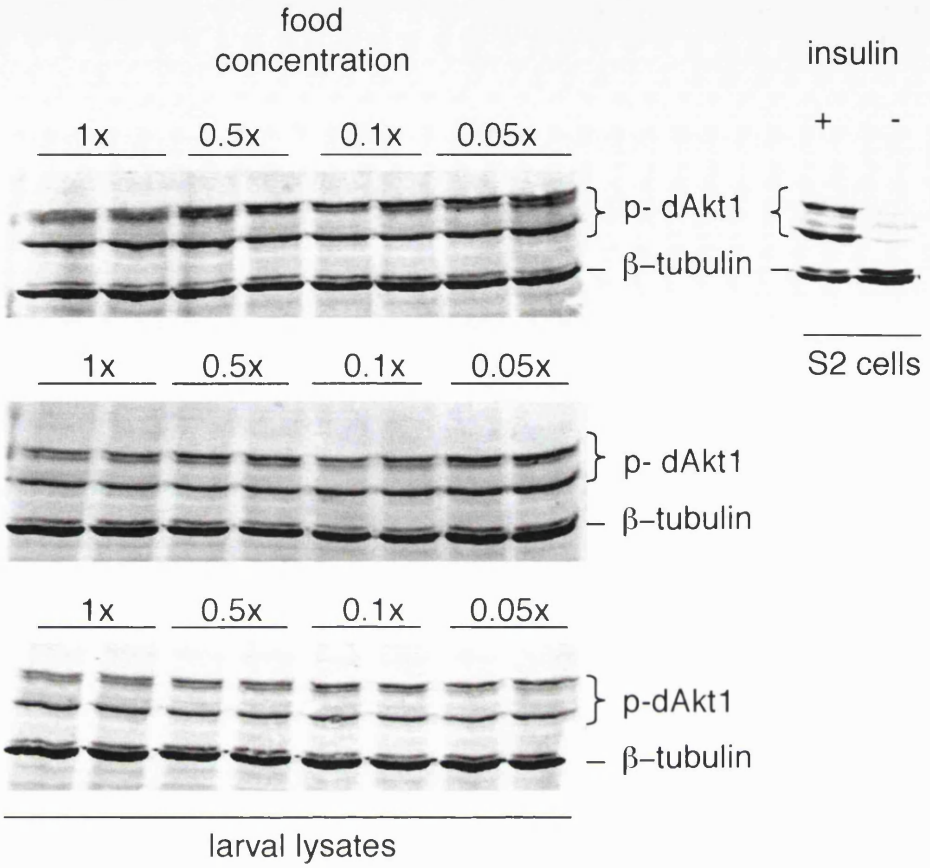

Figure 3.9 Phosphorylation of dAkt in calorically restricted third-instar larvae (revisited)

Wild-type embryos, deposited during a three-hour egg lay were grown up for 80 hours on complete food (100/vial), following which, larvae were harvested and transferred to diluted food (1x, 0.5x, 0.1x and 0.05x) at a density of 50 larvae per vial. After development for 17 hours, these larvae were harvested and snap frozen in N_2(l) in 20mg aliquots. These were lysed in 300μl lysis buffer and the lysates were resolved in duplicate using SDS-PAGE (8% gels). Three independent samples were made for each point. Western blots were probed with α-pSer586 and α–β-tubulin primary antibodies and α-rabbit-800 and α-mouse-680 secondary antibodies. The blots were visualised and quantified using the LI-COR Odyssey Infra-Red scanner. No differences in dAkt phosphorylation could be seen in the lysates from the differently treated larvae.

of protein on the blot is more linear than was possible when using the FLUOR-S Max. Further details on the Western blotting method can be seen in sections 2.4.11 and 2.4.12.

This experiment was performed in triplicate. As can be seen in figure 3.9, no differences were seen in the amount of p-dAkt in the lysates of larvae that had been fed or calorically restricted for 17 hours after feeding for 80 hours. This was not due to differences in loading, shown by the equivalent amounts of β-tubulin in each lane. In contrast to earlier data, these results implied that signalling flux through the PI3K signalling pathway was not altered by the modulation of larval nutritional input.

3.11 Summary

The aim of the experiments presented in this chapter was to discover whether nutrition activated Dp110 in *Drosophila* larvae, either directly or indirectly. In order to do this, first- or third-instar larvae were raised for 24 hours on regimens that provided them with varying levels of nutrients, and the phosphorylation state or activity of dAkt, a downstream component of the PI3K signalling pathway, were then assessed in larval lysates of these larvae using biochemical techniques.

Although in some preliminary experiments, lower levels of dAkt phosphorylation appeared to correlate with a reduction in larval nutrition, the sensitivity of immunoblotting methods used and the low levels of endogenous dAkt protein extracted combined to reduce reliability and reproducibility of these results. Later, when larvae were only calorically restricted for 17 hours, no differences in the phosphorylated dAkt signal were recorded from Western blots by the more sensitive LI-COR Odyssey infrared scanner.

Two different methods were used to measure dAkt kinase activity by assessing the level of phosphorylation of a dAkt peptide substrate, Crosstide, by α-dAkt immunoprecipitates from larval lysates: liquid scintillation counting and phosphoimaging of Tricine gels. Both assays of dAkt kinase activity were subject to high background to signal ratios. In some experiments the high background levels may have masked differences in the dAkt activity in different lysates. In any case, results from these experiments were not highly reproducible. No firm conclusions can be drawn about how nutrition affects larval Dp110 activity despite some experiments showing that severe caloric restriction does lead to a significant reduction in dAkt activity levels.

In order to take this investigation further, for example to examine the impact of re-feeding starved larvae with either amino acids or sucrose, the effect of starvation on larval dAkt phosphorylation and activity needed to be clear. The low reproducibility of experiments hindered the formation of such definite conclusions. We therefore reasoned that our experimental approach was not appropriate to observe physiological changes in larval dAkt phosphorylation or activity in response to changes in larval nutritional input. In addition, other researchers had used a different and more successful experimental approach to investigate the issue of the nutritional control of the PI3K signalling pathway (see section 3.12 for further details). Together these factors made me decide not to continue with these investigations.

3.12 Discussion

Figure 3.3 shows that as the concentration of larval food reduces, the phosphorylation of larval dAkt reduces co-ordinately, yet from figure 3.9 I concluded that larval food concentration had no effect on the phosphorylation of dAkt. Multiple factors could have cause the difference in these results. The most obvious factor is the time spent by larvae on the diluted foods. It is possible that 17 hours was not a sufficient length of time for differences in dAkt phosphorylation to appear. In fact, Jessica Britton and Bruce Edgar report that PI3K activity in larvae only reduces significantly after 24 hours (Britton et al., 2002). However, in support of using an earlier time point, Zinke and collegues have reported differences in some transcript levels as early as one hour after starvation (Zinke et al., 2002). Alternatively, the difference could be ascribed to transferring larvae to the restricted diet at 80 hours, rather than 72 hours AED. This reason seems less plausible, as reductions in larval dAkt activity linked to decreasing larval nutrition had been seen when an 80 hours transfer time point was used (see figures 3.6 and 3.7). A further possibility is that the optimisation of the lysis procedure led to the differences in results. In the later experiment larvae were snap-frozen after harvesting and lysed for an extra 20 min in three times as much lysis buffer. These modifications are likely to lead to more thorough lysis of the larvae, and invite the speculation that the modulation of dAkt phosphorylation occurs only in a small proportion of the larval tissues, and that these tissues are preferentially lysed.

A large amount of inter-experimental variation was seen between the experiments described in this chapter, even when experimental methods remained

constant. This could well have been caused by the nature of the experiments: analysing changes to endogenous larval protein after alteration of external environmental conditions. Perhaps dAkt phosphorylation and activity are affected not just by changes in food availability but also by small fluctuations in temperature, humidity, larval stress levels or other external factors. This would mean that results obtained from biochemical analyses of larval lysates would incorporate all these factors, not only those that were being actively tested. If this is the case, then it may account for the fact that a difference in dAkt activity in larvae raised on 1× and 0.05× food was seen in the experiment presented in figure 3.7, but not in experiment 3.8. Because of the more involved experimental method of the re-feeding experiments, larvae often remained in Eppendorf tubes on the bench after harvesting and before weighing and snap freezing, while other larvae were harvested and transferred to different diets. This delay could easily have increased larval stress levels.

As discussed in section 3.11, the biochemical assays used to monitor dAkt activity were subject to high background to signal ratios. Previously these assays had been used to assess dAkt activity in lysates of *Drosophila* cells over-expressing dAkt protein (Scanga et al., 2000; Verdu et al., 1999) or in lysates of *Drosophila* adults or embryos, both of which contain a higher concentration of dAkt than larvae (Andjelkovic et al., 1995). The assays proved not to be sensitive enough to reproducibly record physiological changes in endogenous larval dAkt activity. Perhaps sensitivity could have been increased by changing immunoprecipitation conditions, for example by reducing the amount of antibody or protein-A used, which may have reduced non-specific binding of larval proteins. Changes that were made to the assay method, both in the lysis and monitoring of radioactive phosphate incorporation into Crosstide, did not increase the sensitivity sufficiently to persuade me that reproducible results would be forthcoming.

3.12.1 Do larval nutritional levels affect PI3K signalling?

It is now clear that nutrition, and in particular amino acids, do feed in to the *Drosophila* PI3K signalling pathway upstream of Dp110. Dp110 activity in amino acid starved and fed second-instar larvae (48-60 hours AED) was monitored using a PIP_3-binding PH domain from *Drosophila* cytohesin1 fused to GFP (GFP-PH). In fed larvae, GFP-PH is localised to the membrane of larval epithelial cells. However, if larvae are starved for 24 hours, the membrane localisation of the fusion protein in

these cells decreases. Further reductions are seen after 48 hours of starvation (Britton et al., 2002). If larvae are re-fed for one or two days, the membrane localisation of GFP-PH is restored (Britton et al., 2002). This suggests that starving larvae of amino acids induces a reversible reduction in PI3K signalling levels. Note that differences in absolute levels of GFP-PH were also observed upon starvation, and that the data were not quantified.

Several models could account for this reduction in PI3K signalling (see figure 3.10):

1. Larval tissues could autonomously monitor the level of nutrients in the larval hemolymph, in part via dTOR. As the concentration of amino acids in the hemolymph drops, down-regulation of dTOR activity could cause not only a cell-autonomous reduction in growth but also a cell-autonomous reduction in Dp110 activity, via an unknown mechanism.
2. The production or secretion of DILPs in the larval brain could be nutritionally regulated. If the concentration of the ligands in the hemolymph reduces as larvae are starved a co-ordinate decrease in signalling flux through the *Drosophila* PI3K pathway in all tissues will be observed.
3. The production or secretion of another molecule, "Factor X", could be negatively regulated by a reduction in larval nutritional input. The function of Factor X would be to positively regulate signalling via Dp110, perhaps by synergising with the DILPs.
4. The production or secretion of another molecule, "Factor Y", could be positively regulated by a reduction in larval nutritional input. The function of Factor Y would be to down regulate signalling via Dp110 perhaps by negatively regulating DILP or receptor function.

3.12.2 How does nutritional input modulate larval growth?

Recent research has begun to shed light on what is actually happening at the molecular level in the larva as larval nutritional input is varied. As discussed earlier, if dTOR activity is lost in clones of cells in the developing *Drosophila* wing imaginal disc, or in the larval ERTs, the cells within that clone are smaller, and divide less than cells in clones of wild type cells (see section 3.1; (Oldham et al., 2000; Zhang et al., 2000). These data partially support the idea that developing cells do respond to

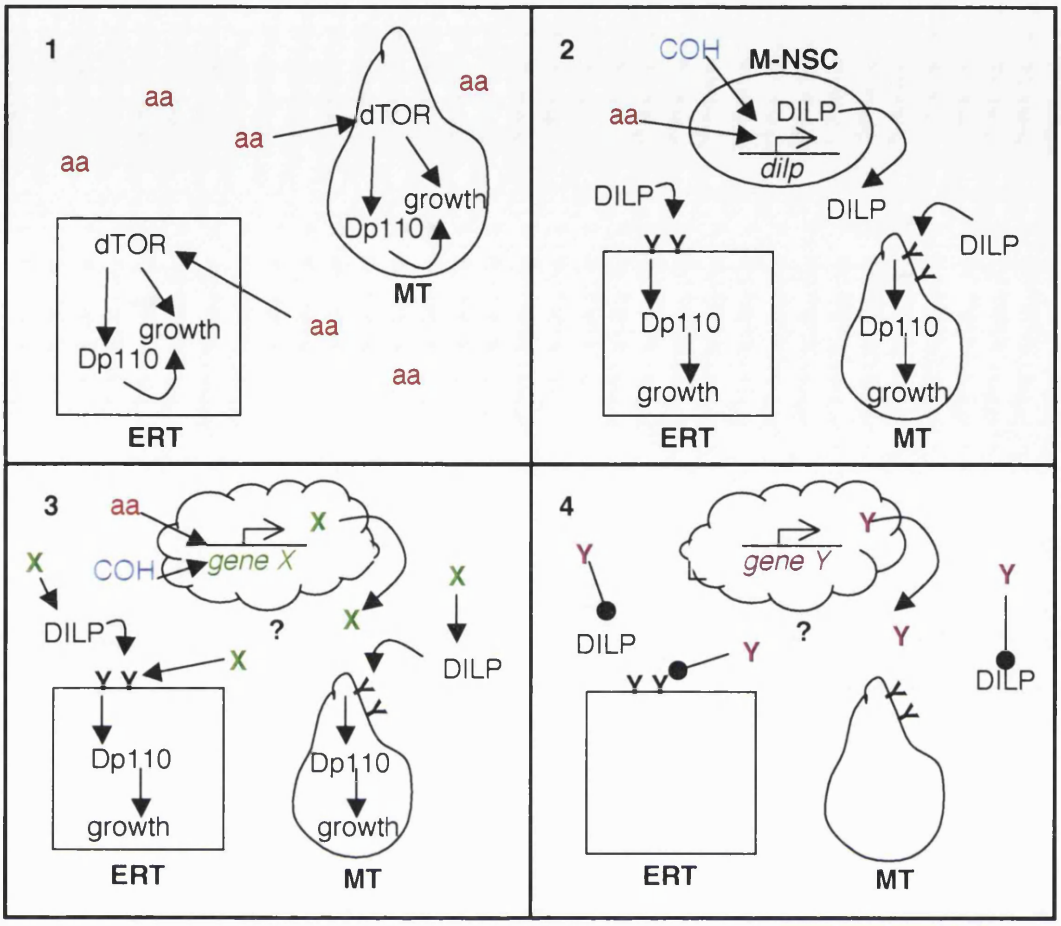

Figure 3.10 Models of the nutritional regulation of PI3K signalling in larvae

MT stands for mitotic tissues. These include the imaginal discs and larval neuroblasts. ERT stands for endoreplicating tissues. These include salivary glands, fat body and larval epidermis. M-NSCs stand for median neurosecretory cells. These are the cells in the larval brain where DILP2, 3 and 5 are produced. COH stands for carbohydrates.
(1) Amino acids (aa) are sensed by all larval tissues. The presence of amino acids leads to dTOR activation. This in turn supports growth, and possibly Dp110 activity, in a cell-autonomous manner.
(2) The production and secretion of *Drosophila* insulin like peptides (DILPs) is regulated by levels of both aa's, and carbohydrates in the hemolymph. When levels are high, DILP production and secretion increases, and the ligands stimulate Dp110 activity in larval tissues via receptor activation.
(3) The production or secretion of a Factor X, from an unidentified larval tissue (?), is up regulated by the presence of nutrients in the hemolymph. Factor X positively regulates signalling via the *Drosophila* PI3K pathway.
(4) When nutrient levels are low in the larval hemolymph, the production and secretion of a Factor Y, from an unknown tissue is up regulated. This negatively regulates signalling via the *Drosophila* PI3K pathway.

circulating amino acid levels and thereby modulate dTOR activity thus altering their growth and division rates accordingly. However there is as yet no evidence that reduction of dTOR activity can lead to negative regulation of PI3K signalling. In contrast, a mechanism of negative feedback on the PI3K pathway downstream of *high* dTOR activity has been proposed, based on evidence from mammalian cell culture. In this mechanism S6 kinase, which is activated via TOR and PI3K signalling, phosphorylates the insulin receptor subunit (IRS). This phosphorylation leads to the degradation of IRS via the proteosome (Haruta et al., 2000).

In favour of the model 2, it has been shown that the transcription of some *Drosophila* insulin like peptide genes *(dilps)* is nutritionally regulated (Ikeya *et al.*, 2002). The particular *dilps* tested, *dilp2, dilp3* and *dilp5*, all have high levels of transcription in a set of seven median neurosecretory cells (m-NSCs) in the larval brain (Brogiolo et al., 2001). The axons of these m-NSCs terminate on the heart and in the corpora cardiaca compartment of the ring gland (Ikeya et al., 2002; Rulifson et al., 2002) and antibodies have recognised DILP2 within these processes. Furthermore, DILP2 has been visualised outside the m-NSCs both on the heart and outside the lumen of the heart (Rulifson et al., 2002). Together these results suggest the heart surface may be a site of DILP release to the openly circulating hemolymph. Out of the three genes tested, the transcription of both *dilp3* and *dilp5* was reduced by complete starvation of larvae for 24 hours at 72 hours AED (Ikeya et al., 2002). Although *dilp2* transcription was unmodified, translation of the resulting mRNA, DILP2 protein processing or DILP2 secretion may have been affected by the starvation regime. These results suggest that the down-regulation of PI3K signalling seen in starved larvae could, in part, be due to reduction in the concentration of circulating DILPs. The lower levels of ligand acting directly on larval tissues would reduce PI3K signalling in those tissues and hence growth. In addition, the resultant down-regulation of PI3K signalling in a specific tissue, such as the fat body, may alter the rate of production or secretion of a second signal, a 'Factor X' or a 'Factor Y'.

Some data supporting the presence of a second humoral signal, originating from the fat body have already been discussed in this chapter. These include the ability of fed larval fat body to support the *in vitro* culture of imaginal discs (Davis and Shearn, 1977) and to induce quiescent larval neuroblasts to enter the cell cycle (Britton and Edgar, 1998). Further evidence for the existence of such a signal is presented below. This suggests firstly that the fat body does monitor amino acids

directly and secondly that the level of amino acids recorded by the fat body has an affect on the growth and behaviour of the whole larva.

Larvae that carry mutations in the *minidiscs* gene have smaller imaginal discs than wild type larvae, yet these discs can grow normally in wild-type larval hosts (Martin et al., 2000). This is consistent with minidiscs being involved in the non-autonomous regulation of growth, probably via a secreted signal. The *minidiscs* gene encodes a protein with twelve putative membrane-spanning domains, whose sequence resembles that of an amino acid transporter. Furthermore, the *minidiscs* transcript accumulates in the fat body (Martin et al., 2000).

More recent data comes from Pierre Leopold's laboratory. They too have identified a putative amino acid transporter that is present in the fat body. They have called this protein Slimfast. Larvae that carry strong hypomorphic mutations for *slimfast* experience developmental delay and some arrest growth at the larval stage. If flies are generated from these mutant larvae, they are smaller and slimmer than wild type, similar to flies from larvae starved after they have reached their critical mass. In addition, the fat bodies of *slimfast* mutants resemble those of starved larvae, with increased vesiculation and a reduction in opacity. If the expression of Slimfast is reduced specifically in the fat body by the targeted expression of anti-sense *slimfast* mRNA, then the larvae look as though they have been starved, with the growth of ERTs being affected more than the growth of discs (Columbani *et al.*, 2003).

Both of these sets of experiments suggest that the uptake of amino acids into the fat body controls the secretion of a growth regulating humoral signal, supporting our third or fourth models. A further experiment showed that when Slimfast expression is reduced in the fat body, levels of PI3K signalling are down regulated in the larval epidermis (Columbani *et al.*, 2003). These data support the idea that at least one of the secreted signals acts as we hypothesised to positively or negatively regulates PI3K signalling. For the sake of argument, let us consider that this signal acts as a Factor X to positively regulate signalling.

The question remains of how the presence of amino acids in the fat body leads to the production or secretion of such a signal. Previous data showed that activating the PI3K signalling pathway specifically in the larval fat body caused larvae to become starvation sensitive. Also, inhibiting PI3K signalling in the fat body, by over-expression of p60 caused larvae to look as though they had been starved (Britton et al., 2002). Together, these data suggest that Factor X production or secretion might

lie downstream of PI3K. However, Columbani and co-workers have questioned this data. When they over expressed dPTEN specifically in the larval fat body, they were unable to see the effects on fat body morphology, developmental delay or body size that had been previously reported as a consequence of down regulating fat body PI3K signalling. In contrast they suggested that the release of the humoral signal was regulated by dTOR activity, as over-expression of the negative regulators of dTOR, dTSC1 and dTSC2 in the fat body, generated a starvation like phenotype.

The discrepancy between these data could well be due to the use of different drivers to induce fat body expression. The *Adh* driver, which was used by (Britton *et al.*, 2002) was not particularly fat body specific: dPTEN or p60 expression would have also been induced in the gut and the salivary glands as well as in other areas at a lower level, such as the trachea. Columbani instead used a *pumpless* driver, which induces expression only in the larval fat body and the salivary glands. Additionally, Jessica Britton's over-expression of p60 in the fat body may have had wider effects than the intended reduction in PI3K pathway signalling. Perhaps another, as yet unknown function of p60 was increased, or perhaps signalling via alternative pathways was reduced, as over expressed p60 bound promiscuously to many different phosphorylated tyrosine motifs. A further possible explanation is that the *Adh* driver induces stronger expression of dPTEN than the *pumpless* driver. This higher level of dPTEN expression may be sufficient to significantly reduce activity of dTOR via a down-regulation of dAkt activity, which would lead to a coordinate increase in dTSC1/2 activity (see chapter 1 for further details). The lower level of dPTEN expressed downstream of the *pumpless* promoter may not have this stronger effect.

A working model for the nutritional control of larval growth is presented in figure 3.11. Firstly, larval tissues respond directly to circulating amino acid levels by activating dTOR when levels are high, via an unknown mechanism. Active dTOR then activates growth in a cell-autonomous manner. The transport of amino acids from the larval hemolymph into the fat body and the resulting activation of dTOR are of particular importance. Not only does active dTOR lead to the growth of the fat body, but it also promotes the production and/or the secretion of a Factor X into the hemolymph. This Factor X activates growth in the other larval tissues, perhaps by cooperating with DILPs. The DILPs stimulate growth of the larva by activating the *Drosophila* insulin/PI3K signalling pathway in the mitotic and endoreplicating tissues. The production, and possibly the secretion, of DILPs is also dependent on levels of

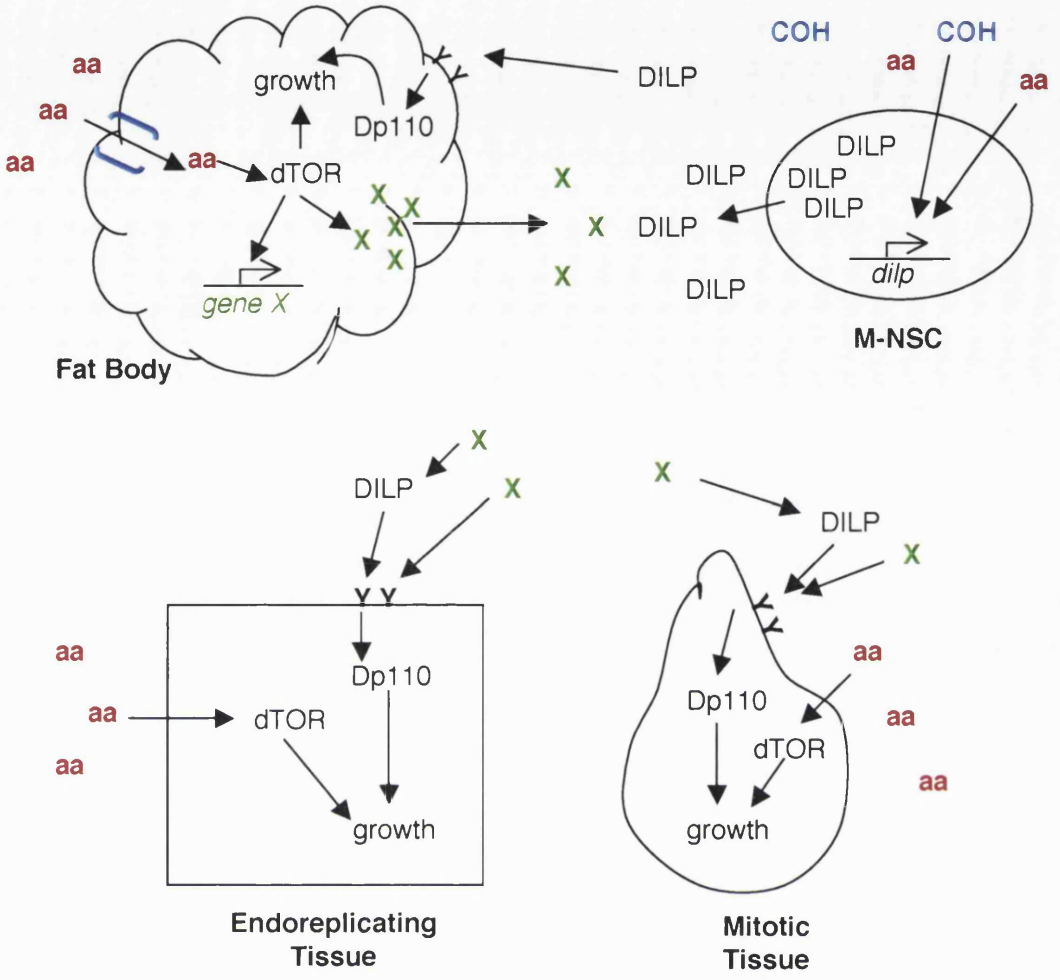

Figure 3.11 The nutritional control of growth in the *Drosophila* larva

Larval tissues respond to circulating amino acid levels directly. When levels are high, dTOR is activated. This activation can then lead to increased tissue growth via a cell autonomous stimulation of cell division and cell growth. PI3K activity in both mitotic and endoreplicating tissues increases the growth of those tissues. This activity is stimulated by the presence of *Drosophila* insulin like peptides in the hemolymph(DILPs). DILP production in the median neurosecretory cells (m-NSCs) and possibly DILP secretion is positively regulated by high levels of circulating nutrients. A second secreted signal from the fat body (Factor X) acts to promote PI3K signalling in both the endoreplicating tissues and the mitotic tissues, via an unknown mechanism. The production and or secretion of this factor X is regulated by the levels of circulating amino acids. Amino acids (aa) enter the fat body through transporters, such as Minidiscs or Slimfast and their presence in fat body cells increases the activity of dTOR. Active dTOR then stimulates the production or secretion of this factor X.

larval nutritional input. The presence of nutrients, possibly carbohydrates in particular, is signalled to the m-NSCs, which respond by secreting DILPs into the hemolymph.

3.12.3 What is Factor X?

There are still outstanding issues to resolve. Most importantly, what is this Factor X, and how does it work? As mentioned previously, one set of candidates are the imaginal disc growth factors (IDGFs). These proteins are strongly expressed in the larval fat body. They are structurally related to chitinases, but are believed to lack chitinase activity (Kawamura et al., 1999). The addition of recombinant IDGF1 or IDGF2 to supplement-free cell culture medium was sufficient to stimulate proliferation of clonal imaginal cells. Furthermore, the IDGFs synergise with insulin to stimulate cell proliferation to a greater degree than the additive effects of the individual growth factors (Kawamura et al., 1999). This observation led Kawamura to suggest, "IDGFs might function as co-factors of *Drosophila* insulin", in much the same way as our hypothetical Factor X.

Clearly, further experiments need to be carried out to discover if IDGFs do work *in vivo* as we are suggesting. One interesting line of investigation would be to look at whether larval ERTs and mitotic tissues have a differential requirement for IDGFs. If so, this may account for the different effects of starvation on these two tissue types. Alternatively, these differential effects could be explained by the existence of other molecules that act as Factor Xs, or indeed Factor Ys, some of which may act specifically on one or the other tissue type.

3.12.4 The effects of Dp110 over-expression in the larval fat body

One further question remains unanswered. If the PI3K pathway is not required for the release of a nutrition dependent signal from the fat body, how is it that over-expression of Dp110 specifically in the fat body leads to a starvation sensitive phenotype (Britton et al., 2002)? Earlier, I suggested that this up-regulation of PI3K pathway signalling in the fat body may lead to the inappropriate expression of a Factor X, causing the larvae to behave as if they were fed, and thus perish prematurely upon starvation (see section 3.1). According to our new model, this could be the case if the up-regulation of PI3K signalling was sufficient to activate dTOR, via the phosphorylation and inhibition of dTSC1/2 by dAkt. As yet, an increase in dTOR activity under these conditions has not been specifically confirmed. My alternative explanation was that high levels of PI3K signalling may inhibit nutrient mobilisation

from the fat body, and this still remains a possibility. In addition, the active PI3K signalling in the fat body could instruct the fat body cells to continue to take up nutrients and this too will accelerate the reduction of circulating nutrients, further sensitising the larva to starvation.

A further effect of over expressing Dp110 in larval fat bodies is intriguing, and worthy of consideration. If these larvae are raised in the presence of plentiful food, they frequently wander away from that food. This behaviour is reminiscent of third instar larvae, which wander away from food sources prior to pupariation. Furthermore, if Dp110 is expressed ubiquitously in *Drosophila* larvae, nearly all the larvae wander out of the food, and pupate precociously (Britton et al., 2002). Data from another laboratory sheds some light on a possible mechanism behind this behaviour.

The *pumpless* gene encodes a protein with homology to a vertebrate enzyme involved in glycine catabolism. *Drosophila* larvae that contain mutations in *pumpless* are initially indistinguishable from wild-type, but after the larvae reach the first instar stage, they become unable to pump food from the pharynx to the oesophagus. Although the larvae are unable to ingest food, they do not behave as if they are starving. They do not up regulate genes associated with starvation, and they begin to move away from any food sources rather than being attracted towards them (Zinke et al., 1999). Again, this behaviour is reminiscent of third instar larvae, that wander away from the food before they pupariate.

The difference in phenotype between larvae carrying loss of function *minidiscs* or *slimfast* mutations, and that of *pumpless* mutants can be explained by the difference in amino acid levels in the fat body. The fat bodies of *pumpless* mutants will contain a high level of amino acids that are unable to be catabolised. This situation may well lead to high levels of dTOR signalling in the fat body. In contrast *minidiscs* and *slimfast* mutants will have low levels of fat body amino acids, and hence low levels of fat body dTOR signalling. Ingo Zinke proposed that perhaps an amino acid-dependent signal that arises from the fat body induces cessation of feeding in the larva. A down-regulation of *pumpless* expression near the end of the third instar stage that would probably increase fat body amino acid levels is consistent with this signal inducing larval wandering behaviour. In fact it is possible that this *pumpless* down regulation is hormonally controlled. As yet, it is unclear whether in wild type larvae this negative feedback on feeding behaviour only takes place at the end of the third larval instar. In

favour of it being operational at other times, there is some evidence that high levels of amino acids in the diet can also decrease larval feeding (Zinke et al., 1999).

If this proposed mechanism, that a high concentration of fat body amino acids leads to the release of a signal that stops the larva from feeding, is correct, then it could explain the behaviour of those larvae that over express Dp110 in their fat bodies. Over expressed Dp110 would lead to the phosphorylation and activation of dAkt, which in turn would phosphorylate and inhibit the dTSC1/2 complex. This would then increase dTOR activity in the fat body, increase the levels of this unidentified signal in the hemolymph, and cause larvae to cease feeding prematurely.

Our initial model now needs refining, as not only can the presence of amino acids in the fat body promote larval growth via secreted signals but if those levels exceed a threshold level then they can also negatively feed back on larval feeding behaviour, thereby indirectly inhibiting growth. In both cases the production and/or secretion of the signals involved in producing the behavioural effects downstream of amino acids is also likely to be downstream of dTOR.

Chapter 4: Functional analysis of Dp110 mutated within its Ras-binding domain

4.1 Introduction

As discussed in chapter one, the catalytic subunits of mammalian class I PI3K molecules, along with Dp110, contain a Ras-binding domain. A homologous domain is present in all Ras effectors and is required for interaction with the small GTPase. Figure 4.1 shows an alignment of the RBDs from the catalytic subunits of several PI3K molecules from different species. Note that the presence of a RBD in PI3K molecules is conserved even in evolutionarily distant species such as the slime mould, *Dictyostelium* (Funamoto et al., 2002). The homology between individual sequences was assessed using the CLUSTAL W programme. This calculated that Dp110 contained a RBD with 37% similarity to the comparative domains in human p110β and p110δand a slightly lower homology to those of the other mammalian p110 molecules.

The presence of this domain has led researchers to question whether the catalytic subunits of Class I PI3K molecules can bind to Ras or a Ras-related small GTPase. Co-immunoprecipitation experiments using a variety of mammalian cell lines showed that all of the Class I PI3K catalytic subunits were capable of binding Ras in a GTP dependent manner (Deora et al., 1998; Rodriguez-Viciana et al., 1994; Rodriguez-Viciana et al., 1996b; Suire et al., 2002) . Furthermore, the p110γ-binding ability of Ras could be increased by the post-translational farnesylation of the small GTPase (Rubio et al., 1999). This farnesylation enables Ras to localise to the membrane.

Now, the crystal structure of porcine p110γ, a class IB PI3K catalytic subunit, bound to N-Ras, which in turn was bound to a nonhydrolysable GTP analogue, has been solved (Pacold et al., 2000). This further supports the likelihood that the catalytic subunits of p110 do bind to Ras *in vivo*. However, the recorded binding affinity of these two molecules is low, with a high dissociation constant of around 3 μM. In order that the two molecules would bind tightly enough to co-crystallise, which was necessary to solve this structure, a mutation in the RBD that increased the affinity of p110γ for Ras needed to be made (Pacold et al., 2000).

Ras is active when it is bound to GTP and inactive when it is GDP bound. Two 'switch' motifs adopt different conformations when Ras is in a GDP or a GTP bound state, thereby modifying the ability of Ras to bind to and activate other molecules. Normally, Ras interacts with its downstream effectors via the first 'switch'

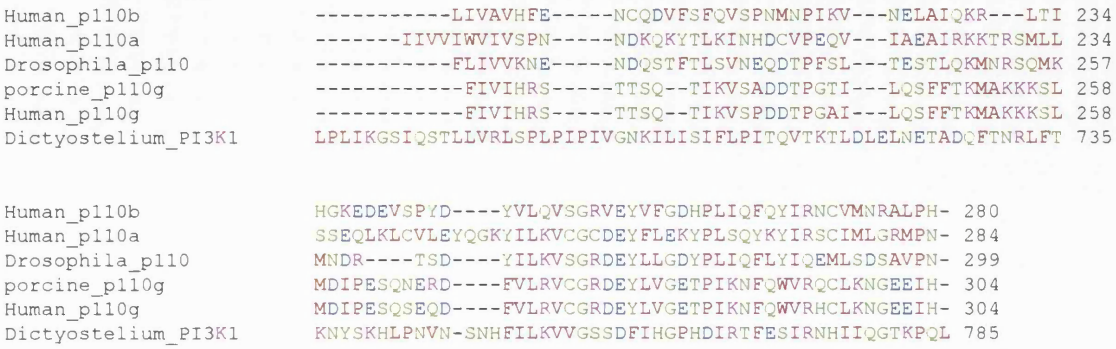

Figure 4.1 An alignment of Ras-binding domains from catalytic PI3K subunits

The figure above shows an alignment of the Ras-binding domains from various PI3K molecules generated using the Clustal W amino acid sequence alignment algorithm (Thompson et al., 1994). Small and hydrophobic amino acids have been marked in red, acidic amino acids are marked in blue, basic amino acids are coloured pink, and those amino acids with a hydroxyl, amine or basic side chain are coloured green.

motif. Interestingly, the structural data suggest that N-Ras uses both the Switch-I and Switch-II motifs to bind PI3K. The orientation of binding of the small-GTPase is determined by a loop in the p110γ, which becomes ordered upon Ras binding. The binding of Ras to p110γ appears to alter the conformation of p110γ, in particular within its C2 domain and the C-terminal lobe of its catalytic domain. These conformational changes could increase the catalytic ability of the lipid kinase (Pacold et al., 2000).

The biological importance of the interaction of Ras with PI3K catalytic subunits has been debated, but there is a large volume of data that supports this idea that p110-Ras binding increases PI3K catalytic activity. Constitutively GTP bound H-Ras, N-Ras, Ki-Ras or R-Ras can increase p110γ activity *in vitro* (Pacold et al., 2000; Suire et al., 2002). The redox-stimulated Ras binding of p110δ and p110β also increases the *in vitro* lipid kinase activity of these PI3K molecules (Deora et al., 1998), and both the *in vitro* and the *in vivo* activity of p110α are increased by the presence of constitutively active Ras (Rodriguez-Viciana et al., 1994; Rodriguez-Viciana et al., 1996b). Furthermore, several publications suggest that by inhibition of the PI3K pathway, some of the effects of transfecting constitutively the active Ras^{G12V} into cells can be blocked (Kauffmann-Zeh et al., 1997; Rodriguez-Viciana et al., 1997). Another approach to this question has been to compare the effects of constitutively active Ras to those of constitutively active Ras that has been mutated within the effector loop in order to abrogate binding to individual downstream effectors. These are known as Ras effector mutants. Using these, Rodriguez-Viciana proposed that the ability of constitutively active Ras to modify the actin cytoskeleton was dependent on PI3K activation (Rodriguez-Viciana et al., 1997). However, a similar approach led Maria Karasarides to conclude that a constitutively active GTP bound Ras containing the mutations Y64G, Y71G and F156L, which could not bind to p110δ or p110α in *in vitro* binding assays, could still activate PI3K lipid kinase activity *in vivo*, even when the effector mutant was present at low levels in the rat intestinal cells used (Karasarides et al., 2001). This observation prompts questions about whether the *in vitro* binding assays give a true representation of *in vivo* binding ability, and also whether the binding of Ras to p110 is necessary for the activation of PI3K catalytic activity.

If Ras binding does increase PI3K activity, as I have suggested, how does it do this? As discussed earlier, it is possible that the binding of Ras to the catalytic subunit

of PI3K alters the conformation of p110 thereby increasing its activity (Pacold et al., 2000). The idea that events occurring in the p110 RBD can influence the molecule's catalytic activity is supported by the observation that although a K227E mutation in the RBD of p110α blocks Ras binding, it also increases the basal lipid kinase activity of the subunit. This may well act by transmitting a conformational change to the p110 catalytic domain (Rodriguez-Viciana et al., 1996b).

PI3K is normally targeted to the membrane, where its substrate resides, via the binding of the adaptor subunit to phosphorylated tyrosine motifs. Further to this, the activation of PI3K lipid kinase activity by constitutively active Ras has been shown to work in synergy with the presence of such phosphorylated tyrosine motifs (Rodriguez-Viciana et al., 1996b). The enhancement of lipid kinase activity by Ras was particularly striking when phosphotyrosines were only present at low levels. One explanation of this observation is that binding to Ras increases the time spent by PI3K at the membrane, therefore increasing its opportunity to phosphorylate its lipid substrate. In practise this would be seen as an increase in the concentration of PIP_3 at the membrane. However, Suire *et al.* demonstrated that the localisation of PI3K in cells was not altered by constitutively active Ras transfection (Suire et al., 2002). An alternative explanation is that active Ras increases the apparent affinity of p110 for phosphatidylinositol 4,5-bisphosphate (PIP_2). Suire postulated that this would occur via binding to Ras orientating the PI3K catalytic subunit so that it can access its substrate more readily (Suire et al., 2002).

One possibility that has not yet been discussed is that Ras binding to p110 increases the activity of Ras rather than PI3K. The evidence for a direct activation of Ras by p110 is not strong, as the main experiment was performed using a constitutively active form of p110 where the inter-SH_2 domain of p85 was attached to the N-terminus of the catalytic subunit (Hu et al., 1995). Although expression of this protein did activate Ras, there is now evidence that the inter-SH_2 domain of p85 can act synergistically with Ras to increase p110 activity (Chan et al., 2002). Other research suggests that increased activation of PI3K does not lead to a co-ordinate increase in Ras activity. Instead, these experiments suggested that the basal activity of PI3K plays a permissive role in the activation of Ras by weak stimuli (Wennstrom and Downward, 1999).

Experiments similar to those described above have not been carried out using *Drosophila* cells or proteins, yet several *in vivo* studies suggest that the two

homologous molecules, Dp110 and Dras1 may functionally interact. The first indication of this link arose from a comparison of the mutant phenotypes resulting from loss of function *dras1/MAPK* pathway mutations and those generated by loss of *dp110* function. $dp110^{A}$ is a null mutation in which the 3´ end of the gene, including part of the *Hairless* genomic sequence, is deleted. If the resulting mRNA were translated the resulting Dp110 protein would be truncated at amino acid 668 and an extra four amino acids would be added to the protein's C-terminus. Most importantly, this protein would lack an intact kinase domain. $dp110^{B}$ is a larger deletion that also uncovers the *dp110* gene. Larvae that are homozygous for $dp110^{A}$ or heterozygous for $dp110^{A}$ and $dp110^{B}$, and contain a genomic rescue construct containing the *Hairless* genomic sequence, arrest growth at the early third larval instar stage and contain no discernable imaginal discs (Weinkove et al., 1999). This phenotype can be rescued by the expression of a genomic rescue construct containing the *dp110* genomic sequence. A similar phenotype is observed in flies carrying loss of function mutations in the *Drosophila* mitogen activated protein kinase, *Rolled* (Biggs et al., 1994) or strong loss of function mutations in *draf-1* (Nishida et al., 1988) both of which are activated downstream of Dras1. In addition, small wing discs are observed in strong loss of function mutants in an epidermal growth factor-like ligand called *vein* that is known to lead to Dras1 activation (Simcox et al., 1996). However, as larval growth arrest and the absence of imaginal discs are not very specific phenotypes these observations alone are not convincing that Dras1 and Dp110 do interact in fruit flies.

A second more convincing indication of a link arose from observations of Dras1 or Dp110 clonal phenotypes. Similarities are seen between clones made in the developing wing imaginal discs of third-instar larvae in which Dp110 or Dras1 activity have been increased by ectopic expression of activated versions of either protein. Likewise, similarities are seen if protein function or expression is reduced in clones. Increasing Dras1 activity in clones, by expressing the constitutively GTP-bound $Dras1^{V12}$, causes an increase in cell and clone size and a faster progression through the G1 phase of the cell cycle in comparison to wild-type clones. No differences in cell doubling time are seen (Prober and Edgar, 2000). The same is seen if Dp110 is over expressed in wing disc clones (Weinkove et al., 1999). PI3K signalling can be reduced in clones, by over-expression of a mutated adaptor subunit (Δp60) that is unable to bind Dp110 and thus competes for binding sites with Dp110-bound p60. Δp60 over-expression leads to a reduction in cell size (to 75% wild-type size), a

reduction in cell number and a cell-cycle profile where increased numbers of cells are in G1 (Weinkove et al., 1999). Cells from wing disc clones homozygous for a loss of function Ras allele are reduced in size compared to cells in a wild-type twin spot clone (Diaz-Benjumea and Hafen, 1994). In addition, over-expression of dominant negative Dras1^{N17} reduces cell size and clone cell number and alters cell cycle profiles in a similar fashion to loss of Dp110 function. Furthermore, both Δp60 and Dras1^{N17} increase cell doubling time, suggesting that cell proliferation is inhibited.

To assess whether these similarities are caused by a direct or indirect activation of PI3K by Dras1, David Prober used a PIP_3-binding PH domain fused to GFP (GFP-PH) to examine the levels of signalling through Dp110 in wing disc clones generated at 72 hours AED where Dras1^{V12} was expressed or Dras1 expression was completely removed. He found that over-expression of Dras1^{V12} led to an increase in membrane localisation of GFP, consistent with over-expression of Dras1^{V12} leading to an increase in membrane PIP_3 concentrations. This increase could be brought about by activation of Dp110 or inhibition of dPTEN in these clones. In contrast, loss of endogenous Dras1 did not alter the membrane localisation of GFP, suggesting that Dras1 is not necessary for the maintenance of normal levels of Dp110 activity in the developing wing disc (Prober and Edgar, 2002). These conclusions were verified by immunostaining imaginal discs containing Dras1^{V12} over expressing or *dras1* null wing disc clones with α-p-Ser586, which specifically recognises phosphorylated dAkt (Alrubaie, 2002). In such experiments, the intensity of antibody staining correlates with the level of PI3K pathway activity.

Although these experiments suggest that endogenous Dras1 is not necessary for PI3K function in developing *Drosophila* imaginal discs, Dp110 does contain a conserved Ras-binding domain, suggesting that Dp110 can interact with a Dras1 or another Ras-family small GTPase. This interaction could influence Dp110 function at another location or another time during the *Drosophila* life cycle. An alternative possibility is that although small-GTPase binding was important in an evolutionarily distant species, the RBD may have be conserved for a function entirely independent of this. In order to test these possibilities we decided to approach the problem by analysing the importance of RBD integrity in the normal function of Dp110. The idea was to make mutations in the RBD domain, and assess whether normal Dp110 function was retained or lost. This experimental approach had not been used before,

although it could turn out to be highly informative, especially as it does not rely on the over-expression of proteins.

4.1.1 Background to the project

In order to obtain mutations in *dPI3K* pathway genes, Hugo Stocker and Ernst Hafen carried out a screen known as the Pinhead screen. This involved the generation of genetically mosaic flies, in which the eye and head capsule are homozygous for a randomly induced mutation on the right arm of the third chromosome, which is where *dp110* is located. Those flies that had small head and eye structures under these conditions were studied further (Oldham et al., 2000). One complementation group isolated contained alleles that were larval lethal when combined with $dp110^{A}$. These are therefore likely to contain loss of function mutations in *dp110*. Sally Leevers was provided with these alleles, which were further characterised by Krishna Vaghela. Sequence analysis revealed that five of the thirteen alleles had premature stop codons. The most severe, $dp110^{1C1}$, would lead to the generation a protein truncated at amino acid 383 in the C2 domain of Dp110 if the resultant mRNA were translated. Two alleles contained mutations in the p60-binding domain of *dp110*, and one, $dp110^{6N3}$, contained a mutation within the RBD.

In $dp110^{6N3}$, a guanine at position 778 in the *dp110* genomic sequence has been altered to an adenine. This translates into a non-conservative mutation at residue 260 in the amino acid sequence from an aspartate to an asparagine (see figures 4.2 and 4.5). The alteration in charge caused by replacing a negatively charged acidic side chain with an uncharged polar side chain may well affect the intra-molecular binding capabilities of Dp110. The analogous residue in porcine p110γ, D260, is involved in the stabilisation of the loop within the RBD that controls the orientation of Ras binding. Mutation of this analogous residue to an alanine causes a two-fold reduction in *in vitro* binding of p110γ to non-hydrolysable GTP-bound N-Ras (Pacold et al., 2000). We hypothesised that the 6N3 mutation would similarly disrupt Ras binding. However, as Pacold found that the introduction of two sets of RBD mutations did not alter the basal lipid kinase activity of p110γ, we hypothesised that basal kinase activity of $Dp110^{6N3}$ would remain the same as that of wild-type Dp110 ($Dp110^{WT}$). It is important to note that both sets of p110γ RBD mutations tested decreased the activity of the lipid kinase when cells were stimulated by the transient transfection of Ras (Pacold et al., 2000).

In order to test that the larval lethality of *dp110*$^{6N3/A}$ was not caused by a lack of Dp110 expression or a severe reduction in Dp110 stability, Krishna Vaghela attempted to assess the Dp110 expression level in these larvae. As the available α-Dp110 antibody, SK50, did not have a high enough affinity for Dp110 to work effectively on Western blots of lysates, Krishna used an α-p60 antibody to immunoprecipitate Dp110 from *dp110*$^{6N3/A}$ and *dp110*$^{+/A}$ larval lysates (where *dp110*$^{+}$ represents the wild-type genomic *dp110* sequence). The immunoprecipitates were then separated using SDS-PAGE. Western blots were probed with SK50 allowing levels of Dp110 protein in the lysates were compared. Unfortunately low levels of protein were consistently isolated from *dp110*$^{6N3/A}$ larval lysates. The phenomenon that the lysates of larvae carrying loss of function *dp110* mutations contain low protein concentrations had previously been commented upon by Thomas Radimerski (personal communication). In conjunction with the low affinity of SK50 for Dp110, these low protein concentrations hindered such analyses. The experiments were limited by the amount of sample material that could be collected, and this was always insufficient to reach a conclusive result.

In this chapter I will present a more in-depth analysis of loss of function *dp110* mutant larvae, which suggests that although *dp110*^{6N3} is a strong mutation it is weaker than either of the presumed null mutations, *dp110*^{A} or *dp110*^{1C1}. New α-Dp110 antibodies were raised in the hope that larval Dp110 expression levels could be tested, and the analysis of these antibodies is also presented. To circumvent the problems of poor antibody recognition and low protein concentrations associated with *in vivo* analyses, stable cell lines were created where expression of HA-p60 and myc-Dp110* could be induced by the addition of copper sulphate ($CuSO_4$) to the cell culture medium (* is used to indicate that the protein could contain no, one or more mutations within the RBD). These cell lines were used as a source of protein for biochemical analyses of Dp110*. The aim of such biochemical experiments was to assess whether the introduction of mutations into the RBD affected Dp110 protein function. Firstly, we needed to assess their effect on protein stability and adaptor binding, as these would automatically reduce PI3K function. In addition, it was important to confirm whether the mutations altered the basal *in vitro* kinase activity of Dp110. As discussed, it is quite possible that the addition of RBD mutations may alter the basal kinase activity of Dp110 by transmitting a conformational change to the kinase domain. The hope was that none of the above characteristics would be altered. If this

turned out to be the case, and yet the mutations do cause a reduction in Dp110 activity *in vivo*, then we would be able to infer that the integrity of the RBD is vital for *in vivo* Dp110 function. One explanation for why this might be the case is that binding to a small GTPase is essential for the full activation of Dp110.

4.2 Growth of loss of function *dp110* mutant larvae.

To compare the strength of the 6N3 RBD mutation to the partial deletion in $dp110^{A}$ and the premature stop codon caused by the 1C1 mutation, the lengths of larvae carrying one or two of these alleles were measured and compared. The reason for using both $dp110^{A}$ and $dp110^{1C1}$ chromosomes as null alleles of *dp110* was because the $dp110^{A}$ chromosome had been maintained for five years over a balancer chromosome. During this time, it may well have acquired additional mutations. Although four years ago the addition of a genomic rescue construct containing the wild type *dp110* sequence could rescue the phenotype of $dp110^{A/A}$ larvae, which also contained a *Hairless* genomic rescue construct, this may no longer be the case. By putting $dp110^{A}$ in trans with $dp110^{1C1}$ we could be confident that the resulting phenotype was caused by the lack of functional Dp110 protein in these larvae, as it is highly unlikely that any additional mutations on the $dp110^{A}$ chromosome are also present on the $dp110^{1C1}$ chromosome.

Flies containing $dp110^{A}$, $dp110^{1C1}$ or $dp110^{6N3}$ stabilised over a TM3 third chromosome balancer that was marked with GFP, were crossed to themselves, to each other, and to the wild-type strain OregonR. Embryos from a four-hour egg lay were collected and placed in vials of fly food at a density of 100 embryos per vial. After developing at 25 C for three, four, five or six days, larvae were harvested using 30% glycerol and monitored for the presence of GFP. Those that lacked GFP, and therefore no longer carried a balancer chromosome, were picked, fixed in 3.7% formaldehyde and stored at 4 C. Larvae were later photographed using a digital camera attached to a dissecting microscope. Figure 4.2 shows the larvae that are closest to the mean larval length after three (A), four (C) and five (E) days' development. These pictures indicate that that between days three and four, the growth of transheterozygous mutant larvae, that is larvae containing two different mutant *dp110* alleles, and that of homozygous mutant larvae, which contain two of the same mutant *dp110* allele, are reduced compared to larvae with one copy of $dp110^{+}$. This reduced growth rate persists through to days five and six (data not shown). It is important to note that

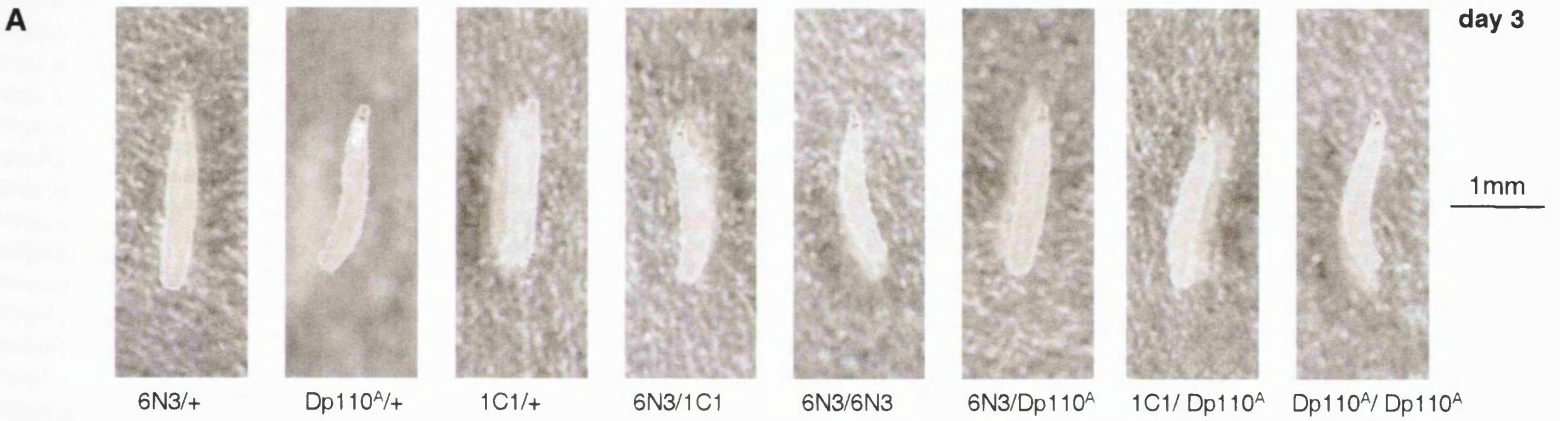

Figure 4.2 Length of larvae carrying mutations in Dp110

Flies containing $Dp110^{6N3}$, $Dp110^{A}$, or $Dp110^{1C1}$ genes stabilised over a GFP-marked balancer chromosome, were crossed to themselves to each other, and to the wild-type $Oregon^{R}$ strain. Embryos from these crosses were transferred to vials (100 embryos/vial) and raised at 25°C for three (**A,B**), four (**C,D**) or five (**E,F**) days. After this time, larvae were collected using 30% glycerol and those lacking GFP were fixed and photographed. The larvae were measured from the images created, using the measuring tool in Adobe Photoshop. **G** shows the collated data. Dp110*/+ larvae continue growing until day 5, when they begin the pupariation process. $Dp110^{A}$ and $Dp110^{1C1}$ appear to be slightly stronger mutations than $Dp110^{6N3}$.

C

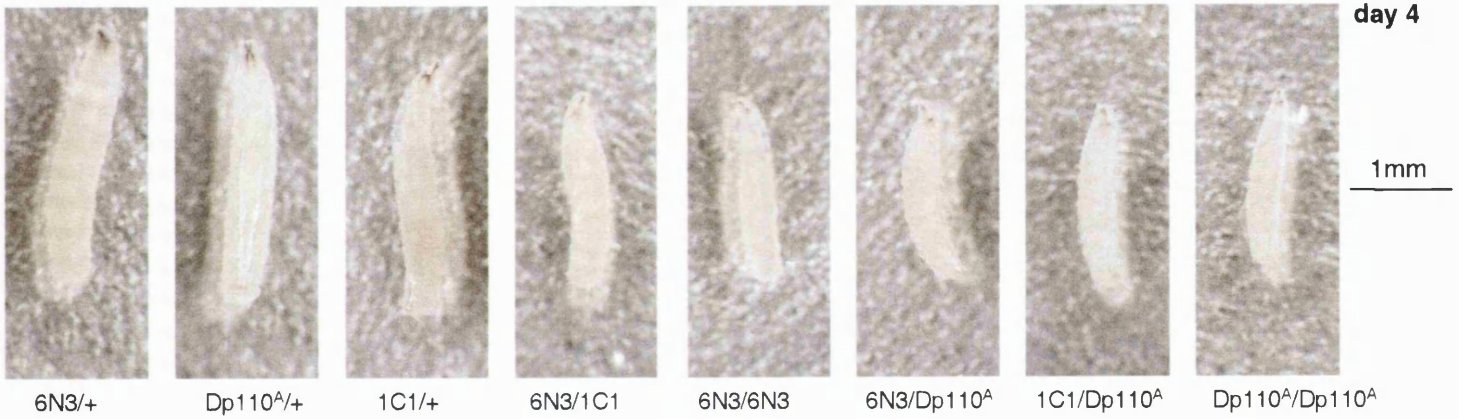

D

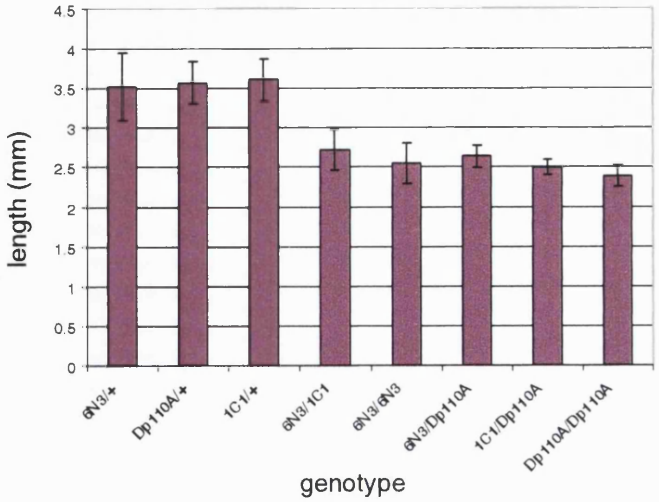

Figure 4.2 cont. Length of larvae carrying mutations in Dp110

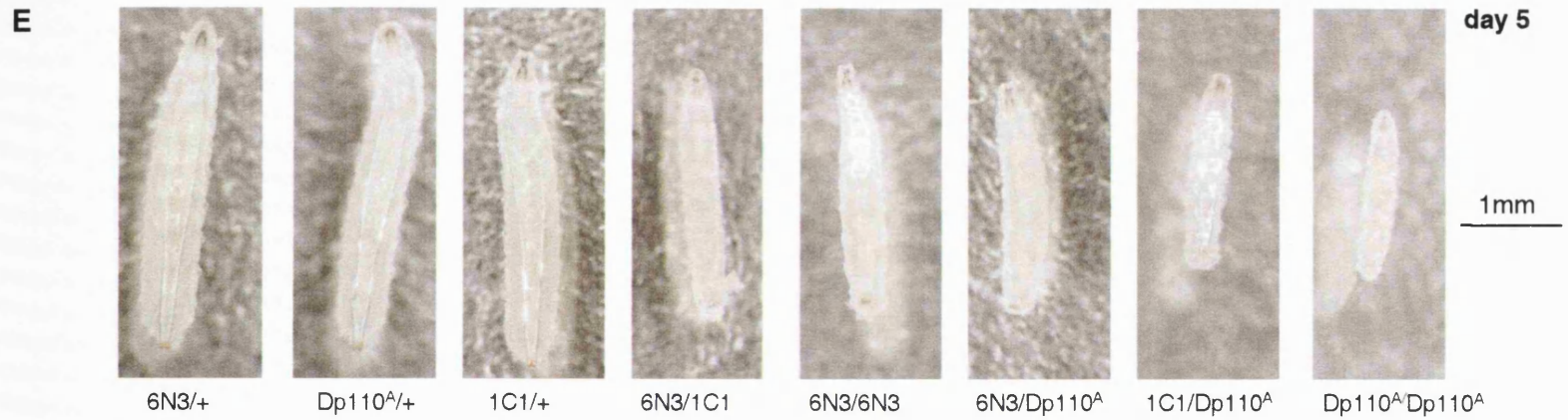

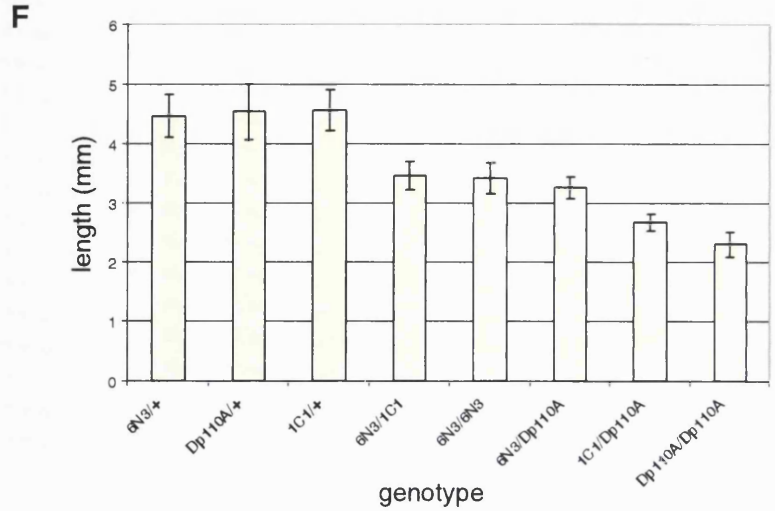

Figure 4.2 cont. Length of larvae carrying mutations in Dp110

G

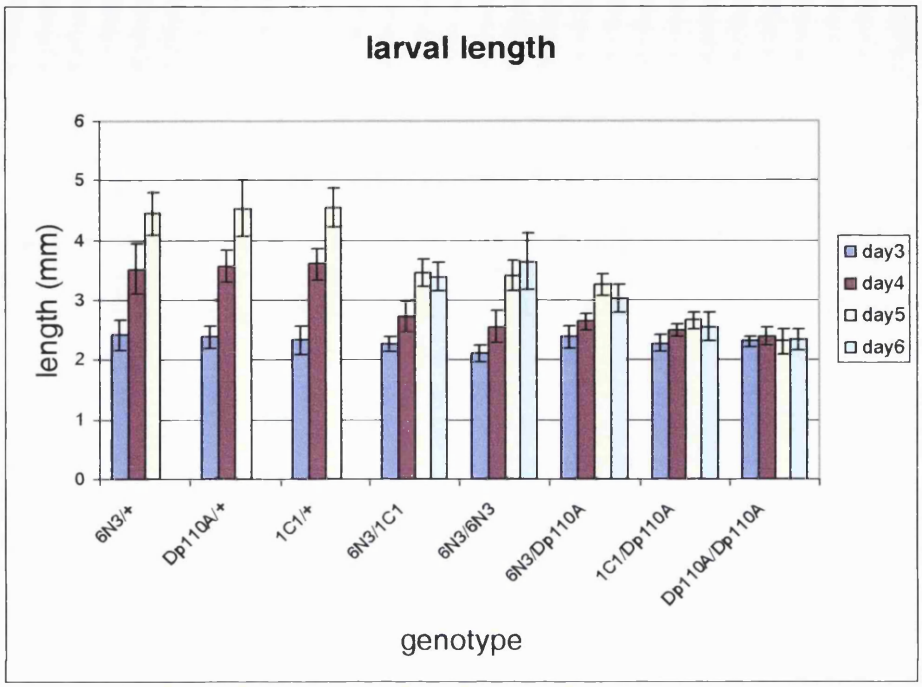

Figure 4.2 cont. Length of larvae carrying mutations in Dp110

heterozygous larvae, which contain one copy of $dp110^{+}$, are indistinguishable from wild type larvae (Sally Leevers, personal communication).

In order to quantify the data, lengths of larvae were measured from the photographs using the measuring tool in Adobe PhotoShop. The number of larvae assessed for each point and the mean lengths of larvae are shown in table 4.1. Length data are shown graphically in figures 4.2 B, D, F and G. Length data for six day-old larvae that carry one copy of $dp110^{+}$ are not shown, as these larvae had begun the pupariation process and their length had therefore begun to reduce. These quantitative analyses confirmed that the larvae containing two mutant alleles of *dp110* have a reduced growth rate compared to those containing one copy of a mutant allele and one copy of the wild-type gene. They also suggested that the growth defect was more severe if the two *dp110* alleles present carried the deletion mutant or the premature stop codon, as opposed to any other combinations. For example, $dp110^{A/A}$ larvae appeared not to grow at all after three days, whereas $dp110^{6N3/6N3}$ or $dp110^{6N3/1C1}$ larvae did continue growing until day five, albeit at a reduced rate.

Student t-tests were used to assess how significant the larval length differences were (see table 4.2). When the lengths of the three day-old larvae were compared, relatively few statistically significant differences were seen. Even if differences were statistically significant, the level of that significance was much lower than that obtained from comparisons of older larvae. Size differences between four day-old larvae that carry one copy of $dp110^{+}$ and those that do not are highly significant, with p-values of less than 6.5×10^{-6}. The significance of these length differences rises after five days of development, with p-values ranging from 3.6×10^{-11} to 9.1×10^{-30}.

From day four onwards $dp110^{A/A}$ larvae are significantly smaller than larvae of all the other genotypes. This may be because the $dp110^{A}$ chromosome contains at least one additional mutation. Alternatively, it could simply be because the flies have a slightly different genetic background.

The statistical analysis of five day-old larvae indicates that 6N3 is a strong loss of function mutation. However, it does appear to generate a slightly weaker phenotype than either of the null mutations. The larger size of larvae containing at least one $dp110^{6N3}$ chromosome, in comparison with either $dp110^{1C1/A}$ *or* $dp110^{A/A}$ larvae, is statistically significant, with p-values of less than 5.5×10^{-12}. This observation is perhaps not surprising, as the translation product from the $dp110^{6N3}$ gene will probably

	6N3/+		Dp110^{A}/+		1C1/+		6N3/1C1		6N3/6N3		6N3/Dp110^{A}		1C1/Dp110^{A}		Dp110^{A}/ Dp110^{A}	
	n	length(mm)	n	length(mm)	n	length(mm)	n	length(mm)	n	length(mm)	n	length(mm)	n	length(mm)	n	length(mm)
Day3	24	2.41	25	2.38	23	2.33	18	2.26	10	2.10	15	2.38	16	2.27	18	2.30
Day4	28	3.52	16	3.57	27	3.60	17	2.72	22	2.55	21	2.64	18	2.50	21	2.39
Day5	27	4.45	23	4.53	26	4.55	21	3.45	20	3.41	14	3.25	20	2.66	24	2.30
Day6	24	Ⓟ	20	Ⓟ	25	Ⓟ	25	3.39	16	3.65	26	3.02	20	2.55	19	2.35

Table 4.1 Average lengths of larvae carrying one or two copies of Dp110 mutant chromosomes

The table shows the number of larvae (n) that were collected and assessed for each genotype on each day and the average length of those larvae determined from the captured photographic images. The six day-old heterozygous larvae are marked with a Ⓟ. These larvae had begun the pupariation process and some had already pupated. As this process reduces the length of larvae, these length data have not been included in the table.

A DAY3	6N3/+	Dp110^{A}/+	1C1/+	6N3/1C1	6N3/6N3	6N3/ Dp110^{A}	1C1/ Dp110^{A}	Dp110A/ Dp110^{A}
6N3/+								
Dp110^{A}/+	0.65							
1C1/+	0.32	0.30						
6N3/1C1	0.045	0.0090	0.31					
6N3/6N3	0.072	0.77	0.12	0.015				
6N3/ Dp110^{A}	0.86	0.94	0.46	0.072	0.0054			
1C1/ Dp110^{A}	0.14	0.043	0.48	0.92	0.014	0.085		
Dp110A/ Dp110^{A}	0.092	0.031	0.63	0.30	0.00020	0.23	0.51	

B DAY4	6N3/+	Dp110^{A}/+	1C1/+	6N3/1C1	6N3/6N3	6N3/ Dp110^{A}	1C1/ Dp110^{A}	Dp110A/ Dp110^{A}
6N3/+								
Dp110^{A}/+	0.19							
1C1/+	0.31	0.57						
6N3/1C1	6.5×10^{-6}	6.2×10^{-10}	5.0×10^{-10}					
6N3/6N3	3.3×10^{-10}	4.0×10^{-12}	3.7×10^{-16}	0.089				
6N3/ Dp110^{A}	1.2×10^{-8}	4.8×10^{-11}	9.5×10^{-15}	0.38	0.21			
1C1/ Dp110^{A}	3.7×10^{-8}	4.0×10^{-12}	8.2×10^{-13}	0.0030	0.36	0.0013		
Dp110A/ Dp110^{A}	8.5×10^{-11}	1.6×10^{-13}	2.7×10^{-23}	9.1×10^{-5}	0.014	2.1×10^{-6}	0.0094	

C DAY5	6N3/+	Dp110^{A}/+	1C1/+	6N3/1C1	6N3/6N3	6N3/ Dp110^{A}	1C1/ Dp110^{A}	Dp110A/ Dp110^{A}
6N3/+								
Dp110^{A}/+	0.46							
1C1/+	0.56	0.78						
6N3/1C1	1.5×10^{-17}	3.6×10^{-11}	2.410^{-17}					
6N3/6N3	2.9×10^{-17}	1.5×10^{-11}	6.7×10^{-17}	0.59				
6N3/ Dp110^{A}	4.2×10^{-19}	7.5×10^{-13}	7.4×10^{-19}	0.0058	0.038			
1C1/ Dp110^{A}	1.5×10^{-24}	2.8×10^{-16}	9.1×10^{-25}	1.0×10^{-14}	5.5×10^{-12}	3.8×10^{-10}		
Dp110A/ Dp110^{A}	2.3×10^{-29}	2.7×10^{-19}	9.1×10^{-30}	2.2×10^{-20}	2.9×10^{-17}	1.3×10^{-15}	2.3×10^{-8}	

Table 4.2 The significance of differences in length of larvae carrying different Dp110 mutations.

Two-tailed student's T-tests were carried out on the raw larval length data, comparing the length values for each genotype with those of the other genotypes collected on the same day. The p-values for these comparisons are shown in the tables. The tables are colour coded, indicating the significance of the length differences seen.

$0.05>p>10^{-3}$ $10^{-3}>p>10^{-8}$ $10^{-8}>p>10^{-13}$ $10^{-13}>p>10^{-20}$ $p<10^{-20}$

be full-length Dp110 protein, with an intact lipid kinase domain. Despite the weaker nature of the mutation, pupae do not develop from $dp110^{6N3/6N3}$ or $dp110^{6N3/1C1}$ larvae.

From these experiments it can be concluded that $dp110^{6N3}$ causes a similar phenotype to a known null *dp110* mutant. This loss of function phenotype could be caused by a lack of expression or an inherent instability of $Dp110^{6N3}$ protein. Alternatively, $Dp110^{6N3}$ might be expressed at normal levels, but the protein's p60-binding ability or its kinase activity may have been destroyed or reduced by conformational changes induced by the presence of the point mutation. The final and most intriguing possibility is that the RBD integrity itself is crucially important for full function of Dp110, and that this integrity is sufficiently disrupted by the presence of the 6N3 mutation to generate a strong loss of function phenotype. From this it could follow that the interaction of Dp110 with Ras or a Ras related protein via its RBD is important for normal Dp110 function.

4.3 Raising new antibodies against Dp110 peptides

In order to confirm whether $Dp110^{6N3}$ was expressed in mutant larvae, new antibodies against Dp110 were raised. It was hoped that these antibodies would have a stronger affinity for Dp110 than the current α-Dp110 antibody (SK50) as SK50 recognises Dp110 only if the protein concentration has been increased via immunoprecipitation or affinity purification. SK50 had been raised against a peptide corresponding to amino acids 480 to 496 of Dp110 (CADDIQSVEVFHPLGTIE).

To decide which peptide sequences should be used in generating the new α-Dp110 antibodies, I consulted the solved structure of p110γ (see chapter one for further details; (Walker et al., 1999). Although p110γ is a Class IB PI3K, whereas Dp110 is a class IA PI3K, the overall degree of sequence similarity between the two proteins is fairly high, at 27%. From an alignment of the *dp110* sequence with the porcine *p110γ* sequence, created using Clustal W, I was able to estimate the positions where the different domains in Dp110 began and ended (see figure 4.3 for alignment, and figure 4.6A for Dp110 schematic). Further to this, I used the solved structure of p110γ to select peptides to use as antigens that were likely to be exposed on the surface of the protein, that were part of a mobile structural element, or that were found within β-turns (Walker et al., 1999). It has been suggested that antibodies raised against peptides with one or more of these properties are more likely to recognise the endogenous protein (Harlow and Lane, 1988).

Figure 4.3 Amino acid sequence comparison of *Drosophila* p110 (Dp110) with porcine p110γ

The alignment of the amino acid sequences of Dp110 and p110γ. The alignment was generated using the CLUSTALW algorithm (Thompson *et al.*, 1994). Amino acids identical in both sequences are shaded red. The Ras-binding domain is marked with a purple line. The asterisk marks the aspartate residue in Dp110 that is mutated to an arginine in the 6N3 fly strain. The sequences used to generate antigenic peptides are underlined and numbered.

Three peptides were chosen as antigens (see figure 4.3). Dp110-1 is taken from a sequence in the third β-strand of the membrane binding C2 domain (KKLCAQRSTDSPNGN). Dp110-2 originates from the linker between the RBD and the membrane binding C2 domain (VTKRPLPKKRTVHLHKS). This linker region is unresolved in the *p110γ* structure and is therefore likely to be highly mobile. Dp110-3 consists of the 20 C-terminal amino acids of Dp110 (NSWKTSLNWASHNFSKNNKQ). C-terminal peptides are often used to raise antibodies, as the C-terminal sequence of a protein is regularly exposed and mobile. In fact, successful α-Dp110δ antibodies have previously been generated against C-terminal peptides (Harlow and Lane, 1988; Vanhaesebroeck et al., 1997b).

Peptides were coupled to Keyhole limpet hemacyanin (KLH), which acts to increase the immune response of the immunised animal and hence increase the likelihood that specific antibodies will be generated. Two rabbits were then immunised with each peptide. After an 11-week course of antigenic peptide boosts and anti-sera collections the rabbits were terminally bled (see section 2.3 for further details). Immunoreactivity of the generated antisera was then tested.

4.4 Testing immunoreactivity of antisera raised against Dp110 peptides

The ability of the antisera to recognise Dp110 on Western blots of S2 cell lysates and α-p60 immunoprecipitates from S2 cell lysates, which would be enriched for Dp110, was tested. Western blots were cut into strips and probed either with the pre-immune serum, or the antisera (final bleeds) from each rabbit. The blots were then reformed and scanned at two different sensitivities, one that was optimum for viewing the IPs (see figure 4.4), and a higher sensitivity for viewing any bands in the lysate lanes (data not shown).

No bands of the predicted molecular weight of approximately 127kDa (Atelier BioInformatique) were seen in the lysate lanes probed with any of the antisera, which were not also seen in the lanes probed with the cognate pre-immune sera. Furthermore, only α–Dp110-3A was able to recognise a band of the appropriate size in α-p60 immunoprecipitates. The Dp110 recognition ability of α–Dp110-3A and SK50 were compared directly in a further experiment (see figure 4.5). Here, strips of Western blots of S2 cell lysates or α-p60 IPs were probed with either the α-Dp110-3 antisera (third bleed) or the cognate pre-immune sera, and in addition one lane of α-

Figure 4.4 Immunoreactivity of antisera raised against Dp110 peptides

80μl α-p60 antibody was used to immunoprecipitate Dp110 from 10ml S2 cell lysate (1.2mg/ml). The α-p60 imunoprecipitates (equivalent to 600μg protein/lane) and S2 cell lysate (c.70μg/lane) were separated on three SDS-PAGE gels (8%). Each Western blot was cut into four strips. These strips were then individually probed with one of the six crude Dp110 antisera (final bleeds) or the cognate preimmune sera. Note that two rabbits (A and B) were immunised with each peptide. All antibodies were used at a 1:1000 dilution. The blots were then visualised using the Odyssey infrared multi-imaging system. The picture shown was exposed for the optimal time for viewing the bands in the IP lanes, not the lysate lanes. Only the Dp110-3A antisera detected a 110kDa band corresponding to Dp110 (see asterisk), and its reactivity was weak (i.e. only recognising the protein in IPs).

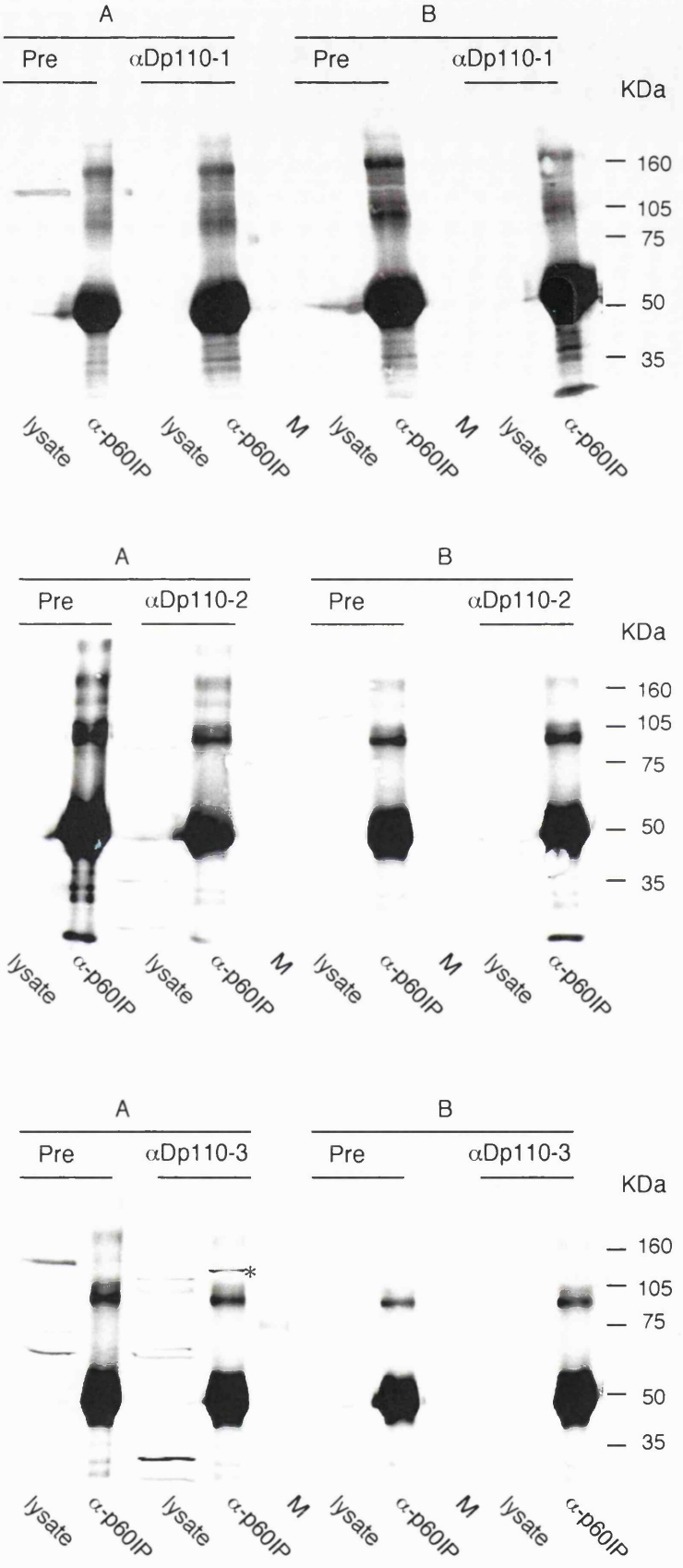
A
B
Pre
αDp110-1
Pre
αDp110-1
KDa
160
105
75
50
35
lysate
α-p60IP
lysate
α-p60IP
M
lysate
α-p60IP
M
lysate
α-p60IP
A
B
Pre
αDp110-2
Pre
αDp110-2
KDa
160
105
75
50
35
lysate
α-p60IP
lysate
α-p60IP
M
lysate
α-p60IP
M
lysate
α-p60IP
A
B
Pre
αDp110-3
Pre
αDp110-3
KDa
160
105
75
50
35
*
lysate
α-p60IP
lysate
α-p60IP
M
lysate
α-p60IP
M
lysate
α-p60IP

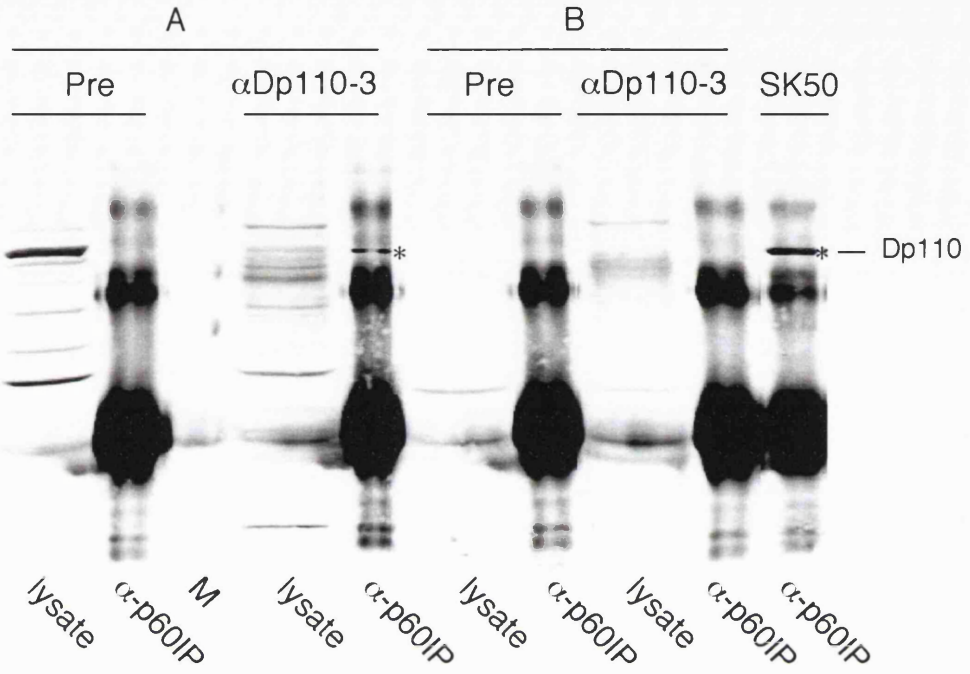

Figure 4.5 Comparing the immunoreactivity of old and new α–Dp110 antisera

A Western blot of Schneider S2 cell lysate (70μg/lane) and α–p60 immunoprecipitates from S2 cells was cut into five strips. Four of the strips were probed individually with either a Dp110-3 crude antisera (third bleed) or a cognate preimmune sera. The fifth strip was probed with the original αDp110 antisera (SK50). M indicates the marker lane. The asterisks mark the bands that are running at the appropriate molecular weight for Dp110 (127kDa). Note that SK50 has a stronger affinity for Dp110 than the α-Dp110-3 antisera.

p60 immunoprecipitates was probed with SK50. The figure clearly shows that SK50 has a higher affinity for Dp110 than α-Dp110-3A.

As the majority of the new antisera did not recognise Dp110 and the only antibody that showed any affinity for Dp110 was less effective than SK50, it was clear that we were not going to be able to test larval $Dp110^{6N3}$ expression directly from larval lysates. In order to test whether $Dp110^{6N3}$ was likely to be stable *in vivo* and to analyse the protein's biochemical properties, an alternative source of protein was needed.

4.5 Establishing stable inducible cell lines to induce expression of Dp110* and p60.

I decided to generate stable cell lines in which expression of $Dp110^{6N3}$ and other Ras binding domain mutants (Dp110*) could be induced. However, if these cell lines were to act not only as a source of protein but also as a tool for *in vivo* experiments then it was important that the Dp110* proteins could be normally activated via the adaptor subunit. To achieve this, the cell lines needed to express p60 at equivalent levels to Dp110*. The level of expression of the two proteins is crucially important, as it has been shown that over-expression of Dp110 on its own can activate downstream signalling, and over-expression of p60 on its own can act as a dominant inhibitor of PI3K signalling. This was visualised by a respective increase or decrease in final fly eye or wing size, when the proteins were over expressed in the imaginal discs (Leevers et al., 1996; Weinkove et al., 1999). However, if p60 and Dp110 are over expressed together in discs, then the final organ size is no different to wild type (Weinkove et al., 1999), suggesting that the protein complex has no innate signalling ability or that the positive and negative signals from the two components cancel each other out. It would follow that net signalling downstream of the p60-Dp110* complex would only occur after an activating event. By making cell lines that over express Dp110 and p60 at equivalent levels we would therefore be able to observe the normal activation of Dp110* following stimulation by receptor-ligand binding or active Dras1 transfection.

Stable *Drosophila* cell lines generally contain multi-copy inserts that form arrays of more than 500 to 1000 copies of transfected plasmid in a head to tail fashion (Kirkpatrick and Shatzman, 1997). Together with the fact that different genes take different lengths of time to transcribe and translation rates of different mRNAs vary, it

is hard to be confident that transgenic Dp110* and p60 will be expressed at equivalent levels, even if equivalent concentrations of the genetic material are transfected into the cells. Because of this, we decided to create polyclonal cell lines, in the hope that over the whole population of cells, the levels of p60 and Dp110* would be equivalent, even if they were not equal in individual cells. Furthermore, manufacturing clonal populations of stably transfected S2 cells would be difficult, as it would necessitate growing stably transfected cells at low density, at least initially. Under such conditions, *Drosophila* S2 cells tend not to survive.

Cells that express higher levels of Dp110* than p60 will have a competitive advantage over other cells, causing the composition of a polyclonal cell line to drift over time to a state in which the majority of cells express higher levels of Dp110* than p60. To minimise this drift, transgene expression was put under the control of the metallothionein (Mt) promoter. Transcription from the Mt promoter is controlled by heavy metal ions, and can be induced experimentally by the addition of $CuSO_4$ to the culture medium, at a concentration of 700μg/ml. If transgene expression is inducible, it means that selection for the transgenes can take place independently of any influence from transfected transgene expression levels.

In order to ensure that the characteristics of the transgenic protein could be analysed, a method of distinguishing it from the endogenous protein was necessary. We decided that transgenic proteins should be fused to an epitope tag. This tagging has an added benefit: antibodies with a high affinity for the epitope tags are commercially available so the poor quality of the available α-Dp110 antibodies is no longer a problem. DNA cassettes encoding HA-tagged p60 and myc-tagged Dp110 were readily available from previous work carried out in the lab (Leevers et al., 1996; Weinkove et al., 1999).

To evaluate the behaviour of $Dp110^{6N3}$ compared to the wild-type protein, stable inducible cell lines containing HA-p60 and myc-$Dp110^{WT}$ transgenes were created alongside those containing HA-p60 and myc-$Dp110^{6N3}$. Additionally, cell lines that had been transfected with empty vectors were included as a further control, to confirm that the transfection or selection processes themselves could not account for any effects seen.

At this stage, we were unsure how well myc-$Dp110^{6N3}$ would fare in functional tests. To improve the chance of being able to assess the importance of RBD integrity in Dp110 function, I decided to create two further cell lines that inducibly expressed

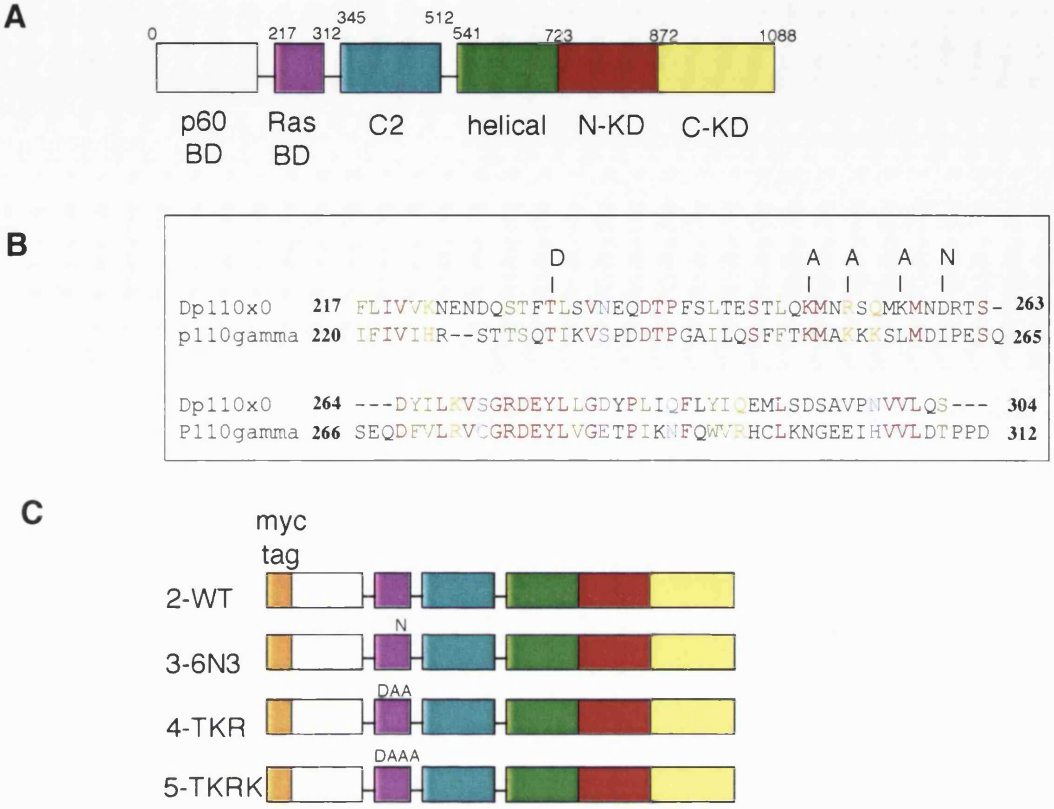

Figure 4.6 Dp110 domain structure and Ras binding domain mutations

A shows the domain structure of Dp110. The numbers above the figure indicate the predicted amino acid positions at which the different domains begin and end. These positions were estimated on an alignment of Dp110 with porcine p110γ using the domain positions of p110γ predicted in Walker et al., 1999. BD indicates a binding domain. The C2 domain is thought to stabilise Dp110 membrane localisation. N-KD and C-KD indicate the N- and C-terminal kinase domain respectively. **B** shows the amino acid (aa) sequence of the predicted Ras binding domain (RBD). Identical aa's are marked in red; similarly placed small aa's are coloured green; acidic residues are purple; basic residues are orange and those aa's containing either a hydroxyl amine or basic group are marked in blue. The mutations made are indicated above the particular aa altered. Schematics of the four epitope-tagged proteins placed under the trancriptional control of the metallothionien promoter are shown in **C**. The homologous residues to those mutated in Dp110 are highlighted overleaf (**D**) on a close up of Ras bound to the RBD of p110γ (from Pacold et al., 2000).

D

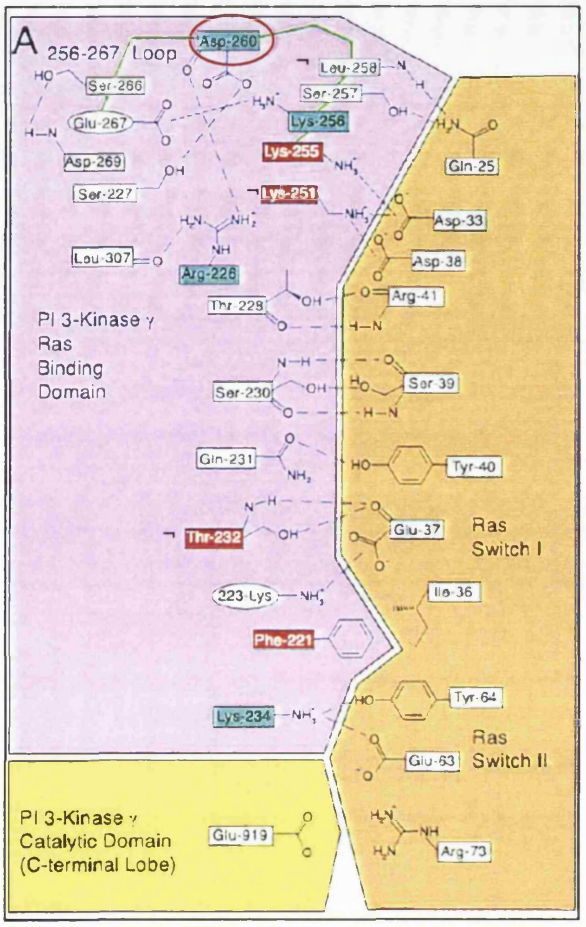

Figure 4.6 cont. Dp110 domain structure and Ras binding domain mutations

This is a schematic of Ras, bound to the RBD of p110γ (from Pacold et al., 2000). D260 (homologous to D259, mutated in the 6N3 flies) is ringed in red. T232, K251 and L258 (homologous to T231, K250 and K257, respectively) are marked with an asterisk.

myc-Dp110 proteins containing multiple mutations within their RBDs (see figure 4.6B and C). To determine which residues in Dp110 should be mutated, studies of p110γ RBD mutants were consulted, in which p110γ-Ras binding and p110γ *in vitro* lipid kinase activity had been assessed. These studies concluded that a 'DASAA' mutant of p110γ has the same basal activity as the wild-type enzyme, but is not activated by H-Ras-GTP-γS *in vitro* (Pacold et al., 2000). The mutations in $p110\gamma^{DASAA}$ are T232D, K251A, K254S, K255A and K256A. Each of these mutations has been shown to individually abrogate Ras binding (Pacold et al., 2000).

T231 and K250 are the residues in Dp110 that are homologous to p110γ T232 and K251. In collaboration with Roger Williams, we decided that any new Dp110 RBD mutants should contain both T231D and K250A mutations. Although K254, K255 and K256 in p110γ do not directly align with lysine residues in Dp110, the *Drosophila* sequence does contain an arginine at an analogous position to K254. As both arginine and lysine have basic side chains, these amino acids will have a similar capacity to form hydrogen bonds. On this basis we decided to introduce a third mutation of R253A into both Dp110 RBD mutants. The final residue, mutated in only one of the proteins, was a second lysine at position 257. This residue was, again, mutated to alanine. This residue is in an analogous position to L258 in p110γ. L258 is thought to play a role in p110γ-Ras binding (shown in figure 4.6D), and also makes up part of the loop that is stabilised upon Ras binding (as discussed in section 4.1.1). However, the main reason for choosing to mutate K257 to an alanine was that Dp110 contains fewer lysines than porcine p110γ in the region thought to interact with Ras. It was hoped that by reducing the number of basic residues in this region, we would decrease the Ras-binding affinity of Dp110 by hindering the formation of strong electrostatic interactions between the two proteins. Dp110 containing the first three RBD mutations was named $Dp110^{TKR}$ and the protein with four RBD mutations was called $Dp110^{TKRK}$ (see figure 4.6C for a schematic).

4.5.1 The method used to generate the stable cell lines

Further details of the methods used to create the cell lines can be found in sections 2.5 and 2.6. Briefly, two commonly used expression vectors, pMTIZ and pMK-33 were used to express the tagged proteins. pMTIZ contains a Zeocin resistance gene and pMK33 contains a Hygromycin resistance gene, both of which will allow Schneider S2 cells containing the vectors to be selected for by growing the

cells in medium containing the appropriate antibiotic. The presence of an Ampicillin resistance gene allowed selection of the both vectors during bacterial culture steps. Also, both vectors contained metallothionein (Mt) promoters, from which $CuSO_4$ dependent transcription occurs.

A DNA cassette encoding HA-p60 was sub-cloned into the vector pMTIZ, downstream of the Mt promoter. In fact, the HA tag in this cassette was unintentionally modified during its generation. Rather than the usual HA sequence of YPYDVPDYA, an extra aspartate residue has been added, to create the sequence: YPYDDVPDYA (for further details see (Weinkove, 1999). However, this mutated tag is still recognised by α-HA antibodies in Western blot analyses and in immunoprecipitation reactions.

The Myc-Dp110* inserts were sub-cloned into the vector PMK-33, downstream of the Mt promoter. The Quikchange PCR based mutagenesis kit was used to add the various RBD mutations to the sequence encoding myc-Dp110, while it was within a Bluescript SKII backbone. DNA sequencing confirmed the addition of the RBD mutations and the absence of any unintentionally induced mutations.

After diagnostic digests and DNA sequencing confirmed the integrity of the expression vectors, S2 cells were simultaneously transfected with both pTIZ-HA-p60 and PMK-myc-Dp110*, or copies of the empty vectors, at a 1:1 concentration ratio. After three days, selection of cell lines began using only Hygromycin, at a concentration of 300μg/ml. This was due to an unfortunate oversight: Zeocin is a copper chelated antibiotic, and as such is distributed in a copper sulphate solution. If this antibiotic is used to select cells, the copper ions in the solution will promote transcription from the Mt promoter, so cell line selection will no longer be independent of transgene expression. This situation was not thought to be a major problem as when different DNAs are included in the same transfection mix, a very high rate of co-transfection into individual cells is observed (Perucho et al., 1980)

After three weeks of selection, during which cells were passaged and replenished with fresh medium and antibiotic, the surviving cells in the established polyclonal cell lines looked healthy. The five cell lines were named 1-control, 2-wt, 3-6N3, 4-TKR and 5-TKRK after the *dp110* gene they expressed. Hitherto, the cell lines may be referred to with these names, or simply their numbers. Inducible transgene expression was then tested.

4.6 Time course of induction of Dp110 and p60 transgene expression

The aim of these first experiments was to test that 700μg/ml $CuSO_4$ induced transcription from the Mt promoter and hence transgene expression. In addition, we wanted to discover the best time point to use in future experiments. Cells from each line were seeded into six-well plates at a density of 5×10^6 cells per ml in media containing Hygromycin (300μg/ml). After eight hours of growth at 23 C, $CuSO_4$ was added to five of the six wells to a final concentration of 700μg/ml. After defined amounts of time (2, 5, 8, 16 and 24 hours) cells were harvested, pelleted and lysed. Lysates were separated by SDS-PAGE, and Western blots were probed with α-myc, α-HA and α-β-tubulin. Blots were then probed with α-mouse secondary antibodies coupled to an 800nm infrared dye (α-mouse-800) and visualised using the Odyssey infrared imaging system (figure 4.7).

The Western blots revealed that no myc- or HA-tagged proteins were expressed in the 1-control cell line, but that they were expressed in all the other cell lines after $CuSO_4$ treatment. Furthermore, they confirmed that the expressed myc- and HA-tagged proteins ran at the molecular weights expected for myc-Dp110* and HA-p60 (approximately 128kDa and 59kDa respectively). When HA-p60 was expressed at a high level, degradation of the protein ensued. It was unclear whether this degradation occurred within the cells, or upon lysis, but previous results suggest that the latter is more likely (Weinkove, 1999).

The level of transgene expression in all cell lines increases with the length of $CuSO_4$ treatment. Note that some 'leaky' expression of transgenes, that is expression in the absence of $CuSO_4$, does occur. This is most apparent in the 3-6N3 and 5-TKRK cell lines, possibly because these uninduced lanes contain a larger amount of total protein, as indicated by the higher levels of β-tubulin.

Although the immunoblot suggests that the levels of HA-p60 protein are higher than those of myc-Dp110*, this is not a justifiable conclusion to draw. Differences in affinity of the primary antibody for its antigen, the concentration of primary antibody used, and the ability of the secondary antibody to recognise the primary may all collude to produce this illusion. However, inter-cell line comparisons of similarly tagged proteins are valid. These suggest that expression levels of HA-p60 are similar in all cell lines after 16 hours of $CuSO_4$ treatment, although higher levels of expression are induced earlier in 3-6N3 and 4-TKR cell lines. However, levels of myc-Dp110*

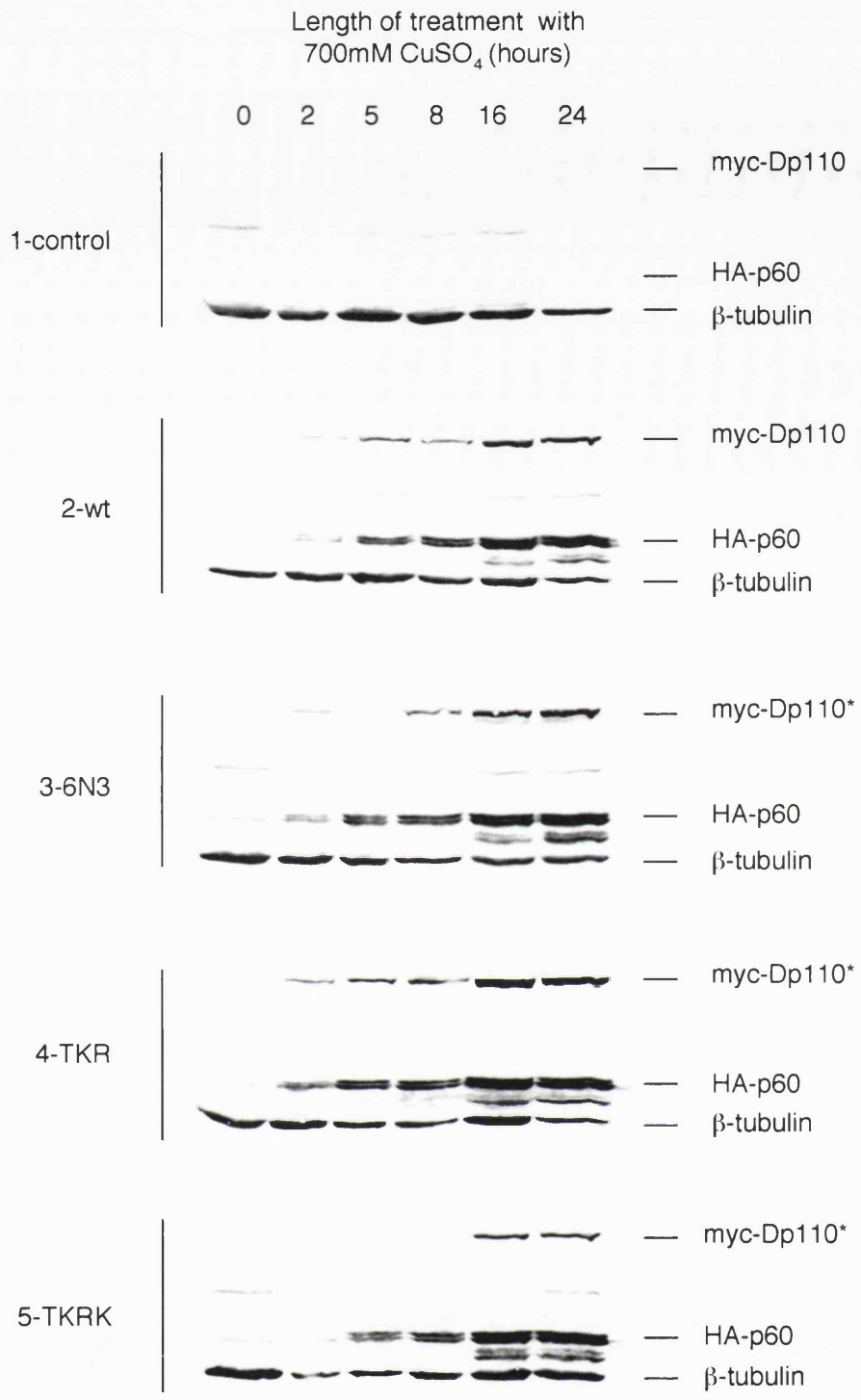

Figure 4.7 Timecourse of Dp110 and p60 transgene induction

Lysates of control transfected or pMt-myc-Dp110*/pMt-HA-p60 cells treated for varying lengths of time with $CuSO_4$ (700μg/ml) were resolved using SDS-PAGE (100μg protein/lane). The blots were then probed with αmyc, αHA and αβ-tubulin. No myc-Dp110 or HA-p60 was seen in control cell lysates. The other cell lines showed increasing levels of transgene expression with increasing time of $CuSO_4$ treatment. Note that HA-p60 appears to be rapidly degraded. This is clearly seen after five hours of induction as HA-p60 appears as a doublet. As the concentration of HA-p60 increases the concentration of a futher degradation product of HA-p60 increases co-ordinately.

n = 3

vary more widely between the cell lines. Dp110^{TKR} appears to be expressed at a higher level, and Dp110^{TKRK} at a lower level than the other myc-tagged proteins.

These results indicate that HA-p60 expression in all cell lines reaches a maximum level after treatment of cells with $CuSO_4$ for 16 hours, with the obvious exception of control lines. Myc-Dp110* is also expressed after this length of treatment, although the levels of expression vary in the different cell lines. Observations of control cell lines and untransfected S2 cells confirmed that 16 hours of $CuSO_4$ treatment had no negative effects on cell viability or β-tubulin expression. Thus, 16 hours was chosen as the time point to use for further experiments.

4.7 Relative myc-Dp110* and HA-p60 expression levels after 16 hours of induction

A more quantitative assessment of the expression levels of the different transgenes after 16 hours of induction was desirable. Cell lines were treated with $CuSO_4$ for 16 hours and then harvested and lysed. Lysates were separated on 8% SDS-PAGE gels, and Western blots were probed as before, with α-myc, α-HA and α−β-tubulin. The relative expression level of each transgene was assessed by quantification of the blot using the Odyssey infrared imaging system. Signals were normalised to the total amount of protein in each lane using the amount of β−tubulin as a guide. In order to combine results from five independent experiments, levels of HA-p60 and myc-Dp110^{WT} in the 2-wt cell line were arbitrarily defined as 1. Relative expression levels of the transgenes in the other cell lines could then be calculated.

The combined results are shown in figure 4.8. As suggested by the time course data, levels of HA-p60 in the different cell lines after 16 hours of $CuSO_4$ treatment are not significantly different. Myc-Dp110^{TKR} expression levels in the 4-TKR cell line are significantly higher than the expression levels of all other myc-Dp110* fusion proteins ($p<0.1$); expression levels of myc-Dp110^{TKRK} are significantly lower than those of the other myc-Dp110* proteins ($p<0.05$). Although the low levels of myc-Dp110^{TKRK} could suggest that the multiple mutations render this protein less stable than the other fusion proteins, other explanations are possible, and potentially more plausible. The low myc-Dp110^{TKRK} expression levels could simply be a function of the concentration of PMK vector that was used to transfect cells. Although as equal concentrations as possible of PMK vectors were used, the assessment of the concentrations could well

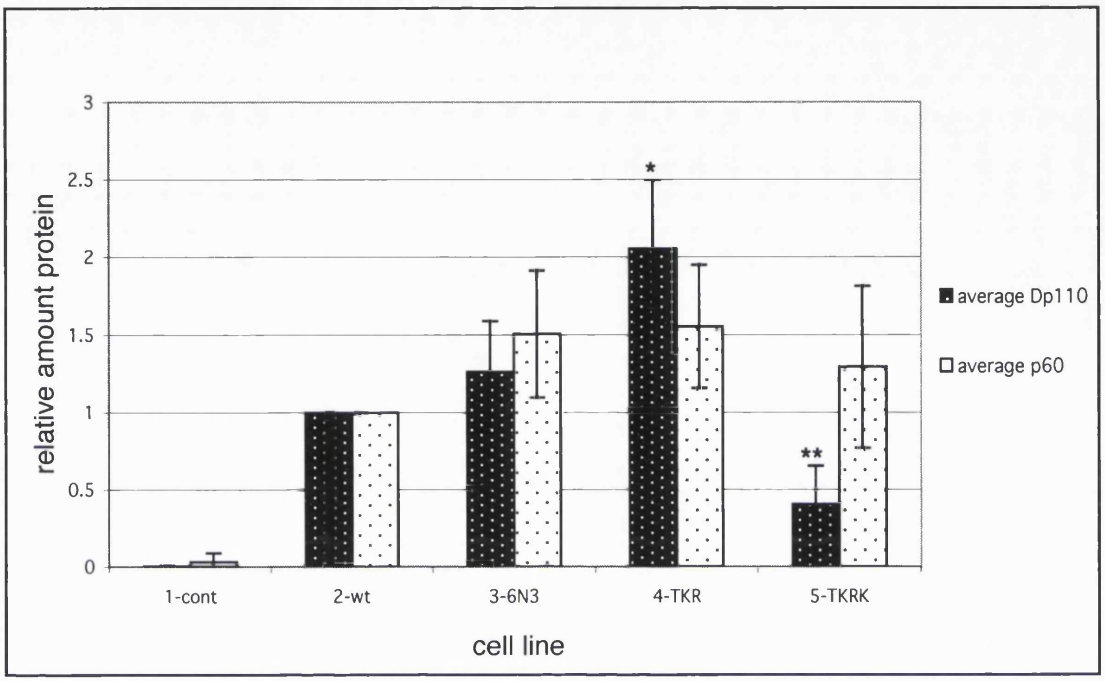

Figure 4.8 Relative expression levels of myc-Dp110* and HA-p60 in transgenic cell lines

Relative myc-Dp110* and HA-p60 expression levels after 16 hours of 700μg/ml $CuSO_4$ treatment were calculated from Western blots of induced cell lysates probed with α–HA, α–myc and α–β-tubulin. Amounts of myc-Dp110* and HA-p60 were normalised for total protein levels using the amount of β-tubulin in the respective lane. Relative values within each experiment were then adjusted by dividing each value by the level of the corresponding transgene in the 2-wt cell lysate. The graph shows data compiled from five independent experiments. The levels of HA-p60 expressed in each cell line are not significantly different. myc-$Dp110^{TKR}$ is expressed at a higher level ($p<0.05$, *) and myc-$Dp110^{TKRK}$ is expressed at a lower level ($p<0.01$, **) than any of the other myc-Dp110* proteins.

Error bars show standard deviation

have been incorrect. This explanation could equally well explain why the same treatment with $CuSO_4$ induces a higher level of $Dp110^{TKR}$ expression.

As discussed before, a direct comparison of HA-p60 and myc-Dp110* expression levels is not possible using these data (see section 4.10 for an explanation of how this can be achieved). What is clear from figures 4.7 and 4.8 is that $Dp110^{6N3}$ is expressed, and is stable. The results indicate that unless further, unidentified promoter mutations are present on the 6N3 chromosome, the reduced size of $dp110^{6N3/6N3}$ larvae is unlikely to be caused by a reduction in Dp110 protein expression.

4.8 Immunofluorescence of stable cell lines

Although biochemical analyses give us an idea of what is happening globally in the cell lines, they do not give us any indication of how individual cells respond to treatment, nor do they tell us how heterogeneous the populations of cells are. For example, although we know that HA-p60 can be expressed in the cell line as a whole, we have no idea whether all cells are able to express the fusion protein, and this anxiety is accentuated by the fact that we were unable to select for the pTIZ-HA-p60 vector. In addition, we do not know whether the ratio of HA-p60 to myc-Dp110* expression is constant within a cell line, or whether it varies. That is to say, if a particular cell expresses a lower than average level of HA-p60, is the level of myc-Dp110 co-ordinately reduced or does it vary independently? One way of addressing these issues is to use immunofluorescence to look at small populations of the stably transfected cells.

Cells from each cell line were cultured in six well plates at a density of 5×10^6 cells/ml for eight hours. $CuSO_4$ was added to half the wells to a final concentration of 700μg/ml, for 16 hours. Induced and uninduced cells were seeded onto lysine-coated coverslips, fixed and permeablilised. Coverslips were then incubated with Fluorescein conjugated α-myc antibody (α-myc-FITC) or with α-HA followed by a Rhodamine conjugated α-mouse antibody (α-mouse-TRITC), then mounted on slides in a mountant containing the nuclear dye, DAPI (Vectashield).

Comparing the level of staining in control and induced 2-wt cell lines revealed that the available α-HA antibodies did not recognise the mutated HA epitope tag in cells. It is unclear whether this difficulty arose directly as a result of the mutation, as HA has a reputation for performing poorly in immunofluorescence experiments even

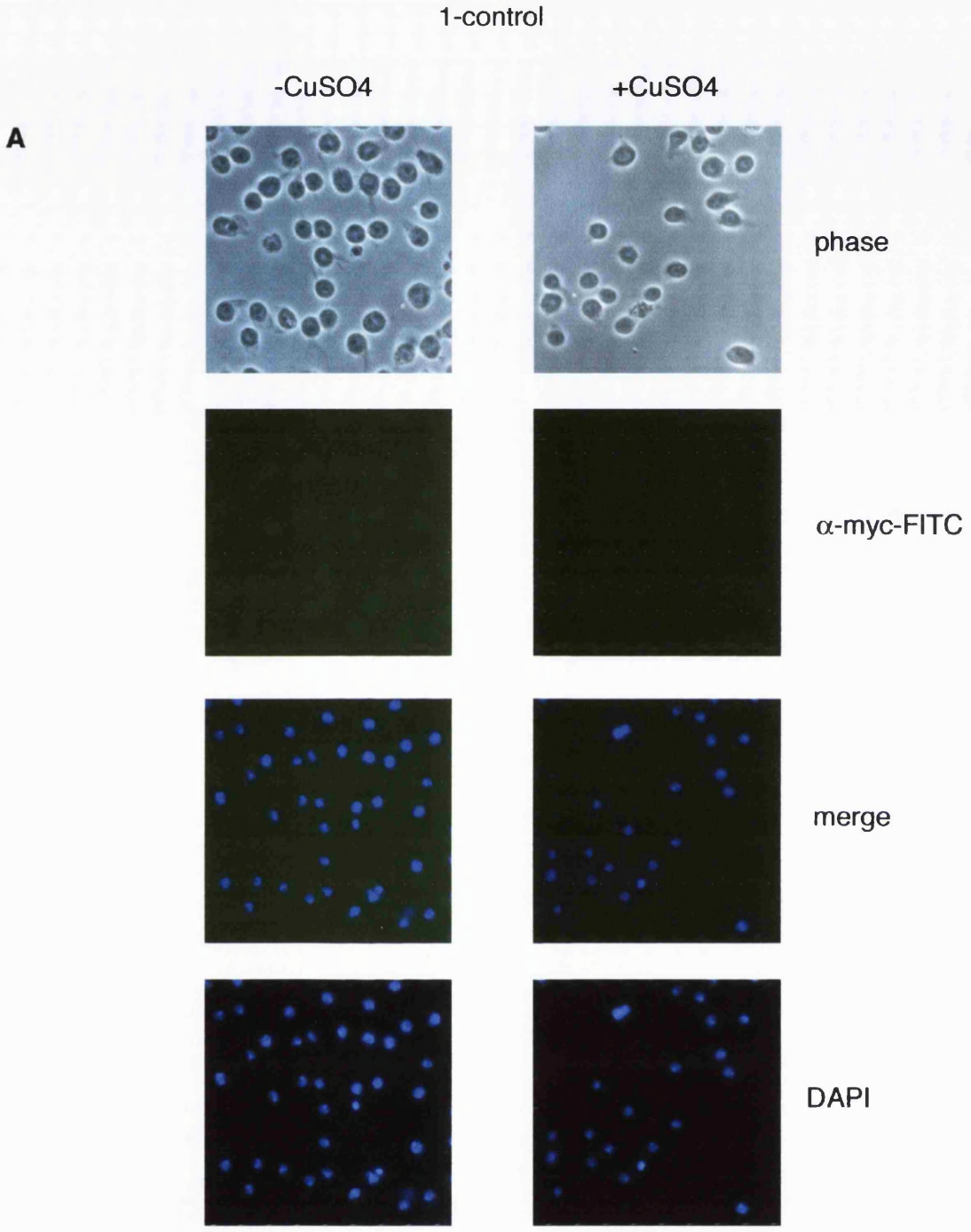

Figure 4.9 Induction of myc-Dp110* in transgenic cell lines

Control transfected or pMt-myc-Dp110*/pMt-HA-p60 cells were fixed after no treatment or treatment with $CuSO_4$ for 16 hours. Cells were immunostained with Fluorescein conjugated α-myc antibodies (α-myc-FITC) and mounted in DAPI-containing Vectashield. Untreated (-$CuSO_4$) and treated (+$CuSO_4$) cells were photographed. **A** shows control transfected cells. Note that there is only minimal background reactivity with the α-myc-FITC antibody. **B**, **C**, **D** and **E** show treated and untreated 2-wt, 3-6N3, 4-TKR and 5-TKRK cells respectively. A strong induction of myc-Dp110* expression is induced upon $CuSO_4$ treatment.

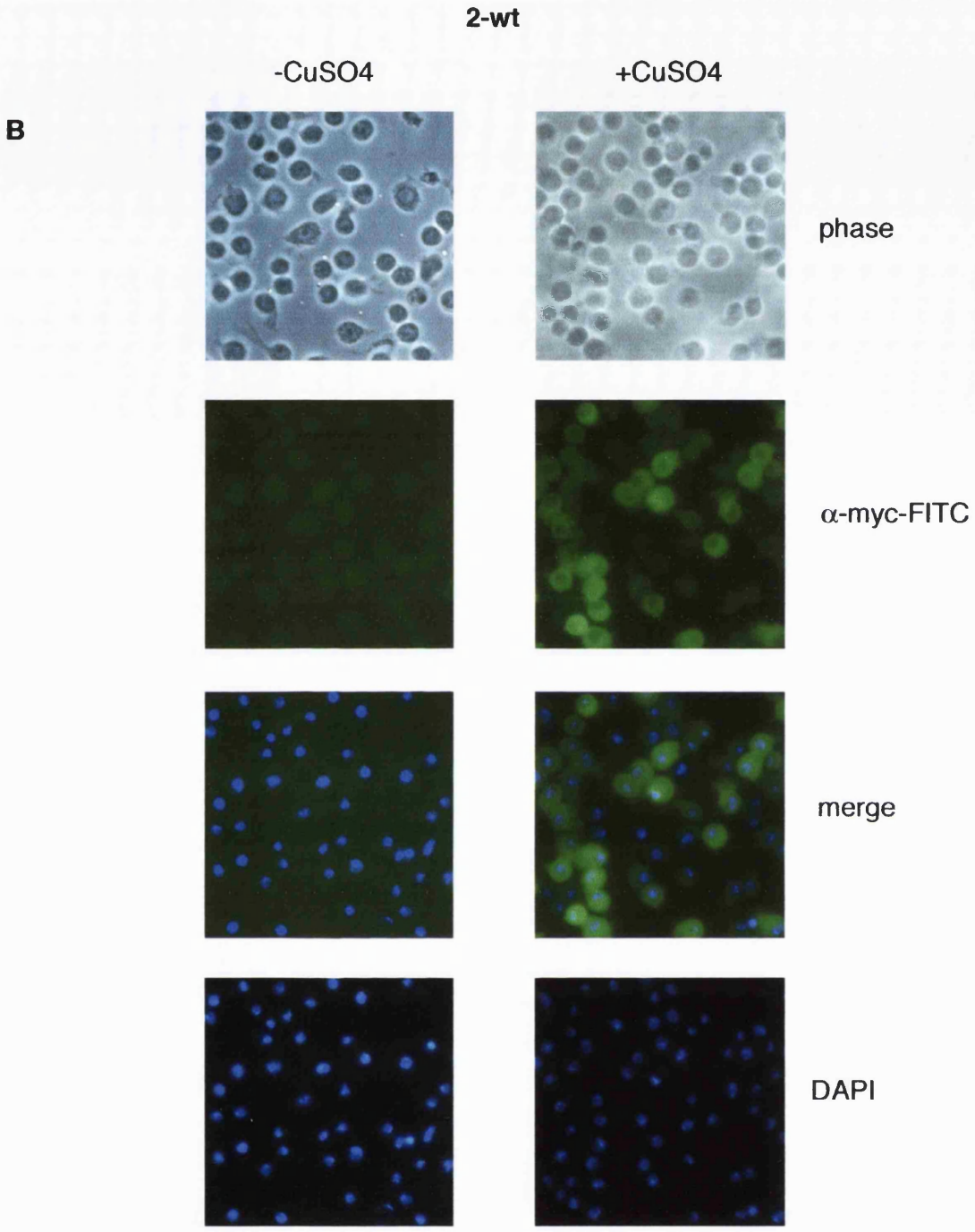
2-wt
-CuSO4
+CuSO4
B
phase
α-myc-FITC
merge
DAPI

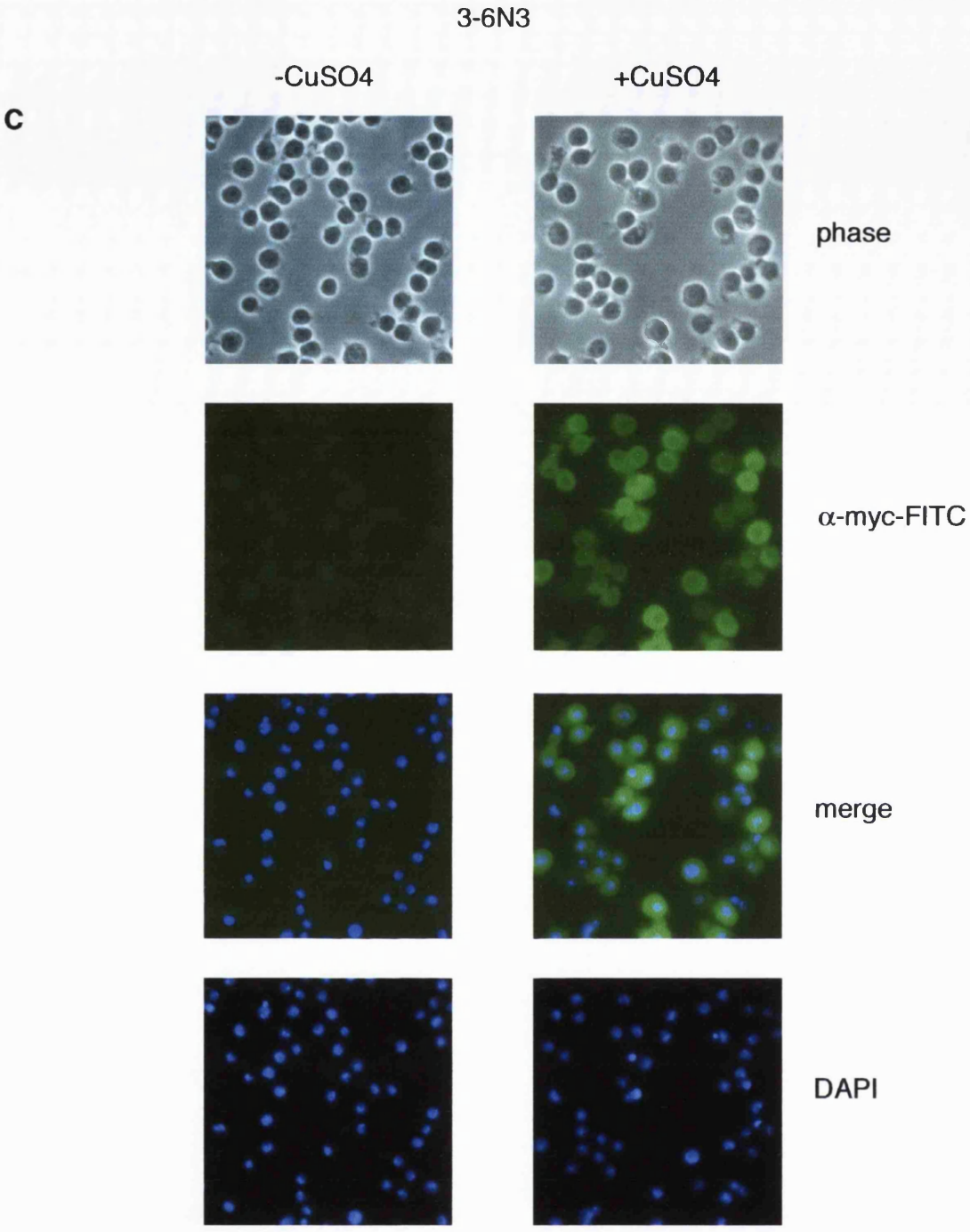
3-6N3
-CuSO4
+CuSO4
C
phase
α-myc-FITC
merge
DAPI

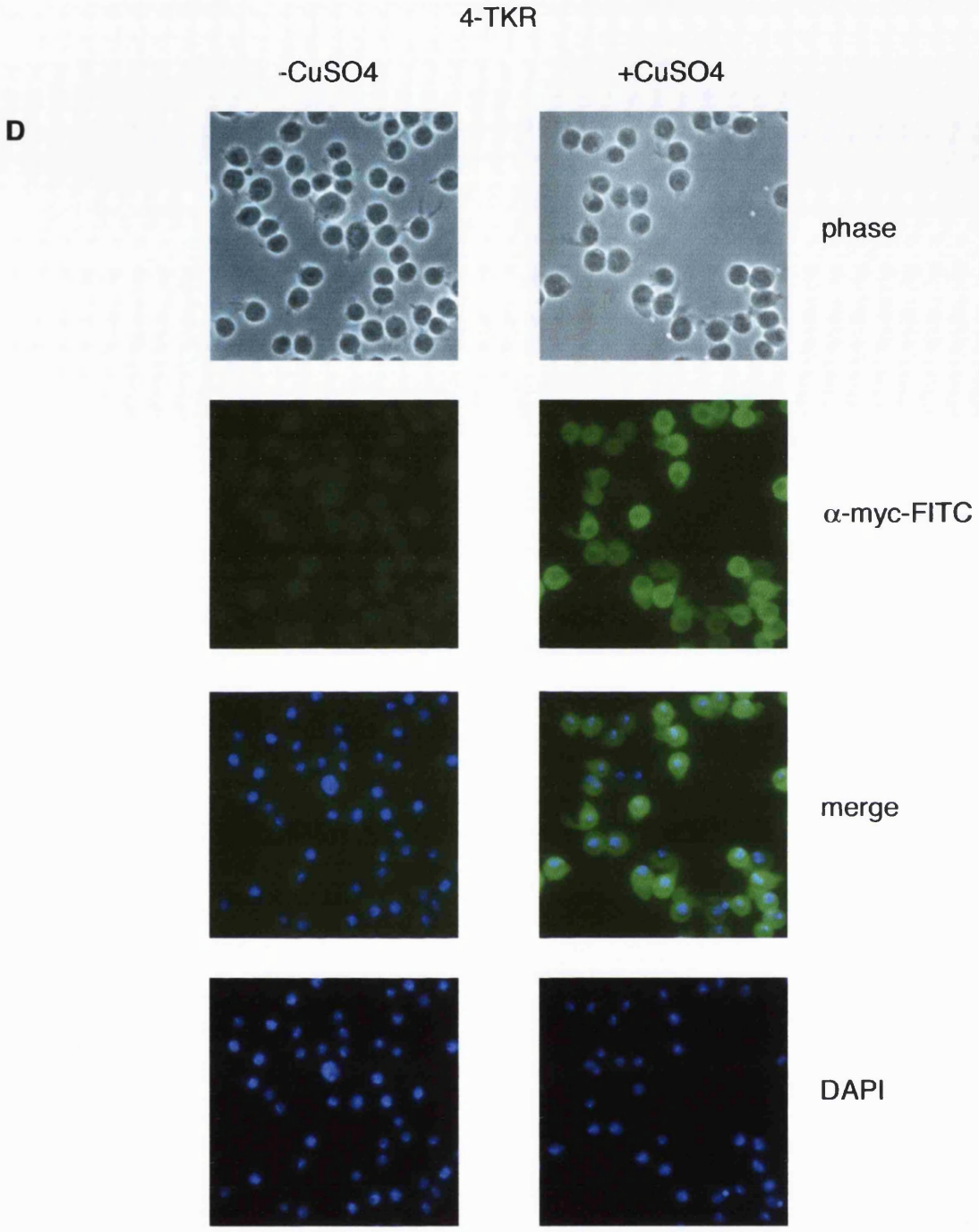
4-TKR
-CuSO4
+CuSO4
D
phase
α-myc-FITC
merge
DAPI

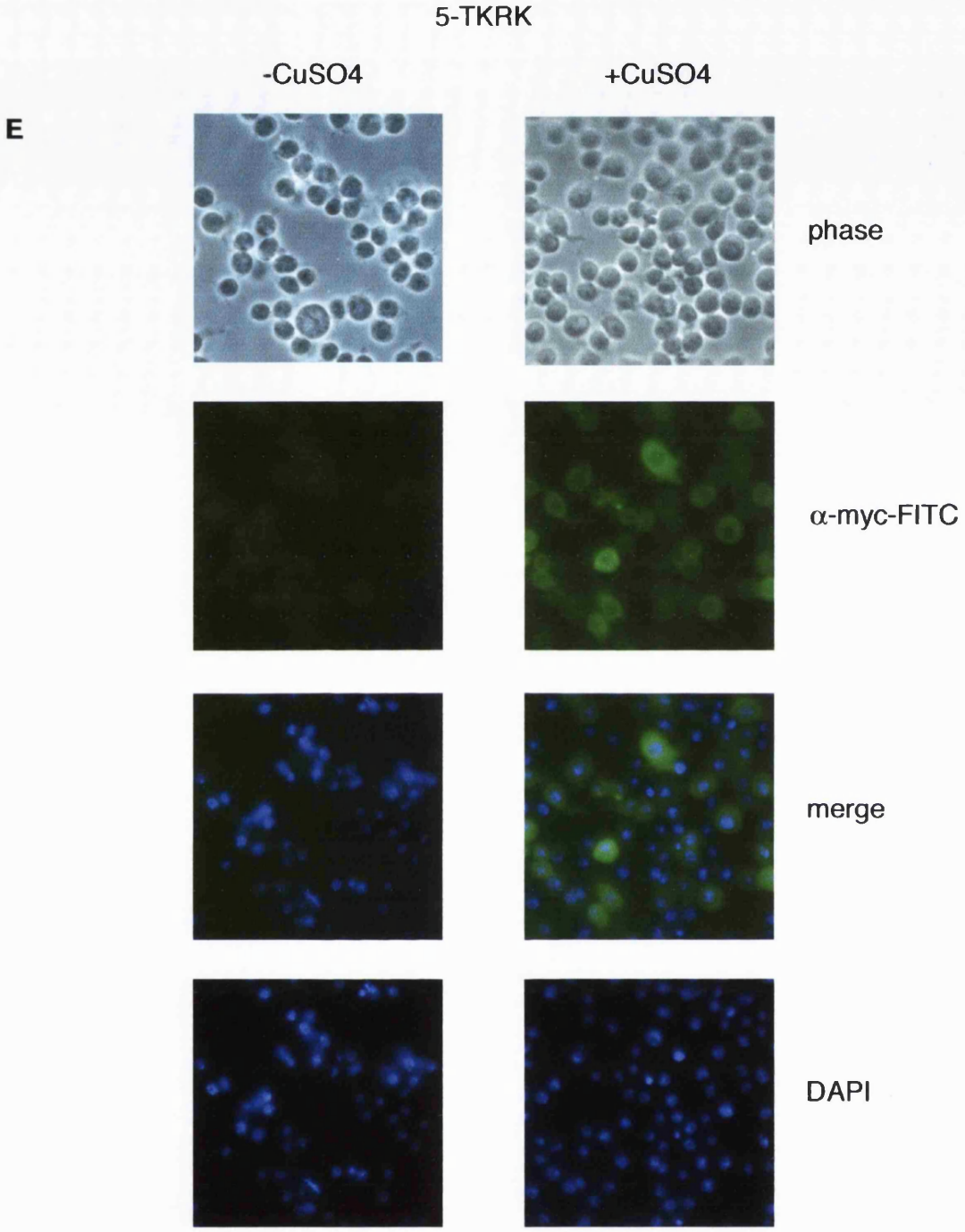
5-TKRK
-CuSO4
+CuSO4
E
phase
α-myc-FITC
merge
DAPI

when it is not mutated (Daniel Zicha, personal communication). The α-myc antibodies worked well and a significant increase in myc-tagged protein expression in 2-wt cells was seen after induction with $CuSO_4$.

Figures 4.9A to 4.9E show the changes in myc-Dp110* expression level upon treatment of all five cell lines with $CuSO_4$ for 16 hours. Pictures of the cells were captured using a digital camera (Axiocam) attached to an imaging microscope (Zeiss Axioplan 2). All comparable images were captured using the same objective and at the same sensitivity and resolution. These images confirm that myc-Dp110* is induced in all cell lines after 16 hours, with the exception of the 1-control cell line. The sensitivity of the immunofluorescence is not high enough to register any leaky myc-Dp110* expression in uninduced cells. The phase contrast images confirm that no major morphological changes are caused by $CuSO_4$ treatment or by myc-Dp110* or HA-p60 expression.

From a comparison of the myc-Dp110* expression levels in each of the cell lines (see figure 4.10), myc-$Dp110^{TKR}$ appears to be expressed in the majority of cells at a higher level than the other fusion proteins; $Dp110^{TKRK}$ is expressed at a lower level, and in a lower percentage of the cells than the other myc-tagged proteins. This is directly comparable with the biochemical data presented in section 4.7. Information about the variations in brightness across an image can be collected in PhotoShop. This was used to assess the proportion of cells were expressing the transgenes at a visible level. In order to quantify this information, a $3cm^2$ area was marked out on three separate images of each cell line. The proportion of cells expressing visible levels of the transgenes within each square was then assessed, and an average of these proportions was then calculated. 96.5 +/- 5.5% of 2-wt cells, 98.3 +/- 2.9% of 3-6N3 cells and 100+/- 0% of 4-TKR cells express myc-Dp110* at visible levels. In contrast, only 69.1 +/- 7.0% of 5-TKRK cells express myc-$Dp110^{TKRK}$ at visible levels.

As all cells are grown in the presence of Hygromycin, it follows that all cells must be resistant to the antibiotic. The invisible levels of myc-$Dp110^{TKRK}$ expression in 31% of the 5-TKRK cells could be because the cells have incorporated only the Hygromycin resistance gene into their genome independently of the *myc-dp110^{TKR}* sequence, so no fusion protein is expressed. Alternatively, the myc-$Dp110^{TKRK}$ protein may be inherently unstable. A further possibility, discussed previously, is that the amount of PMK-myc-$Dp110^{TKRK}$ that was used to transfect the S2 cells may have been lower than the amount of the other PMK vectors, so although the myc-$Dp110^{TKRK}$

Figure 4.10 Comparative myc-Dp110* levels in cell lines

Control transfected or pMt-myc-Dp110*/pMt-HA-p60 cell lines were treated with $CuSO_4$ for 16 hours. Cells were fixed, immunostained with α-myc-FITC, and mounted on slides in DAPI-containing vectashield. The number of cells expressing visible levels of myc-Dp110* was assessed in PhotoShop from the captured images. Control transfected cells were used as a reference as they expressed no myc-Dp110* protein. >96% of 2-wt, 3-6N3 and 4-TKR cells expressed visible levels of myc tagged protein. Only 69% of the 5-TKRK cells express visible levels of myc-$Dp110^{TKRK}$. The 4-TKRK cell line also appeared to have higher levels of protein expressed in comparison with other cell lines. Note that this figure is made up of the same data as the previous figure.

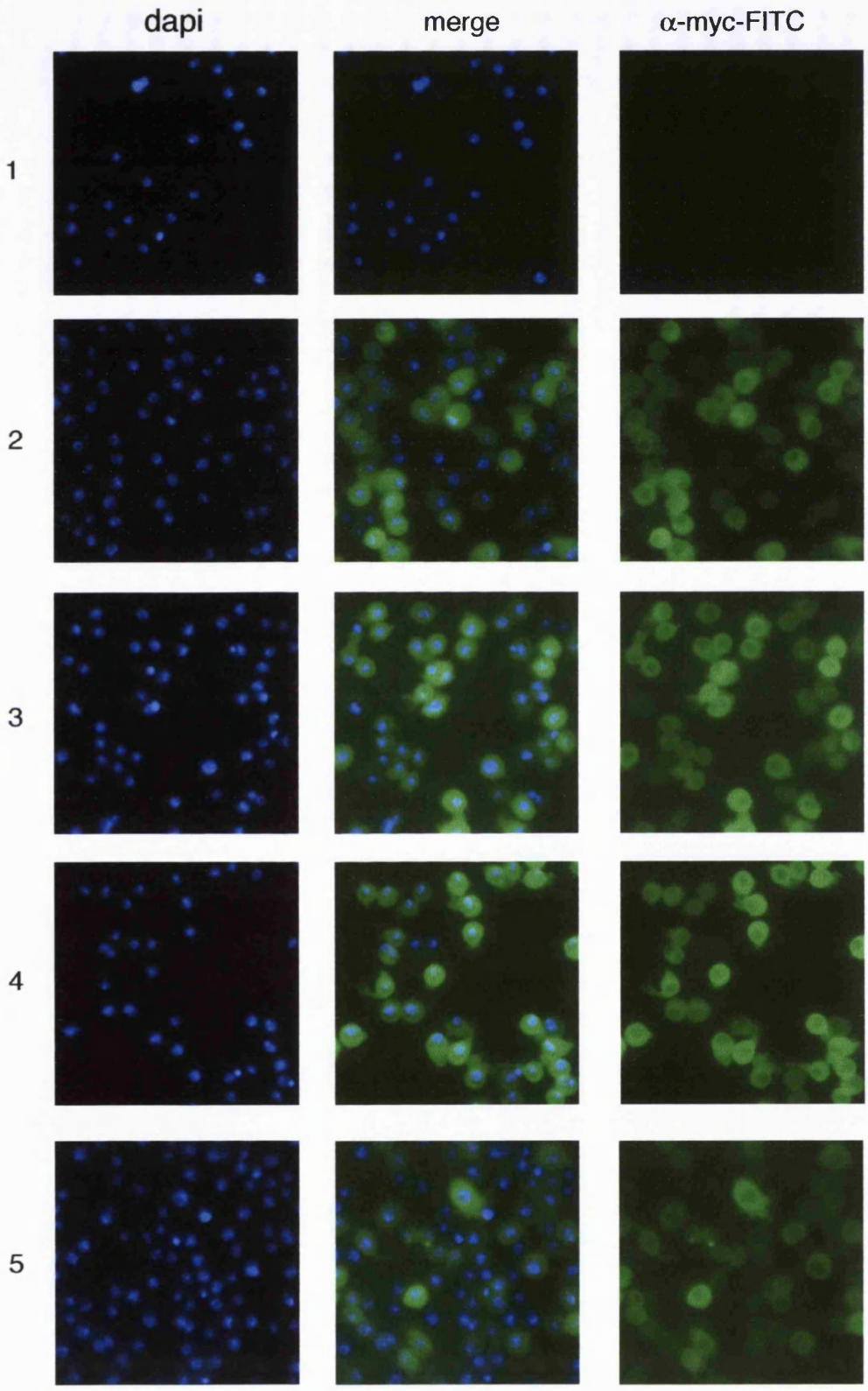
dapi
merge
α-myc-FITC
1
2
3
4
5

encoding vector is present in the cells there are fewer copies of the vector in each cell, so the levels of expression are too low to be recorded using this technique.

Although the immunofluorescence data were not able to confirm whether all transfected cells expressed HA-p60, they did highlight the polyclonal nature of the cell lines with respect to myc-Dp110* expression. Although greater than 96% of cells from cell lines 2-wt, 3-6N3 and 4-TKR express visible amounts of myc-tagged protein, the protein expression levels within the cell populations vary widely. In addition, the low level of $Dp110^{TKRK}$ expression seen in the 5-TKRK cell lines, which had been suggested by the biochemistry experiments, was confirmed.

4.9 Co-immunoprecipitation of myc-Dp110* with HA-p60

In order for Dp110 to function *in vivo,* it needs to access its lipid substrates in the cell membrane. This is primarily achieved via the binding of p60 to phosphorylated tyrosine motifs resident within the cytoplasmic domain of activated receptor tyrosine kinase molecules. If Dp110 is unable to bind p60, the ligand stimulated Dp110 activation will be impaired. Thus, if any of the RBD mutations have a negative effect on the p60 binding ability of Dp110, then associated loss of function phenotypes could be a result of an inability of the protein to be membrane localised.

To ensure that the RBD mutations did not affect Dp110*-p60 binding, I carried out co-immunoprecipitation experiments. Cells from each cell line were untreated, or treated with $CuSO_4$ for 16 or 24 hours, and then pelleted and lysed. The lysates (2mg/point) were incubated for one hour with α-myc or α-HA antibodies (1.5μl/point) and then protein-A sepharose beads (15μl/point) were used to capture immune complexes. Immunoprecipitates (IPs) were washed extensively in lysis buffer and then separated using SDS-PAGE. Lysates were separated in the same way.

Western blots of the SDS-PAGE gels were probed first with α-myc, α-HA, α-p60 and α-Dp110 (SK50) antibodies and then α-mouse-800 and α-rabbit-680 secondary antibodies. The blots were scanned on the LI-COR Odyssey infrared scanner and visualised via the associated software package. This software represents the 800nm channel in green and the 680nm channel in red (see figure 4.11) and thus allows the signals originating from α-rabbit and α-mouse primary antibodies to be distinguished.

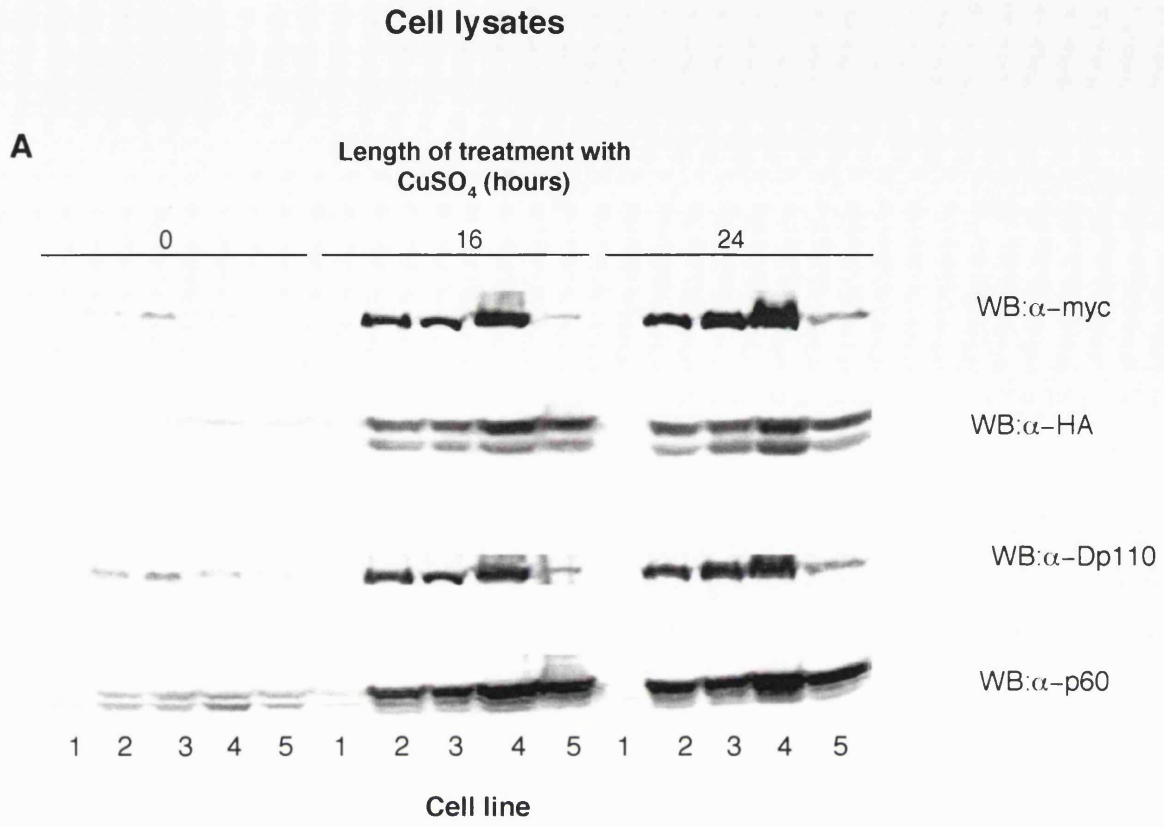

Figure 4.11 Immunoprecipitation of myc-Dp110* and HA-p60 from transgenic cell lines

α-myc and α-HA were used to immunoprecipitate myc-Dp110* and HA-p60 respectively from lysates of control transfected or pMt-myc-Dp110*/ pMt-HA-p60 cells that were untreated or treated with $CuSO_4$ for 16 hours or 24 hours. Lysates **(A)**, α-myc immunoprecipitates **(B,C)** and α-HA immunoprecipitates **(D,E)** were resolved on three SDS-PAGE gels (8%). Western blots were probed first with α-myc, α-HA (mouse antibodies), α-Dp110 and α-p60 (rabbit antibodies) and then with α-mouse-800 (green) and α-rabbit-680 (red) secondary antibodies. **B** and **D** show the single channel images, whereas **C** and **E** show the merged images. The Dp110 proteins containing RBD mutations are able to co-immunoprecipitate with HA tagged and endogenous p60 (see **C**). The presence of HA-p60 and myc-Dp110* in the lysates of and immunoprecipitates from untreated cells confirms that some leaky expression of these transgenes occurs. Note that $Dp110^{TKR}$ (4) and $Dp110^{TKRK}$ (5) run at a higher apparent molecular weight than the wt (2) and 6N3-mutation containing proteins (3).

Similar results were obtained more than three times

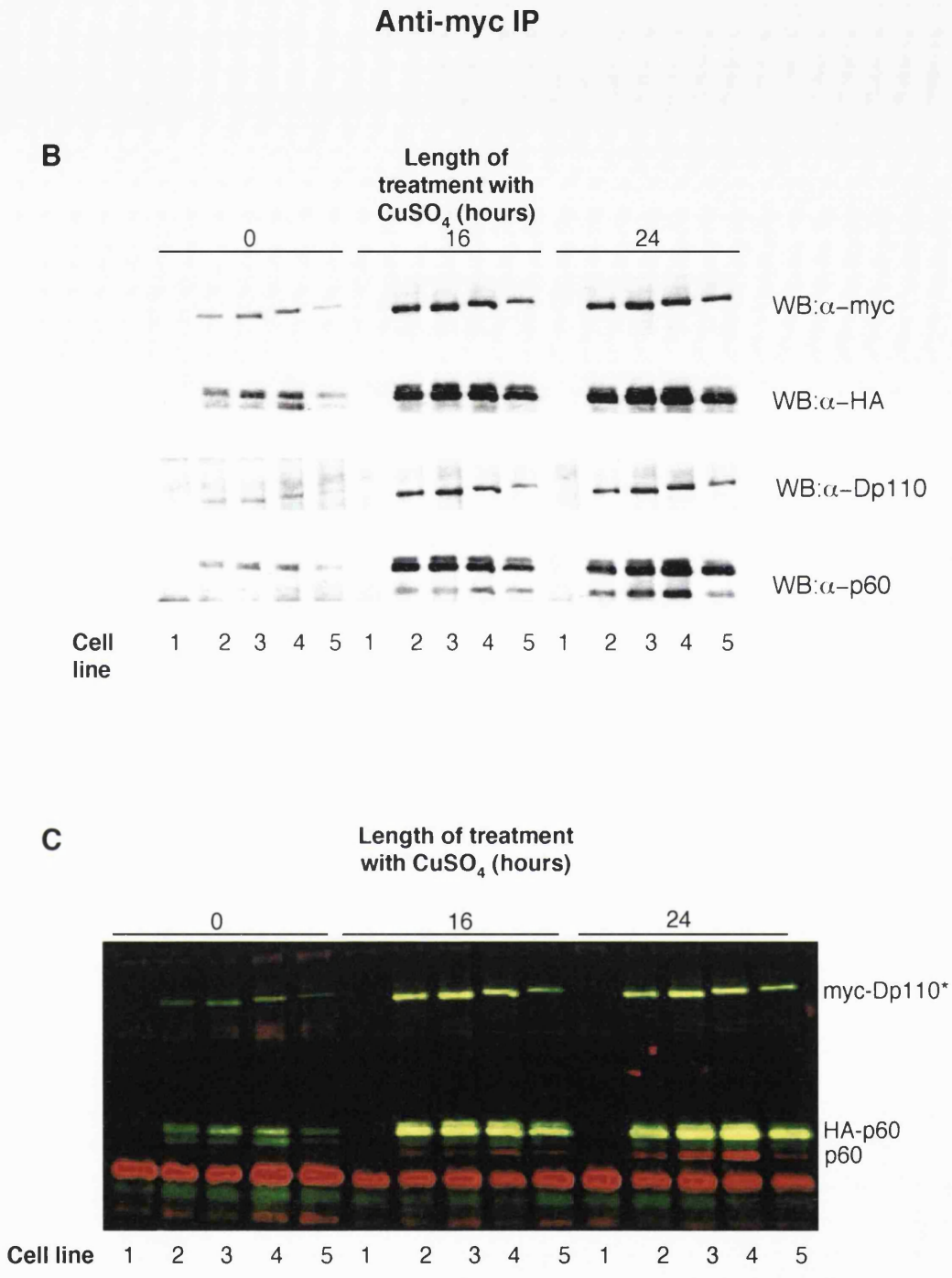
Anti-myc IP
B
Length of treatment with CuSO4 (hours)
0
16
24
WB:α-myc
WB:α-HA
WB:α-Dp110
WB:α-p60
Cell line
1 2 3 4 5 1 2 3 4 5 1 2 3 4 5
C
Length of treatment with CuSO4 (hours)
0
16
24
myc-Dp110*
HA-p60
p60
Cell line
1 2 3 4 5 1 2 3 4 5 1 2 3 4 5

Anti-HA IP

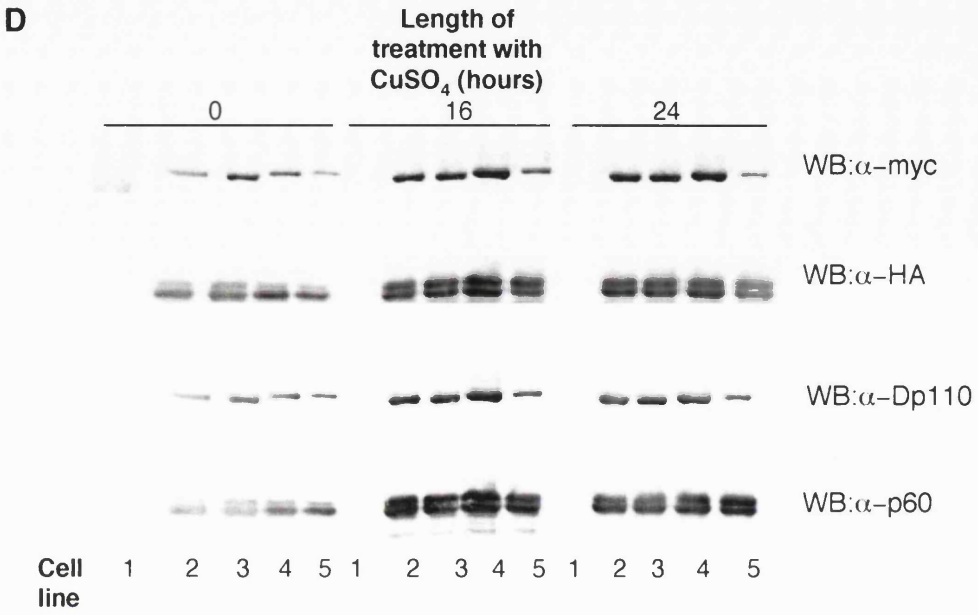
D
Length of treatment with CuSO4 (hours)
0
16
24
WB:α-myc
WB:α-HA
WB:α-Dp110
WB:α-p60
Cell line
1 2 3 4 5 1 2 3 4 5 1 2 3 4 5

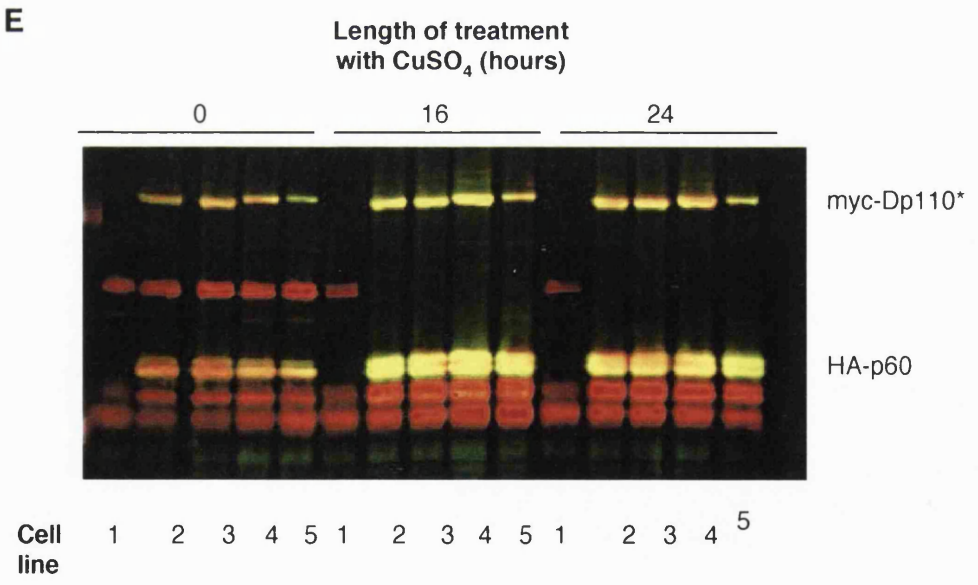
E
Length of treatment with CuSO4 (hours)
0
16
24
myc-Dp110*
HA-p60
Cell line
1 2 3 4 5 1 2 3 4 5 1 2 3 4 5

These experiments clearly demonstrate that HA-p60 co-immunoprecipitates with each myc-Dp110* protein and vice versa (see figure 4.11B-E). This observation confirms that none of the RBD mutations abolish the p60 binding domain of the myc-Dp110* sufficiently to abolish p60 binding. It additionally confirms that the myc tag itself does not abrogate p60 binding. Furthermore, by quantifying the relative levels of HA-tagged and myc-tagged protein in the α-myc immunoprecipitates from the different cell lines visualised on several independent Western blots, I was able to confirm that the p60-binding abilities of the different mutants were remarkably similar.

The association of endogenous p60 with each of the α-myc immune complexes (see figure 4.11C) suggests that the binding of myc-Dp110* to HA-p60 is not dependent on the presence of the HA tag, consistent with the assumption that myc-Dp110*-HA-p60 binding takes place via the p60 binding site on myc-Dp110*.

From these blots it can be seen that myc-Dp110^{TKR} and Dp110^{TKRK} have reduced electrophoretic mobility compared to the other tagged proteins as they run through the polyacrylamide gel. This characteristic of these mutant proteins is not particularly surprising and is probably caused by the point mutations altering the overall charge of the protein.

The level of myc-Dp110^{TKRK} compared to the other myc-tagged proteins is lower in the Western blots of the lysates (see figure 4.11A) than in those of the immunoprecipitates. This difference suggests that the immunoprecipitation reaction (at least the α-myc IP) is not progressing to completion and is therefore limited by some component of the reaction (see figure 4.11).

From the data described in this section we can be confident that the phenotype of *dp110$^{6N3/6N3}$* flies is not caused by an inability of Dp110^{6N3} to bind p60. If this had been the case, the inability of the catalytic subunit to be localised to the cell membrane thereby could have caused a reduction in *in vivo* Dp110 kinase activity. In addition, the data confirm that neither the myc tag nor the other RBD mutations inhibit Dp110-p60 binding. These results were corroborated by data from a further three independent experiments.

4.10 Revisiting relative expression levels of myc-Dp110* and HA-p60 in cell lines

By quantifying the data obtained from co-immunoprecipitation experiments it should be possible to assess the comparative expression levels of myc-Dp110 to

HA-p60 in the different lines. This assessment would be based on the assumption that as Dp110 and p60 constitutively associate with one another and thus that unbound p60 or Dp110 would only exist if the particular subunit were present in the cell in excess of its binding partner. In order to make this calculation, it is also necessary to assume that the protein composition of the immunoprecipitate reflects the overall protein composition of the cell.

If the ratio of HA- to myc-tagged protein in the α-HA and α-myc IPs are calculated and compared and no difference is seen, then we can be confident that the myc-Dp110* and HA-p60 are expressed at a 1:1 ratio in these cells. However, if the fraction of HA-tagged protein over myc-tagged protein were higher in the α-HA IP than in the α-myc IP, it would suggest that HA-p60 is present in the cell in excess of myc-Dp110*. If the fraction of HA-protein to myc tagged protein were lower in the α-HA IP than in the α-myc IP then this observation would suggest that myc-Dp110* is present in excess. These calculations are independent of antibody affinity but the same lysate must be used for both immunoprecipitation reactions, and care must be taken to develop the blots from those two reactions simultaneously. Furthermore, replicate experiments would have to be assessed to ensure the validity of the conclusion.

Unfortunately, as I tried to optimise the experimental method while performing experiments described in section 4.9, the results from the four experiments cannot be directly combined and compared. As a result, I cannot conclusively calculate the relative levels of HA-p60 or myc-Dp110* in the different cell lines.

4.11 Assessing the *in vitro* kinase activity of myc-Dp110*

It was important to assess whether the RBD domain mutations altered the basal *in vitro* kinase activity of the myc-Dp110* proteins. If basal kinase activity is reduced, this reduction could account for any phenotype seen in flies containing only the RBD mutated forms of Dp110. Kinase assay data from p110γ and p110γ-DASAA, suggests that no difference in basal kinase activity should result from the addition of RBD mutations to p110γ, although large differences in activity do result if the two p110γ molecules are stimulated with constitutively active Ras (Pacold et al., 2000).

Basal kinase activity can be determined *in vitro* by quantifying the ability of α-myc immunoprecipitates to phosphorylate phospho-inositide lipids in the presence of [γ-^{32}P]-ATP. Although phosphatidylinositol 4,5-bisphosphate (PIP_2) is the substrate

required to produce the second messenger, phosphatidylinositol 3,4,5-trisphosphate (PIP_3), and is therefore the most relevant substrate to use in such assays, phosphatidylinositol (PI), and phosphatidylinositol 4-phosphate (PIP) are also commonly used as substrates (Chan et al., 2002; Suire et al., 2002). In fact, the recorded levels of PI phosphorylation in *in vitro* PI3K assays are often higher than those of other lipid substrates. Owing to this observation, we decided to use PI as a substrate in preliminary experiments, with the intention of assaying PIP_2 phosphorylation in later experiments.

Stably transfected cells were grown in flasks at 23 C until they reached a density of greater than 6×10^6 cells per ml media. $CuSO_4$ was then added to the flasks to a final concentration of 700μg/ml. After a further 16 hours, cells were pelleted and lysed, and α-myc (3μl) was used to immunoprecipitate myc-Dp110* from lysates of cell lines 1 to 5 (18mg protein/point). Protein-G sepharose (25μl/point) was added to capture the immune complexes. S2 cells were lysed co-ordinately, and endogenous Dp110/p60 complexes were affinity purified using agarose beads that had been coated in a tyrosine-phosphorylated peptide from the cytoplasmic tail of human PDGFβ receptor (15μl/point). This phosphopeptide (GGpYMDMSKDESVDpYVPML) contains two pYXXM motifs and is recognised and bound by the SH2 domain of p60 (Weinkove et al., 1997).

Lipid kinase assay methods are described in detail in section 2.4.7. Briefly, IPs were washed in lysis buffer and kinase assay buffer, and one tenth of the IP was removed during the final wash to be used in Western blotting analysis. The remaining beads were then incubated at 30 C for 30 min with kinase assay buffer, PI vesicles, magnesium-ATP (100μM), and 5μCi [γ-^{32}P]-ATP. The kinase reaction was stopped with hydrochloric acid (1M), and a 1:1 methanol: chloroform solution was used to separate the aqueous and non-aqueous layers of the reaction mix. 80μl of the non-aqueous phase was spotted onto warmed TLC plates and separated overnight. The plates were visualised (see figure 4.12A), and the incorporation of radioactive phosphate into PI was quantified using a phosphoimager.

The amount of myc-Dp110* or $Dp110^{WT}$ added to the reaction was assessed from Western blots of the immunoprecipitates, probed with α-Dp110 (SK50) (see figure 4.12B). The activity of the different Dp110 proteins was determined by dividing the level of radioactive phosphate incorporated into PI by the amount of Dp110* protein included in the assay. Relative activities were calculated, after the

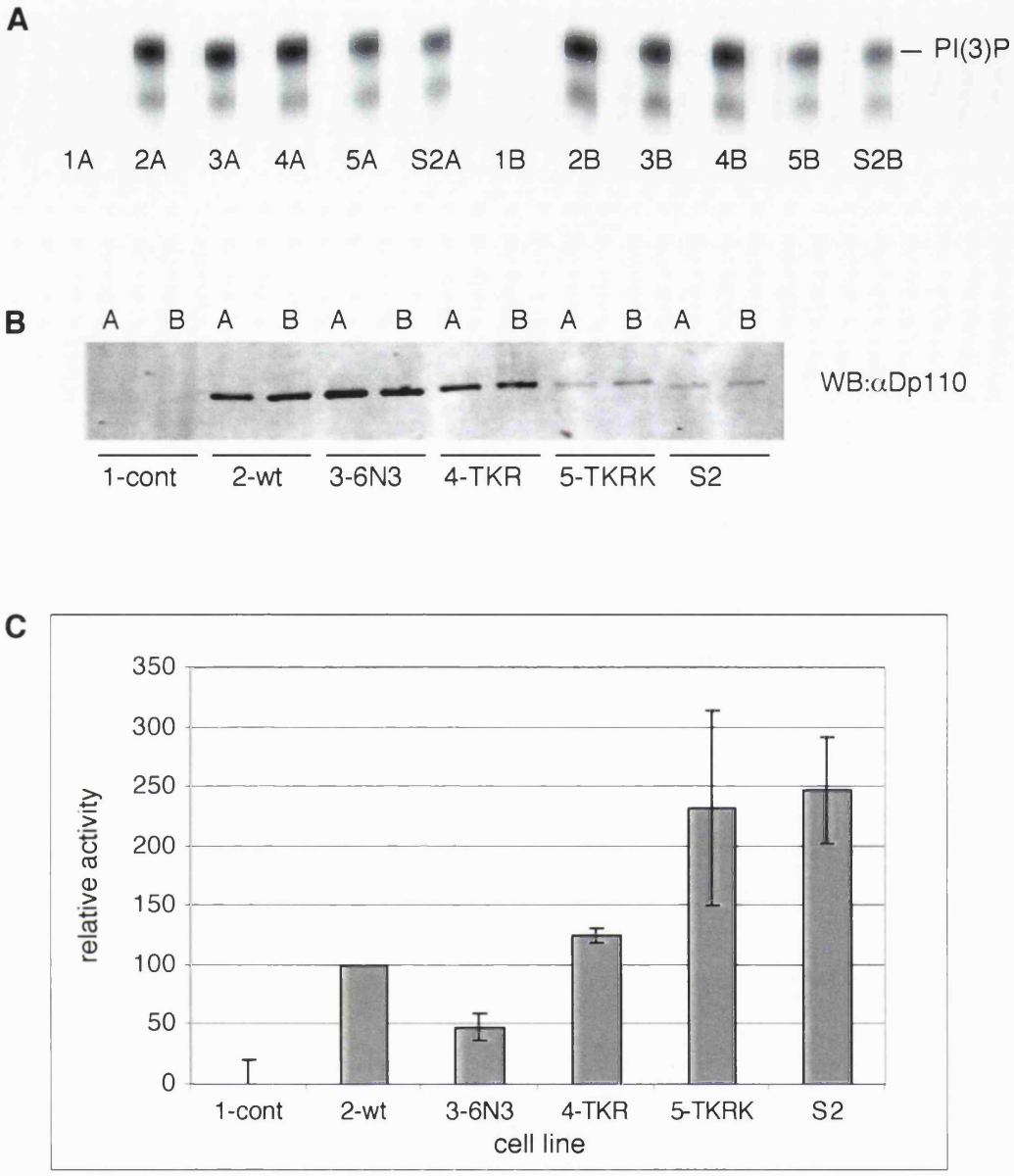

Figure 4.12 *In vitro* myc-Dp110* activity levels

α-myc immunoprecipitation reactions were performed from lysates of induced pMt-myc-Dp110*/pMt-HA-p60 cell lines, or control transfected cell lines (18mg protein/point). Nine tenths of the IP was assayed for its ability to phosphorylate phospatidyl inositol (PI) lipid vesicles in the presence of [γ-^{32}P]-ATP. **A** 80μl of the non-aqueous phase of the kinase assay reaction was separated using thin layer chromatography and the incoporation of radioactive phosphate into PI was visualised and quantified using a Storm phosphoimager. The remaining one tenth of the IP was separated using SDS-PAGE. **B** Western blots were probed with α-Dp110 (SK50) and the levels of myc-Dp110* present in the IP were quantified using the LI-COR Odyssey infrared imaging system. **C** Relative activity of the myc-Dp110* was calculated by dividing the value of radioactive phosphate incorporation by the relative amount of Dp110 present in the IP.

Similar results were obtained in one other experiment

Error bars show standard deviation

activity of myc-Dp110^{WT} was defined as 100 percent, and are displayed graphically in figure 4.12C.

The RBD mutations in myc-Dp110^{TKR} and myc-Dp110^{TKRK} do not appear to adversely affect basal activity of the kinase. If anything, myc-Dp110^{TKRK} has a higher activity than the myc-tagged wild-type kinase. However, these particular data are subject to a large amount of error, primarily because of the low levels of myc-Dp110^{TKRK} protein present in the immunoprecipitations. In contrast, a 50% reduction in basal kinase activity is caused by the 6N3 point mutation. A replicate experiment confirmed these observations (data not shown).

One concern that could arise from these data is that attachment of the myc-tag to the N-terminus of the protein causes kinase activity of Dp110 to be reduced. Although the differences between the activities of myc-Dp110^{WT}/HA-p60 in α-myc IPs and endogenous Dp110/p60 in phosphotyrosine affinity purification do suggest this, an alternative explanation is possible. Myc-tagged Dp110* was purified from cell lysate via its N-terminally placed myc tag, whereas untagged Dp110 was pulled out of the S2 cell lysate via p60 binding to a phosphotyrosine motif. The latter situation is clearly more reminiscent of the physiological activation of Dp110. It is possible that phosphotyrosine binding causes conformational changes in p60 that are transmitted to Dp110. These changes may well increase the activity of the kinase. In fact, constitutive membrane localisation of p85 via the N-terminal addition of a peptide encoding the Src myristoylation signal does not increase mammalian PI3K activity in NIH3T3 cells as much as would be expected if membrane localisation of the catalytic subunit were the only factor involved in kinase activation (Chan et al., 2002). Furthermore, the binding of p85 to phosphorylated tyrosine motifs has been shown to increase PI3K catalytic activity *in vitro* (Backer et al., 1992; Carpenter et al., 1993).

In trying to assess whether normalisation of Dp110 activity using the amount of protein present in the IPs was justified, I realised that the immunoprecipitation procedure being used was not optimal. Increasing the amount of input lysate and the amount of antibody used in a proportional manner did not lead to the recovery of larger amounts of Dp110 protein. This result suggested that the volume of beads being used in the experiment was limiting the amount of Dp110 precipitated, and led me to repeat the experiment after optimisation of the IP conditions (see section 2.4.4 for further details). Time constraints restricted the number of new experiments that

could be performed, but results from the experiment carried out indicated that $Dp110^{6N3}$ may not be less active than $Dp110^{WT}$ (data not shown).

It is hard to reach a firm conclusion about the activity level of myc-$Dp110^{6N3}$ from these experiments. If activity is reduced by 50% by the introduction of the non-conservative mutation at D260, as implied by figure 4.12, then this could well account for the phenotype of larvae whose only full-length Dp110 contains the 6N3 mutation. However, if the activity were not reduced, as has been observed in preliminary experiments carried out using different IP conditions, then the phenotype would have to be explained by loss of RBD integrity. In order to be sure of which of these conclusions is valid, experiments should be repeated, and additional experiments, using PIP_2 as a substrate should also be carried out.

4.12 The story so far

The results so far are summarised in table 4.3. Western blots of lysed control transfected or pMt-myc-Dp110*/pMt-HA-p60 cells treated for 16 hours with $CuSO_4$ showed that although the expression levels of HA-p60 did not vary significantly between cell lines, there were significant differences in the levels of myc-Dp110* expression. The 2-wt and 3-6N3 cell lines expressed very similar amounts of myc-Dp110* when induced for 16 hours, but the level of $Dp110^{TKR}$ expressed in the 4-TKR cell line was significantly greater, and the level of $Dp110^{TKRK}$ expressed in the 5-TKRK cell line was significantly lower than this amount after the same length of transgene induction. These results were confirmed using immunofluorescence. Co-immunoprecipitation experiments using α-myc or α-HA antibodies as bait demonstrated that all the myc-Dp110 RBD mutants were able to bind HA-p60, and suggested that no significant differences in this binding ability were caused by the introduction of the RBD mutations. Most recently discussed are the experiments in which *in vitro* lipid kinase activity of Dp110 was assessed. The preliminary data suggested that myc-$Dp110^{6N3}$ was 50% less active than its wild type counterpart, and that myc-$Dp110^{TKRK}$ was more active. The problems associated with drawing these conclusions have already been examined. For firmer conclusions to be reached, the *in vitro* kinase activity experiments should be repeated using both PI and PIP_2 as substrates.

Cell line	Myc-Dp110* expression level	HA-p60 expression level	Myc-Dp110*/ HA-p60 binding	*In vitro* Myc-Dp110* kinase activity
1-control	-	-	-	-
2-wt	++	++	++	++
3-6N3	++	++	++	+(+)
4-TKR	++++	++	++	++
5-TKRK	+	++	++	++(+)

Table 4.3 Summary of cell line properties

This table summarises the results of the experiments shown in figures 4.7 to 4.12. Details are given in the text. The greater the number of crosses, the higher the expression level, binding ability, or kinase activity. The brackets indicate that the result is has been questioned, either because replicate experiements showed variable results or because experimental error was high, as is the case with the in vitro kinase activity of $Dp110^{6N3}$ and $Dp110^{TKRK}$ respectively.

Together these results imply that the small larva phenotype of $Dp110^{6N3/A}$ larvae described in section 4.2 is not due to lack of $Dp110^{6N3}$ expression, nor is it due to an inability of $Dp110^{6N3}$ to bind p60. If p60-binding had been disrupted the phenotype could be explained by a reduction in *in vivo* kinase activity caused by an inability of the $Dp110^{6N3}$ protein to be localised appropriately to the membrane. However, it is still unclear whether the phenotype is caused by a reduction in the innate catalytic activity of the subunit.

Secondly, the experiments performed demonstrate that both myc-$Dp110^{TKR}$ and myc-$Dp110^{TKRK}$ are expressed, are able to bind to p60 and have similar or greater lipid kinase than myc-$Dp110^{WT}$. These results suggest that myc-$Dp110^{TKR}$ and myc-$Dp110^{TKRK}$ are good candidate proteins for use in further experiments testing the *in vivo* activity of Dp110 proteins that are unable to bind Ras-family small GTPases.

4.13 Assessing the *in vivo* activity of myc-Dp110*

As discussed in section 3.1, signalling flux through the *Drosophila* PI3K pathway can be monitored using antibodies that specifically recognise phosphorylated dAkt. This technique was used to assess whether over-expression of the different transgenes activated signalling downstream of Dp110* in these cell lines. As discussed in section 4.5, the PI3K signalling activity downstream of transgene expression may be affected by the relative expression levels of myc-Dp110* and HA-p60 as the former activates signalling whereas the latter is thought to negatively regulate signalling. In addition, the activity of the different myc-Dp110* proteins may be altered by the differing abilities of the proteins to be regulated by other activating proteins, such as Ras-family small GTPases.

In a preliminary experiment (see figure 4.13), the Western blots showing the time course of transgene induction in cells that were actively growing in normal culture medium (see figure 4.6) were re-probed with α-p-Ser586 antibodies, which recognise dAkt only after it has been phosphorylated within its hydrophobic motif. Transgene expression in 2-wt and 3-6N3 cell lines appears to induce high levels of dAkt phosphorylation. Much lower levels of dAkt phosphorylation are seen when transgenes are expressed in the 4-TKR or 5-TKRK cell lines.

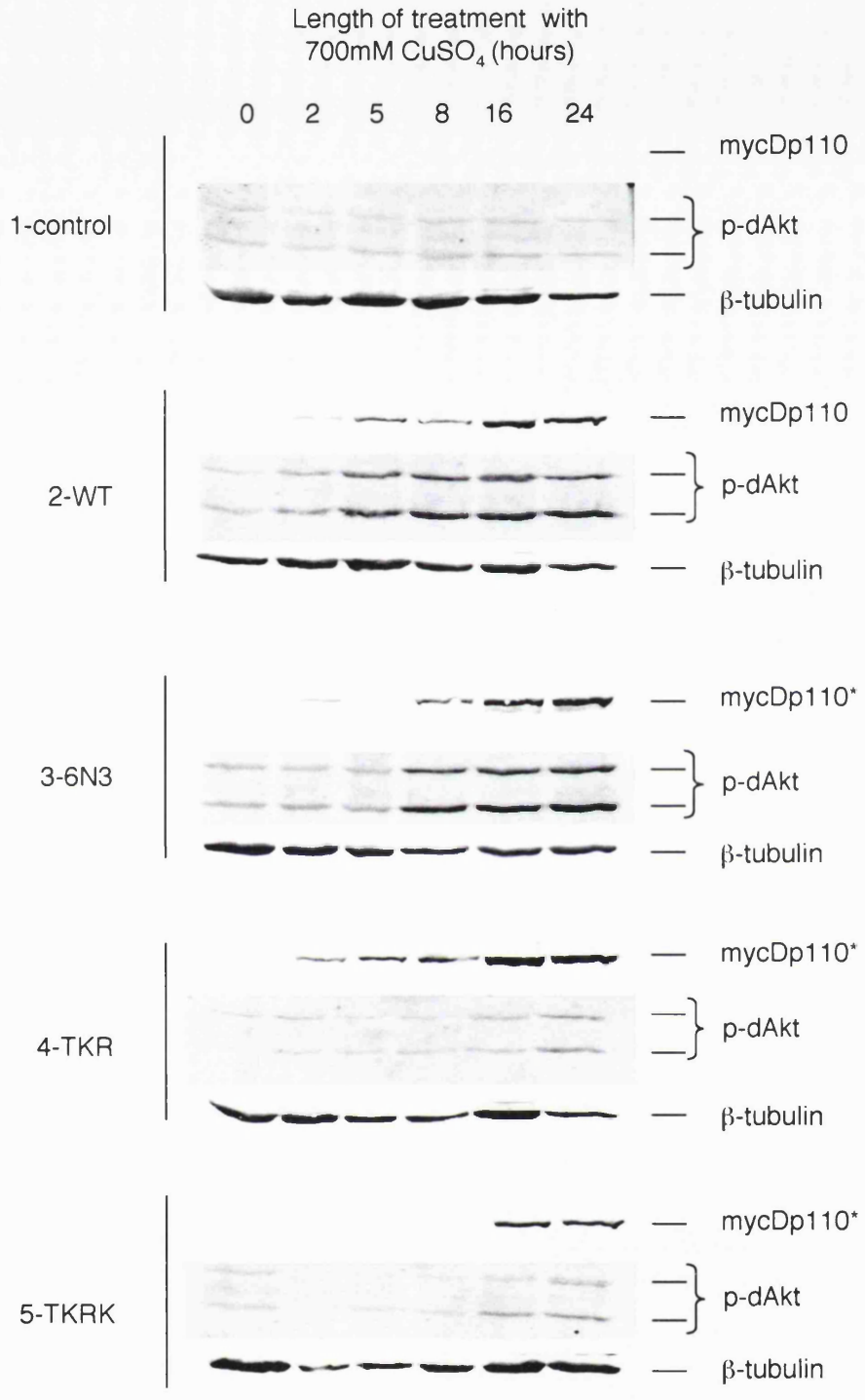

Figure 4.13 dAkt phosphorylation after varying lengths of transgene expression

Western blots of the five cell lines treated for varying lengths of time with $CuSO_4$ (see figure 4.6) were re-probed with α-p-Ser586 antibodies that recognise phosphorylated dAkt. Expression of wild-type Dp110, and $Dp110^{6N3}$ appears to induce high levels of dAkt phosphorylation. $Dp110^{TKR}$ and $Dp110^{TKRK}$ expression appears to lead to lower levels of dAkt phosphorylation.

To quantify the levels of phosphorylation, and by implication, the *in vivo* activities of the different myc-Dp110* proteins, four further independent experiments were carried out. In these, transgene expression was induced in the cell lines by treating the cells for 16 hours with $CuSO_4$. This time point was chosen as a good level of dAkt phosphorylation had been seen after 16 hours in the previous experiment. $CuSO_4$ treated cells were lysed and lysates separated on two SDS-PAGE gels. Western blots of these gels were probed with either α-HA, α-dAkt and α–β-tubulin or α-myc, α-p-Ser586 and α–β-tubulin. Representative Western blots are shown in 4.14A and 4.14B respectively. Immunoblots were scanned and quantified using the LI-COR Odyssey infrared imaging system. These blots confirmed that induction of transgenes leads to dAkt phosphorylation in both the 2-wt and 3-6N3 cell lines and that there was little or no phosphorylation of dAkt after transgene expression was induced in either the 4-TKR or 5-TKRK cell lines.

Two different calculations were used to assess PI3K pathway activity in the different cell lines upon transgene over-expression in a quantitative manner. For both methods, the relative level of dAkt phosphorylation in 2-wt cells was arbitrarily set at 100%. In the first method, the level of p-dAkt recorded was divided by the amount of myc-Dp110* present in the lysate (see figure 4.13C). In the second method the fraction of dAkt that was phosphorylated was divided by the amount of myc-Dp110* present in the lysate (see figure 4.13D). The two graphs generated similar results.

Both suggest that while PI3K pathway activity in induced 3-6N3 cells is almost equal to that seen in induced 2-wt cells, transgene induction alone has little effect on dAkt phosphorylation in 4-TKR cells. Relative activity of myc-$Dp110^{TKRK}$ appears higher than that of myc-$Dp110^{TKR}$ and lower than myc-$Dp110^{WT}$ or myc-$Dp110^{6N3}$. However, the low levels of myc-$Dp110^{TKRK}$ expressed in induced 5-TKRK cells hinder the evaluation of the protein's *in vivo* activity, as dividing by such a small value introduces a large degree of error to the method.

As these experiments assess what is happening inside cells, the comparative levels of HA-p60 and myc-Dp110* in the different cell lines must be taken into consideration when evaluating the data (see figure 4.7). For example, the reduced level of p-dAkt seen in 5-TKR cell lysates could well be a result of PI3K pathway activity being negatively regulated by the relatively high levels of free HA-p60 expressed in these cells. This argument cannot however be used to explain the low levels of p-dAkt in the 4-TKR cells. In fact, these cells have a much higher level of

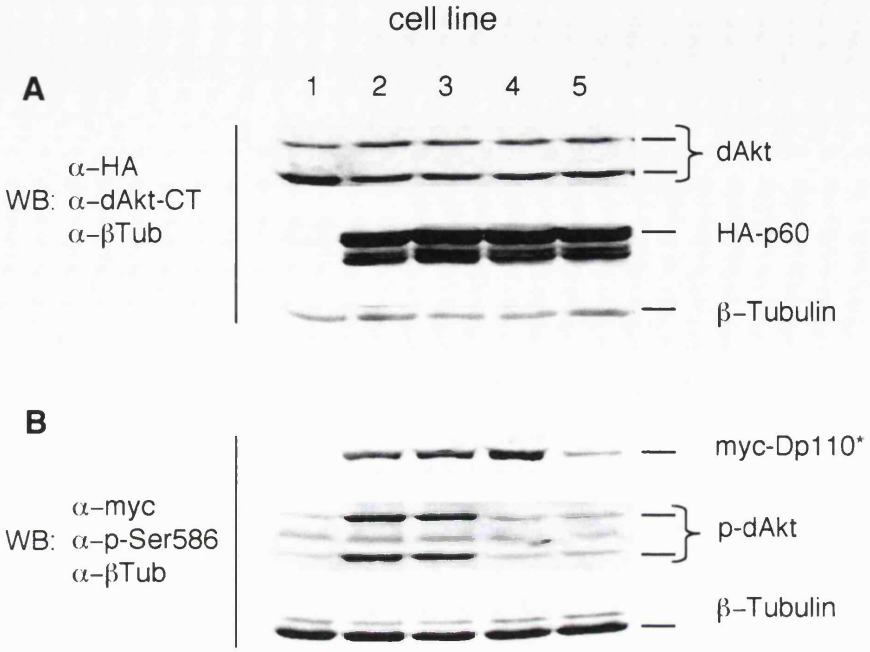

Figure 4.14 Induction of dAkt phosphorylation upon myc-Dp110* expression.

Lysates of control transfected or pMt-myc-Dp110*/pMt-HA-p60 cells treated for 16 hours with $CuSO_4$ (700μg/ml) were separated on two separate gels (8%) using SDS-PAGE (100μg protein/ lane). The blots were probed with α-HA, α-dAkt and α–β-tubulin **(A)** or α-myc, α-p-Ser586 and α–β-tubulin **(B)**. Western blots were quantified and data from four experiments were combined to create the graphs overleaf. The relative activity of Dp110* in the cells was assessed by dividing the total amount of p-dAkt **(C)**, or the fraction of dAkt that was phosphorylated **(D)** by the total amount of Dp110* present.

Error bars show standard deviation

C

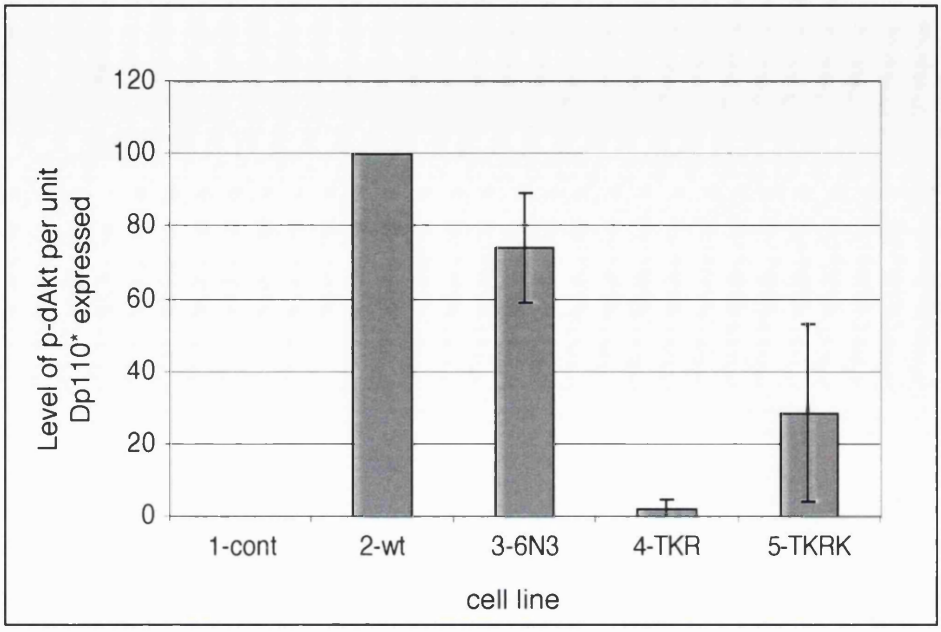

D

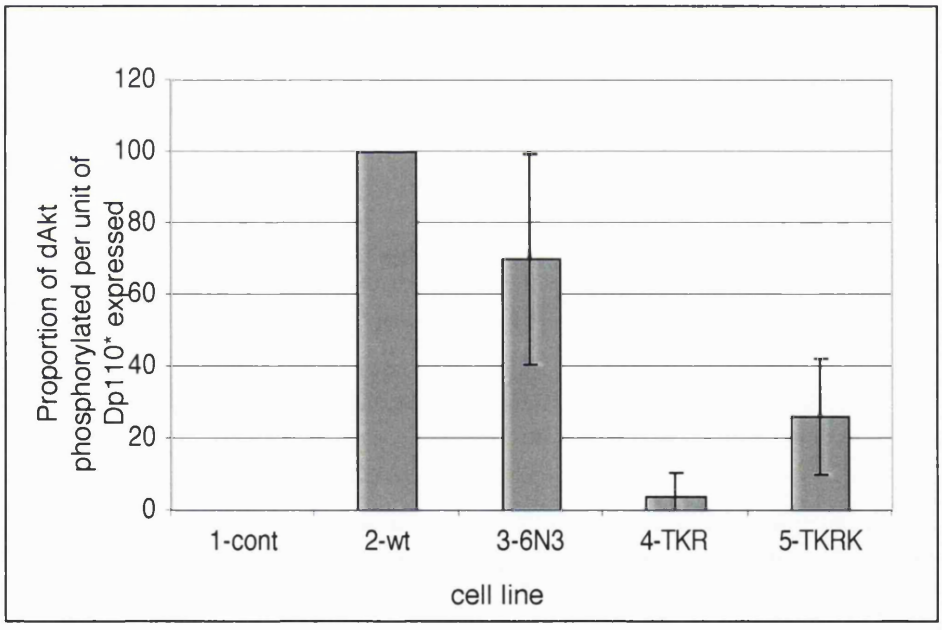

Figure 4.14 cont. Induction of dAkt phosphorylation upon myc-Dp110* expression.

myc-Dp110* protein expressed than those of the other lines. Even after taking this factor into account, the results suggest that the mutations present in myc-Dp110^{TKR}, namely T231D, K250A and R253A do disrupt the *in vivo* kinase activity of the protein. Yet, from this hypothesis it would follow that addition of a further lysine to alanine mutation in the RBD increases the *in vivo* activity of the kinase. Although this seems counterintuitive, a lysine to glutamate mutation at position 227 in the p110α RBD does increase the basal activity of p110α (Rodriguez-Viciana et al., 1996b), providing a precedent from mutations in the RBD positively affect kinase activity. However, it is not clear whether this is what is happening with the addition of the K257A mutation to Dp110^{TKR}.

The ability of myc-Dp110^{6N3} over-expression to lead to levels of dAkt phosphorylation that are comparable with those induced by myc-Dp110^{WT} over-expression forces me to question the data presented in figure 4.12. If *in vitro* kinase activity were truly reduced by 50% by the introduction of the 6N3 mutation, I would have expected its *in vivo* activity to also be reduced. The data also raise an issue of whether the 6N3 mutation has *any* affect on *in vivo* kinase activity. This could imply that other promoter or enhancer mutations do exist on the 6N3 chromosome and that the phenotype is therefore caused by a lack of protein expression. However, it is important to remember that stimulation of these cells, either by the addition of insulin or the transient transfection of constitutively active Ras or Dras1 was not attempted. If the signalling pathway were activated in this way larger differences in PI3K signalling may well have been seen.

From these experiments I can conclude that over-expression of myc-Dp110^{TKR} leads to minimal activation of downstream PI3K pathway components, whereas over-expression of myc-Dp110^{WT} or myc-Dp110^{6N3} does activate downstream signalling. Coupled with the results that indicate that myc-Dp110^{TKR} is expressed and is stable, is able to bind p60 and has wild-type *in vitro* kinase activity, it seems appropriate to propose that the triple RBD mutant is used in further *in vitro* and *in vivo* analyses of the importance of RBD integrity (see section 4.16.3 for further details).

4.14 Evaluation of dAkt phosphorylation in S2 and 2-wt cells upon insulin stimulation

As discussed above, to evaluate the full functional capabilities of the Dp110 RBD mutants it would be useful to assess whether the PI3K pathway activity in cells over expressing the myc-Dp110* proteins is modulated by insulin treatment or transient transfection with constitutively active Dras1 or Ras. Both these procedures have been shown to increase PI3K pathway activity in mammalian cell culture (Alessi et al., 1996; Rodriguez-Viciana et al., 1996b), and a thirty-minute insulin stimulation leads to the phosphorylation and activation of dAkt in non-transfected S2 cells (Alrubaie, 2002; Verdu et al., 1999). To examine whether performing this type of experiment would generate interpretable results, a preliminary experiment was carried out using untransfected and 2-wt cells.

Untransfected S2 and 2-wt cells were seeded into six-well plates at a density of 5×10^6 cells per ml media. $CuSO_4$ was added to half the wells for 16 hours. After this time, half the $CuSO_4$-treated and half the $CuSO_4$-untreated cells were stimulated with 1μM insulin for 30 min. Cells were harvested and lysed, and lysates were separated using SDS-PAGE. Phosphorylation of dAkt in the differently treated cells was assessed by Western blotting (see figure 4.15).

Insulin stimulation of S2 cells leads to the same level of dAkt phosphorylation regardless of whether or not $CuSO_4$ was added to the cells (figure 4.15 left hand panel). The same cannot be said for the 2-wt cells however. Induction of transgene expression with $CuSO_4$ leads to a low level of dAkt phosphorylation, and surprisingly this is not enhanced by further treatment with insulin (figure 4.15 right hand panel). In contrast, insulin stimulation of uninduced 2-wt cells leads to a higher level of dAkt phosphorylation than stimulation of induced 2-wt cells, although this level is still below that seen in insulin treated untransfected S2 cells.

This latter result leads me to hypothesise that chronic low-level transgene expression in the 2-wt cells has dampened the PI3K signalling pathway in these cells. In addition, although increasing the level of myc-Dp110^{WT} in these cells, via addition of $CuSO_4$ for 16 hours, does increase signalling through the pathway, this treatment co-ordinately leads to an increase in negative feedback to other components of the pathway, thereby ensuring that signalling flux cannot increase upon insulin stimulation. Note that no differences in dAkt expression level were seen after any

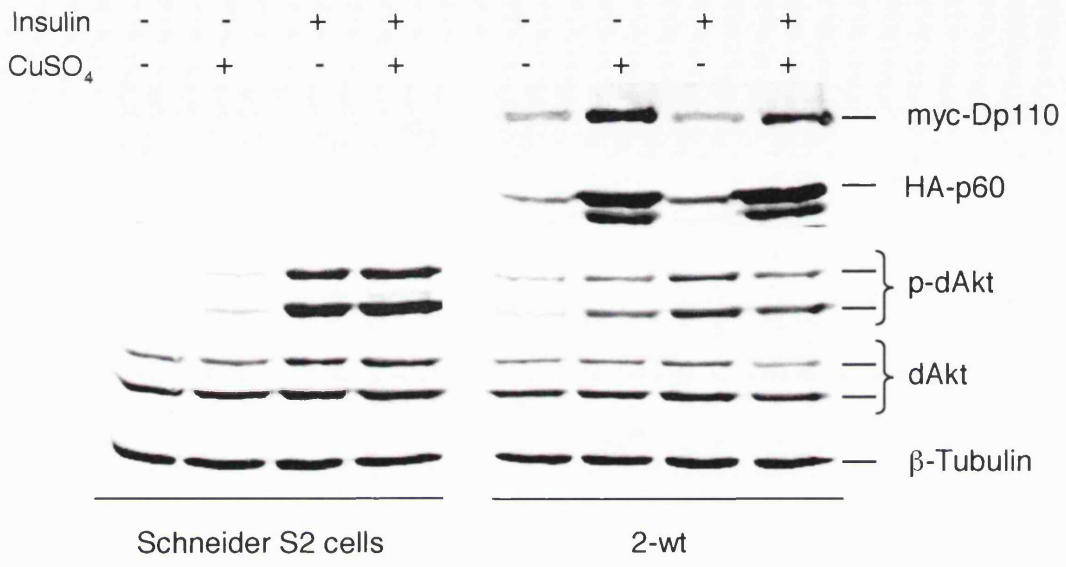

Figure 4.15 Insulin stimulation of Schneider S2 and 2-wt cells

Schneider S2 and 2-wt cells untreated or treated with CuSO4 for 16 hours were unstimulated or subjected to insulin stimulation (1μM, 30 min). Lysates of these cells were resolved using SDS-PAGE (8% gel) and Western blots were probed with α-myc, α-HA, α-p-Ser586, α-dAkt and α–β-tubulin. dAkt was phosphorylated upon insulin stimulation of S2 cells or of untreated 2-wt cells (at a lower level). Induction of $Dp110^{wt}$ expression in 2-wt cells led to low levels of dAkt phosphorylation and this was only very marginally increased upon stimulation by insulin.

Similar results were obtained when $CuSO_4$ was added to the cells for 8 hours or 24 hours prior to insulin stimulation.

treatment (data not shown), ruling out the modulation of dAkt expression levels as a mechanism for this negative feedback.

If this hypothesis is correct, it could follow that, contrary to prior conclusions, myc-Dp110^{TKR} may be active *in vivo*. However, the higher levels of induced myc-Dp110^{TKR} expressed compared with the other myc-Dp110* proteins, may be mimicked by higher levels of leaky expression. If this is the case, it would follow from our theory that the PI3K pathway in the 4-TKR cells would continually be subjected to an increased level of negative feedback, perhaps to such a degree that phosphorylation of dAkt can never be induced. If this were the case, it would also explain how the introduction of a further mutation in the RBD could lead to an apparent increase in *in vivo* protein activity (see section 4.12), as the lower expression levels of Dp110^{TKRK} would lead to less negative feedback, and hence more *in vivo* signalling is possible.

To test this, experiments similar to the one in this section could be carried out on 4-TKR cells and 5-TKRK cells. We would expect that insulin stimulation of both induced and uninduced 4-TKR cells would have less of an effect on dAkt phosphorylation than the same treatments on 2-wt cells. In contrast, as we would expect the low level of myc-Dp110^{TKRK} expression to have less of an effect on dampening down PI3K signalling, a greater response to insulin should be seen.

More importantly, this final experiment highlights the problems with data interpretation that are encountered when performing more *in vivo* analyses using these transgenic cell lines. On the basis of these results, I would advise that, in future, these cell lines are used only as a source of tagged protein for biochemistry experiments, rather than being used to carry out *in vivo* studies.

4.15 Summary

The phenotypic analysis of larvae whose only full-length *dp110* gene contains a mutation encoding a non-conservative mutation in the Ras binding domain (RBD) suggested that RBD integrity is important for full Dp110 function. However, the larval expression of Dp110^{6N3} protein could not be tested owing to the low affinity of α-Dp110 antibodies for Dp110, and the mysteriously low protein concentration of *dp110*$^{6N3/A}$ larval lysates. In order to rule out other possible explanations of the phenotype, further experiments were carried out, in which the biochemical properties

of Dp110 RBD mutants were tested. Stable, inducible cell lines were generated as a source of myc-tagged Dp110* protein, and the stability, p60 binding ability and *in vitro* kinase activity of these proteins were assessed.

RBD mutations did not affect overall protein stability, determined by the assessment of protein expression levels, nor did they compromise Dp110-p60 binding. Preliminary experiments, where the ability of myc-Dp110* to phosphorylate PI *in vitro* was tested, indicated that $Dp110^{6N3}$ may have a reduced basal kinase activity. However, this finding was not confirmed after immunoprecipitation conditions were altered and should therefore be further tested. In addition, it is important to test the ability of myc-Dp110* to phosphorylate PIP_2, as this substrate is more meaningful in the context of downstream PI3K signalling. None of the other RBD mutations appeared to negatively affect the *in vitro* kinase activity of Dp110.

Further experiments observing the activity of myc-Dp110* within the cell lines were carried out, using the phosphorylation of dAkt as a measure of signalling activity via the PI3K pathway activity. It was hoped that these experiments would give some indication as to whether the *in vivo* kinase activity of Dp110 was adversely affected by the RBD mutations. This scenario could easily be envisaged, despite no differences in *in vitro* activity having been recorded, as other regulatory factors are present in cells that are removed from the purified Dp110 in the *in vitro* system. Unfortunately, the interpretation of the data from these experiments was problematic. In part this was due to variations in the myc-Dp110* to HA-p60 ratios between the cell lines. For example, the inability of myc-$Dp110^{TKRK}$ over-expression to lead to the phosphorylation of dAkt could well have been caused by a comparably high level of HA-p60 expression in the 5-TKR cells that negatively regulated the PI3K pathway. Additional problems were highlighted from preliminary experiments where induced and uninduced 2-wt cells were stimulated with insulin. The resulting data suggested that expression of the transgenes themselves could down regulate signalling. Possible mechanisms for this down regulation are discussed in section 4.16.

4.16 Discussion

Various questions have been raised during the course of this chapter: Is p60-bound Dp110 really basally inactive, as we might hypothesise from the co-over-expression experiments carried out in developing imaginal discs? What mechanisms could explain the apparent dampening of the PI3K signalling pathway

after chronic expression of HA-p60 and myc-Dp110^{WT}? How could the RBD-mutants of Dp110 be used to further assess the importance of RBD integrity to Dp110 activity? And finally, can Ras or indeed another small GTPase bind and activate Dp110? Each of these questions will be addressed in turn during the following discussion.

4.16.1 The relationship between the adaptor and catalytic subunits of PI3K

The results presented in figures 4.13 and 4.14 showed that induction of transgene expression could lead to the serine phosphorylation of dAkt at position 586. This phosphorylation, as discussed before, can act as a marker for PI3K pathway activity. This result was surprising as I had envisaged that if myc-Dp110* and HA-p60 were co-expressed, no increase in pathway activity would result, as the positive and negative effects of the two tagged proteins on PI3K signalling would cancel one another out. This idea was based on the co-over-expression experiments discussed in section 4.5 (Weinkove, 1999).

Other experiments using mammalian cells and/or proteins have suggested a similar regulatory effect of the adaptor subunit of PI3K on the activity of the catalytic subunit. One such experiment was performed using the yeast *Schizosaccharomyces pombe*, in which transfection of mammalian p110α into the yeast cells induced a growth arrest. This phenotype was rescued by the co-transfection of the p85α catalytic subunit. Contrary to what one might imagine, this rescue was not caused by a reduction in p110α expression levels, rather an increase in both p110α and p85α expression levels were seen in comparison to the singly transfected cells, suggesting that the two proteins co-stabilise (Kodaki et al., 1994). A further experiment showed that co-transfection of p85α can inhibit the PI3K dependent Ras transformation of Swiss3T3 cells (Rodriguez-Viciana et al., 1997).

Several possible mechanisms by which p60 or p85 could respectively inhibit Dp110 or p110 have been proposed. Firstly, the lone adaptor subunits could compete with adapter-catalytic subunit complexes for phosphorylated tyrosine motif binding. If this were the case, then it would imply that the inhibition was dependent on the adaptor subunit being present in excess of the catalytic subunit. The observation that a deletion mutant of p85α that is unable to bind p110α can inhibit phosphotyrosine associated PI3K activity in L6 myotubes suggests that this mechanism is used (Ueki et al., 2000).

Secondly, the adaptor subunit, when bound to the catalytic subunit, could directly inhibit the lipid kinase activity of the complex, perhaps by causing a conformational change in the kinase domain that renders it inactive. The reduction in *in vitro* lipid kinase activity seen when p110α is bound to p85α, in comparison to its activity when it is unbound, suggests that some direct regulation of the two subunits is occurring (Yu et al., 1998). Exactly how this inhibition works, has not been fully characterised. However, it is important to note that much of this repression can be removed, *in vitro* at least, by co-expression of tyrosine-phosphorylated peptides (Yu et al., 1998). In fact, recent data suggest that phosphorylation of a serine at the C-terminus of p85, downstream of phosphotyrosine binding is responsible for removing this inhibition (Chan et al., 2002).

Thirdly, the adaptor subunit, when not bound to phosphorylated tyrosine residues, could sequester the catalytic subunit away from its substrate, reducing the basal activity level of the kinase. This would be a good explanation for reduced levels of basal downstream signalling upon expression of adaptor and catalytic subunits at a 1:1 ratio.

The fact that dAkt phosphorylation did result from treating the 2-wt and 3-6N3 cells with $CuSO_4$ for 16 hours could be explained in a number of ways. One possibility is that the levels of HA-p60 may not be as great as the levels of myc-Dp110* in the 2-wt and 3-6N3 cells and this discrepancy could lead to a net positive effect on PI3K signalling. Quantitative data on the relative expression levels of the tagged protein calculated from the Westerns of α-myc and α-HA immunoprecipitates would be able to corroborate or disprove this hypothesis.

Another possibility is that p60 may not act to negatively regulate Dp110 at all in the stably transfected Schneider S2 cells. As S2 cells have been generated from a heterogeneous population of embryonic cells, and are mostly haemocytes, they are very different in origin to the epithelial cells that make up the imaginal discs where these competing effects were observed (Weinkove, 1999). The dominant negative effects of p85 have previously been shown to be cell-type specific, as experiments using COS cells showed no inhibitory effect of p85α (Rodriguez-Viciana et al., 1996b).

One very important detail that has been overlooked up until now is that the stable cell lines are grown in complete media, albeit in the presence of antibiotic. Although no insulin was added to the cells, S2 cells are renowned for being able to

condition their own media with growth factors. This could mean that the tyrosine kinase receptors on the cell surface are being activated by growth factors in the media and the active nature of the over expressed myc-Dp110*-HA-p60 complex is due to the presence of phosphorylated tyrosine motifs within the cells, which remove the inhibitory effects of HA-p60 upon binding.

4.16.2 Negative regulation of PI3K signalling

The idea that signalling via PI3K can negatively feed back on various pathway components, thereby reducing PI3K signalling is not new. For example it has been shown that PI3K has serine-threonine protein kinase activity as well as lipid kinase activity, and that this activity is directed toward itself (Vanhaesebroeck et al., 1999) and its adaptor (Dhand et al., 1994). When either subunit is phosphorylated the *in vitro* lipid kinase activity of the complex is reduced. The importance of the adaptor subunit phosphorylation *in vivo* has not been confirmed, yet phosphorylation and coordinate inhibition of p110δ has been shown to increase with the length of time of insulin stimulation in Jurkat T-cells (Vanhaesebroeck et al., 1999).

Although a similar down-regulation of myc-Dp110* activity could be occurring in the stable cell lines (see figure 4.16), I do not think that this mechanism could account for the refractory nature of the induced cells to insulin. The increase in phosphorylated dAkt seen upon transgene induction could well be due to the activation of the myc-Dp110*-HA-p60 complex by low levels of growth factor dependent phosphorylated tyrosine motifs at the membrane. An increase in signalling is therefore seen when increased levels of the complex are present, simply as a function of the increased concentration of PI3K in the cell, as PI3K molecules are more frequently found in contact with phospho-tyrosine motifs. However, the proportion of PI3K molecules active at any one time may not be all that great. It would then follow that only a small proportion of the expressed Dp110 would be subjected to inhibitory phosphorylation, and so a large proportion of the pool would still be able to respond when the cell is stimulated with insulin.

Other negative feedback mechanisms could include the up regulation of PI3K pathway inhibitors, such as PTEN or PP2A, the phosphatase for dAkt. Again, this mechanism seems somewhat unlikely. Aside from the fact that PP2A has multiple functions within the cell, which would be activated as the protein concentration rises,

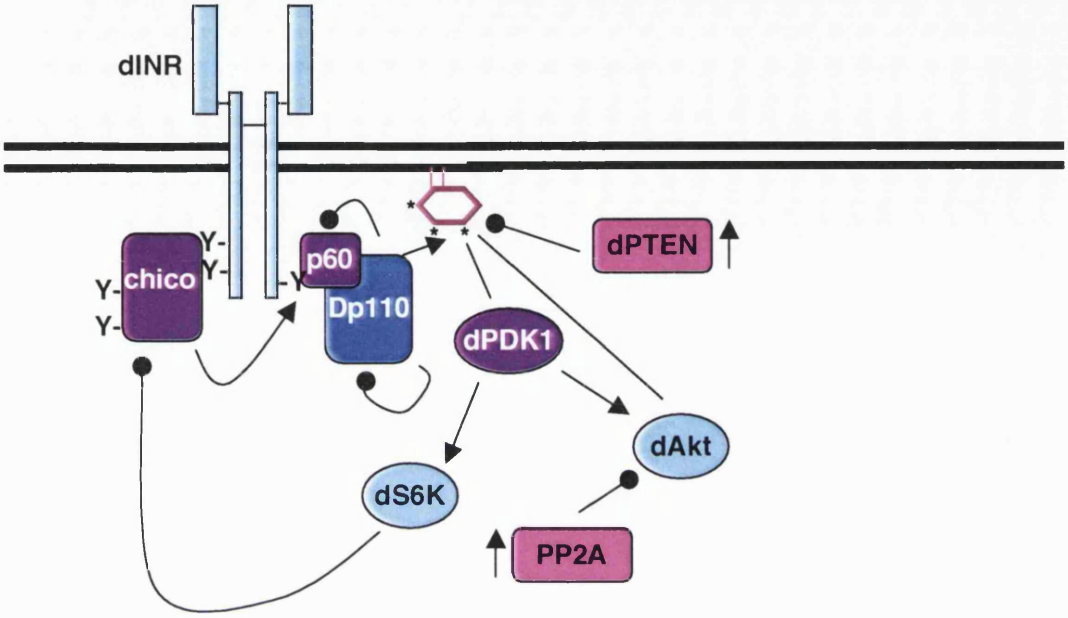

Figure 4.16 A model depicting possible routes through which myc-Dp110* may feed back to negatively regulate PI3K pathway signalling

Active Dp110 may have serine-threonine protein kinase activity as well as lipid kinase activity and could phosphorylate and inhibit both itself or its bound adaptor subunit. Alternatively PI3K-activated dS6K may phosphorylate the *Drosophila* insulin receptor subunit, Chico. In mammalian systems such a phosphorylation event has been shown to lead to the degradation of IRS via the proteosome (Haruta et al., 2000). Other methods of negative feedback could include the up-regulation of pathway inhibitors, such as PTEN or PP2A, a phosphatase that acts on dAkt.

if phosphatase levels were increased a net increase in kinase activity should still be seen upon insulin stimulation, yet is not.

Alternatively, the down-regulation might not be dependent on the inhibition of the complex itself and therefore would not depend on each and every complex being inhibited, which in an over-expression context is hard to imagine. In mammalian cells, Haruta and colleagues noticed that IRS-1 was first phosphorylated and then degraded via the proteosome, following prolonged stimulation of 3T3-L1 adipocytes with insulin. This response was both wortmannin and rapamycin sensitive, suggesting that S6K was the enzyme responsible for the action (Haruta et al., 2000). These results suggest that regulation might occur at the level of the insulin receptor subunit (IRS) and be dependent on the overall signalling flux through the pathway.

There is evidence that a similar negative feedback pathway may be active downstream of *Drosophila* S6K. dAkt purified from larvae lacking both copies of the *dS6K* gene is more active in *in vitro* kinase assays than the same total amount of dAkt purified from wild type larvae (Radimerski et al., 2002a; Radimerski et al., 2002b). This suggests that dS6K can somehow act to inhibit dAkt phosphorylation, and this may well be via the phosphorylation and degradation of the insulin receptor subunit, Chico.

To test whether this mechanism is decreasing the 2-wt cells' responsiveness to insulin, the levels of chico protein in the cells could be compared with the levels in the control-transfected cell line. It is hard to judge whether this mechanism would be sufficient to account for the inability of dAkt to be further phosphorylated when induced cells are subjected to insulin stimulation. Unlike in mammalian cells, phosphorylation of tyrosine motifs on the insulin receptor, creates consensus p60 binding sites suggesting the receptor can activate PI3K directly. It would therefore be expected that insulin could increase PI3K activity via insulin receptor phosphorylation even when Chico was not present.

4.16.3 How can we assess whether RBD integrity is necessary for maximal in vivo Dp110 function?

Despite the limitations of the cell lines, other approaches could be used to assess the importance of Dp110 RBD integrity *in vivo*. For example a genomic *dp110* rescue construct exists which has been shown to rescue the null phenotype of $dp110^{A/A}$ larvae (Weinkove et al., 1999). If the same RBD mutations were introduced into this

construct as have been tested *in vitro*, the ability of these new constructs to rescue the $dp110^{A/A}$ phenotype could be assessed. Any resulting phenotype could be assigned to the RBD mutations, without fear that the proteins were not expressed or that they contained other mutations.

Flies that are rescued in such a manner would be equivalent to flies that carried one copy of a null allele of *dp110* and one copy of the *dp110**. If the developing larvae contain imaginal discs, which may well not be the case if the phenotype of the $Dp110^{6N3/A}$ larvae can be trusted, the ability of constitutively active Dras1 to activate Dp110* could be tested by making clones in the developing wing imaginal discs that over express $Dras1^{V12}$. These could be studied using immunofluorescence to observe whether phosphorylation of dAkt is increased in these clones. An alternative strategy would be to use the GFP fused PH domain construct described by David Prober (Prober and Edgar, 2002) to visualise whether there is a greater proportion of GFP bound to cell membranes within the clone. This would give some indication as to whether the mutations disrupted the ability of Dp110 to bind to Ras-family small GTPases.

As yet, the Ras-binding ability of the Dp110 RBD mutants has not been assessed directly. It seems sensible to test whether the introduced mutations can reduce Ras binding, and indeed whether wild-type Dp110 can bind to Ras in a GTP dependent manner, before embarking on these genomic rescue experiments. There are a number of ways in which these could be performed. Co-immunoprecipitation of the mammalian PI3K complex with Ras has been achieved in the past, although these assays are notoriously difficult to carry out (Deora et al., 1998). Owing to this, the majority of assays that are used to address such questions involve observing *in vitro* binding capability. Purified GST-tagged p110 protein is mixed with GTP- or GDP-bound Ras *in vitro* and then any complexes are recovered using glutathione-agarose (Rodriguez-Viciana et al., 1996b). Alternatively immobilised GTP- or GDP-bound Ras proteins can be incubated with the lysate of cells over expressing p110 proteins and the formation of complexes assessed (Karasarides et al., 2001). This latter assay would seem to be appropriate in our case, as we have already generated appropriate cell lines.

4.16.4 Which, if any, small GTPase is likely to be involved in Dp110 activation?

Although the activation of PI3K by Ras has been most extensively investigated in mammalian systems, more recent reports have indicated that other small GTPases could also be involved in its activation. For example, the activation of Akt by PI3K in Jurkat cells downstream of T-cell antigen receptor engagement is inhibited by a dominant negative form of the Rho-family GTPase, Rac1 (Genot et al., 2000). That PI3K can be activated by Rac1 has since been confirmed in Mast cells (Djouder et al., 2001). This observation was particularly surprising as prior experiments identified Rac1 as an effector of PI3K (Rodriguez-Viciana et al., 1997). However, Genot and colleagues showed that although Rac1 was upstream of the lipid kinase in the PI3K-dependent activation of Akt, it was downstream of PI3K in the PI3K-dependent cytoskeletal reorganisation.

Another Rho-family small GTPase, Cdc42, has been implicated in PI3K-dependent Akt activation following integrin binding to extracellular matrix components. Dominant negative Cdc42 inhibited the three-fold activation of Akt *in vitro* caused by plating Rat1 cells onto fibronectin (Clark et al., 1998). In conjunction with evidence that Cdc42 can bind to p110 in a GTP dependent manner (Zheng et al., 1994), this result highlights Cdc42 as another strong candidate for PI3K activation.

Finally, inhibition of Rap1 by cyclic AMP in glioma cells was shown to inhibit PI3K-dependent Akt phosphorylation. Conversely, increasing the activity of Rap1 in these cells co-ordinately increased dAkt phosphorylation (Wang et al., 2001).

With respect to the *Drosophila* pathway only the possibility that Dras1 activates Dp110 has been discussed. However, the described experiments in mammalian cell systems suggest that other small GTPases could also lead to PI3K activation. Seventy proteins are classified as monomeric small GTPases in the FlyBase database. It is therefore possible that one or more of these normally regulates PI3K activity.

Dras2 is another Ras homolog in *Drosophila*, which causes embryonic lethality when mutated. However, no effect on dAkt phosphorylation levels is seen in developing wing disc clones that over express an activated Dras2 or in clones that do not contain any Dras2 protein (Alrubaie, 2002). It therefore seems unlikely that Dras2 is involved in Dp110 activation, at least in the developing imaginal discs.

A more promising candidate is the Ras-family protein, Rheb, as this was identified as a growth regulator in the pinhead screen described in section 4.1.1

(Stocker et al., 2003). Localised over-expression of Rheb during larval life increases cell size in multiple fly tissues including the eye, wing and fat body, in a manner reminiscent of activation of PI3K pathway members (Saucedo et al., 2003). Furthermore the increase in eye size seen upon removal of PTEN function in the developing eye imaginal disc is suppressed if the disc also lacks Rheb function (Stocker et al., 2003). However, further investigation revealed that Rheb does not function upstream of Dp110. Rather, it is located downstream of PI3K and upstream of S6K and TOR, acting to promote TOR activity.

The fact that the Ras-binding domain is conserved in Dp110, and that over-expression of constitutively active Dras1 *can* increase dAkt phosphorylation in developing wing-disc clones suggests one or more Ras-family small GTPases do normally function to directly activate PI3K. However, it remains to be seen, which, if any, of the *Drosophila* Ras-family small GTPases are playing that role.

Acknowledgements

I would like to thank all my friends and colleagues who helped me during my time at the *Ludwig Institute of Cancer Research* and *Cancer Research UK*. Thanks especially to Graham, Katherine, Dave and Olga for their technical support, advice and friendship.

Thank you to Pascal Meier for the vectors, and Ernst Hafen and Hugo Stocker for the flies.

Thank you to all the members of the *Growth Regulation Lab*: Ben Kolevski, Steven Marygold, and Carmen Coelho, for their friendship, support and poor jokes throughout my time in the lab. In particular thank you to Krishna Vaghela who started the work on the Ras-binding domain project and to Saif Alrubaie who persuaded me to carry on where she left off. I would also like to thank Caroline Bunn for proof reading this thesis, for her scientific advice, her understanding of statistics and her good humour.

A special thanks to Sally Leevers for giving me the chance to work in her lab, for her guidance throughout and her eternal hope that one day it might just work. Thank you too for taking so much time to read and correct this thesis, and for your understanding.

Most of all, thank you to my Mum and Dad and to Steve for putting up with all the heartache that is hidden behind this thesis. Let's just say, it won't happen again.

Bibliography

Alessi, D. R., Andjelkovic, M., Caudwell, B., Cron, P., Morrice, N., Cohen, P., and Hemmings, B. A. (1996). Mechanism of activation of protein kinase B by insulin and IGF-1. Embo J *15*, 6541-6551.

Alessi, D. R., Deak, M., Casamayor, A., Caudwell, F. B., Morrice, N., Norman, D. G., Gaffney, P., Reese, C. B., MacDougall, C. N., Harbison, D., *et al.* (1997a). 3-Phosphoinositide-dependent protein kinase-1 (PDK1): structural and functional homology with the Drosophila DSTPK61 kinase. Curr Biol *7*, 776-789.

Alessi, D. R., and Downes, C. P. (1998). The role of PI 3-kinase in insulin action. Biochim Biophys Acta *1436*, 151-164.

Alessi, D. R., James, S. R., Downes, C. P., Holmes, A. B., Gaffney, P. R., Reese, C. B., and Cohen, P. (1997b). Characterization of a 3-phosphoinositide-dependent protein kinase which phosphorylates and activates protein kinase Balpha. Curr Biol *7*, 261-269.

Alrubaie, S. (2002) Analysis of the *Drosophila* insulin pathway using phosphorylation state-specific antibodies to *Drosophila* Akt; Identification and characterisation of an apoptosis-associated signal, PhD, University College, London.

Anderson, K. E., Coadwell, J., Stephens, L. R., and Hawkins, P. T. (1998). Translocation of PDK-1 to the plasma membrane is important in allowing PDK-1 to activate protein kinase B. Curr Biol *8*, 684-691.

Andjelkovic, M., Alessi, D. R., Meier, R., Fernandez, A., Lamb, N. J., Frech, M., Cron, P., Cohen, P., Lucocq, J. M., and Hemmings, B. A. (1997). Role of translocation in the activation and function of protein kinase B. J Biol Chem *272*, 31515-31524.

Andjelkovic, M., Jakubowicz, T., Cron, P., Ming, X. F., Han, J. W., and Hemmings, B. A. (1996). Activation and phosphorylation of a pleckstrin homology domain containing protein kinase (RAC-PK/PKB) promoted by serum and protein phosphatase inhibitors. Proc Natl Acad Sci U S A *93*, 5699-5704.

Andjelkovic, M., Jones, P. F., Grossniklaus, U., Cron, P., Schier, A. F., Dick, M., Bilbe, G., and Hemmings, B. A. (1995). Developmental regulation of expression and activity of multiple forms of the Drosophila RAC protein kinase. J Biol Chem *270*, 4066-4075.

Araki, E., Lipes, M. A., Patti, M. E., Bruning, J. C., Haag, B., 3rd, Johnson, R. S., and Kahn, C. R. (1994). Alternative pathway of insulin signalling in mice with targeted disruption of the IRS-1 gene. Nature *372*, 186-190.

Atkinson, W. D. (1979). A field investigation of larval competition in domestic *Drosophila.* Journal of Animal Ecology *48*, 91-102.

Backer, J. M., Myers, M. G., Jr., Shoelson, S. E., Chin, D. J., Sun, X. J., Miralpeix, M., Hu, P., Margolis, B., Skolnik, Y., Schlessinger, J., and White, M. F. (1992). Phosphatidylinositol 3'-kinase is activated by association with IRS-1 during insulin stimulation. EMBO J *11*, 3469-3479.

Backman, S. A., Stambolic, V., Suzuki, A., Haight, J., Elia, A., Pretorius, J., Tsao, M. S., Shannon, P., Bolon, B., Ivy, G. O., and Mak, T. W. (2001). Deletion of Pten in mouse brain causes seizures, ataxia and defects in soma size resembling Lhermitte-Duclos disease. Nat Genet *29*, 396-403.

Bakker, K. (1959). Feeding period, growth and pupation in larvae of *Drosophila melanogaster.* Entomolgia Experimentalis et Applicata *2*, 171-186.

Balendran, A., Casamayor, A., Deak, M., Paterson, A., Gaffney, P., Currie, R., Downes, C. P., and Alessi, D. R. (1999). PDK1 acquires PDK2 activity in the presence of a synthetic peptide derived from the carboxyl terminus of PRK2. Curr Biol *9*, 393-404.

Barbet, N. C., Schneider, U., Helliwell, S. B., Stansfield, I., Tuite, M. F., and Hall, M. N. (1996). TOR controls translation initiation and early G1 progression in yeast. Mol Biol Cell *7*, 25-42.

Bernal, A., and Kimbrell, D. A. (2000). Drosophila Thor participates in host immune defense and connects a translational regulator with innate immunity. Proc Natl Acad Sci U S A *97*, 6019-6024.

Biggs, W. H., 3rd, Zavitz, K. H., Dickson, B., van der Straten, A., Brunner, D., Hafen, E., and Zipursky, S. L. (1994). The Drosophila rolled locus encodes a MAP kinase required in the sevenless signal transduction pathway. Embo J *13*, 1628-1635.

Biondi, R. M., Kieloch, A., Currie, R. A., Deak, M., and Alessi, D. R. (2001). The PIF-binding pocket in PDK1 is essential for activation of S6K and SGK, but not PKB. Embo J *20*, 4380-4390.

Blume-Jensen, P., Janknecht, R., and Hunter, T. (1998). The kit receptor promotes cell survival via activation of PI 3-kinase and subsequent Akt-mediated phosphorylation of Bad on Ser136. Curr Biol *8*, 779-782.

Bohni, R., Riesgo-Escovar, J., Oldham, S., Brogiolo, W., Stocker, H., Andruss, B. F., Beckingham, K., and Hafen, E. (1999). Autonomous control of cell and organ size by CHICO, a Drosophila homolog of vertebrate IRS1-4. Cell *97*, 865-875.

Britton, J. S., and Edgar, B. A. (1998). Environmental control of the cell cycle in Drosophila: nutrition activates mitotic and endoreplicative cells by distinct mechanisms. Development *125*, 2149-2158.

Britton, J. S., Lockwood, W. K., Li, L., Cohen, S. M., and Edgar, B. A. (2002). Drosophila's insulin/PI3-kinase pathway coordinates cellular metabolism with nutritional conditions. Dev Cell *2*, 239-249.

Brogiolo, W., Stocker, H., Ikeya, T., Rintelen, F., Fernandez, R., and Hafen, E. (2001). An evolutionarily conserved function of the Drosophila insulin receptor and insulin-like peptides in growth control. Curr Biol *11*, 213-221.

Bryant, P. J., and Simpson, P. (1984). Intrinsic and extrinsic control of growth in developing organs. Q Rev Biol *59*, 387-415.

Burgering, B. M., and Medema, R. H. (2003). Decisions on life and death: FOXO Forkhead transcription factors are in command when PKB/Akt is off duty. J Leukoc Biol *73*, 689-701.

Cardenas, M. E., Cutler, N. S., Lorenz, M. C., Di Como, C. J., and Heitman, J. (1999). The TOR signaling cascade regulates gene expression in response to nutrients. Genes Dev *13*, 3271-3279.

Carpenter, C. L., Auger, K. R., Chanudhuri, M., Yoakim, M., Schaffhausen, B., Shoelson, S., and Cantley, L. C. (1993). Phosphoinositide 3-kinase is activated by phosphopeptides that bind to the SH2 domains of the 85-kDa subunit. J Biol Chem *268*, 9478-9483.

Casso, D., Ramirez-Weber, F., and Kornberg, T. B. (2000). GFP-tagged balancer chromosomes for Drosophila melanogaster. Mech Dev *91*, 451-454.

Chan, T. O., Rodeck, U., Chan, A. M., Kimmelman, A. C., Rittenhouse, S. E., Panayotou, G., and Tsichlis, P. N. (2002). Small GTPases and tyrosine kinases coregulate a molecular switch in the phosphoinositide 3-kinase regulatory subunit. Cancer Cell *1*, 181-191.

Cho, K. S., Lee, J. H., Kim, S., Kim, D., Koh, H., Lee, J., Kim, C., Kim, J., and Chung, J. (2001). Drosophila phosphoinositide-dependent kinase-1 regulates apoptosis and growth via the phosphoinositide 3-kinase-dependent signaling pathway. Proc Natl Acad Sci U S A *98*, 6144-6149.

Chu, D. T. W., and Klymkowsky, M. W. (1989). The appearance of acetylated α-tubulin during early development and cellular differentiation in Xenopus. Dev Biol *136*, 104-117.

Clark, E. A., King, W. G., Brugge, J. S., Symons, M., and Hynes, R. O. (1998). Integrin-mediated signals regulated by members of the rho family of GTPases. J Cell Biol *142*, 573-586.

Coelho, C. M., and Leevers, S. J. (2000). Do growth and cell division rates determine cell size in multicellular organisms? J Cell Sci *113*, 2927-2934.

Conlon, I., and Raff, M. (1999). Size control in animal development. Cell *96*, 235-244.

Cross, D. A., Alessi, D. R., Cohen, P., Andjelkovich, M., and Hemmings, B. A. (1995). Inhibition of glycogen synthase kinase-3 by insulin mediated by protein kinase B. Nature *378*, 785-789.

Cross, D. A., Alessi, D. R., Vandenheede, J. R., McDowell, H. E., Hundal, H. S., and Cohen, P. (1994). The inhibition of glycogen synthase kinase-3 by insulin or insulin-like growth factor 1 in the rat skeletal muscle cell line L6 is blocked by wortmannin, but not by rapamycin: evidence that wortmannin blocks activation of the mitogen-activated protein kinase pathway in L6 cells between Ras and Raf. Biochem J *303*, 21-26.

Currie, R. A., Walker, K. S., Gray, A., Deak, M., Casamayor, A., Downes, C. P., Cohen, P., Alessi, D. R., and Lucocq, J. (1999). Role of phosphatidylinositol 3,4,5-trisphosphate in regulating the activity and localization of 3-phosphoinositide-dependent protein kinase-1. Biochem J *337*, 575-583.

Datar, S. A., Jacobs, H. W., de la Cruz, A. F., Lehner, C. F., and Edgar, B. A. (2000). The Drosophila cyclin D-Cdk4 complex promotes cellular growth. Embo J *19*, 4543-4554.

Datta, S. R., Dudek, H., Tao, X., Masters, S., Fu, H., Gotoh, Y., and Greenberg, M. E. (1997). Akt phosphorylation of BAD couples survival signals to the cell- intrinsic death machinery. Cell *91*, 231-241.

Davis, K. T., and Shearn, A. (1977). In vitro growth of imaginal disks from Drosophila melanogaster. Science *196*, 438-440.

Day, S. J., and Lawrence, P. A. (2000). Measuring dimensions: the regulation of size and shape. Development *127*, 2977-2987.

Deeney, J. T., Prentki, M., and Corkey, B. E. (2000). Metabolic control of beta-cell function. Semin Cell Dev Biol *11*, 267-275.

Delcommenne, M., Tan, C., Gray, V., Rue, L., Woodgett, J., and Dedhar, S. (1998). Phosphoinositide-3-OH kinase-dependent regulation of glycogen synthase kinase 3 and protein kinase B/AKT by the integrin-linked kinase. Proc Natl Acad Sci U S A *95*, 11211-11216.

Dennis, P. B., Pullen, N., Kozma, S. C., and Thomas, G. (1996). The principal rapamycin-sensitive p70(s6k) phosphorylation sites, T-229 and T-389, are differentially regulated by rapamycin-insensitive kinase kinases. Mol Cell Biol *16*, 6242-6251.

Colombani, J., Raisin, S., Pantalacci, S., Radimerski, T., Montagne, J., and Leopold, P. (2003). A nutrient sensor mechanism controls *Drosophila* growth. Cell *114*, 739-749.

Deora, A. A., Win, T., Vanhaesebroeck, B., and Lander, H. M. (1998). A redox-triggered ras-effector interaction. Recruitment of phosphatidylinositol 3'-kinase to Ras by redox stress. J Biol Chem *273*, 29923-29928.

Dhand, R., Hiles, I., Panayotou, G., Roche, S., Fry, M. J., Gout, I., Totty, N. F., Truong, O., Vicendo, P., Yonezawa, K., *et al.* (1994). PI 3-kinase is a dual specificity enzyme: autoregulation by an intrinsic protein-serine kinase activity. EMBO J *13*, 522-533.

Di Como, C. J., and Arndt, K. T. (1996). Nutrients, via the Tor proteins, stimulate the association of Tap42 with type 2A phosphatases. Genes Dev *10*, 1904-1916.

Diaz-Benjumea, F. J., and Hafen, E. (1994). The sevenless signalling cassette mediates Drosophila EGF receptor function during epidermal development. Development *120*, 569-578.

Dickson, B., Sprenger, F., Morrison, D., and Hafen, E. (1992). Raf functions downstream of Ras1 in the Sevenless signal transduction pathway. Nature *360*, 600-603.

Djordjevic, S., and Driscoll, P. C. (2002). Structural insight into substrate specificity and regulatory mechanisms of phosphoinositide 3-kinases. Trends Biochem Sci *27*, 426-432.

Djouder, N., Schmidt, G., Frings, M., Cavalie, A., Thelen, M., and Aktories, K. (2001). Rac and phosphatidylinositol 3-kinase regulate the protein kinase B in Fc epsilon RI signaling in RBL 2H3 mast cells. J Immunol *166*, 1627-1634.

Dowler, S., Currie, R. A., Downes, C. P., and Alessi, D. R. (1999). DAPP1: a dual adaptor for phosphotyrosine and 3-phosphoinositides. Biochem J *342*, 7-12.

Downward, J. (1992). Regulatory mechanisms for ras proteins. Bioessays *14*, 177-184.

Dufner, A., and Thomas, G. (1999). Ribosomal S6 kinase signaling and the control of translation. Exp Cell Res *253*, 100-109.

Efstratiadis, A. (1998). Genetics of mouse growth. Int J Dev Biol *42*, 955-976.

Evan, G. I., Lewis, G. K., Ramsay, G., and Bishop, J. M. (1985). Isolation of monoclonal antibodies specific for human c-myc proto- oncogene product. Mol Cell Biol *5*, 3610-3616.

Fankhauser, G. (1952). Nucleo-cytoplasmic relations in amphibian development. Int Rev Cytol *1*, 165-193.

Feige, J. J., and Chambaz, E. M. (1987). Membrane receptors with protein-tyrosine kinase activity. Biochimie *69*, 379-385.

Fernandez, R., Tabarini, D., Azpiazu, N., Frasch, M., and Schlessinger, J. (1995). The Drosophila insulin receptor homolog: a gene essential for embryonic development encodes two receptor isoforms with different signaling potential. Embo J *14*, 3373-3384.

Franke, T. F., Yang, S. I., Chan, T. O., Datta, K., Kazlauskas, A., Morrison, D. K., Kaplan, D. R., and Tsichlis, P. N. (1995). The protein kinase encoded by the Akt proto-oncogene is a target of the PDGF-activated phosphatidylinositol 3-kinase. Cell *81*, 727-736.

French, V., Bryant, P. J., and Bryant, S. V. (1976). Pattern regulation in epimorphic fields. Science *193*, 969-981.

Fry, M. J., Panayotou, G., Dhand, R., Ruiz Larrea, F., Gout, I., Nguyen, O., Courtneidge, S. A., and Waterfield, M. D. (1992). Purification and characterization of a phosphatidylinositol 3-kinase complex from bovine brain by using phosphopeptide affinity columns. Biochem J *288*, 383-393.

Funamoto, S., Meili, R., Lee, S., Parry, L., and Firtel, R. A. (2002). Spatial and temporal regulation of 3-phosphoinositides by PI 3-kinase and PTEN mediates chemotaxis. Cell *109*, 611-623.

Gao, X., Neufeld, T. P., and Pan, D. (2000). Drosophila PTEN regulates cell growth and proliferation through PI3K- dependent and -independent pathways. Dev Biol *221*, 404-418.

Gao, X., and Pan, D. (2001). TSC1 and TSC2 tumor suppressors antagonize insulin signaling in cell growth. Genes Dev *15*, 1383-1392.

Gao, X., Zhang, Y., Arrazola, P., Hino, O., Kobayashi, T., Yeung, R. S., Ru, B., and Pan, D. (2002). Tsc tumour suppressor proteins antagonize amino-acid-TOR signalling. Nat Cell Biol *4*, 699-704.

Garofalo, R. S. (2002). Genetic analysis of insulin signaling in Drosophila. Trends Endocrinol Metab *13*, 156-162.

Genot, E. M., Arrieumerlou, C., Ku, G., Burgering, B. M., Weiss, A., and Kramer, I. M. (2000). The T-cell receptor regulates Akt (protein kinase B) via a pathway involving Rac1 and phosphatidylinositide 3-kinase. Mol Cell Biol *20*, 5469-5478.

Gingras, A. C., Raught, B., and Sonenberg, N. (1999). eIF4 initiation factors: effectors of mRNA recruitment to ribosomes and regulators of translation. Annu Rev Biochem *68*, 913-963.

Goberdhan, D. C., Paricio, N., Goodman, E. C., Mlodzik, M., and Wilson, C. (1999). Drosophila tumor suppressor PTEN controls cell size and number by antagonizing the Chico/PI3-kinase signaling pathway. Genes Dev *13*, 3244-3258.

Gonzalez-Gaitan, M., Capdevila, M. P., and Garcia-Bellido, A. (1994). Cell proliferation patterns in the wing imaginal disc of Drosophila. Mech Dev *46*, 183-200.

Goodge, K. A., and Hutton, J. C. (2000). Translational regulation of proinsulin biosynthesis and proinsulin conversion in the pancreatic beta-cell. Semin Cell Dev Biol *11*, 235-242.

Groszer, M., Erickson, R., Scripture-Adams, D. D., Lesche, R., Trumpp, A., Zack, J. A., Kornblum, H. I., Liu, X., and Wu, H. (2001). Negative regulation of neural stem/progenitor cell proliferation by the Pten tumor suppressor gene in vivo. Science *294*, 2186-2189.

Halfar, K., Rommel, C., Stocker, H., and Hafen, E. (2001). Ras controls growth, survival and differentiation in the Drosophila eye by different thresholds of MAP kinase activity. Development *128*, 1687-1696.

Hara, K., Yonezawa, K., Weng, Q. P., Kozlowski, M. T., Belham, C., and Avruch, J. (1998). Amino acid sufficiency and mTOR regulate p70 S6 kinase and eIF-4E BP1 through a common effector mechanism. J Biol Chem *273*, 14484-14494.

Harlow, E., and Lane, D. P. (1988). Antibodies. A Laboratory Manual, Cold Spring Harbor Laboratory).

Haruta, T., Uno, T., Kawahara, J., Takano, A., Egawa, K., Sharma, P. M., Olefsky, J. M., and Kobayashi, M. (2000). A rapamycin-sensitive pathway down-regulates insulin signaling via phosphorylation and proteasomal degradation of insulin receptor substrate-1. Mol Endocrinol *14*, 783-794.

Hiles, I. D., Otsu, M., Volinia, S., Fry, M. J., Gout, I., Dhand, R., Panayotou, G., Ruiz Larrea, F., Thompson, A., Totty, N. F., *et al.* (1992). Phosphatidylinositol 3-kinase: structure and expression of the 110 kd catalytic subunit. Cell *70*, 419-429.

Holt, K. H., Olson, L., Moye-Rowley, W. S., and Pessin, J. E. (1994). Phosphatidylinositol 3-kinase activation is mediated by high-affinity interactions between distinct domains within the p110 and p85 subunits. Mol Cell Biol *14*, 42-49.

Hu, Q., Klippel, A., Muslin, A. J., Fantl, W. J., and Williams, L. T. (1995). Ras-dependent induction of cellular responses by constitutively active phosphatidylinositol-3 kinase. Science *268*, 100-102.

Huang, H., Potter, C. J., Tao, W., Li, D. M., Brogiolo, W., Hafen, E., Sun, H., and Xu, T. (1999). PTEN affects cell size, cell proliferation and apoptosis during Drosophila eye development. Development *126*, 5365-5372.

Hunter, T., Lindberg, R. A., Middlemas, D. S., Tracy, S., and van der Geer, P. (1992). Receptor protein tyrosine kinases and phosphatases. Cold Spring Harb Symp Quant Biol *57*, 25-41.

Iiboshi, Y., Papst, P. J., Kawasome, H., Hosoi, H., Abraham, R. T., Houghton, P. J., and Terada, N. (1999). Amino acid-dependent control of p70(s6k). Involvement of tRNA aminoacylation in the regulation. J Biol Chem *274*, 1092-1099.

Ikeya, T., Galic, M., Belawat, P., Nairz, K., and Hafen, E. (2002). Nutrient-Dependent Expression of Insulin-like Peptides from Neuroendocrine Cells in the CNS Contributes to Growth Regulation in Drosophila. Curr Biol *12*, 1293.

Inoki, K., Li, Y., Zhu, T., Wu, J., and Guan, K. L. (2002). TSC2 is phosphorylated and inhibited by Akt and suppresses mTOR signalling. Nature Cell Biology *4*, 648-657.

Ito, N., and Rubin, G. M. (1999). gigas, a Drosophila homolog of tuberous sclerosis gene product-2, regulates the cell cycle. Cell *96*, 529-539.

Jaeschke, A., Hartkamp, J., Saitoh, M., Roworth, W., Nobukuni, T., Hodges, A., Sampson, J., Thomas, G., and Lamb, R. (2002). Tuberous sclerosis complex tumor suppressor-mediated S6 kinase inhibition by phosphatidylinositide-3-OH kinase is mTOR independent. Journal of Cell Biology *159*, 217-224.

Jefferies, H. B., Fumagalli, S., Dennis, P. B., Reinhard, C., Pearson, R. B., and Thomas, G. (1997). Rapamycin suppresses 5'TOP mRNA translation through inhibition of p70s6k. Embo J *16*, 3693-3704.

Jefferies, H. B., Reinhard, C., Kozma, S. C., and Thomas, G. (1994). Rapamycin selectively represses translation of the "polypyrimidine tract" mRNA family. Proc Natl Acad Sci U S A *91*, 4441-4445.

Johnston, L. A., Prober, D. A., Edgar, B. A., Eisenman, R. N., and Gallant, P. (1999). Drosophila myc regulates cellular growth during development. Cell *98*, 779-790.

Karasarides, M., Anand-Apte, B., and Wolfman, A. (2001). A direct interaction between oncogenic Ha-Ras and phosphatidylinositol 3-kinase is not required for Ha-Ras-dependent transformation of epithelial cells. J Biol Chem *276*, 39755-39764.

Karim, F. D., and Rubin, G. M. (1998). Ectopic expression of activated Ras1 induces hyperplastic growth and increased cell death in Drosophila imaginal tissues. Development *125*, 1-9.

Kauffmann-Zeh, A., Rodriguez-Viciana, P., Ulrich, E., Gilbert, C., Coffer, P., Downward, J., and Evan, G. (1997). Suppression of c-Myc-induced apoptosis by Ras signalling through PI(3)K and PKB. Nature *385*, 544-548.

Kawamura, K., Shibata, T., Saget, O., Peel, D., and Bryant, P. J. (1999). A new family of growth factors produced by the fat body and active on Drosophila imaginal disc cells. Development *126*, 211-219.

Kimball, S. R., and Jefferson, L. S. (2000). Regulation of Translation Initiation in Mammalian Cells by Amino acids. In Translational control of Gene Expression, N. Sonenberg, J. W. B. Hershey, and M. B. Mathews, eds. (New York, Cold Spring Harbor Laboratory Press), pp. 561-580.

Klippel, A., Reinhard, C., Kavanaugh, W. M., Apell, G., Escobedo, M. A., and Williams, L. T. (1996). Membrane localization of phosphatidylinositol 3-kinase is sufficient to activate multiple signal-transducing kinase pathways. Mol Cell Biol *16*, 4117-4127.

Kodaki, T., Woscholski, R., Hallberg, B., Rodriguez-Viciana, P., Downward, J., and Parker, P. J. (1994). The activation of phosphatidylinositol 3-kinase by Ras. Curr Biol *4*, 798-806.

Kotani, K., Yonezawa, K., Hara, K., Ueda, H., Kitamura, Y., Sakaue, H., Ando, A., Chavanieu, A., Calas, B., Grigorescu, F., and et al. (1994). Involvement of phosphoinositide 3-kinase in insulin- or IGF-1-induced membrane ruffling. Embo J *13*, 2313-2321.

Kozma, S. C., and Thomas, G. (2002). Regulation of cell size in growth, development and human disease: PI3K, PKB and S6K. Bioessays *24*, 65-71.

Kwon, C. H., Zhu, X., Zhang, J., Knoop, L. L., Tharp, R., Smeyne, R. J., Eberhart, C. G., Burger, P. C., and Baker, S. J. (2001). Pten regulates neuronal soma size: a mouse model of Lhermitte-Duclos disease. Nat Genet *29*, 404-411.

Lambertsson, A. (1998). The minute genes in Drosophila and their molecular functions. Adv Genet *38*, 69-134.

Lawlor, M. A., and Alessi, D. R. (2001). PKB/Akt: a key mediator of cell proliferation, survival and insulin responses? J Cell Sci *114*, 2903-2910.

Lawrence, P. A. (1992). The Making of a Fly (Oxford, Blackwell Science Publications).

Layton, M. J., Harpur, A. G., Panayotou, G., Bastiaens, P. I. H., and Waterfield, M. D. (1998). Binding of a diphosphotyrosine-containing peptide that mimics activated platelet-derived growth factor receptor beta induces oligomerization of phosphatidylinositol 3-kinase [In Process Citation]. J Biol Chem *273*, 33379-33385.

Lee, J. O., Yang, H., Georgescu, M. M., Di Cristofano, A., Maehama, T., Shi, Y., Dixon, J. E., Pandolfi, P., and Pavletich, N. P. (1999). Crystal structure of the PTEN tumor suppressor: implications for its phosphoinositide phosphatase activity and membrane association. Cell *99*, 323-334.

Leevers, S. J., Weinkove, D., MacDougall, L. K., Hafen, E., and Waterfield, M. D. (1996). The Drosophila phosphoinositide 3-kinase Dp110 promotes cell growth. Embo J *15*, 6584-6594.

Lemmon, M. A., Ferguson, K. M., and Schlessinger, J. (1996). PH domains: diverse sequences with a common fold recruit signaling molecules to the cell surface. Cell *85*, 621-624.

Lewis, E. B. (1978). A gene complex controlling segmentation in *Drosophila*. Nature *276*, 565-570.

Li, J., Yen, C., Liaw, D., Podsypanina, K., Bose, S., Wang, S. I., Puc, J., Miliaresis, C., Rodgers, L., McCombie, R., *et al.* (1997). PTEN, a putative protein tyrosine phosphatase gene mutated in human brain, breast, and prostate cancer. Science *275*, 1943-1947.

Lin, T. A., Kong, X., Haystead, T. A., Pause, A., Belsham, G., Sonenberg, N., and Lawrence, J. C., Jr. (1994). PHAS-I as a link between mitogen-activated protein kinase and translation initiation. Science *266*, 653-656.

Lynch, D. K., Ellis, C. A., Edwards, P. A., and Hiles, I. D. (1999). Integrin-linked kinase regulates phosphorylation of serine 473 of protein kinase B by an indirect mechanism. Oncogene *18*, 8024-8032.

Madhavan, M. M., and Scheiderman, H. A. (1977). Histological analysis of the dynamicas of growth of the imaginal discs and histoblast nests during larval development of *Drosophila melanogaster*. Wilhelm Roux's Archives *183*, 269-305.

Maehama, T., and Dixon, J. E. (1998). The tumor suppressor, PTEN/MMAC1, dephosphorylates the lipid second messenger, phosphatidylinositol 3,4,5-trisphosphate. J Biol Chem *273*, 13375-13378.

Maffucci, T., and Falasca, M. (2001). Specificity in pleckstrin homology (PH) domain membrane targeting: a role for a phosphoinositide-protein co-operative mechanism. FEBS Lett *506*, 173-179.

Martin, J. F., Hersperger, E., Simcox, A., and Shearn, A. (2000). minidiscs encodes a putative amino acid transporter subunit required non-autonomously for imaginal cell proliferation. Mech Dev *92*, 155-167.

Marygold, S. J., and Leevers, S. J. (2002). Growth Signaling: TSC Takes Its Place. Curr Biol *12*, R785-787.

Mayer, B. J., Ren, R., Clark, K. L., and Baltimore, D. (1993). A putative modular domain present in diverse signaling proteins. Cell *73*, 629-630.

McCabe, J., French, V., and Partridge, L. (1997). Joint regulation of cell size and cell number in the wing blade of Drosophila melanogaster. Genet Res *69*, 61-68.

McManus, E. J., and Alessi, D. R. (2002). TSC1-TSC2: a complex tale of PKB-mediated S6K regulation. Nat Cell Biol *4*, E214-216.

Meyer, C. A., Jacobs, H. W., Datar, S. A., Du, W., Edgar, B. A., and Lehner, C. F. (2000). Drosophila Cdk4 is required for normal growth and is dispensable for cell cycle progression. Embo J *19*, 4533-4542.

Michalopoulos, G. K., and DeFrances, M. C. (1997). Liver regeneration. Science *276*, 60-66.

Milan, M., Campuzano, S., and Garcia-Bellido, A. (1997). Developmental parameters of cell death in the wing disc of Drosophila. Proc Natl Acad Sci U S A *94*, 5691-5696.

Miron, M., Verdu, J., Lachance, P. E., Birnbaum, M. J., Lasko, P. F., and Sonenberg, N. (2001). The translational inhibitor 4E-BP is an effector of PI(3)K/Akt signalling and cell growth in Drosophila. Nat Cell Biol *3*, 596-601.

Morata, G., and Lawrence, P. A. (1975). Control of compartment development by the engrailed gene in Drosophila. Nature *255*, 614-617.

Morata, G., and Ripoll, P. (1975). Minutes: mutants of drosophila autonomously affecting cell division rate. Dev Biol *42*, 211-221.

Myers, M. G., Jr., Sun, X. J., and White, M. F. (1994). The IRS-1 signaling system. Trends Biochem Sci *19*, 289-293.

Nave, B. T., Ouwens, M., Withers, D. J., Alessi, D. R., and Shepherd, P. R. (1999). Mammalian target of rapamycin is a direct target for protein kinase B: identification of a convergence point for opposing effects of insulin and amino-acid deficiency on protein translation. Biochem J *344 Pt 2*, 427-431.

Nellen, D., Burke, R., Struhl, G., and Basler, K. (1996). Direct and long-range action of a DPP morphogen gradient. Cell *85*, 357-368.

Neufeld, T. P., de la Cruz, A. F., Johnston, L. A., and Edgar, B. A. (1998). Coordination of growth and cell division in the Drosophila wing. Cell *93*, 1183-1193.

Nijhout, H. F., and Emlen, D. J. (1998). Competition among body parts in the development and evolution of insect morphology. Proc Natl Acad Sci U S A *95*, 3685-3689.

Niman, H. L., Houghten, R. A., Walker, L. E., Reisfeld, R. A., Wilson, I. A., Hogle, J. M., and Lerner, R. A. (1983). Generation of protein-reactive antibodies by short peptides is an event of high frequency: implications for the structural basis of immune recognition. Proc Natl Acad Sci U S A *80*, 4949-4953.

Nishida, Y., Hata, M., Ayaki, T., Ryo, H., Yamagata, M., Shimizu, K., and Nishizuka, Y. (1988). Proliferation of both somatic and germ cells is affected in the Drosophila mutants of raf proto-oncogene. Embo J *7*, 775-781.

Obata, T., Yaffe, M. B., Leparc, G. G., Piro, E. T., Maegawa, H., Kashiwagi, A., Kikkawa, R., and Cantley, L. C. (2000). Peptide and protein library screening defines optimal substrate motifs for AKT/PKB. J Biol Chem *275*, 36108-36115.

Ohneda, K., Ee, H., and German, M. (2000). Regulation of insulin gene transcription. Semin Cell Dev Biol *11*, 227-233.

Oldham, S., Montagne, J., Radimerski, T., Thomas, G., and Hafen, E. (2000). Genetic and biochemical characterization of dTOR, the Drosophila homolog of the target of rapamycin. Genes Dev *14*, 2689-2694.

Oldham, S., Stocker, H., Laffargue, M., Wittwer, F., Wymann, M., and Hafen, E. (2002). The Drosophila insulin/IGF receptor controls growth and size by modulating PtdInsP(3) levels. Development *129*, 4103-4109.

Pacold, M. E., Suire, S., Perisic, O., Lara-Gonzalez, S., Davis, C. T., Walker, E. H., Hawkins, P. T., Stephens, L., Eccleston, J. F., and Williams, R. L. (2000). Crystal structure and functional analysis of Ras binding to its effector phosphoinositide 3-kinase gamma. Cell *103*, 931-943.

Park, I. H., Bachmann, R., Shirazi, H., and Chen, J. (2002). Regulation of ribosomal S6 kinase 2 by mammalian target of rapamycin. J Biol Chem *26*, 26.

Partridge, L., Langelan, R., Fowler, K., Zwaan, B., and French, V. (1999). Correlated responses to selection on body size in Drosophila melanogaster. Genet Res *74*, 43-54.

Pelengaris, S., Khan, M., and Evan, G. (2002). c-MYC: more than just a matter of life and death. Nat Rev Cancer *2*, 764-776.

Perucho, M., Hanahan, D., and Wigler, M. (1980). Genetic and physical linkage of exogenous sequences in transformed cells. Cell *22*, 309-317.

Polymenis, M., and Schmidt, E. V. (1997). Coupling of cell division to cell growth by translational control of the G1 cyclin CLN3 in yeast. Genes Dev *11*, 2522-2531.

Potter, C. J., Huang, H., and Xu, T. (2001). Drosophila Tsc1 functions with Tsc2 to antagonize insulin signaling in regulating cell growth, cell proliferation, and organ size. Cell *105*, 357-368.

Potter, C. J., Pedraza, L. G., and Xu, T. (2002). Akt regulates growth by directly phosphorylating Tsc2. Nat Cell Biol *4*, 658-665.

Prober, D. A., and Edgar, B. A. (2000). Ras1 promotes cellular growth in the Drosophila wing. Cell *100*, 435-446.

Prober, D. A., and Edgar, B. A. (2002). Interactions between Ras1, dMyc, and dPI3K signaling in the developing Drosophila wing. Genes Dev *16*, 2286-2299.

Pullen, N., Dennis, P. B., Andjelkovic, M., Dufner, A., Kozma, S. C., Hemmings, B. A., and Thomas, G. (1998). Phosphorylation and activation of p70S6K by PDK1. Science *279*, 707-710.

Radimerski, T., Montagne, J., Hemmings-Mieszczak, M., and Thomas, G. (2002a). Lethality of Drosophila lacking TSC tumor suppressor function rescued by reducing dS6K signaling. Genes & Development *16*, 2627-2632.

Radimerski, T., Montagne, J., Rintelen, F., Stocker, H., van Der Kaay, J., Downes, C. P., Hafen, E., and Thomas, G. (2002b). dS6K-regulated cell growth is dPKB/dPI(3)K-independent, but requires dPDK1. Nat Cell Biol *4*, 251-255.

Richardson, H. E., O'Keefe, L. V., Reed, S. I., and Saint, R. (1993). A Drosophila G1-specific cyclin E homolog exhibits different modes of expression during embryogenesis. Development *119*, 673-690.

Rintelen, F., Stocker, H., Thomas, G., and Hafen, E. (2001). PDK1 regulates growth through Akt and S6K in Drosophila. Proc Natl Acad Sci U S A *98*, 15020-15025.

Robertson, F. W. (1959). Studies in quantitative inheritance XII. Cell size and numberin relation to genetic and environmental variation of body size in Drosophila. Genetics *44*, 869-896.

Robertson, F. W. (1963). The ecological genetics of growth in Drosophila 6. The genetic correlation between the duration of the larval period and body size in relation to the larval diet. Genet Res *4*, 74-92.

Rodriguez-Viciana, P., Marte, B. M., Warne, P. H., and Downward, J. (1996a). Phosphatidylinositol 3' kinase: one of the effectors of Ras. Philos Trans R Soc Lond B Biol Sci *351*, 225-231; discussion 231-222.

Rodriguez-Viciana, P., Warne, P. H., Dhand, R., Vanhaesebroeck, B., Gout, I., Fry, M. J., Waterfield, M. D., and Downward, J. (1994). Phosphatidylinositol-3-OH kinase as a direct target of Ras. Nature *370*, 527-532.

Rodriguez-Viciana, P., Warne, P. H., Khwaja, A., Marte, B. M., Pappin, D., Das, P., Waterfield, M. D., Ridley, A., and Downward, J. (1997). Role of phosphoinositide 3-OH kinase in cell transformation and control of the actin cytoskeleton by Ras. Cell *89*, 457-467.

Rodriguez-Viciana, P., Warne, P. H., Vanhaesebroeck, B., Waterfield, M. D., and Downward, J. (1996b). Activation of phosphoinositide 3-kinase by interaction with Ras and by point mutation. Embo J *15*, 2442-2451.

Rubio, I., Wittig, U., Meyer, C., Heinze, R., Kadereit, D., Waldmann, H., Downward, J., and Wetzker, R. (1999). Farnesylation of Ras is important for the interaction with phosphoinositide 3-kinase gamma. Eur J Biochem *266*, 70-82.

Rulifson, E. J., Kim, S. K., and Nusse, R. (2002). Ablation of insulin-producing neurons in flies: growth and diabetic phenotypes. Science *296*, 1118-1120.

Sambrook, J., Fritsch, E. F., and Maniatis, T. (2001). Molecular cloning: A laboratory manual (Cold Spring Harbor, Cold Spring Harbor Laboratory Press).

Sang, J. H. (1978). The nutritional requirements of *Drosophila*. In The genetics and biology of *Drosophila*, M. Ashburner, and T. R. F. Wright, eds. (London and New York, Academic Press), pp. 159-192.

Saucedo, L. J., Gao, X., Chiarelli, D. A., Li, L., Pan, D., and Edgar, B. A. (2003). Rheb promotes cell growth as a component of the insulin/TOR signalling network. Nat Cell Biol *5*, 566-571.

Scanga, S. E., Ruel, L., Binari, R. C., Snow, B., Stambolic, V., Bouchard, D., Peters, M., Calvieri, B., Mak, T. W., Woodgett, J. R., and Manoukian, A. S. (2000). The conserved PI3'K/PTEN/Akt signaling pathway regulates both cell size and survival in Drosophila. Oncogene *19*, 3971-3977.

Schagger, H., and von Jagow, G. (1987). Tricine-sodium dodecyl sulfate-polyacrylamide gel electrophoresis for the separation of proteins in the range from 1 to 100 kDa. Anal Biochem *166*, 368-379.

Schmelzle, T., and Hall, M. N. (2000). TOR, a central controller of cell growth. Cell *103*, 253-262.

Schmidt, A., Beck, T., Koller, A., Kunz, J., and Hall, M. N. (1998). The TOR nutrient signalling pathway phosphorylates NPR1 and inhibits turnover of the tryptophan permease [In Process Citation]. Embo J *17*, 6924-6931.

Scott, P. H., Brunn, G. J., Kohn, A. D., Roth, R. A., and Lawrence, J. C., Jr. (1998). Evidence of insulin-stimulated phosphorylation and activation of the mammalian target of rapamycin mediated by a protein kinase B signaling pathway. Proc Natl Acad Sci U S A *95*, 7772-7777.

Sekulic, A., Hudson, C. C., Homme, J. L., Yin, P., Otterness, D. M., Karnitz, L. M., and Abraham, R. T. (2000). A direct linkage between the phosphoinositide 3-kinase-AKT signaling pathway and the mammalian target of rapamycin in mitogen-stimulated and transformed cells. Cancer Res *60*, 3504-3513.

Shima, H., Pende, M., Chen, Y., Fumagalli, S., Thomas, G., and Kozma, S. C. (1998). Disruption of the p70(s6k)/p85(s6k) gene reveals a small mouse phenotype and a new functional S6 kinase. Embo J *17*, 6649-6659.

Shioi, T., Kang, P. M., Douglas, P. S., Hampe, J., Yballe, C. M., Lawitts, J., Cantley, L. C., and Izumo, S. (2000). The conserved phosphoinositide 3-kinase pathway determines heart size in mice. Embo J *19*, 2537-2548.

Shioi, T., McMullen, J. R., Kang, P. M., Douglas, P. S., Obata, T., Franke, T. F., Cantley, L. C., and Izumo, S. (2002). Akt/protein kinase B promotes organ growth in transgenic mice. Mol Cell Biol *22*, 2799-2809.

Simcox, A. A., Grumbling, G., Schnepp, B., Bennington-Mathias, C., Hersperger, E., and Shearn, A. (1996). Molecular, phenotypic, and expression analysis of vein, a gene required for growth of the Drosophila wing disc. Dev Biol *177*, 475-489.

Smith, A., Alrubaie, S., Coehlo, C., Leevers, S. J., and Ashworth, A. (1999). Alternative splicing of the Drosophila PTEN gene. Biochim Biophys Acta *1447*, 313-317.

Smith, A. V., and Orr-Weaver, T. L. (1991). The regulation of the cell cycle during Drosophila embryogenesis: the transition to polyteny. Development *112*, 997-1008.

Songyang, Z., Shoelson, S. E., Chaudhuri, M., Gish, G., Pawson, T., Haser, W. G., King, F., Roberts, T., Ratnofsky, S., Lechleider, R. J., *et al.* (1993). SH2 domains recognize specific phosphopeptide sequences. Cell *72*, 767-778.

Stambolic, V., Suzuki, A., de la Pompa, J. L., Brothers, G. M., Mirtsos, C., Sasaki, T., Ruland, J., Penninger, J. M., Siderovski, D. P., and Mak, T. W. (1998). Negative regulation of PKB/Akt-dependent cell survival by the tumor suppressor PTEN. Cell *95*, 29-39.

Stephens, L., Anderson, K., Stokoe, D., Erdjument-Bromage, H., Painter, G. F., Holmes, A. B., Gaffney, P. R., Reese, C. B., McCormick, F., Tempst, P., *et al.* (1998). Protein kinase B kinases that mediate phosphatidylinositol 3,4,5- trisphosphate-dependent activation of protein kinase B. Science *279*, 710-714.

Stephens, L. R., Eguinoa, A., Erdjument-Bromage, H., Lui, M., Cooke, F., Coadwell, J., Smrcka, A. S., Thelen, M., Cadwallader, K., Tempst, P., and Hawkins, P. T. (1997). The G beta gamma sensitivity of a PI3K is dependent upon a tightly associated adaptor, p101. Cell *89*, 105-114.

Stephens, L. R., Jackson, T. R., and Hawkins, P. T. (1993). Agonist-stimulated synthesis of phosphatidylinositol(3,4,5)- trisphosphate: a new intracellular signalling system? Biochim Biophys Acta *1179*, 27-75.

Stern, D. L., and Emlen, D. J. (1999). The developmental basis for allometry in insects. Development *126*, 1091-1101.

Stocker, H., Radimerski, T., Schindelholz, B., Wittwer, F., Belawat, P., Daram, P., Breuer, S., Thomas, G., and Hafen, E. (2003). The small GTPase dRheb is an essential regulator of sS6K in controlling cell growth in Drosophila. Nat Cell Biol *in press*.

Stokoe, D., Stephens, L. R., Copeland, T., Gaffney, P. R., Reese, C. B., Painter, G. F., Holmes, A. B., McCormick, F., and Hawkins, P. T. (1997). Dual role of phosphatidylinositol-3,4,5-trisphosphate in the activation of protein kinase B. Science *277*, 567-570.

Suire, S., Hawkins, P., and Stephens, L. (2002). Activation of phosphoinositide 3-kinase gamma by Ras. Curr Biol *12*, 1068-1075.

Tamemoto, H., Kadowaki, T., Tobe, K., Yagi, T., Sakura, H., Hayakawa, T., Terauchi, Y., Ueki, K., Kaburagi, Y., Satoh, S., and et al. (1994). Insulin resistance and growth retardation in mice lacking insulin receptor substrate-1. Nature *372*, 182-186.

Tapon, N., Ito, N., Dickson, B. J., Treisman, J. E., and Hariharan, I. K. (2001). The Drosophila tuberous sclerosis complex gene homologs restrict cell growth and cell proliferation. Cell *105*, 345-355.

Toker, A., and Newton, A. C. (2000). Akt/protein kinase B is regulated by autophosphorylation at the hypothetical PDK-2 site. J Biol Chem *275*, 8271-8274.

Ueki, K., Algenstaedt, P., Mauvais-Jarvis, F., and Kahn, C. R. (2000). Positive and negative regulation of phosphoinositide 3-kinase-dependent signaling pathways by three different gene products of the p85alpha regulatory subunit. Mol Cell Biol *20*, 8035-8046.

Vanhaesebroeck, B., and Alessi, D. R. (2000). The PI3K-PDK1 connection: more than just a road to PKB. Biochem J *346 Pt 3*, 561-576.

Vanhaesebroeck, B., Higashi, K., Raven, C., Welham, M., Anderson, S., Brennan, P., Ward, S. G., and Waterfield, M. D. (1999). Autophosphorylation of p110delta phosphoinositide 3-kinase: a new paradigm for the regulation of lipid kinases in vitro and in vivo. EMBO J *18*, 1292-1302.

Vanhaesebroeck, B., Leevers, S. J., Ahmadi, K., Timms, J., Katso, R., Driscoll, P. C., Woscholski, R., Parker, P. J., and Waterfield, M. D. (2001). Synthesis and function of 3-phosphorylated inositol lipids. Annu Rev Biochem *70*, 535-602.

Vanhaesebroeck, B., Leevers, S. J., Panayotou, G., and Waterfield, M. D. (1997a). Phosphoinositide 3-kinases: a conserved family of signal transducers. Trends Biochem Sci *22*, 267-272.

Vanhaesebroeck, B., Welham, M. J., Kotani, K., Stein, R., Warne, P. H., Zvelebil, M. J., Higashi, K., Volinia, S., Downward, J., and Waterfield, M. D. (1997b). p110δ, a novel phosphoinositide 3-kinase in leukocytes. Proc Natl Acad Sci USA *94*, 4330-4335.

Verdu, J., Buratovich, M. A., Wilder, E. L., and Birnbaum, M. J. (1999). Cell-autonomous regulation of cell and organ growth in Drosophila by Akt/PKB. Nat Cell Biol *1*, 500-506.

Vlahos, C. J., Matter, W. F., Hui, K. Y., and Brown, R. F. (1994). A specific inhibitor of phosphatidylinositol 3-kinase, 2-(4- morpholinyl)-8-phenyl-4H-1-benzopyran-4-one (LY294002). J Biol Chem *269*, 5241-5248.

Walker, E. H., Perisic, O., Ried, C., Stephens, L., and Williams, R. L. (1999). Structural insights into phosphoinositide 3-kinase catalysis and signalling. Nature *402*, 313-320.

Wang, L., Liu, F., and Adamo, M. L. (2001). Cyclic amp inhibits extracellular signal-regulated kinase and phosphatidylinositol 3-kinase/akt pathways by inhibiting rap1. J Biol Chem *276*, 37242-37249.

Watson, K. L., Chou, M. M., Blenis, J., Gelbart, W. M., and Erikson, R. L. (1996). A Drosophila gene structurally and functionally homologous to the mammalian 70-kDa s6 kinase gene. Proc Natl Acad Sci U S A *93*, 13694-13698.

Weigmann, K., Cohen, S. M., and Lehner, C. F. (1997). Cell cycle progression, growth and patterning in imaginal discs despite inhibition of cell division after inactivation of Drosophila Cdc2 kinase. Development *124*, 3555-3563.

Weinkove, D. (1999) Identification of an adaptor for the *Drosophila* Class IA phosphoinositide 3-kinase and the study of its function *in vivo* and *in vitro*, University College, London.

Weinkove, D., Leevers, S. J., MacDougall, L. K., and Waterfield, M. D. (1997). p60 is an adaptor for the Drosophila phosphoinositide 3-kinase, Dp110. J Biol Chem *272*, 14606-14610.

Weinkove, D., Neufeld, T. P., Twardzik, T., Waterfield, M. D., and Leevers, S. J. (1999). Regulation of imaginal disc cell size, cell number and organ size by Drosophila class I(A) phosphoinositide 3-kinase and its adaptor. Curr Biol *9*, 1019-1029.

Wennstrom, S., and Downward, J. (1999). Role of phosphoinositide 3-kinase in activation of ras and mitogen- activated protein kinase by epidermal growth factor. Mol Cell Biol *19*, 4279-4288.

Wheelhouse, N. M., Stubbs, A. K., Lomax, M. A., MacRae, J. C., and Hazlerigg, D. G. (1999). Growth hormone and amino acid supply interact synergistically to control insulin-like growth factor-I production and gene expression in cultured ovine hepatocytes. J Endocrinol *163*, 353-361.

Whittle, J. R. (1990). Pattern formation in imaginal discs. Semin Cell Biol *1*, 241-252.

Williams, M. R., Arthur, J. S., Balendran, A., van der Kaay, J., Poli, V., Cohen, P., and Alessi, D. R. (2000). The role of 3-phosphoinositide-dependent protein kinase 1 in activating AGC kinases defined in embryonic stem cells. Curr Biol *10*, 439-448.

Withers, D. J., Burks, D. J., Towery, H. H., Altamuro, S. L., Flint, C. L., and White, M. F. (1999). Irs-2 coordinates Igf-1 receptor-mediated beta-cell development and peripheral insulin signalling. Nat Genet *23*, 32-40.

Wolpert, L., Beddington, R., Brockes, J., Jessel, T., Lawrence, P. A., and Meyerowitz, E. (1998). Principles of Development (London, Current Biology Ltd.).

Wymann, M. P., Bulgarelli-Leva, G., Zvelebil, M. J., Pirola, L., Vanhaesebroeck, B., Waterfield, M. D., and Panayotou, G. (1996). Wortmannin inactivates phosphoinositide 3-kinase by covalent modification of Lys-802, a residue involved in the phosphate transfer reaction. Mol Cell Biol *16*, 1722-1733.

Yenush, L., Fernandez, R., Myers, M. G., Jr., Grammer, T. C., Sun, X. J., Blenis, J., Pierce, J. H., Schlessinger, J., and White, M. F. (1996). The Drosophila insulin receptor activates multiple signaling pathways but requires insulin receptor substrate proteins for DNA synthesis. Mol Cell Biol *16*, 2509-2517.

Yu, J., Zhang, Y., McIlroy, J., Rordorf-Nikolic, T., Orr, G. A., and Backer, J. M. (1998). Regulation of the p85/p110 phosphatidylinositol 3'-kinase: stabilization and inhibition of the p110alpha catalytic subunit by the p85 regulatory subunit. Mol Cell Biol *18*, 1379-1387.

Zhang, H., Stallock, J. P., Ng, J. C., Reinhard, C., and Neufeld, T. P. (2000). Regulation of cellular growth by the Drosophila target of rapamycin dTOR. Genes Dev *14*, 2712-2724.

Zheng, Y., Bagrodia, S., and Cerione, R. A. (1994). Activation of phosphoinositide 3-kinase activity by Cdc42Hs binding to p85. J Biol Chem *269*, 18727-18730.

Zinke, I., Kirchner, C., Chao, L. C., Tetzlaff, M. T., and Pankratz, M. J. (1999). Suppression of food intake and growth by amino acids in Drosophila: the role of pumpless, a fat body expressed gene with homology to vertebrate glycine cleavage system. Development *126*, 5275-5284.

Zinke, I., Schutz, C. S., Katzenberger, J. D., Bauer, M., and Pankratz, M. J. (2002). Nutrient control of gene expression in Drosophila: microarray analysis of starvation and sugar-dependent response. EMBO Journal *21*, 6162-6173.